LUND UNIVERSITY

Impact of Fuel Properties on Partially Premixed Combustion

Solaka, Hadeel

2014

Link to publication

Citation for published version (APA):
Solaka, H. (2014). *Impact of Fuel Properties on Partially Premixed Combustion*. [Doctoral Thesis (monograph), Combustion Engines].

Total number of authors:
1

General rights
Unless other specific re-use rights are stated the following general rights apply:
Copyright and moral rights for the publications made accessible in the public portal are retained by the authors and/or other copyright owners and it is a condition of accessing publications that users recognise and abide by the legal requirements associated with these rights.
• Users may download and print one copy of any publication from the public portal for the purpose of private study or research.
• You may not further distribute the material or use it for any profit-making activity or commercial gain
• You may freely distribute the URL identifying the publication in the public portal

Read more about Creative commons licenses: https://creativecommons.org/licenses/

Take down policy
If you believe that this document breaches copyright please contact us providing details, and we will remove access to the work immediately and investigate your claim.

LUND UNIVERSITY

PO Box 117
221 00 Lund
+46 46-222 00 00

Impact of Fuel Properties on Partially Premixed Combustion

Hadeel Solaka Aronsson

DOCTORAL DISSERTATION
by due permission of the Faculty Engineering, Lund University, Sweden.

To be defended at M-building, LTH, room M:B 05/09 2014, 10.00.

Faculty opponent

Bianca Maria Vaglieco, Istituto Motori-CNR, Italy

Organization LUND UNIVERSITY	Document name DOCTORAL DISSERTATION
	Date of issue
Author Hadeel Solaka Aronsson	Sponsoring organization KCFP and Swedish Energy Agency

Title and subtitle

Impact of Fuel Properties on Partially Premixed Combustion

Abstract

Compression ignited engines generally have higher efficiency than spark ignition engines. However, the most common combustion concept in compression ignited engines, conventional diesel combustion, struggles with high levels of particulate matter and NO_x emissions. Therefore, new combustion strategies are used in compression ignited engines to reduce engine-out particulate matter and NO_x emissions. One such promising strategy, Partially Premixed Combustion (PPC), is analyzed in this thesis. Independently of its properties, if a combustion concept should be possible to put in production in a near future it is important that it can utilize the available fuel on the market. Hence, it is important to understand how PPC responds to fuel properties, especially research octane number value and ignition quality.

The objective of this work is to gain knowledge of fuel effects on the combustion and engine-out emissions in PPC. The topics are divided into three main parts.

The first part investigates the impact of research octane number (RON) and fuel composition on combustion, emissions and load range for PPC. A clear interaction between RON and ignition delay was found; higher research octane number results in longer ignition delay. Also, an interaction between ignition delay and fraction of low temperature reaction was found, a prolonged ignition delay results in higher fraction of low temperature reactions. A load range comparison between four gasoline-like fuels and Swedish diesel class 1 (MK1) at a specific air-fuel ratio and exhaust gas recirculation rate was performed. A clear interaction between RON and the feasible load range was found, fuels with lower RON values could be operated at lower loads.

The second part investigates the effects of engine operating parameters on combustion and emissions. As expected, the inlet oxygen concentration had a significant effect on ignition delay; reducing the inlet oxygen concentration resulted in a longer ignition delay. Also, when low inlet O_2 concentration is used in combination with high RON values the effect on ignition delay is enhanced compared to the added effects of each parameter. All emissions were influenced by inlet O_2 concentration; CO and HC emissions were increased with reduced inlet O_2 concentration, while the trend was the opposite for NO_x. A more retarded combustion phasing gave higher levels of CO and HC and lower levels of NO_x. However, at lower inlet O_2 concentrations the NO_x values were suppressed to very low levels independently of CA50. The emission levels of smoke decreased with increasing injection pressure.

The third part predicts the RON and motor octane number (MON) for oxygenated surrogate gasoline fuels using quadratic regression models. The models perform remarkably well in predicting RON and MON for any fuel blend of n-heptane, toluene, ethanol and isooctane. A similar model for Ignition delay is also presented in the thesis. By using these regression models for predicting ignition delay and RON value, it is possible to design a specific fuel to meet both emissions legislations and reducing fuel consumption.

Key words

PPC, Reference Fuels, Gasline, Diesel, Ignition Delay, Quadratic Regression Model

Classification system and/or index terms (if any)

Supplementary bibliographical information		Language English
ISSN and key title 0282-1990		ISBN 978-91-7623-032-9
Recipient's notes	Number of pages 193	Price
	Security classification	

Signature Hadeel Aronsson Date 2014-06-12

Impact of Fuel Properties on Partially Premixed Combustion

Hadeel Solaka Aronsson

LUND UNIVERSITY

Copyright © Hadeel Solaka Aronsson

Division of Combustion Engines
Department of Energy Sciences
Faculty of Engineering
Lund University
P.O. Box 118
SE-22100 Lund
Sweden

ISBN 978-91-7623-032-9 (Printed)
IBSN 978-91-7623-033-6 (Electronic version)
ISRN LUTMDN/TMHP-14/1104-SE
ISSN 0282-1990

Printed in Sweden by Tryckeriet E-huset, Lund University
Lund 2014

To my son

Abstract

Compression ignited engines generally have higher efficiency than spark ignition engines. However, the most common combustion concept in compression ignited engines, conventional diesel combustion, struggles with high levels of particulate matter and NO_x emissions. Therefore, new combustion strategies are used in compression ignited engines to reduce engine-out particulate matter and NO_x emissions. One such promising strategy, Partially Premixed Combustion (PPC), is analyzed in this thesis. Independently of its properties, if a combustion concept should be possible to put in production in a near future it is important that it can utilize the available fuel on the market. Hence, it is important to understand how PPC responds to fuel properties, especially research octane number value and ignition quality.

The objective of this work is to gain knowledge of fuel effects on the combustion and engine-out emissions in PPC. The topics are divided into three main parts.

The first part investigates the impact of research octane number (RON) and fuel composition on combustion, emissions and load range for PPC. A clear interaction between RON and ignition delay was found; higher research octane number results in longer ignition delay. Also, an interaction between ignition delay and fraction of low temperature reaction was found, a prolonged ignition delay results in higher fraction of low temperature reactions. A load range comparison between four gasoline-like fuels and Swedish diesel class 1 (MK1) at a specific air-fuel ratio and exhaust gas recirculation rate was performed. A clear interaction between RON and the feasible load range was found, fuels with lower RON values could be operated at lower loads.

The second part investigates the effects of engine operating parameters on combustion and emissions. As expected, the inlet oxygen concentration had a significant effect on ignition delay; reducing the inlet oxygen concentration resulted in a longer ignition delay. Also, when low inlet O_2 concentration is used in combination with high RON values the effect on ignition delay is enhanced compared to the added effects of each parameter. All emissions were influenced by inlet O_2 concentration; CO and HC emissions were increased with reduced inlet O_2 concentration, while the trend was the opposite for NO_x. A more retarded combustion phasing gave higher levels of CO and HC and lower levels of NO_x. However, at lower inlet O_2 concentrations the NO_x values were suppressed to very

low levels independently of CA50. The emission levels of smoke decreased with increasing injection pressure.

The third part predicts the RON and motor octane number (MON) for oxygenated surrogate gasoline fuels using quadratic regression models. The models perform remarkably well in predicting RON and MON for any fuel blend of n-heptane, toluene, ethanol and isooctane. A similar model for Ignition delay is also presented in the thesis. By using these regression models for predicting ignition delay and RON value, it is possible to design a specific fuel to meet both emissions legislations and reducing fuel consumption.

Populärvetenskaplig sammanfattning

Kompressionsantända (CI) motorer har generellt högre verkningsgrad än ottomotorer. Men det vanligaste förbränningskonceptet i motorer med kompressionständning, konventionell dieselförbränning, medför höga halter av partiklar (PM) och kväveoxider. Därför är målet med nya förbränningsstrategier som används i motorer med kompressionständning att minska motorns utsläpp av PM och NOx. En lovande strategi, delvis förblandad förbränning (PPC), analyseras i denna avhandling. Oberoende av egenskaperna, är det viktigt att tillgängliga bränslen på marknaden kan utnyttjas om ett förbränningskoncept skall vara möjligt att sätta i produktion inom en snar framtid. Därför är det viktigt att förstå hur PPC svarar på bränsleegenskaper, speciellt RON värde och antändningskvalitet.

Syftet med detta arbete är att få kunskap om bränsleeffekter på förbrännings processen och utsläppen med PPC. Avhandlingen är indelad i tre huvuddelar.

Den första delen undersöker från effekterna av RON värde och bränslesammansättning på förbränningsprocessen, utsläpp och lastområde för PPC. En tydlig växelverkan mellan RON värde och tändfördröjning hittades, högre RON värde gav längre tändfördröjning. Dessutom har en interaktion mellan tändfördröjning och fraktion av lågtemperaturreaktion hittats: en förlängd tändfördröjning gav högre fraktion av lågtemperaturförbränning. Vid ett visst luft-bränsleförhållande och EGR-mängd med användning av fyra bensinliknande bränslen i jämförelse med diesel, hittades en tydlig växelverkan mellan RON och det genomförbara lastområdet: bränslen med lägre RON värden möjliggör drift vid lägre laster.

Den andra delen undersöker effekterna av motorns driftsparametrar på förbränningsprocesser och utsläpp. Som väntat hade koncentrationen av syre i inkommande gaser en signifikant effekt på tändfördröjningen, i vilken en minskad koncentration av syre resulterade i en längre tändningsfördröjning. När låga koncentrationer av syre används i kombination med höga RON värden ökar effekten på tändfördröjningen jämfört med den summerade effekten av varje enskild parameter. Alla utsläpp påverkades av koncentrationen av syre. CO och HC-utsläpp ökade med minskad koncentration av syre, medan utvecklingen var den motsatta för NO_x. En senarelagd förbränningsfasning (CA50) gav högre halter av CO och HC och lägre nivåer av NO_x. Vid lägre syrekoncentrationer, undertrycktes NO_x värdena till

mycket låga nivåer oberoende av CA50. Utsläppsnivåerna av partiklar minskade med ökande insprutningstryck.

Den tredje delen beskriver skapandet av en kvadratisk regretionsmodell som förutspår RON och MON värden för bränsleblandningar av n-heptan, toluen, etanol, och isooktan. Modellen fungerar anmärkningsvärt väl och är en stor förbättring för att förutsäga RON och MON jämfört med de modeller som tidigare beskrivits i litteraturen.

List of Papers

Paper I

Investigation of Partially Premixed Combustion characteristics in Low Load Range with Regards to Fuel Octane Number in a Light-Duty Diesel Engine

Hadeel Solaka, Ulf Aronsson, Martin Tunér, Bengt Johansson

SAE Technical Paper 2012-01-0684

Paper II

Investigation on the Impact of Fuel Properties on Partially Premixed Combustion Characteristics in a Light Duty Diesel Engine

Hadeel Solaka, Martin Tunér, Bengt Johansson

ASME Technical Paper ICES2012-81184

Paper III

Analysis of Surrogate Fuels Effect on Ignition delay and Low Temperature Reaction during Partially Premixed Combustion

Hadeel Solaka, Martin Tunér, Bengt Johansson

SAE Technical Paper 2013-01-0903

Paper IV

Gasoline Surrogate Fuels for Partially Premixed Combustion, of Toluene Ethanol Reference Fuels

Hadeel Solaka, Martin Tunér, Bengt Johansson, William Cannella

SAE Technical Paper 2013-01-2540

Paper V

Using Oxygenated Gasoline Surrogate Composition to Map RON and MON

Hadeel Solaka, Martin Tunér, Bengt Johansson

SAE Technical Paper 2014-01-1303

Paper VI

Submitted to SAE 2014 International Powertrain, Fuels and Lubricants meeting

Comparison of Fuel Effects on Low Temperature Reactions in PPC and HCCI Combustion

Hadeel Solaka, Ida Truedsson, Martin Tunér, Bengt Johansson, William Cannella

Other publications

Impact of Mechanical Deformation due to Pressure, Mass, and Thermal Forces on the In-Cylinder Volume Trace in Optical Engines of Bowditch Design

Ulf Aronsson, Hadeel Solaka, Clément Chartier, Öivind Andersson, Bengt Johansson

SAE Technical Paper 2011-26-0082

Analysis of Errors in Heat Release Calculations Due to Distortion of the In-Cylinder Volume Trace from Mechanical Deformation in Optical Diesel Engines

Ulf Aronsson, Hadeel Solaka, Guillaume Lequien, Öivind Andersson, Bengt Johansson

SAE Technical Paper 2012-01-1604

Acknowledgment

Many people have contributed to the content of this thesis and I am grateful to all of them.

I would like to thank the department of Energy Sciences for giving me the opportunity to do this project. Also I would like to thanks the Centre of Competence for Combustion Processes (KCFP) and Swedish Energy Agency for financing my project.

I would like to thank my supervisors, Bengt Johansson and Martin Tunér for being helpful and supportive during my tenure as a PhD. I would also like to thank both Per Tunestål and Öivind Andersson for many interesting and valuable discussions and feedback.

Special thanks for William Cannella from Chevron for his interesting discussions, helpful paper- and thesis corrections, and for supplying fuels.

I would like to thank all the technicians for their support in the lab, special thanks for Mats Bengtsson for helping me out with the emission system and Krister Olsson for his help with the computers.

To all my colleagues at the division of combustion engines, it has been fun to work with all of you. I would like to give my special thanks for the female colleagues especially, Mengqin, Ida, Jessica and Maja for being there when I needed them. I would also like to thank my officemates, Ashish and Nhut for interesting discussions and making the day easier.

Finally, I would like to thank my husband for the enormous support and for all help that I got during the PhD especially during the last couple of months; you have made and are making my life brighter. I would also like to thank my parents and siblings for all their support. To my unborn child I apologized for the long and stressful period that I have put you in. At last, mom's book is finished and you will be the main focus from now on.

Nomenclature

ATDC	After top dead centre
ASTM	American Society for Testing and Materials
BTDC	Before top dead centre
CA0	Crank angle at 0% completion of heat release
CA10	Crank angle at 10% completion of heat release
CA50	Crank angle at 50% completion of heat release
CA90	Crank angle at 90% completion of heat release
CAD	Crank angle degree
CD	Combustion duration
CFR	Cooperative fuel research
CI	Compression ignition
CN	Cetane number
CO	Carbon monoxide
CO_2	Carbon dioxide
DOE	Design of experiment
E	Ethanol
EGR	Exhaust gas recirculation
EN	European standards
EOI	End of injection
ERF	Primary reference fuel with ethanol
EU	European Union
FSN	Filter smoke number
HC	Unburned hydrocarbon
HCCI	Homogeneous charge compression ignition
I	Isooctane
ID	Ignition Delay
$IMEP_g$	Indicated mean effective pressure gross
LbV	Linear by volume
LTC	Low temperature combustion
LTR	Low temperature reaction
MBT	Maximum brake torque
MK	Modulated Kinetics
MK1	Swedish diesel class 1
MON	Motor octane number
N	n-Heptane
NO_x	Nitrogen oxides i.e. NO, NO_2
O_2	Oxygen
OI	Octane index
ON	Octane number
PCCI	Premixed charge compression ignition
PCI	Premixed compression ignition
PM	Particulate matter
PPC	Partially premixed combustion

PPCI	Partially premixed compression ignition
PRF	Primary reference fuel
RCCI	Reactivity controlled compression ignition
RoHR	Rate of heat release
RON	Research octane number
S	Sensitivity
SI	Spark ignition
SOC	Start of combustion
SOI	Start of injection
T	Toluene
TDC	Top dead centre
$TERF_{cp}$	Primary reference fuel with toluene and ethanol, centre
$TERF_{critical}$	Primary reference fuel with toluene and ethanol, critical
TRF	Primary reference fuel with toluene
UNIBUS	Uniform bulky combustion system
λ	Relative air/fuel ratio
ϕ	Fuel/air equivalence ratio

Contents

Chapter 1

Introduction

1.1 Background

The internal combustion engine has a long history. In 1820 Cecil built the first working engine, but it did not get commercialized until 1860 when Lenoir sold his first engine. Since that time engines have been developed and improved by many inventors. Important developments are Nikolaus Otto's flame ignited (spark ignited) engine from 1876 and Rudolf Diesel's compression-ignited engine from 1892 [1]. Since then the internal combustion engine has been important for society in the fields of power generation and transport. In recent years, engine research has been challenged to solve air pollution issues and reduce fuel consumption.

Most climate scientists agree that the main cause of the global warming is from human development on the greenhouse gas effect. In the European Union (EU) the second biggest source of greenhouse gas after power generation is from road transport. A recent analysis showed that road transport is the source of one-fifth of the EU's total emissions of greenhouse gas and continues to increase [2]. The most important greenhouse gas from internal combustion engines is carbon dioxide (CO_2). This shows the need for research towards more fuel-efficient engines leading to lower CO_2 emissions.

Other pollutants from combustion engines are carbon monoxide (CO), hydrocarbons (HC), nitrogen oxide (NO_x) and particulate matter (PM). They are harmful not just to the environment but also to human health. CO emissions are dangerous to humans because they bind to hemoglobin and cause blood poisoning. HC emissions increase incidence of leukemia and lung cancer. PM emissions contain microscopic solids or liquid droplets that can get deep into the lungs and cause serious health problems. NO_x emissions together with HC influence the formation of ground-level ozone, which are also linked to a number of adverse effects on the respiratory system [3].

The pollutant legislations force a reduction of emissions that are emitted from road transportation. Therefore the focus is to develop clean combustion engines that minimize the environmental impact.

1.2 Engine Research and Development

Increasingly strict emissions regulations for internal combustion engines and market forces have been and are the motivation for engine research and development. Since the first emission-control legislation for gasoline engines came into effect in the U.S. in the mid-1960s, the permissible emission levels have been reduced in many steps. Complying with legislation has been the prime focus of research and development since then. However, the focus of engine research is also directed by consumer requirements of vehicle drivability and economy. Therefore, the goal with combustion engine development is to minimize the fuel consumption with legal emission levels while ensuring that the engine performance meet customer requirements.

Compression ignited (CI) engines generally have higher efficiency than spark ignited (SI) engines. However, the most common combustion concept in CI engines, conventional diesel combustion, struggles with high levels of PM and NO_x emissions. A significant portion of the PM consists of combustion generated soot. The soot and NO_x emissions can be individually suppressed but generally there is a tradeoff [4], methods that reduce NO_x emissions lead to increased soot emissions and vice-versa. One reason for this is that conditions leading to a sufficient soot oxidation also lead to high NO_x formation [5]. Creating diesel engines that meet the forthcoming emissions standards requires significant development of the diesel engine system. Decreasing the level of engine-out emissions reduces demand on the aftertreatment system. Furthermore, improving an engine by varying the combustion strategy and using existing components are more cost effective. However, methods of reducing the engine-out emissions must not sacrifice fuel economy as this will increase end user fuel costs and CO_2 emissions levels.

1.3 Advanced Combustion Strategies

In response to the strict legislation on engine-out emissions, especially PM and NO_x, new strategies for diesel combustion have been developed. Many of these strategies can be classified as low temperature combustion (LTC) concepts which strive for a low combustion temperature to reduce NO_x and PM [6]. A few examples of the concept included in this group are homogeneous charge compression ignition (HCCI) [7-12], premixed charge compression ignition (PCCI) [13, 14], reactivity controlled compression ignition (RCCI) [15, 16], and partially premixed combustion (PPC) [17].

1.3.1 Homogeneous Charge Compression Ignition

Homogeneous charge compression ignition is a combustion process that facilitates homogeneous operation in CI engine. In HCCI fuel is injected into the inlet or into the cylinder during an early phase of the compression stroke enabling a homogenous mixture of air and fuel before the auto-ignition occurs. The concept is known for its high thermodynamic efficiency and low emissions [5]. The disadvantages of HCCI engine are:

1. Limited load range.
2. Difficult to control the auto-ignition event.
3. High heat release and pressure rise rates.
4. Emission levels of HC and CO for HCCI engine are higher than SI engine.

1.3.2 Modulated Kinetics combustion

Nissan Modulated Kinetics (MK) combustion was introduced to the market in 1998. In MK combustion the swirl level in the cylinder is increased, the exhaust gas recirculation (EGR) level raised and the single injection timing significantly retarded after top dead center (TDC) [18, 19]. The retarded injection timing with EGR ratio prolongs the ignition delay. This results in somewhat homogenous charge that auto-ignites with volumetric energy release. The first generation of MK was only used during low load conditions. In order to expand the load range, one key was to make the ignition delay longer than the injection duration. To achieve that high injection pressure, reduced compression ratio and cooled EGR are used in the second generation of MK [20].

1.3.3 Uniform Bulky Combustion System

This concept was described by Hasegawa and Yanagihara [21] and was introduced to the market 1997. Toyota's Uniform Bulky Combustion System (UNIBUS) uses early injection of diesel fuel with low temperature and high rates of EGR to extend the ignition delay. Toyota UNIBUS is two-stage injection diesel combustion. The first injection is introduced early during the compression stroke to form premixed mixture and low temperature reaction. The second injection is introduced before TDC to trigger the combustion [22].

1.3.4 Reactivity Controlled Compression Ignition

The concept was developed by Reitz at the University of Wisconsin [15]. The RCCI process uses in-cylinder fuel blending with at least two fuels having very different reactivities. The process involves port injection of a low reactivity fuel, such as gasoline, to create a well-mixed charge of fuel, air and EGR which is ignited with direct injections of a high reactivity fuel, such as diesel. By changing the ratios of the low- and high- reactivity fuels, the combustion event can be better controlled. One issue with RCCI is the need to have and maintain two fuel tanks.

1.3.5 Partially Premixed Combustion

Partially Premixed Combustion PPC is a combustion process that can be applied in CI. In this system the fuel is injected near TDC during the compression stroke, which allows air and fuel to be partially premixed before the mixture auto-ignites. This concept can be considered to be an intermediate between HCCI and conventional diesel combustion. The difference between PPC, HCCI and conventional diesel is the ignition delay which is defined as the time between the start of injection (SOI) to the start of combustion (SOC). The mixing period is the period between end of injection (EOI) and the SOC. The mixing period for PPC should be greater than zero, in other words there should be a separation between EOI and SOC. This separation enables larger degree of premixing at start of combustion [23, 24]. By using high level of cooled EGR the combustion temperature is reduced. Lower temperature during the combustion and expansion events gives lower levels of NO_x emissions and lower heat losses. The EGR also slows down the kinetic reactions and gives longer ignition delay. If the EGR rate reaches as high as 60% the soot formation is prevented [25]. Unfortunately, high EGR levels reduce the oxidation of soot, HC and CO due to lower oxygen content in the mixture [26].

Fuels that have lower cetane number (CN) (and thus higher octane number (ON)) can be used instead of the conventional diesel fuel during the PPC operating mode. Using moderate cetane fuels allow an extended delay with more time for mixing prior to ignition. Therefore, the EGR level must be adjusted according to the octane numbers: lower EGR for a high octane number. Using a balanced combination of fuel reactivity and EGR during PPC can lead to low levels of soot, NO_x, HC and CO emissions simultaneously.

1.4 Objective

This work aims to answer questions regarding partially premixed combustion. The focus is on the coupling between fuel properties and combustion characteristics, mainly heat release and engine-out emissions. Compared to traditional diesel combustion PPC relies on a prolonged ignition delay to get enough mixing between fuel and air before the combustion event. Thus, understanding the effect of the fuel in the early stages, i.e. mixing period, ignition delay and low temperature reaction phase (LTR) is critical to understand fuel effects on PPC.

Given the large operating range for a modern combustion engine, it is not obvious that a fuel suited for one operating condition would be a proper fuel for PPC in general. Thus, in this work an effort is made to sort out interactions between fuel characteristics and engine settings such as engine load, combustion phasing, intake composition, injection pressure and boost level. The final goal is to find a group of fuels more suitable for PPC which give low pollutant levels, high efficiency and good controllability.

1.5 Method

The approach adopted in this work is to use in-cylinder pressure analysis, heat release calculations and exhaust gas analysis. Different fuels are used in this work, such as well-defined gasoline fuels and surrogate fuels. Examples of surrogate fuels used are: blends of n-heptane, isooctane, toluene and ethanol.

1.6 Contributions

This thesis contributes to the understanding of Partially Premixed Combustion in the following areas:

- Effect of RON on ignition delay.
- The operating range for different fuels in relation to inlet boost.
- Fuel composition effects on combustion events, such as: Ignition delay, low temperature reactions and combustion duration.
- Fuel composition effect on emissions.
- The limits in combustion phasing with high and low octane fuels.
- The effect of fuel composition on low temperature reactions for PPC and HCCI combustion.
- Predicting RON and MON for surrogate fuel blends.

- Engine operating parameters, for example, inlet O_2-level, CA50 and injection pressure influence the links between fuel properties and combustion characteristics.

Chapter 2

Fuels and low temperature combustion

This chapter gives an overview of different types of fuels and their specifications. The most common fuels used in internal combustion engines are diesel, gasoline, natural gas and ethanol. In internal combustion engine research studies of a great variety of single component fuels are used neat and in mixtures.

2.1 Gasoline fuels

Gasoline is a petroleum product and consists of hundreds of different hydrocarbons with a variety of the chain lengths [27]. These chains have different characteristics and properties. The lighter components in gasoline are highly volatile and evaporate quickly at ambient conditions. Depending on the region, the aromatic compounds content in gasoline varies between 22% to 42% and also smaller amounts of alkane cyclic are present. The quality of a fuel is measured by octane number. High octane number is equal to higher resistance to auto-ignition in internal combustion engines [3, 4]. There are two types of octane number: Research octane number (RON) and motor octane number (MON) which are explained in the following sub-sections.

2.1.1 Research octane number

Research octane number is a measure of antiknock quality of a gasoline as determined by the American Society for Testing and Materials (ASTM) D 2699 standard [3]. RON is determined in a single cylinder variable compression engine called Cooperative Fuel Research (CFR). The engine operates with an inlet air temperature of 52^{o}C and atmospheric pressure at an engine speed of 600 rpm. Spark advance is fixed at 13 degree before top dead center (BTDC) with the fuel/air ratio adjusted for maximum knock. The compression ratio is adjusted to get a knock of maximum intensity. The level of knock obtained with the test fuel is determined between the range of two blends of the reference fuels, which have two octane numbers (one knocking more and one less than the tested fuel). The octane number for the tested fuel is obtained by interpolation between the knock meter scale

reading for the two reference fuels and their octane numbers. For fuels below 100 octane numbers, the primary reference fuels are blends of isooctane and n-heptane, where the octane number in the blend is the volume percent of isooctane. The antiknock quality of the fuel is obtained, for fuels above 100 octane number, by a polynomial with isooctane and milliliters per U.S Gallon of the antiknock additive tetraethyl lead [4].

ISO 5164 is the European standards (EN) method to measure RON which is developed by the International Organization for Standardization. This method is essentially the same as the ASTM method [28].

2.1.2 Motor octane number

Motor octane number is a measure of the antiknock quality of a fuel as determined by the ASTM D 2700 standard [3]. The MON method uses the same standard test engine as RON but with different operating conditions. The engine is run at 900 rpm with a 149 ^{o}C inlet mixture temperature and at atmospheric inlet pressure. The spark advanced varies with compression ratio between 19 to 26 degrees BTDC. The fuel/air ratio is adjusted for the maximum knock. Using more sever operating condition for MON, the motor octane number is usually lower than the research octane number.

ISO 5163 is the European standards method to measure MON which is developed by the International Organization for Standardization. This method is the same as the ASTM method [28].

2.2 Diesel fuels

Diesel is a petroleum-based fuel and is produced by distillation in oil refineries. Diesel is composed of a blend of different type of hydrocarbons including paraffin, naphthenes, olefins and aromatics. Diesel consists mainly of hydrocarbons in various combinations of chain length. Diesel has 18% higher density than gasoline fuel because of the higher C/H ratio. The ignition quality of diesel fuel is measured by its cetane number [3].

2.2.1 Cetane number

Cetane number is a measure of the ignition quality of a diesel fuel based on ignition delay in a CFR engine. A higher cetane number gives shorter ignition delay [3]. The standard for this test is ASTM D 613. The engine is run at 900 rpm with an intake

temperature of 65.6 ^{o}C. The injection timing is fixed at 13 degrees BTDC with injection pressure 10.3 MPa. The compression ratio is varied until combustion starts at TDC, giving an ignition delay of 13 degrees. The procedure is then repeated for two reference fuel blends, one with higher and one with lower cetane number [4]. The difference should be less than five cetane numbers between the reference fuels. The cetane number for the tested fuel is then obtained by interpolation between the compression ratios required for the two reference blends. The blends consists of two pure hydrocarbon fuels N-Hexadecane and heptamethylnonane. N-Hexadecane ($C_{16}H_{34}$) with cetane number 100 is a hydrocarbon with high ignition quality which represents the top of the cetane scale. The bottom of the scale is represented by heptamethylnonane, which has a lower ignition quality and a cetane number of 15. In the original procedure α-methylnapthalene ($C_{11}H_{10}$) represented the bottom of the scale with a cetane number of zero but it was replaced by the more stable heptamethylnonane [3, 4] .

2.3 Fuel components

Diesel and gasoline fuels are blends of many different hydrocarbon compounds and are not always well defined. Therefore simplified surrogate fuels are frequently used for modeling and experimental work. Surrogate fuels are mixtures of one or more of hydrocarbon compounds that are designed to emulate either the chemical or physical properties of a more complex fuel such as diesel or gasoline. Individual hydrocarbon compound vary extremely in their ability to auto-ignite depending on their molecular structure and size. The different types of molecular structure of hydrocarbon compounds can be classified according to their knocking tendency as follows:

2.3.1 Alkanes (Paraffins)

Hydrocarbons which contain only single carbon-carbon (C-C) bonds are called alkanes. They are open-chain and called saturated because there is a hydrogen atom in every possible location. For larger molecules there are two types of chains; straight-chain which is called normal (n-) and branched-chain which is called (iso) compounds. This gives them a general formulaC_nH_{2n+2}. Examples: methane (CH_4), ethane (C_2H_6), n-heptane (C_7H_{16}) and isooctane (C_8H_{18}). N-heptane is a long straight-chain while isooctane is a branched-chain. Increasing the length of the carbon chain decreases the resistance to auto-ignition whereas shortening the length of the basic chain (by joining side chains to build a branched chain), and

adding methyl group at the second end of the basic carbon chain will decrease the tendency for knocking [3, 4], as shown in Figure 2-1.

2.3.2 Cycloalkanes (Napthenes)

Hydrocarbons which have single (C-C) bonds in their structure forming ring are called cycloalkanes. They are unsaturated hydrocarbons since the ring can be broken and additional hydrogen can be added. This gives them a general formula C_nH_{2n}. Examples: cyclopropane (C_3H_6) and cyclobutane (C_4H_8). Napthenes have stronger knocking tendency than aromatics having the same number of carbon atoms in the ring [3, 4], as shown in Figure 2-1.

2.3.3 Alkenes (Olefins)

Hydrocarbons which consist of one double bond are called alkenes. They are open-chain and called unsaturated because there is at least one carbon to carbon double bond. There are two types of chains, straight-chain and branched-chain. This gives them a general formula C_nH_{2n}. Alkenes have higher resistance to auto-ignition than alkanes. Examples: ethene (C_2H_4), propene (C_3H_6) and butene (C_4H_8). Generally, increasing number of bonds from one to two or three will result in a reduced knocking tendency [3, 4], as shown in Figure 2-1.

2.3.4 Aromatics

Aromatics are hydrocarbon with alternating single and double bonds between carbon atoms forming rings. Aromatics are based on benzene rings. The simplest is benzene C_6H_6. The ring structure is very stable and accommodates additional $–CH_2$ groups in side chains and not by ring expansion. Examples: toluene (C_7H_8) and xylene (C_8H_{10}). Increasing number of bond to two and three double bonds decreases the knocking tendency [3, 4], as shown in Figure 2-1.

2.3.5 Alcohols

Alcohols are compounds in which one or more hydrogen atom(s) are replaced by an –OH group in an alkane. The general formula for alcohol is $C_nH_{2n+1}OH$. Thus methane becomes methanol (CH_3OH) and ethane becomes ethanol (C_2H_5OH). Alcohols are saturated compounds and have higher boiling points and higher octane number than alkanes [3, 4].

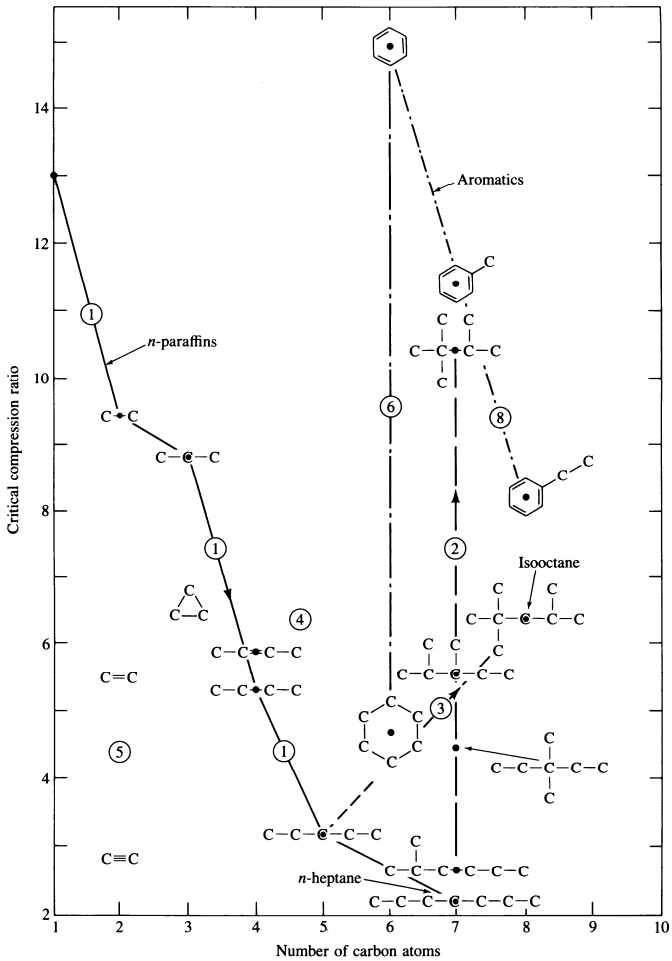

Figure 2-1 critical compression ratio as a function of carbon atoms in hydrocarbon molecule [4].

2.4 Surrogate fuels

As mentioned in the previous section, the surrogate fuels are used in modeling and experimental works. A surrogate fuel is defined as a fuel that consist of a number of pure compounds and which their performance match the conventional fuel in terms of combustion and emissions characteristics [29]. The benefit with surrogate fuels is that they, despite their simpler composition, can be designed to have similar properties such as; volatility, lower heating value, RON value and density as gasoline fuels. The chemical reaction mechanisms applicable to auto-ignition in IC engines

have only been developed for a few pure compounds. Thus, the chemical kinetic schemes have been developed for mixtures of iso-octane and n-heptane, known as Primary Reference Fuels (PRF). The gasoline fuels can be mimicked if aromatic compounds (aromatics are often represented by toluene) are added to PRF, since there are aromatics in conventional gasoline. This mixture of PRF and toluene is called Toluene Reference Fuels (TRF). Authors in [30] suggested that oxygenated surrogate fuels can represent the performance of oxygenated gasolines in commercial engines. These oxygenated surrogate fuels consisted of four compounds: n-heptane, isooctane, toluene and ethanol. These four compounds are used in this thesis and called Toluene Ethanol Reference Fuels (TERF). Beside these four compounds, also TRF and Ethanol Reference Fuels (ERF) are used in this thesis.

2.5 The effect of fuel properties on LTC

Recently, different LTC concepts have been used to reduce engine-out emissions and achieve higher efficiency. Researchers have published articles which analyze the effect of different fuel properties on engine performance and emissions. However, the effects measured may not be universal effects, but effects of a specific engine operating conditions and combustion mode.

2.5.1 The effect of fuel properties on HCCI

It is known that RON and MON play major roles in spark ignition combustion. However, several researchers have studied fuel properties effect on HCCI combustion and concluded that RON and MON are insufficient to explain the fuel behavior in HCCI. Therefore, new methods were developed by several researchers called Octane index (OI) [31-33], Shibata-Urushihara index [34, 35] and HCCI number [36]. This method depends on the temperature and pressure evolution in the unburnt gas.

One of the challenging features of HCCI combustion is to control the combustion. The difficulty lies in controlling the auto-ignition phenomena. This is due to variation in temperature and fuel composition. Each single hydrocarbon has its specific auto-ignition temperature. Therefore, the combustion with diesel or gasoline fuel in an HCCI engine is difficult to explain and predict. However, there are some means to control the combustion such as the inlet temperature, variable compression ratio or use dual fuel where the two fuels have very different auto-ignition temperature.

A well-known phenomena in HCCI is the low temperature reaction, which exhibits a characteristics bump in the rate of heat release before the main combustion. LTR depends both on fuel composition and gas temperature in the cylinder. A fuel chemical composition containing a significant amount of n-paraffin such as n-heptane, will contribute toward a large low temperature reaction heating value [37, 38]. Tanaka indicates that in HCCI [39] the oxidation mechanism of hydrocarbon is initiated by abstraction of an H• atom from a fuel molecule (RH) by O_2 to form an alkyl radical, R•, and HO_2•. At low temperatures, the LTR addition of R• + O_2 to form RO_2• then initiates a highly exothermic cycle that produces H_2O and an alkylperoxide. This continues until the temperature rises to a value where competing reactions starts to produce H_2O_2 and olefins. This intermediate stage occurs between low temperature heat release and high temperature heat release and is referred to as intermediate temperature heat release (ITHR) [40]. The temperature gradually increases until H_2O_2 decomposes leading to a branched thermal explosion. LTR is present with most diesel fuels, but using a fuel with an octane number of 100 or higher no detectable LTR appears before the main combustion. When n-heptane is added to the blend the LTR appears before the main combustion. Christensen et al. [41] noted that LTR appears for HCCI type operation with gasoline-like fuels that exhibits an octane number lower than 83, while Bunting et al. [42] noted that diesel-like fuels or a cetane number higher than 33 exhibits LTR.

LTR is strongly related to the structure of hydrocarbon, Shibata et al. concluded in [37]. They also mentioned that aromatics, olefins and some naphthenes have a mechanism that reduces the LTR. In [35] Shibata et al. noted that a small change in chemical composition can change the HCCI combustion characteristics, such as the amount and phasing of LTR. Ethanol and toluene have quenching effects on LTR and the strongest was for ethanol [43].

2.5.2 The effect of fuel properties on PPC

Manufacturing CI that can meet the future emissions legislation requires significant development of the combustion system. Several new combustion strategies for compression ignition have been developed. Many researchers have developed, such as premixed charge compression ignition [44], premixed compression ignition (PCI) [45], partially premixed compression ignition (PPCI) [46], and others. They all share general features and have similar objectives.

The main advantage of these combustion strategies is the low levels of engine-out soot and NO_x. The common method for this is to use high levels of cooled EGR which

increases the heat capacity resulting in a reduced combustion temperature to avoid zones with high production of soot and NO_x. The EGR also slows down the kinetic reactions which results in a greater amount of fuel and air being premixed before ignition. However, there are significant drawbacks of using high levels of EGR since it will elevate levels of CO and HC emissions. The use of high EGR rates also suppresses soot oxidation late in the cycle [47]. At low loads, high EGR ratio may lead to incomplete combustion. In order to achieve a long ignition delay and a sufficient time for fuel and air to be mixed before ignition without using high levels of EGR, different fuel properties can be utilized.

The impact of the fuel properties on combustion relates to their impact on the mixing process and ignition delay. Generally, a fuel with high cetane number exhibits a shorter ignition delay, resulting in a smaller premixed burn period of combustion. On the contrary, fuels with high octane number have longer ignition delay [48, 49]. A longer ignition delay gives the fuel and air more time to mix before the time of ignition, which results in a larger fraction of premixed combustion. However, too long ignition delay may result in over-lean mixture and wetting on combustion chamber wall which might lead to misfire, which causes high levels of HC. Studies by Kalghatgi and Kitano showed that with injection timings near TDC, for any given set of operating conditions, gasoline has a much larger ignition delay than diesel fuel, which enables higher engine loads with low levels of smoke with no disadvantage to NO_x, CO, HC and fuel consumption [49-51].

The engine-out emissions of CO and HC are connected to the interaction between the injection process and fuel properties. In [52] it was reported that a higher cetane number decrease HC and CO emissions levels using a single injection strategy. It has also been demonstrated that engine-out NO_x emissions can be reduced by decreasing the aromatic content of a fuel [53]. This is because decreasing aromatic content reduces the flame temperature.

Lee et al. investigated the effects of fuel distillation characteristics and cetane number on PCCI combustion [54]. Their research indicated that decreasing fuel cetane number reduce NO_x emissions by suppression of the combustion temperature. Moreover, their study indicates that lighter and more volatile fuels improve mixture formation. The improved mixture formation result in a large fraction of overly lean mixtures leading to increased emissions of HC. There have been more studies investigating the effect of fuel properties on LTC concepts. Studies by Wary et al., and Manente et al. showed that fuel properties had an influence on emission and performance in PCI and PPC combustion modes [55, 56]. Fuels with high octane number (low cetane number) had lower NO_x and smoke

emission in low temperature combustion due to longer ignition delay, but they produced higher level of HC and CO emissions.

Furthermore, there are few studies that investigated the operable load range as a function of octane number. Manente et al. showed that it is possible to operate in a large operating range with high octane fuels since their longer ignition delay allows for additional premixing as load and engine speed increased [57]. However, it was not possible to run at low load with high octane number due to misfire. Gasoline PPC typically have problem with combustion stability and combustion efficiency at low load. Borgqvist et al. [58] addressed this problem with means of negative valve overlap (NVO) and managed to extend the low load limit of a single cylinder light duty engine at 800 rpm engine speed down to 1 bar $IMEP_g$.

Another important aspect for PPC is the auto-ignition properties of the fuel. Kaiadi et al. [59] investigated ethanol effect on PPC using sensitivity analysis to understand how the required parameters for ethanol PPC such as lambda, EGR rate, injection pressure and inlet temperature influence the combustion in terms of controllability, stability, emissions and thermodynamic efficiency. Another study showed that the smoke emissions were significantly reduced for ethanol in comparison to gasoline and diesel fuel, while operating near stoichiometric conditions [60].

Chapter 3

Methods and definitions

This chapter presents the methods employed for experimental design and post processing to obtain characteristics of the combustion process.

3.1 Heat release analysis

Heat release analysis gives quantitative information on the progress of the combustion in the cylinder. A brief explanation of the heat release theory is presented in this chapter based on [4, 61]. For heat release analysis, the cylinder is considered to be a thermodynamically closed system. According to the first law of thermodynamics the energy balance of such a system can be expressed as

$$\frac{dQ}{dt} = \frac{dU}{dt} + \frac{dW}{dt} \tag{3.1}$$

where dQ/dt is the rate of heat transfer to the system, dU/dt is the rate of change of internal energy of the system, and dW/dt is the rate of work transfer from the system. The internal energy, U, can be expressed as

$$U = mC_vT \tag{3.2}$$

where m is the mass in the system, C_v is the specific heat at constant volume and T is the temperature. If the mass in the system is constant the derivative of U is

$$\frac{dU}{dt} = mC_v\frac{dT}{dt} \tag{3.3}$$

From the ideal gas law

$$pV = mRT \tag{3.4}$$

where V is the volume and R is the specific gas constant and with m and R assumed constant, it follows that

$$\frac{dT}{T} = \frac{dV}{V} + \frac{dp}{p} \tag{3.5}$$

Using Eq. 3.4 and 3.5, Eq. 3.3 can be rewritten in the form

$$\frac{dU}{dt} = \frac{C_v}{R}\left(p\frac{dV}{dt} + V\frac{dp}{dt}\right) \tag{3.6}$$

The work performed by the system can be expressed as

$$\frac{dW}{dt} = p\frac{dV}{dt} \tag{3.7}$$

Neglecting mass exchange and using Eq. 3.6 and 3.7, Eq. 3.1 can be rewritten as

$$\frac{dQ}{dt} = \frac{C_v}{R}\left(p\frac{dV}{dt} + V\frac{dp}{dt}\right) + p\frac{dV}{dt} \tag{3.8}$$

The specific gas constant can be expressed as

$$R = C_p - C_v \tag{3.9}$$

where C_p is the specific heat ratio at constant pressure. Eq. 3.9 and the ratio

$$\gamma = \frac{C_p}{C_v} \tag{3.10}$$

Equation (3.10) can be used to simplify Eq. 3.8 into

$$\frac{dQ}{dt} = \frac{\gamma}{\gamma-1}p\frac{dV}{dt} + \frac{1}{\gamma-1}V\frac{dp}{dt} \tag{3.11}$$

It is of interest to study the heat release rate as a function of crank angle degree (CAD), θ, hence Eq. 3.11 can be rewritten as:

$$\frac{dQ}{d\theta} = \frac{\gamma}{\gamma-1}p\frac{dV}{d\theta} + \frac{1}{\gamma-1}V\frac{dp}{d\theta} \tag{3.12}$$

The heat release rate estimated using Eq. 3.12 is often termed as 'Apparent' heat release rate. However, in reality, there is more energy exchange like the heat losses to the combustion chamber wall and mass losses to the crank-case (blow-by) and to crevices in the combustion chamber. For the experiments presented in this thesis the heat transfer to cylinder walls has been estimated using the model proposed by

Woschni [4]. The effects of mass losses are often small and thus has been neglected. The Eq. 3.12 can now be re-written as:

$$\frac{dQ}{d\theta} = \frac{\gamma}{\gamma-1} p \frac{dV}{d\theta} + \frac{1}{\gamma-1} V \frac{dp}{d\theta} + \frac{dQ_{losses}}{d\theta} \tag{3.13}$$

Where $dQ_{losses}/d\theta$ consists of mass and heat losses. The convective heat transfer, dQ_{HT}/dt, to the cylinder wall

$$\frac{dQ_{HT}}{dt} = h \cdot A_{wall}\left(T_{gas} - T_{wall}\right) \tag{3.14}$$

depends on the heat transfer coefficient, h, the wall area, A_{wall}, and the difference between the mean gas-temperature and the mean wall temperature [3]. Woschni's correlation for the heat transfer coefficient can be expressed as

$$h = 3.26 \cdot B^{-0.2} \cdot p^{0.8} \cdot T^{-0.55} \cdot w^{0.8} \tag{3.15}$$

where B is the cylinder bore in meter, p is the cylinder pressure in kilo Pascal. The average cylinder gas velocity w, can be expressed as

$$w = C_1 S_p + C_2 \left(\frac{V_d \cdot T_{ivc}}{p_{ivc} \cdot V_{ivc}}\right)(p_c - p_m) \tag{3.16}$$

Where C_1 and C_2 are parameters to adjust the heat transfer to a specific engine, S_p is the mean piston speed, V_d is the displacement volume, V_{ivo}, p_{ivc} and T_{ivc} are the volume, pressure and temperature at inlet valve closing (IVC), p_c is the instantaneous cylinder pressure, p_m the motored cylinder pressure at the same crank angle as p_c [4].

The specific heat ratio, γ, in this thesis is estimated for a given temperature and gas composition at the inlet conditions [4, 62]. During the engine cycle γ will changes due to the change in combustion temperature.

3.1.1 Heat release characteristics

From the calculated rate of heat release Eq. 3.13, information about the combustion events can be extracted. The conventional diesel combustion process usually is divided into three main phases: ignition delay, premixed combustion, and mixing–controlled combustion. The mixing controlled combustion can be divided into two sub phases, spray driven and late combustion, see Figure 3-1. The spray driven phase is also referred to as the quasi steady lifted flame phase.

The HCCI combustion process is very different from conventional diesel combustion and typically (but not always) it can be divided into three phases: low temperature reaction, intermediate temperature heat release, and premixed combustion phase, see Figure 3-2. Also conventional diesel combustion may have low temperature reactions but this phase is more pronounced for HCCI.

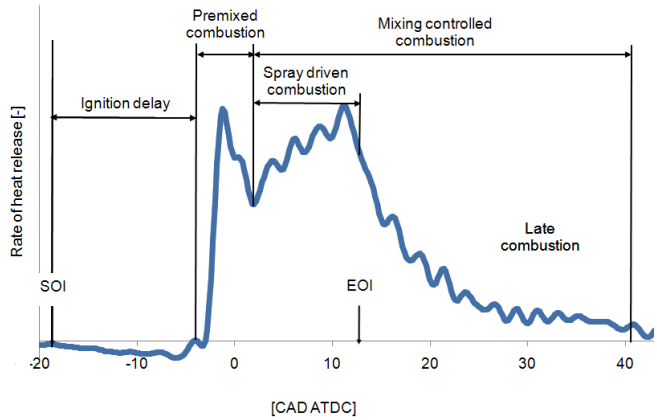

Figure 3-1 Typical diesel heat release rate diagram identifying different combustion phases [63].

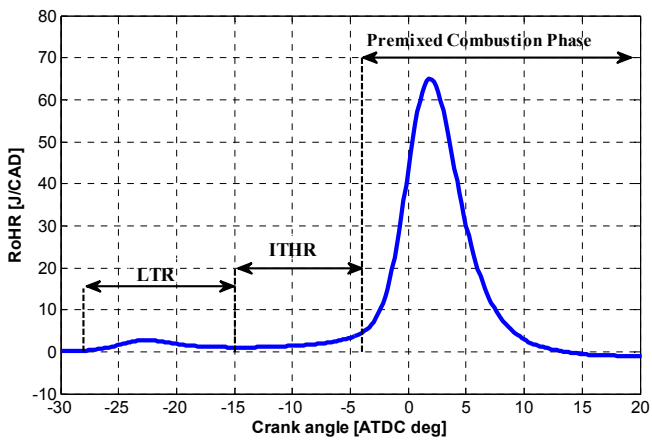

Figure 3-2 Typical HCCI heat release rate diagram identifying different combustion phases.

The Partially Premixed Combustion is something in-between HCCI and conventional diesel combustion. In the analysis, the combustion is divided into four phases: the

ignition delay (ID), low temperature reactions, premixed combustion and late mixing controlled combustion phase, see Figure 3-3.

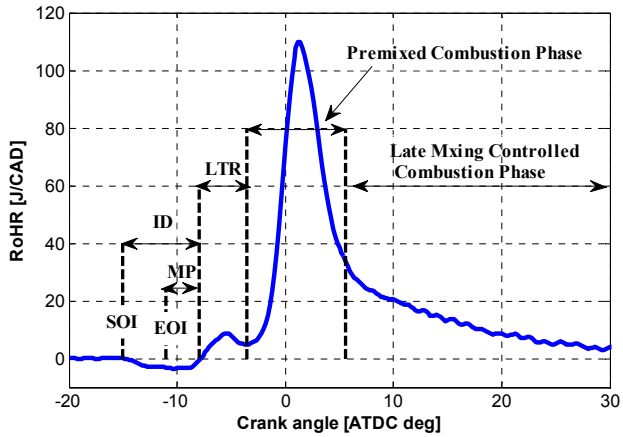

Figure 3-3 Typical PPC heat release rate diagram identifying different PPC phases.

Ignition delay phase is the period between the start of fuel injection and start of combustion, as shown in Figure 3-3. For the experiments presented in this thesis, start of injection is determined from the gradient of injection pressure. The SOI is the point where the gradient reaches its maximum value due to needle opening, as shown in Figure 3-4. The SOC is the point where the rate of heat release becomes positive after the start of injection, which is 0% heat release completion (CA0). In this phase most of the fuel injected into the combustion chamber is heated and evaporated before the ignition occurs. This phase is important in PPC mode because it influence the premixed combustion. With longer ignition delay the air and fuel are more premixed before the ignition occurs.

Low temperature reactions phase is a combustion phase with low reaction temperature, where several reactions occur simultaneously and lead to the main combustion. The LTR is characterised by a small peak before the main premixed heat release. There is a clear negative temperature coefficient region between the LTR and the high temperature reaction phase. The LTR typically occurs between 700 K and 900 K. In this thesis the LTR duration and fraction definitions are used in the analysis.

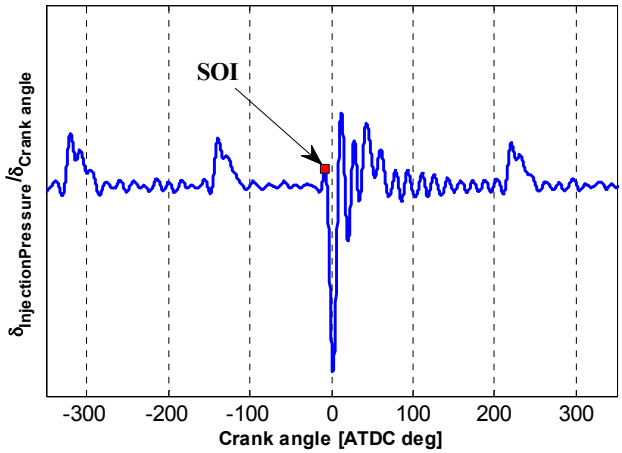

Figure 3-4 Gradient of injection pressure as a function of crank angle degree. Start of injection in red square marker.

The LTR duration is defined as the time between the SOC and the end of LTR. Two different methods for defining end of LTR were used in this thesis; the first method defined the end of LTR as the point where the gradient of rate of heat release reaches 0.05 J/CAD^2. This threshold was selected as the lowest value that gave a robust definition. The second method was developed to also handle case when the low temperature reactions are less separated from the premixed combustion, where the first method was insufficient. In order to separate the phases (LTR phase and premixed combustion phase) in a well-defined manner, a Gaussian profile is fitted to the raising flank of the premixed peak, between a threshold of 15 J/CAD and the actual peak. The rate of heat release is then subtracted from the Gaussian profile, and the integrated area between the start of combustion and the threshold point is used as a measure of the LTR fraction as shown in Figure 3-5.

For HCCI a third definition of LTR fraction was used. A Gaussian profile was fitted to the rising flank of the LTR peak, between a threshold of 0.15 J/CAD and the actual peak of the LTR as seen in Figure 3-6. This method work well for HCCI since the LTR phase is clearly distinguished from the main heat release. The integrated area of the Gaussian profile is used as a measure of the low temperature reactions.

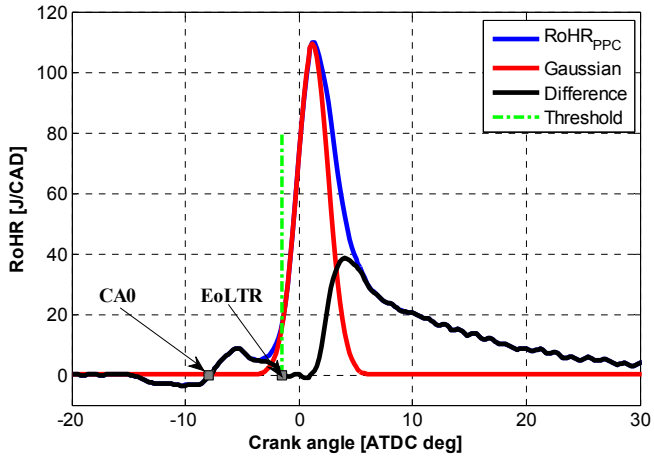

Figure 3-5 Gaussian profile (red), RoHR (blue), difference (black) and threshold (green dashed line) as a function of crank angle degree. Shows the LTR phase.

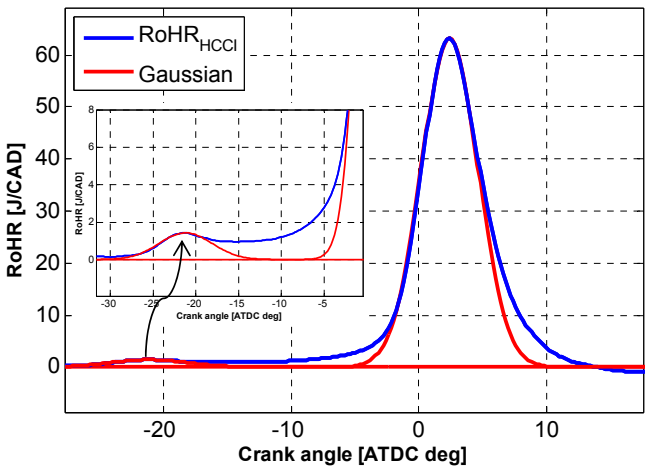

Figure 3-6 Gaussian profiles fits (red) to HCCI RoHR (blue). Two Gaussian profile are used the first one is fitted to the rate of heat release and the second one is fitted to the low temperature reaction phase as seen in the zoomed figure.

Premixed combustion phase is characterised by a rapid combustion that occurs after the LTR phase. This phase is controlled by chemical kinetics and the reaction speed depends mainly on the temperature. In the heat release analysis in this thesis, the premixed- and late- heat release rates are normally not distinctly separated. This is because part of the premixed combustion phase is limited by mixing, and part of the

late combustion phase depends on slow reactions rather than mixing. In order to separate the phases in a well-defined manner, a Gaussian profile

$$G(x) = h \cdot e^{-\left(\frac{x-x_0}{2\alpha^2}\right)^2} \tag{3.17}$$

is fitted to the rising flank of the premixed peak, between the end of LTR and the actual peak, and the integrated area of the profile is used as a measure of the premixed reactions. In Eq. 3.17 x_0 is the central position of the peak, h and α representing the height and width of the Gaussian profile. Figure 3-7 shows the rate of heat release as a function of crank angle together with the Gaussian profile. As is evident, the fit follows the premixed heat release closely. The Gaussian profile is a mathematical rather than a physical representation of the premixed reaction phase. However, it provides a robust measure of the premixed reactions for all operated cases.

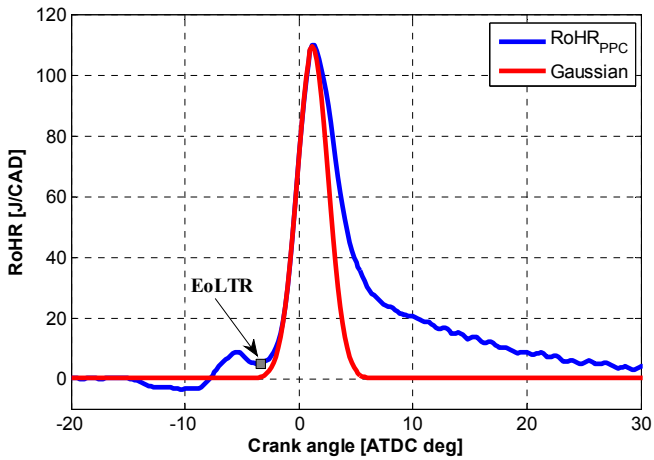

Figure 3-7 Gaussian profile (red) and RoHR (blue) as a function of crank angle degree. Gaussian profile is a fit for the premixed combustion.

Late mixing controlled combustion phase in which its burning rate is primarily controlled by the fuel vapor-air mixing process. The heat release continues at lower rate into the expansion stroke. The low rate of heat release at this phase is because a small fraction of the fuel may not yet combust and/or a fraction of the fuel energy is present in form of soot and fuel-rich combustion products. The chemical reaction processes become slower at this phase due to the reduced in-cylinder temperature during the expansion.

3.1.2 Combustion duration and phasing

The rate of heat release can be integrated over crank angles (time) to obtain the accumulated heat release from which two important parameters are defined, namely, combustion phasing and combustion duration as shown in Figure 3-8. Combustion phasing is defined as the crank angle degree where 50% of the total heat is released (CA50). Combustion duration is defined as the time between 10 and 90% of total heat release (CA90-CA10). The combustion duration is used as an indication of the type of combustion, a shorter combustion duration indicates a large fraction of rapid premixed combustion, while a long combustion duration indicates a more slow diffusion controlled combustion.

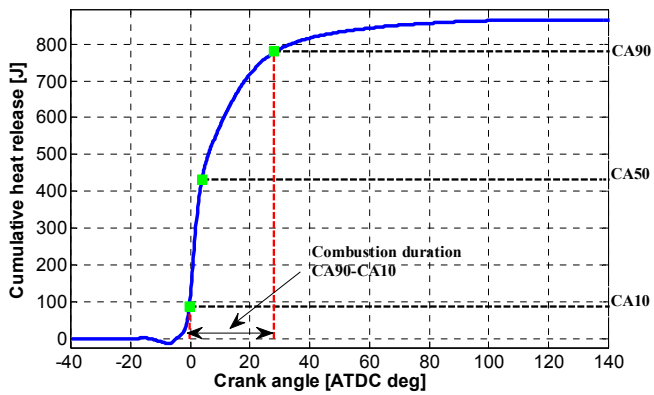

Figure 3-8 Cumulative heat release with combustion timings when 10%, 50% and 90% of the total heat is released.

3.2 Design of experiments

Experimental methods are widely used in research and development both in academia and industry. Several goals can be met with a design of experiments (DOE) methodology; one goal is to show the statistical significance of an effect that a particular factor applies on the dependent variable of interest. The other goal is to extract the maximum amount of unbiased information regarding the factors affecting the process.

In this work, A central composite two-level full-factorial design is used in which axes are drawn through the centre of the cube and the axial points are located on the face of the cube [64], as shown in Figure 3-9. The number of experiments can be described as $2^{k-p} + 2k + cp$, where k is the number of studied variables, p is the

fractionalization element (p = 0, full design), and cp is the number of centre points. The centre point was replicated three times, meaning that test matrix consisted of 17 blends where 3 of them have the same composition, i.e., $2^3 + (2 \times 3) + 3$.

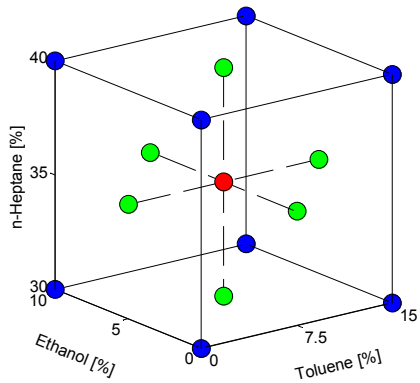

Figure 3-9 Graphical representation of the experimental factors and their levels.

The basic design was based on three fuels: n-heptane, toluene and ethanol but a fourth fuel, isooctane, was used as a filler. The isooctane was chosen to model gasoline fuel over a wide ignition-quality range. The isooctane content of the blends was calculated according to Eq. 3.18

$$\mathrm{Isooctane}_{C_I} = 100 - \left(\mathrm{nheptane}_{C_N} + \mathrm{toluene}_{C_T} + \mathrm{ethanol}_{C_E}\right) \tag{3.18}$$

The quadratic regression model was used to predict the variable in interest and correlate to the data gained from the measurement using Eq. 3.19.

$$\mathrm{Variable}_{\mathrm{Predicted}} = \beta + \alpha_N \cdot X_N + \alpha_T \cdot X_T + \alpha_E \cdot X_E + \gamma_{NT} \cdot X_N \cdot X_T + \gamma_{NE} \cdot X_N \cdot X_E + \gamma_{TE} \cdot X_T \cdot X_E + \delta_{N^2} \cdot X_N^2 + \delta_{T^2} \cdot X_T^2 + \delta_{E^2} \cdot X_E^2 \tag{3.19}$$

where β is a constant and α, γ and δ are coefficients for linear, interaction, and quadratic terms, respectively, and are generated from the regression model. X_N, X_T, and X_E are fuel concentration in volume fraction for n-heptane, toluene, and ethanol, respectively.

Chapter 4

Experimental details

This chapter presents an overview of the experimental apparatus and methods used for the research covered in the thesis.

4.1 Measurement equipment

4.1.1 Engine setup

The experimental engine is a Volvo D5 five cylinder passenger car diesel engine operated on a single cylinder. The engine and injector specifications are listed in Table 4-1. The engine test rig was equipped with an adjustable EGR system and two adjustable heating systems, one for varying the inlet air temperature and the other one for controlling the engine cooling water temperature. For HCCI experiments a CFR engine was used the engine specification are listed in Table 4-1.

Table 4-1 Engine and injection system specifications.

Engine specifications		
Engine type	Volvo D5	CFR
Number of cylinders	1	1
Bore [mm]	81	83
Stroke [mm]	93.2	114
Displacement Volume [cm^2/cylinder]	480	
IVC [CAD BTDC]	174	146±2.5
Compression ratio	16.5	Variable(4:1 to 18:1)
Swirl ratio	2.2	
Number of intake valves	2	1
Number of exhaust valves	2	1
Injector		
Type	Solenoid	Port injection
Injection nozzle holes	7	
Injection nozzle diameter [mm]	0.14	
Included angle [degrees]	140	

4.1.2 Data acquisition

There are several parameters that are measured from the engine. Some of them are recorded with high temporal resolution and others with low temporal resolution. The crank shaft position is determined by an encoder with a resolution of 0.2 CAD. The cylinder head is equipped with piezo-electric pressure sensor to monitor cylinder pressure which is used for heat release analysis and in-cylinder temperature calculations. High temporal data is also giving feedback to the rail pressure PID controller.

There are many engine parameters recorded with low temporal resolution. Examples: inlet /exhaust manifold pressure measured with pressure sensor of type Keller. All temperatures were measured by Pentronic Type K thermocouples.

4.1.3 Engine hardware

Injection system

The injection system consists of a common rail, a high-pressure pipe, high- and low-pressure pumps and a solenoid injector, see Table 4-1 for injector specifications.

Air and Fuel mass flows

The intake air mass flow is measured by a thermal mass flow meter (Bronckhorst IN-FLOW). It is installed approximately 3 m upstream from the intake manifold in order to prevent pressure oscillations from the engine or EGR system to propagate into the flow meter. Fuel mass flow is measured as the mean value of the mass gradient by a fuel balance (Sartorius CPA 62025).

Emission analyzer

Smoke emissions are measured with the AVL415S smoke meter, while NO_x, HC, exhaust CO_2, CO emissions and intake CO_2 are measured with a Horiba measurement system (MEXA9200DF). NO_x emissions are measured with a chemiluminescence analyser whereas HC is measured with a hydrogen flame ionization detector (FID).

The piping to the analyser is heated to approximately 191^{o}C to avoid condensation of unburned fuel components. Both inlet and exhaust Oxygen (O_2) are measured by a magneto-pneumatic condenser microphone method (MPA), whereas CO, intake and exhaust CO_2 are measured with an infrared analyser.

The exhaust gas recirculation, EGR_{ratio}, is defined as the ratio of CO_2 concentrations in the inlet manifold to the CO_2 concentrations in the exhaust gases from the engine.

$$EGR_{ratio} = \frac{CO_{2Inlet}}{CO_{2Exhaust}} \quad (4.1)$$

The circulated exhaust gases are cooled in a heat exchanger, using the engine's coolant water as a heat absorber, before it is mixed with the inlet air. The mixture temperature is controlled by heating the fresh charge before it is blended with the EGR.

4.2 Fuels

Four groups of fuels have been used in this thesis. The first group of fuels was used to study the fuel effect on operating load range for PPC. Four fuels of well-defined gasoline are compared to diesel fuel MK1 in Papers I and II. These gasoline fuels (A, B, C and D) were provided by Chevron and blended from refinery in the gasoline boiling range. Fuel specifications are presented in Table 4-2.

In Table 4-2 x, y and z are normalized value of the gasoline fuel components. In order to ensure that no damage was caused to the injection system, lubricity additive *Infineum R655* was added to each gasoline fuel and other fuel blends. The impact of the additive on combustion phasing and emission formation is expected to be negligible at such small fraction of 100 ppm.

Table 4-2 Fuel specifications.

Fuel	RON	MON	C	H/C	O/C	LHV[MJ/kg]	A/F_s	N-paraffin	Iso-paraffin	Olefins
A	69.4	66.1	7.11	1.98	0	43.80	14.7	6.89x	1.08y	2.94z
B	78.2	73.4	7.16	1.97	0	43.70	14.7	5.71x	1.13y	z
C	87.1	80.5	7.20	1.92	0	43.50	14.6	2.77x	1.46y	4z
D	88.6	79.5	7.21	1.88	0	43.50	14.5	x	y	16.4z
MK1	n.a	-	16	1.87	0	43.15	14.4	38.2%	-	1%

The second group of fuel consists of four single components of n-heptane (N), toluene (T), ethanol (E) and isooctane (I). These were blended by volume to create mixtures of PRF, TRF, ERF and TERF. Design of experiment model was used to break down the fuel effect in details and presented in Papers III and IV. The setting for the

three factors is given in Table 4-3 and graphically is illustrated in Chapter 3.2 Figure 3-9. The isooctane acted as a filer.

Table 4-3 Surrogate fuel composition.

Fuel	High [%]	Average [%]	Low [%]
n-Heptane	40	35	30
Toluene	15	7.5	0
Ethanol	10	5	0

The third group was used to map RON and MON in Paper V. These fuel blends consisted of n-heptane, isooctane, ethanol and toluene. This group consists of three sets of fuel blends, the first two sets of fuels were mixed according to design of experiment using central composite two level full factorial designs as explained in Chapter 3.2. The first set of fuel blends can be found in section 3.2 Figure 3-9 and the second set of fuel blends is shown in Figure 4-1.

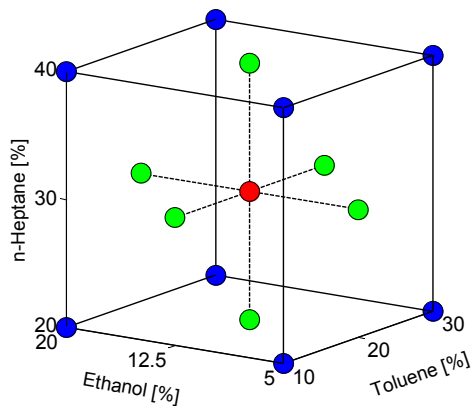

Figure 4-1 Graphical representation of the experimental factors and their levels. The data are taken from [43].

The third set of fuel blends was predicted using quadratic regression models to have specific RON and sensitivity (S) values. Measured fuel properties of the third set can be found in Table 4-4.

Table 4-4 Measured RON, MON, and S for seventeen surrogate fuels.

Fuel	N [v %]	T [v %]	E [v %]	I [v %]	RON measured	MON measured	S measured
ERF1	10	0	10	80	96.4	92.9	3.5
ERF2	38.5	0	16	45.5	75	71.7	3.3
ERF3	43	0	38	19	84.4	78.7	5.7
TRF1	8.5	22	0	69.5	96.1	91.8	4.3
TRF2	30	20	0	50	75	72	3
TRF3	17.5	12	0	70.5	85.1	83.3	1.8
TRF4	13.5	38	0	48.5	94.8	87.8	7
TRF5	34.5	37	0	28.5	75.6	69.8	5.8
TRF6	20	22	0	58	85.1	81.6	3.5
TERF1	38.5	25	10	26.5	74.8	69.8	5
TERF2	15	21	10	54	95.5	89.2	6.3
TERF3	22.5	7.5	8	62	85.1	82.5	2.6
TERF4	33.5	7.5	8	51	74.8	72	2.8
TERF5	10.5	6	8	75.5	96.3	92.4	3.9
TERF6	19	4	4	73	84.9	83.6	1.3
PRF1	5	0	0	95	94.8	94.8	0
PRF2	25	0	0	75	74.8	74.9	-0.1

The fourth group of fuel blends was created using a quadratic regression model based on ignition delay value from Paper III and were used to verify the accuracy of the model in Paper V. The fuel properties are listed in Table 4-5.

Table 4-5 Fuel composition and octane rating.

Fuel T/E	*N [v%]*	*T [v%]*	*E [v%]*	*I [v%]*	*RON DoE*	*MON DoE*
3	31.52	15	5	48.48	77.28	73.6
0.75	35.66	7.5	10	46.84	75.58	73.12
0	34.24	0	10	55.76	75.58	72.15

Table 4-6 illustrate fuel specifications for fuel blends that are used in the Chapters 5 and 6. Each acronym is used for two fuel blends except the toluene ethanol reference fuel centre point ($TERF_{cp}$) which consists of three fuel blends. In the result presented in Chapters 5 and 6 the lowest n-heptane concentration is used, when not specified, for all acronyms.

Table 4-6 Fuel blend composition.

Fuel	N [v %]	T [v %]	E [v %]	I [v %]	RON measured	MON measured
PRF	30	0	0	70	70.3	70.4
	40	0	0	60	60.6	60.8
TRF	30	15	0	55	74.2	71.9
	40	15	0	45	64.3	62.3
ERF	30	0	10	60	78.7	76.7
	40	0	10	50	69.7	66.8
$TERF_{critical}$	30	15	10	45	81.6	77.2
	40	15	10	35	72.2	69.0
$TERF_{cp}$	30	7.5	5	57.5	76.8	74.2
	35	7.5	5	52.5	71.9	69.4
	40	7.5	5	47.5	66.6	64.0

4.3 Operating conditions

In all cases, the engine was heated up until the coolant water and engine oil temperatures reached to 90°C by an external heater. The engine was then operated with combustion until the coolant water and engine oil temperatures reached 95 °C. During data accusation, 300 cycles of cylinder pressure were saved and data was logged during 3 minutes.

4.3.1 Operating load range

The obtainable load region for stable PPC was examined for four fuels in the gasoline boiling range together with MK1 as a reference fuel in Paper I. The fuels were tested at loads between 2 and 8 bar $IMEP_g$ at 1500 rpm with 50% heat release completion at 6 crank angle degree after top dead centre (ATDC) as shown in Table 4-7. A single injection strategy was used, where the start of injection and the injection duration were adjusted to achieve desired loads with fixed CA50, as the injection pressure was kept constant at 1000 bar. During the experiments the desired λ value was 1.5 at an EGR ratio of approximately 50%. Due to the characteristics of the EGR valve, the target level was set to 53 ±1%. The inlet mixture temperature was kept at 335 K.

Table 4-7 Inlet conditions for obtainable load region for stable PPC.

Engine speed [rpm]	1500
CA50 [ATDC deg]	6
Inlet temperature mixture [K]	335
Loads $IMEP_g$ [bar]	2,3,4,5,6,7 & 8
Injection pressure [bar]	1000
EGR [%]	53±1
λ [-]	1.5 -7.5
Absolut inlet pressure [bar]	1-2.5

4.3.2 Combustion phasing effects on PPC

Fuel aspects within the context of combustion phasing during PPC mode was examined for four fuels in the gasoline boiling range together with Swedish diesel MK1 as a reference fuel in Paper II. The experiments were performed at base case: 8 bar IMEPg at 1500 rpm and 1000 bar injection pressure where a single injection strategy was used as shown in Table 4-8. During the experiments the desired relative air/fuel ratio (λ) value was 1.5 at an EGR ratio of 53±1%. This relation gave an inlet mole fraction of approximately 5% CO_2 and 13% O_2. The combustion phasing was adjusted by means of start of injection, for all fuels, over the range with stable combustion and acceptable pressure rise rate combined with maintained λ, EGR ratio, inlet pressure and temperature, and load.

Table 4-8 Inlet conditions for studying fuel aspects on PPC.

Engine speed [rpm]	1500
CA50 [ATDC deg]	3-14
Inlet temperature mixture [K]	335
Loads $IMEP_g$ [bar]	8
Injection pressure [bar]	1000
EGR [%]	53±1
λ [-]	1.5
Absolut inlet pressure [bar]	2.5
Inlet oxygen concentration [%]	13
Inlet CO_2 concentration [%]	5
COV [%]	2

4.3.3 Operating parameter effects on PPC using surrogate fuels

The testing condition used for this part of the work center around the base conditions: 1500 rpm with 8 bar $IMEP_g$ as in previous studies. A single injection strategy was used where the start of injection and the injection duration were adjusted to achieve the desired load and CA50 as shown in Tables 4-9 and 4-10. The

inlet mixture temperature and pressure were kept constant at 345 K and 2.8±0.2 bar respectively. At this condition, several parameters were varied to examine surrogate fuel effect and engine behavior during PPC. These parameters included inlet O_2 concentration, combustion phasing and injection pressure. The inlet O_2 concentration was tested at three different mole fractions: 11, 13 and 15%. At each oxygen concentration level the combustion phasing and injection pressure were varied. The combustion phasing was varied at 3, 6, 8 and 10 degrees after top dead center, while the injection pressures of 800, 1000 and 1200 bar were used at each O_2 concentration and combustion phasing as listed in Table 4-10.

Table 4-9 Operating conditions.

Engine speed [rpm]	1500
Inlet temperature mixture [K]	345
Loads $IMEP_g$ [bar]	8
Absolut inlet pressure [bar]	2.8±0.2

Table 4-10 Engine operating parameters.

Inlet oxygen concentration [%]	11 (Low)	13 (base)	14 (high)
CA50 [ATDC deg]	3, 6, 8 &10	3, 6, 8 &10	3, 6, 8 &10
Injection Pressure	800 (Low)	1000 (base)	1200 (high)

Chapter 5

Effects of Fuel properties

This section presents observations regarding effect of fuel properties on combustion event, emissions and load range for PPC. The results are retrieved from Paper I, II, III, IV, V, and VI.

5.1 Combustion characteristics

5.1.1 Ignition delay

Ignition delay plays an important role in Partially Premixed Combustion. Achieving the desired premixed portion of combustion requires an increased mixing between fuel and air prior to ignition in CI engines. Therefore, understanding the effect of these changes on the early combustion stages is essential. The impact of fuel properties on combustion relates to cooling effect from evaporation, the mixing process and the fuel ignitability. When analyzing fuel effects on ignition delay it is thereby of interest to differentiate between physical and chemical fuel properties.

Relation to RON

As can be seen in Figure 5-1 the effect of octane number on the ID is clear, with distinct differences between each fuel of different octane number for a constant CA50 timing. This is not surprising since a higher RON means that the fuel is more resistant to auto-ignition. To maintain the same CA50 the injection timing for higher RON fuels must thereby be advanced. The dependence of fuel molecular structure on RON is as follows: straight-chain paraffinic compounds (such as n-heptane which has a RON=0) have the highest ignition quality (easiest to ignite) compared to branched-chain paraffinic compounds (such as isooctane which has a RON=100), which have higher auto-ignition resistance and are more difficult to ignite. Aromatics and alcohols also have poor ignition quality which means their auto-ignition resistance is very high. If the injection timing (rather than CA50) is kept constant while the octane number increases, the combustion phasing is retarded and beyond a certain extent the combustion become unstable.

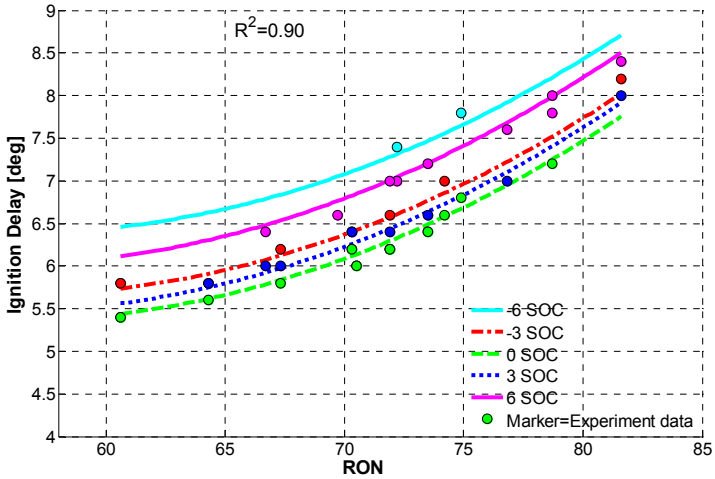

Figure 5-1. Ignition delay predicted as a function of RON. Measured ignition delay presented as markers.

The relation between RON and ID is explained more in detailed in the following sections

Farrell and Bunting [65] studied fuel composition effects at constant RON and MON in HCCI. Their studies showed that neither RON nor MON is complete predictors of ignition quality in HCCI. Their results indicate that fuel composition affects ignition delay for fuels with the same RON and MON. However, results from Paper II and III indicated that this is not the case for PPC. Instead fuels with similar RON had similar ignition delay despite the differences in fuel composition and operating conditions as seen in Figure 5-2. The subscripts in the legend are as follows: PRF=Primary Reference Fuel; ERF=Ethanol Reference Fuel; TERF=Toluene Ethanol Reference Fuel; G=blend of refinery gasoline components. In contrast to HCCI, fuels with similar RON behave similarly in PPC even at different operating conditions. Gasoline fuels with RON 87.1_G and 88.6_G show similar ignition delays despite the difference in fuel composition and MON. The RON is thereby of more importance in terms of affecting ID than MON and fuel composition in PPC.

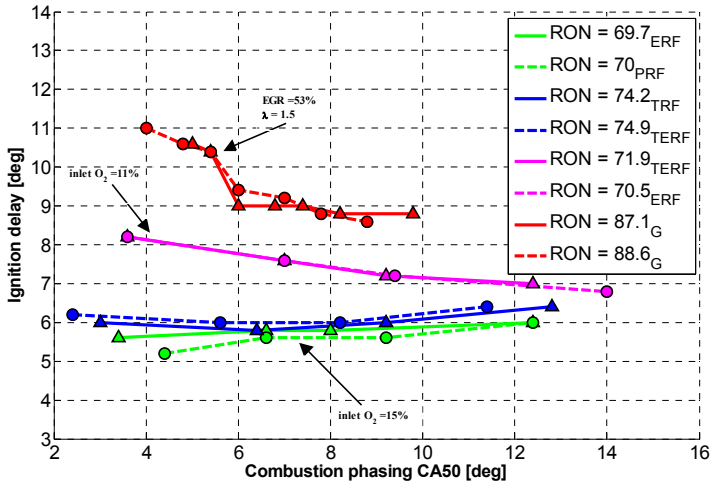

Figure 5-2 Ignition delay as a function of combustion phasing. Different operating conditions and RON are presented.

As shown earlier, an increase in RON leads to an increase ID for a constant CA50. Also, it was shown that similar RON numbers resulted in similar ignition delays. We now address the question: At a given ID at constant operating conditions for different fuel blends what is the RON value? Figure 5-3 shows ignition delay for different fuel blends as a function of start of injection. These fuel blends were predicted using a regression model for ID presented in paper III. The RON numbers for the three fuels were calculated to range from 75.58-77.28 using fuel composition and the regression model presented in paper V the ratio of toluene to ethanol (T/E) was set to 3, 0.75 and 0. Despite the differences in fuel composition, a relation between RON numbers and ignition delays is found. This relation is reversible, meaning similar RON numbers result in similar ignition delays and vice versa ($RON \rightleftharpoons ID$).

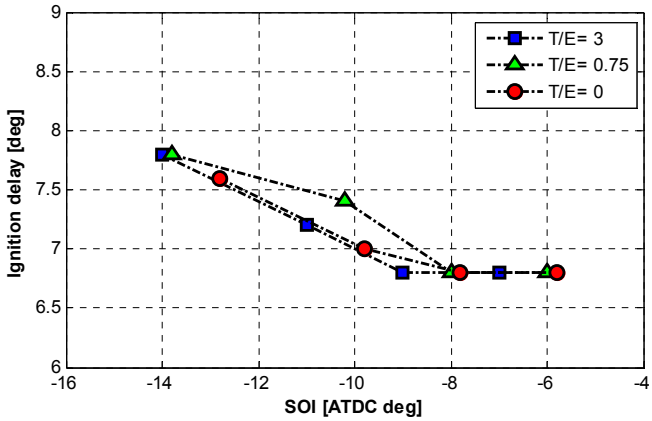

Figure 5-3 Ignition delay as a function of start of injection for three fuel blends with different composition but similar RON.

Fuel composition effect

Octane number is a measure of the fuels propensity to resist auto-ignition and is as shown above related to ID. Fuel octane number is also related to fuel composition. So ID should also be related to fuel composition. To study the relation between ID and fuel composition a matrix of blends of different fuel compositions was designed and tested.

Experimental results showed that fuel composition has a notable impact on ignition delay. Results at constant operating conditions of 13% O_2, 1000 bar injection pressure and CA50 at 3 degrees ATDC are shown in Figure 5-4. In this investigation, PRFs (PRF60 and PRF70) were considered as a base fuel. For TRFs, ERFs, and TERFs fuels the isooctane fraction in PRFs was replaced either by 10% ethanol, 15% toluene or both together. The fuel blends composition is illustrated in Table 4-6 in Chapter 4. Increasing isooctane and decreasing n-heptane in PRFs (black solid line) increased the ignition delay but with less than one degree. At a given n-heptane concentration, the ignition delay was higher for the TRFs, ERFs, and the TERs than the PRFs. This is attributed to the increasing the octane number of the fuel and thus advancing the SOI. Ethanol had stronger impact on ID than toluene, shown by comparing the ERF results with the TRF results. Naturally, when the alcohol and aromatics where at their highest levels the ID was the longest and the sensitivity to n-heptane the strongest. In general, the difference in ID between fuels is close to proportional to the difference in RON numbers.

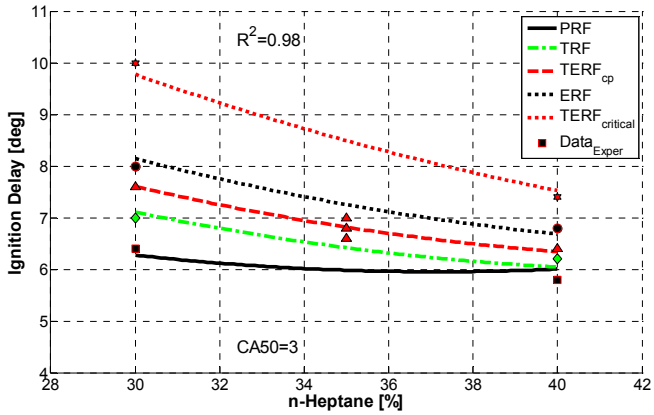

Figure 5-4 Ignition delay as a function of n-heptane for different surrogate fuel blends at 13% O_2, 1000 bar injection pressure at CA50 3 CAD ATDC.

5.1.2 Low temperature reactions

Generally, in HCCI and in other types of low temperature combustion the rate of heat release exhibits an initial bump before the main peak of the rate of heat release. This first peak is called low temperature reaction. The amount of low temperature reaction depends on fuel composition, gas temperature in the cylinder and engine speed. Fuel compositions containing significant amount of n-paraffins such n-heptane exhibit a large amount of low temperature reactions. As mentioned in Chapter 2.4.1 high cetane number, diesel-like fuels generally exhibit LTR. Bunting et.al didn't detect any LTR for fuels with a cetane number lower than 34 in HCCI runs. However, this is not the case for PPC since also high octane number (lower cetane number) fuel can produce LTR. In this section, the behavior of LTR in PPC will be discussed.

Fuel composition effect

As mentioned previously, fuel composition affects the amount of LTR fraction. For example in HCCI combustion both ethanol and toluene are known to reduce the LTR by acting as radical scavengers. However, in the current PPC studies where CA50 is kept constant, both ethanol and toluene increase the LTR fraction as seen in Figure 5-5. When both ethanol and toluene is added to the fuel blend the effect is enhanced, therefore TERFs showed the largest fractions of LTR. Also in contradiction to observations in HCCI combustion, the LTR fraction is increased as n-heptane decreases for all fuel blends. The trends in LTR are related to the ignition

quality. With an increased RON SOI had to be advanced to maintain the same CA50. With advanced SOI means that the cylinder pressure and temperature are lower at SOI. Thus, the chemical reaction rates are slowed down and the LTR is increased. A certain level of mixing before SOC is also required to produce LTR because if the high temperature heat release starts to soon there is no time for LTR.

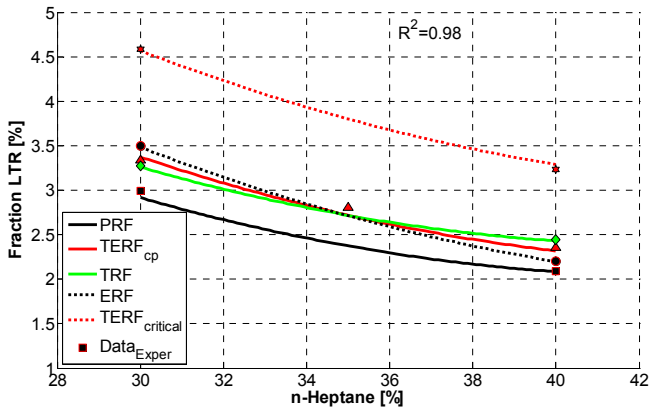

Figure 5-5 LTR Fraction as a function of n-heptane concentration for different surrogate fuel blends at 13% O_2, 1000 bar injection pressure and at CA50 3 CAD ATDC.

As was explained in paper VI, the observed fuel effect on LTR in PPC was the opposite compared to HCCI. Chemical fuel effects dominate over physical effects for port injected HCCI since the fuel can be expected to be vaporized and fairly well mixed when the inlet valve close. The difference in fuel effects between PPC and HCCI indicate that; the processes behind LTR are more complex in PPC than in HCCI. It is not certain that a fuel with more pronounced chemical prerequisites for LTR will produce more LTR. This is since the physical properties and the ignition quality will be of larger importance in PPC. The physical properties in form of mixing and cooling due to vaporization, and the ignition quality in form of available time before the main heat release initiations. Figure 5-6 shows the LTR fraction for different fuel blends with similar RON and ignition delay. The fraction of LTR is similar between the fuels which indicate that the ignition quality is central for the fraction of LTR in PPC. The fuel blends were chosen so that the ratios of toluene to ethanol (T/E) are 3, 0.75 and 0 while the RON numbers were calculated to range from 75.58-77.28. All fuel blends show a similar trend and similar values of LTR fraction with small variation. These variations might be affected by the resolution of the encoder which gives measurement every 0.2 crank angle degree. It was mentioned in section 5.1.1 that similar ignition delays gave similar RON numbers and vice versa. This can explain the similar trend and values of LTR fractions. In other words there is a

relation between ignition delay and LTR fraction which is explained in the next section.

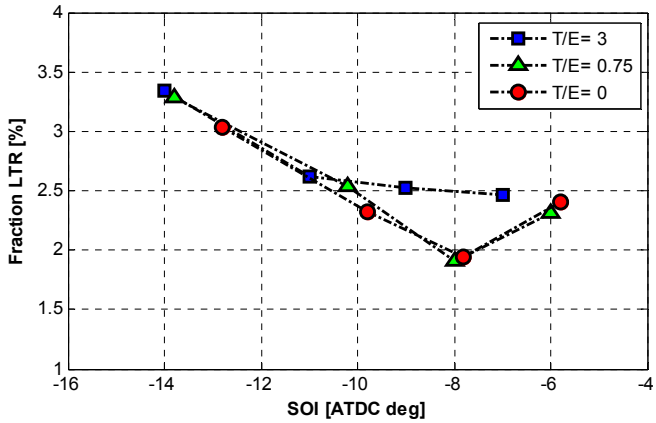

Figure 5-6 LTR Fraction as a function of start of injection for different fuel blends at 13% O_2, 1000 bar injection pressure.

Relation between ignition delay and LTR

As shown above ID and LTR have similar response to fuel composition. They also show similar trends when inlet oxygen concentrations and injection pressure are changed. A close to linear relation was found between the LTR and ID as shown in Figure 5-7 at different O_2 concentrations. It is of interest to know whether ID and LTR are influenced more by inlet O_2 concentration or alcohol concentration (which also introduces oxygen atoms into the combustion process). At 15% O_2, the LTR was 1% higher for ERF (RON 78.7) than PRF60 while the ignition delay was prolonged with 2 degrees. Reducing the inlet O_2 concentration from 15% to 11% the LTR increased by 2% for PRF60, while the ignition delay increased by 2 degrees. Thus, the slope of LTR-ID curve was influenced more by inlet O_2 concentration than alcohol fraction. Due to an insufficient amount of oxygen available in the air charge, the mixing period was longer and the chemical reaction rates occurred slower at lower inlet O_2. Furthermore, the fraction of LTR was sensitive to combustion phasing especially at the highest inlet O_2 concentration, see Figure 19 in Paper III.

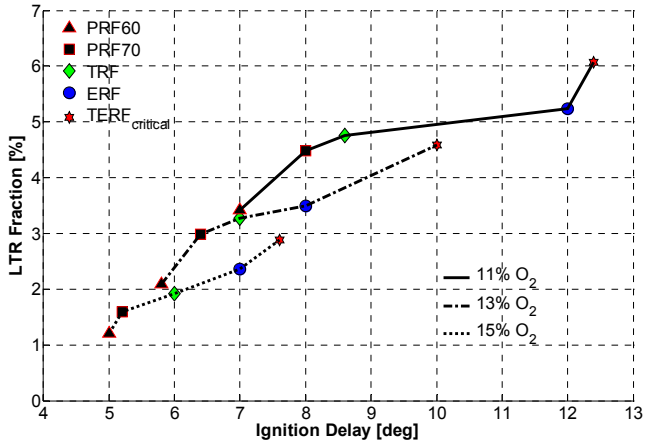

Figure 5-7 Fraction of LTR as a function of ignition delay for different surrogate fuel mixtures and O_2 fractions at 1000 bar injection pressure and at CA50 3 CAD ATDC.

5.1.3 Combustion duration

Combustion duration (defined as CA90-CA10) is one of the factors that have a significant effect on PPC engine performance. Several fuels were tested to study the effect of fuel properties such as RON and fuel composition on combustion duration as well as the effect of combustion duration on the engine performance and emission parameters.

Fuel octane number effect

Combustion duration (CD) is important for PPC since a long CD is an indication of a large fraction of late mixing controlled combustion. When comparing CD for different fuel blends at a given CA50 a higher RON gave a shorter CD as shown in the left hand side of Figure 5-8. Looking at the right hand side of Figure 5-8, the CA10 values are rather similar for all fuels but the CA90 values vary. The highest RON fuel had the earliest CA90 while the lowest RON fuel had the latest CA90. This is mainly due to a larger fraction of premixed combustion for high RON fuels. In order to maintain a constant CA50 the SOI has to be more advanced for high RON fuel and the longer ID gives more combustible air fuel mixture at ignition producing a larger fraction of rapid premixed combustion.

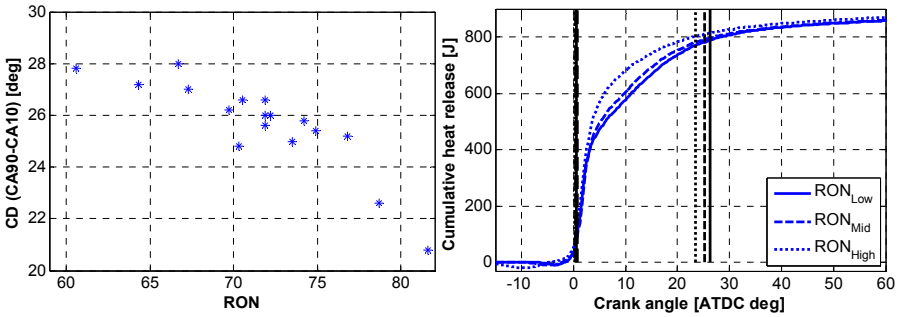

Figure 5-8 Combustion duration as a function of RON (on the left hand side) and cumulative heat release as a function of crank angle degree (on the right hand side) showing the CA10 and CA90 for different RON values: CA50 is 3 crank angle degree ATDC for all fuel blends.

Fuel composition effect

The effect of fuel composition on combustion duration was studied using a regression model according to Eq. 3.19. Independently of n-heptane fraction PRFs had longer CD than TRFs, ERFs, and TERFs fuels, see Figure 5-9. The TERFs fuels with both ethanol and toluene together have the shortest CDs. For all fuels blends, increasing n-heptane while reducing the isooctane concentration, the CD is prolonged. This behavior can be explained by the RON numbers. As previously mentioned, increasing RON the CD is shortened. Both toluene and ethanol are octane enhancer which increasing the fuel RON as they are substituted for isooctane.

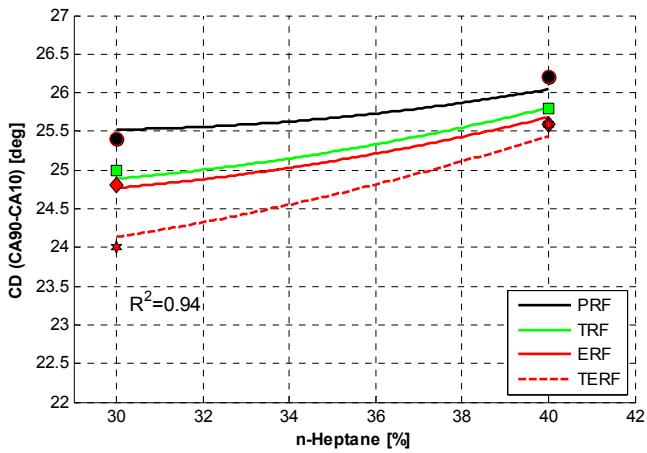

Figure 5-9 Combustion duration as a function of n-heptane concentration at constant operating conditions.

To determine any chemical effects of toluene and ethanol beyond their RON influence, both ignition delay and RON were kept constant for three fuel blends. These blends had different fuel compositions with the ratios of toluene to ethanol (T/E) set to 0, 0.75 and 3. The combustion duration values were similar for all 3 fuels as seen in Figure 5-10. In summary, the RON had a much more significant influence on Partially Premixed Combustion events than fuel composition.

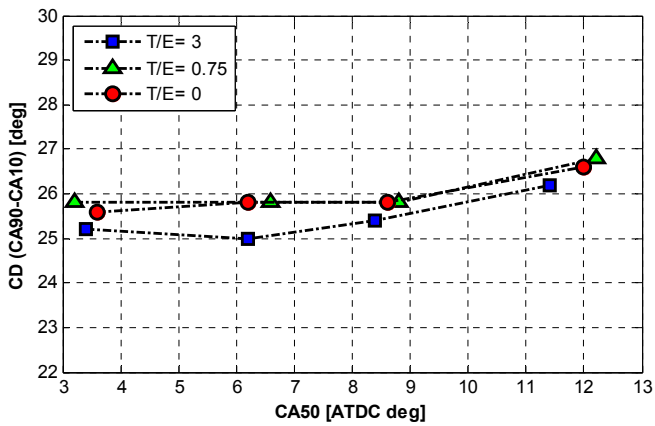

Figure 5-10 Combustion duration as a function of combustion phasing CA50 for three fuel blends with different composition but similar RON.

5.2 Emissions

A diesel engine operating on diesel fuel suffers from high emissions of NO_x and smoke which are difficult to control and require expensive atftertreatment. Diesel fuels are meant to auto-ignite easily. In most cases the fuel is injected late in the compression stroke and combustion starts before all fuel is injected into the cylinder, especially at high loads. Thus diesel burns in a quasi-steady jet with a large fraction of diffusion combustion. To suppress soot formation the local fuel/air equivalence ratio (ϕ) should be below $\phi<\sim2$. NO_x formation can be significantly decreased by reducing the combustion temperature below ~2200 K, which can be achieved by introducing a large amount of cooled EGR. However, suppressing smoke and NO_x simultaneously normally results in higher levels of HC and CO emissions especially with low temperature combustion such as PPC. Therefore in this section the effect of fuel properties on emissions in PPC is reported.

Fuel octane number effect

Diesel fuel generally has a cetane number above ~40, with Swedish diesel MK1 having cetane number 54. As mentioned previously conventional diesel combustion have issues with smoke and NO_x emissions. The effects on emissions of using gasoline-type reference fuels and blends of refinery streams having a range of RON numbers are examined and compared to MK1 for PPC in Paper II. NO_x emissions are not dependent on RON as seen in Figure 5-11, while there is a clear trend between RON and emissions of smoke, HC and CO. Similar trends between RON and emissions for gasoline fuels were reported in Paper II. Smoke levels are almost zero FSN for RON >65. The reason behind increasing smoke level for RON <65 is that the ignition delay is shorter and thus there are rich mixture pockets where soot forms. Both HC and CO emissions have similar trend as RON increases, however the trend is stronger for CO. HC and CO increase as RON increases because the SOI is advanced to maintain a constant CA50. Advancing the SOI may result in fuel being injected into the squish volume creating a liquid film, which is difficult to oxidize and thus lead to incomplete combustion and high levels of HC and CO [66, 67].

It is of interest to compare the results from the surrogate fuel blends presented here to results from MK1 in paper II, where MK1 was run at similar operating conditions. Such comparison shows that the emission performance of the surrogate fuel blends is better than MK1. NO_x and smoke levels are much lower than MK1 and also HC and CO had similar levels as MK1.

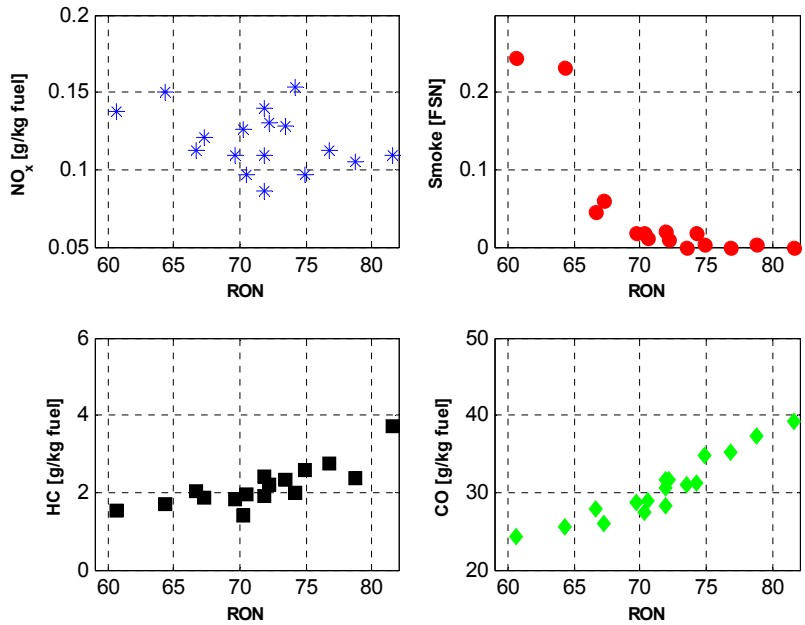

Figure 5-11 NO_x, smoke, HC and CO emissions as a function of RON numbers at constant operating conditions.

Fuel composition effect

Fuel composition effects on emissions have been studied for different gasoline fuels, MK1, and surrogate gasoline blends of PRF, TRF, ERF and TERF. As mentioned before, MK1 and gasoline fuels are complex and consist of hundreds to thousands of different hydrocarbons. Therefore, fuel composition effects on emissions were not clear for MK1 and gasoline fuels. Looking at surrogate fuels in the previous section, NO_x and smoke emissions did not correlate to RON numbers, especially not NO_x emissions. However, a correlation between fuel composition and NO_x and smoke emissions are clear, see Figure 5-12. Treating PRF as a base fuel, it is evident that adding toluene increases both NO_x and smoke levels. The effect on smoke was only evident at late CA50. Ethanol has the effect of decreasing both NO_x and smoke; smoke is decreased to almost zero. It has previously been reported that fuels with aromatics extend the duration of NO_x formation due to local high-temperature regions with combustion of decomposed hydrocarbons [68]. Also, it is known that increasing aromatics content in the fuel can leads to an increased production of soot [69, 70]. On the other hand, fuel composition did not show an effect on HC and CO emissions, the observed trend shown in Figure 15-12 is due to RON variation.

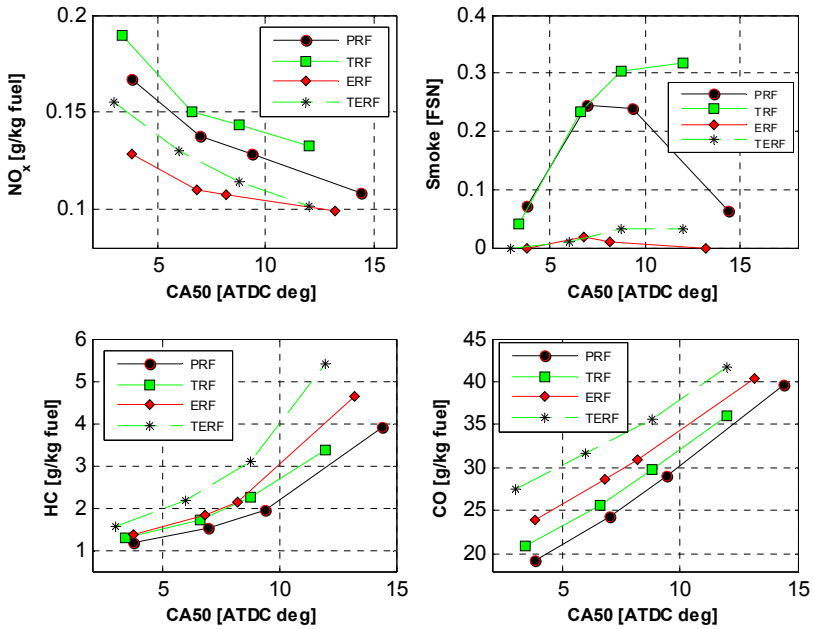

Figure 5-12 NO_x, smoke, HC and CO emissions as a function of combustion phasing for different fuel blends.

Furthermore, the RON and ID effect were decoupled from the emissions by using fixed values of RON and ID for three fuel blends. As explained before, the ratio of toluene to ethanol was varied with values of 0, 0.75 and 3. As illustrated in Figure 5-13, higher level of toluene resulted in higher level of NO_x, smoke and HC emissions. The CO emissions were insensitive to fuel composition. The smoke levels were almost zero even for the fuel blend with the highest toluene concentration except at the latest CA50.

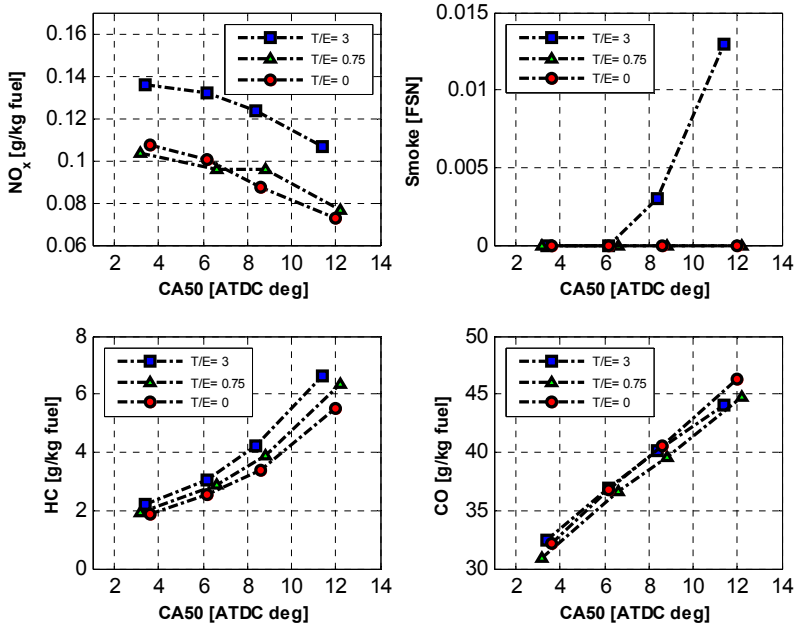

Figure 5-13 NO_x, smoke, HC and CO emissions as a function of combustion phasing for different fuel composition but with similar ID and RON.

5.3 Load range

There is very little published work regarding the fuel effects on partially premixed combustion at low load in light duty diesel engines. Manente et al. (2010) investigated the effect of octane number for low load PPC in a heavy duty diesel engine [57]. The authors in [57] suggested that the optimum EGR rate and air-fuel ratio for PPC are about 50% and 1.5 respectively. These setting were shown to give low emissions of soot and NO_x, together with high combustion- and indicated efficiency. However, it was not possible to achieve stable combustion at low loads for high RON fuels during these conditions. Since the experiments were performed in a heavy-duty diesel engine the operating range for PPC in light-duty diesel engines were still unknown. Accordingly, this section analyzes the load-limit range for PPC in a light duty diesel engine at the suggested setting (50% EGR and λ=1.5) for four fuels in the gasoline boiling range together with Swedish diesel MK1.

The results showed that higher RON fuels had a higher low-load limit since a high RON is the same as high resistance to auto-ignition. With the low-load limits means the turning point where the suggest setting in [57] cannot be applicable anymore.

The low-load limits were different depending on fuel octane number. The low-load limit for MK1 was at 3 bar $IMEP_g$, 5 bar $IMEP_g$ for low RON gasoline fuels and at 7 bar $IMEP_g$ for the high RON gasoline fuels as shown in Figure 5-14.

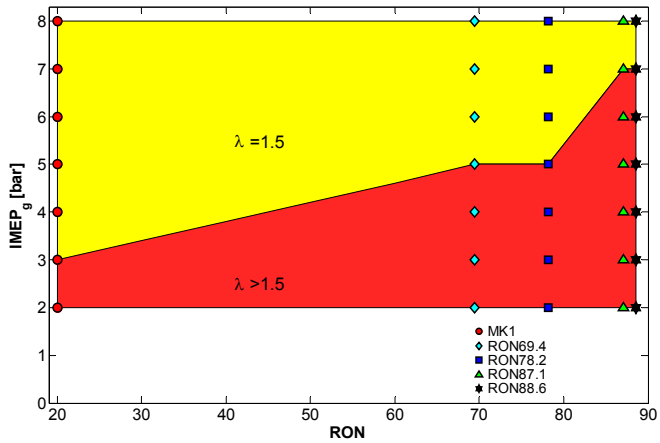

Figure 5-14 Low-load limit regions for different gasoline fuels and MK1.

In order to extend the load below the low-load limits for all fuels, while EGR was kept constant, an increased boosting was used to maintain stable combustion as seen on the left hand side Figure. However, the air-fuel ratios become a function of load below the low-load limits as illustrated in Figure 5-15.

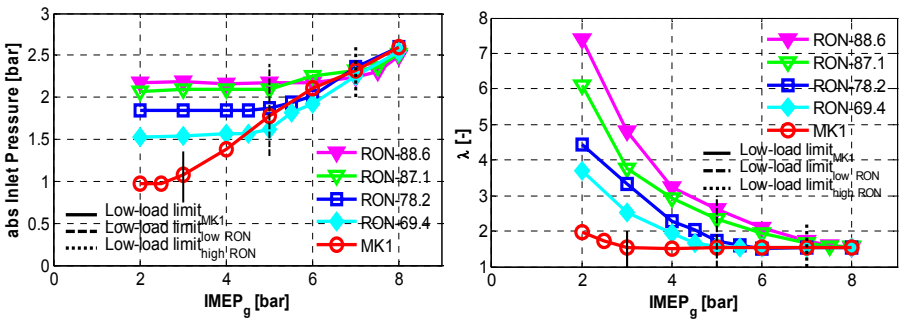

Figure 5-15 Absolute inlet pressure (on the left hand side) and air-fuel ratio (on the right hand side) as a function of gross indicated mean effective pressure.

Chapter 6

Effects of engine operating parameters

This section presents observations regarding engine operating conditions on the combustion event, and emissions for PPC. The results are retrieved from Paper I, II, III, and IV.

6.1 Combustion characteristics

6.1.1 Ignition delay

As explained in chapter 5, the ignition delay is related to the fuels resistance to auto ignition. However, ID is also affected by engine-operating parameters such as: injection timing, injection pressure, injection quantity, charge temperature and pressure, engine speed and EGR level. In this section effects of inlet O_2 concentration, injection pressure, and combustion phasing CA50 on ID are examined during PPC conditions.

Inlet oxygen concentration effect

Inlet O_2 concentration effects were analysed with DoE using a design matrix of the same principle as in Figure 3-9. Values of ID were determined according to section 3.1.1 and a regression model according to Eq. 3.19 was fitted to the data. The inlet O_2 concentration was varied at three levels of 11, 13 and 15%. Decreased inlet O_2 concentration increased the ID as seen in Figure 6-1. This occurs because more time is needed for mixing between fuel and charge gases to reach an ignitable equivalence ratio. SOI was advanced to maintain a constant CA50 when the inlet O_2 was decreased. An advanced SOI also means that the initial chemical reactions occur more slowly due to lower charge cylinder pressure and temperature. The ID trend to inlet O_2 concentration is similar for all fuels at different operating conditions. However, the slope is different depending on fuel blend: for instance ERF and $TERF_{critical}$ have steeper slope comparing to TRF and PRF.

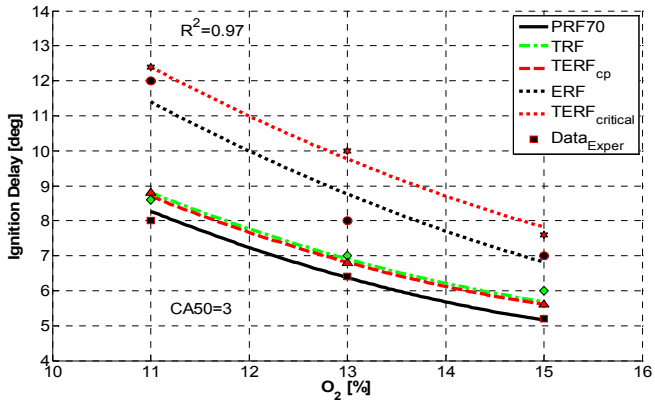

Figure 6-1 Ignition delay as a function of inlet O_2 concentration. The lines represent the quadratic regression model, while the markers represent the calculated ID from the experiment data.

Injection pressure effect

Generally, increasing injection pressure advances the combustion phasing due to improved spray breakup and shorter physical mixing time, yielding a shorter ignition delay [71]. However, the ignition delays in the range tested here are insensitive to injection pressures, as shown in Figure 6-2. This is partially due to a rather small variation in injection pressure and thus the effect was not strong enough to be seen on ignition delay.

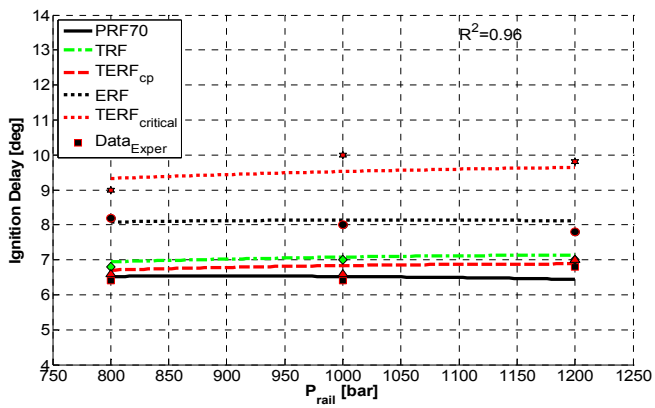

Figure 6-2 Ignition delay as a function of injection pressure. The lines represent the quadratic regression model and the markers represent the calculated ignition delay from the experiment.

6.1.2 Low temperature reactions

The amount of LTR fractions are determined using the second method presented in chapter 3. The values are used in the regression model to predict the behaviour of LTR fractions that are influenced by engine-operating parameters.

Inlet oxygen concentration effect

Similar to ignition delay the LTR fraction decreases by increasing the inlet O_2 concentration as illustrated in Figure 6-3. At low O_2 concentration the flame temperature is lower and so chemical reaction rates can be expected to be slower. Also, at lower O_2 concentration more ambient gases must be mixed with the fuel spray to oxidize the same amount of fuel. Thus, additional time is required for the mixing process. Therefore, in order to achieve the same CA50, the SOI must be advanced. Thus, the cylinder temperature and pressure are lower at SOI for the earliest CA50s. The trends were similar at different operating condition and different fuel blends.

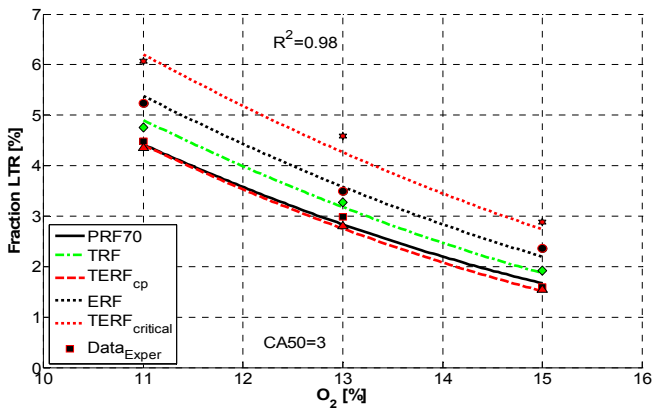

Figure 6-3 LTR fraction as a function of inlet O_2 concentration. The lines represent the quadratic regression model, while the markers represent the calculated LTR fraction from the experiment data.

6.1.3 Combustion phasing

At fixed injection timing and inlet O_2 concentration or EGR level, low octane number fuels require an advanced combustion phasing to maintain a constant combustion phasing. Therefore higher octane number fuels needs earlier injection timings, as illustrated in Figure 6-4, for four gasoline fuels and diesel fuel MK1.

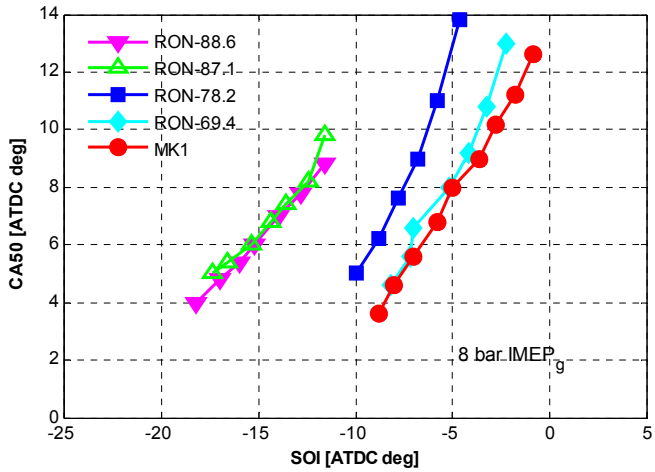

Figure 6-4 Combustion phasing as a function of start of injection.

The combustion phasing was adjusted by means of start of injection over the range with stable combustion and acceptable pressure rise rate for each fuel. For MK1 and the low RON fuels the range was limited by the range of the maximum brake torque (MBT) plateau since an increased fueling (and decreased λ) to maintain the load was not accepted. For the high RON fuels the range was limited by combustion instability: a too early injection timing places more fuel in the squish volume which has less chance to burn. As expected higher RON fuels requires a more advanced SOI since a high RON is the same as high resistance to auto-ignition. MK1 showed the largest span in achievable combustion phasing range. The CA50 for high RON fuels are less sensitive to injection timing because with an early injection the limiting factor for the ignition is temperature rather than mixing. The in cylinder temperature mainly depends on crank angle degree prior ignition.

There are other parameters beside the injection timing that affect the combustion phasing such as the EGR level, inlet O_2 concentration, and inlet air charge temperature and pressure. Decreasing the inlet O_2 concentration retards the combustion phasing due to the increase in ignition delay as shown earlier.

6.1.4 Combustion duration

It is generally known that decreasing the amount of premixed burn reduces the peak pressure and temperature in combustion. A decrease in in premixed burn with low octane number fuels causes an extended late mixing controlled combustion and thus increases the combustion duration.

Inlet oxygen concentration effect

The effect of inlet O_2 concentration on combustion duration was studied. At all inlet O_2 concentrations studied, retarded combustion gave a lower peak rate of heat release indicating that the reaction rate during the most rapid part of the premixed combustion was slower, see Figure 6-5. The trend in CD, however, was not consistent for the different O_2 concentrations. Retarded combustion phasing gave an increased CD at the lowest O_2 fraction, while the CD was stable at the medium inlet O_2 concentration and decreased at the high inlet O_2 concentration. This observation can be explained by differences between early and late combustion. It is evident that combustion starts later when CA50 is retarded at all O_2 concentrations, which also means that CA10 is retarded. At the lowest O_2 concentration, late combustion is slower, leading to a larger retardation in CA90 than in CA10 as well as increased CD. At a higher O_2 concentration, the reaction rate is higher and CA90 is more stable than CA10, while at the medium O_2 concentration, the retardation in CA10 and CA90 is about the same.

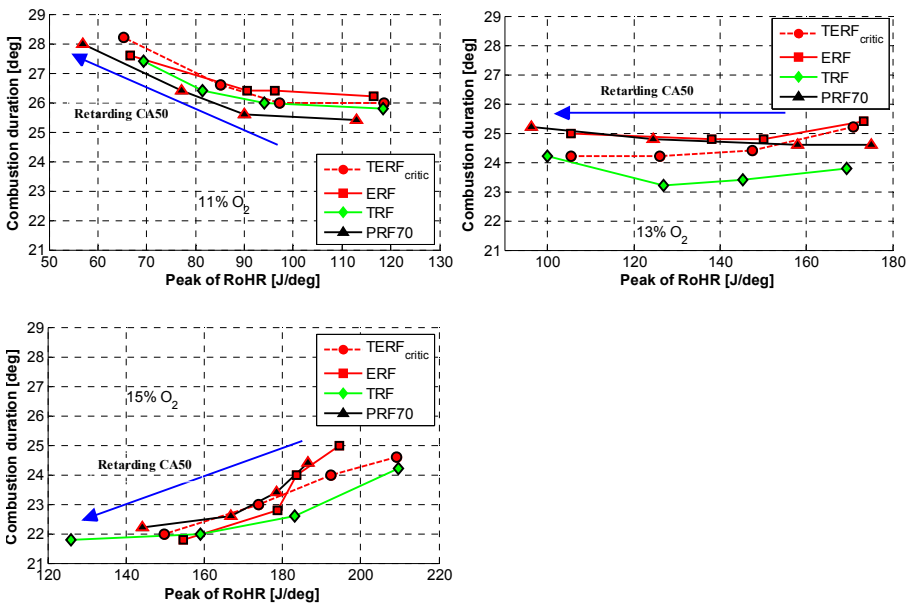

Figure 6-5 Combustion duration as a function of rate of peak heat release at different inlet O_2 concentration and CA50s.

6.2 Emissions

This section discusses the influence of engine operating parameters on emissions. The effect of inlet O_2 concentration, combustion phasing and injection pressure on NO_x, smoke, HC and CO emissions were analyzed. For a description of the emissions measurement systems refer to Chapter 4.2.

Combustion phasing effect

Engine-out emissions were found to be closely related to the combustion phasing. NO_x decreases by retarding the combustion phasing independent on the fuels octane number, as illustrated in Figure 5-12. Thermal NO_x formation is usually assumed to be the most significant contributor to the engine-out emission. NO_x emissions are therefore a function of cylinder conditions rather than fuel properties directly. The time between the point when the thermal NO_x formation starts and when the NO_x reaction chemistry is frozen by the cylinder expansion is restricted at late CA50s. The reduction mechanism for NO_x is very slow at lower temperatures meaning that the engine-out emissions levels of NO_x mostly depends on the in cylinder conditions during the period of highest temperatures which result in NO_x formation.

In contrast to NO_x, emissions of HC and CO increased with retarded CA50 as illustrated in Figure 5-12. An increase in HC and CO emissions implies an incomplete combustion. There are several potential reasons for an incomplete combustion but the main explanation for the relation to CA50 is that the decrease in in-cylinder temperature during expansion, where it reaches a point when the combustion is less completed while CA50 is retarded. The decrease in temperature leads to lower reaction rate.

Another emission of concern in compression ignition engines is smoke or particulate matter which consists to a large extent of combustion generated soot. Generally, soot formation is reduced at low combustion temperatures and lower equivalence ratios which is a feature of LTC concepts such as PPC. Still the soot formation is generally not fully suppressed since local zones with rich mixtures and high temperatures may exist. However in contrast to NO_x even cases with a lot of initial soot formation the engine-out emission levels of smoke could be close to zero if the subsequent oxidization of soot is significant. In the cases described by Figure 5-12 most of the fuels showed smoke level below the detectable limit (0.01 FSN) of the AVL soot meter. The exceptions are two fuels such as PRF fuel that had a peak of smoke around CA50 6 degree ATDC, as seen in Figure 5-12.

Inlet oxygen concentration effect

The effects from inlet O_2 concentration on emissions were studied and reported in Paper IV. The trends for NO_x, HC and CO emissions for different inlet O_2 concentrations are illustrated in Figure 6-6. As expected the NO_x levels decreases with decreasing inlet O_2. As mentioned previously, the inlet O_2 was controlled by the amount of EGR. Cooled EGR serve as a thermal sink and thus decreases the combustion temperature. Imagine two cases with combustion of the same amount of fuel at the same equivalence ratio but different O_2 concentration. In order to reach the same equivalence ratio the case with lower O_2 concentration has to mix in more non-reactive bulk gases leading to a higher heat capacity of the mixture. Since the same amount of heat is released in both cases the combustion temperature will be lower in the more diluted case. In reality the equivalence ratio may different between cases with different O_2 concentration but examples from the literature [72, 73] imply that it is not a given that a more diluted case will have higher local equivalence ratio. Also, reducing the inlet O_2 concentration lowers the ratio of specific heat of the cylinder charge resulting in lower compression temperatures which decreases peak combustion temperature further.

Smoke emissions peaked at 13% inlet O_2 concentration and were close to zero at 15% O_2. This trend is understood by different characteristics for formation and oxidation of soot. Generally, soot formation is higher at higher O_2 levels since the combustion temperature is higher at any given equivalence ratio [74]. This explains why the 11% O_2 case has less smoke than the peak. However, a higher O_2 concentration also gives more effective soot oxidization and apparently the oxidization is almost complete at 15% O_2 since the smoke level is close to zero. The increase in smoke when the O_2 level is decreased from 15% implies that the rate of oxidization decays more rapidly than the rate of formation [63].

As the inlet O_2 concentration is decreased the local combustion temperatures become lower, leading to substantial increases in HC and CO emissions. At a lower inlet O_2 concentration, the light components of the fuel evaporate easily due to longer ID and LTR. However, heavier components that are not quickly vaporized will remain on the combustion chamber walls. These heavier components evaporate during the expansion stroke but, due to a shortage of oxygen and lower combustion temperature, their oxidation reactions suffer [75]. As the ignition delay increases, there is a risk that the fuel will mix to the point where it is too lean for combustion to occur. As the inlet O_2 concentration decreases, the magnitude of CO emissions increases, more than HC emissions.

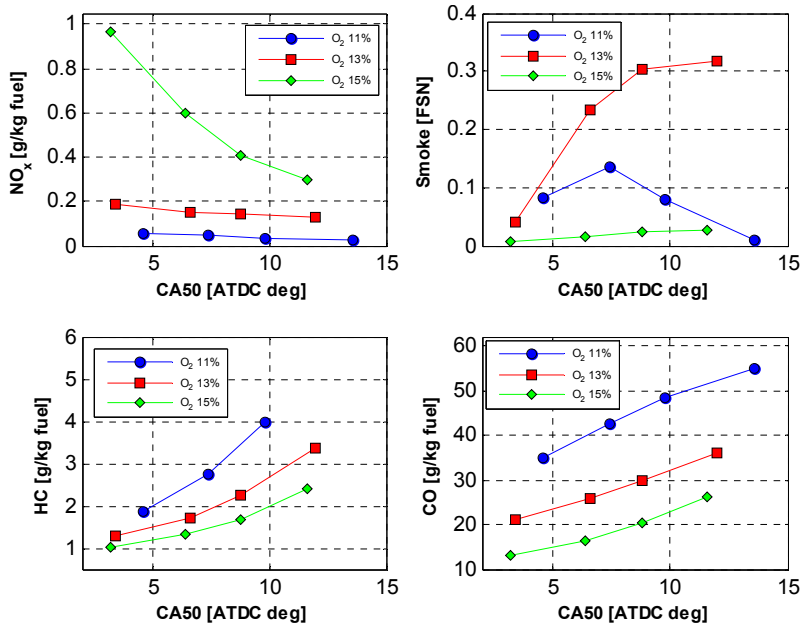

Figure 6-6 Emissions of NO_x, Smoke, HC and CO as a function of combustion phasing at three different inlet O_2 concentrations for TRF fuel.

Injection pressure effect

The injection pressure strongly affected the smoke levels as illustrated in Figure 6-7. Smoke values above the threshold for the AVL415S smoke meter (≥0.01 FSN) were analyzed, yielding results for 188 of 612 measurement points under different operating conditions. As the injection pressure increased from 800 to 1200 bar, the smoke levels declined by approximately 0.4 FSN for TRF fuel. There are several reasons why an increased injection pressure may decrease the engine out smoke level. First the residence time in the region with rapid soot formation in the fuel jet is decreased when the penetrating speed of the jet is increased. Second, at higher injection pressure, the spray breakup and fuel-air mixing are more effective at preventing the formation of locally rich regions, which would produce significant amount of soot. Third, the turbulence is increased which gives a more effective soot oxidization.

The ERF fuel produced lower levels of smoke than the PRF60 and the TRF fuels. This is since ethanol contains oxygen, leading to different characteristics of the soot formation and also a more effective oxidization [60, 76].

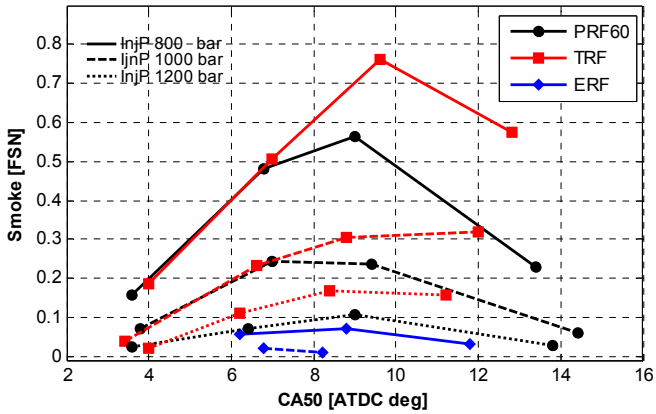

Figure 6-7 Smoke emissions as a function of combustion phasing at three different injection pressures, at 13% inlet O_2 concentration for three different fuels.

Chapter 7

A novel model to predict RON and MON

This section presents development of an empirical model for determining RON and MON. The results were published in Paper V.

7.1 Predicting RON and MON

Fuel composition and properties are known to affect engine performance and emissions. Two important fuel properties are RON and MON which are measured according to the ASTM and EN standard described in Chapter 2. The ASTM and EN methods are widely accepted and work well but unfortunately also expensive and time consuming. Therefore, research groups both in industry and academia desire more convenient methods to predict RON and MON for experimental work as well as for modeling. There are a couple of such methods to predict the RON and MON described in the literature, one which is well-known method called linear by volume (LbV) correlation.

Generally, the linear by volume method is used to calculate RON and MON for any reference fuel PRF consisting of isooctane and n-heptane. This is a sum of the contribution of the two components weighted by their volume fractions, the equation can be written as

$$RON = \propto_N \cdot x_N + \propto_I \cdot x_I \tag{7.1}$$

Where $\propto_N$ and $\propto_I$ are the RON numbers for pure n-heptane (N) and isooctane (I) and are equal to 0 and 100 respectively. x_N and x_I are the volume fractions of n-heptane and isooctane respectively.

In the current study, the ability of the LbV model to predict RON and MON was tested on some reference fuel blends composed of n-heptane, isooctane, toluene, and/or ethanol. The fuel blends were sent to a commercial fuels analytical lab and tested according to the EN standard. In order to take into account the impact from all four components in the fuel blends LbV equation was extended:

$$RON = \theta_N X_N + \theta_T X_T + \theta_E X_E + \theta_I X_I \quad (7.2)$$

Where the θs represent the RON numbers for pure n-heptane (N), toluene (T), ethanol (E) and isooctane (I) and are equal to 0, 120, 107, and 100 respectively. X_N, X_T, X_E and X_I are the volume fractions of n-heptane, toluene, ethanol and isooctane respectively. In order to calculate MON Eq. 7.2 is used but unlike n-heptane and isooctane, the MON numbers for toluene and ethanol are different from The RONs. The MON numbers are 109 and 89 for toluene and ethanol, respectively.

The predicted RON and MON from the linear by volume model calculated according to Eq. 7.2 are compared to the measured RON and MON in Figure 7-1.

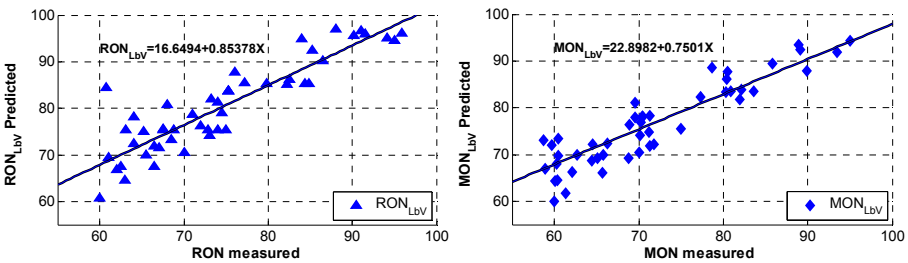

Figure 7-1 The predicted RON and MON from linear by volume model as a function of measured RON and MON.

There are a few known weaknesses with LbV that might explain the somewhat poor performance of the data described in Figure 7-1. The models lack any ability to describe antagonistic or synergistic interactions between the components. There is clear evidence that the blending of certain components is non-linear especially the blends with toluene, ethanol or both together.

Other methods to predict RON and MON have been developed by Morgan et al. [77] and by Anderson et al. [78]. Anderson used a linear molar octane blending model to describe most of the nonlinearity in the RON and MON data of blends of ethanol and gasoline. However their measured values were greater than predicted. Morgan used a 2nd order response surface model to map the toluene, isooctane, and n-heptane space with respect to RON and MON and used the model to determine the RON and MON for TRF blends. The model developed by Morgan et al. is applicable just for TRF blends but not for ERF or TERF blends. Therefore, in the current thesis work, another model was developed to predict RON and MON of blends containing one or more of the components n-heptane, isooctane, toluene, and ethanol. The model is explained and compared with the linear by volume model in the section below.

7.1.1 Regression model

In order to predict RON and MON, a regression model was developed. The data for the regression models consisted of two matrices of fuel blends of n-heptane, toluene, ethanol, and isooctane covering a wide range of RON from 60.6 to 97. The fuel matrices are shown in Table 7-1. Regression models according to Eq. 7.3 were fitted to the measured RON and MON. The R^2 value for both RON and MON was 0.99. R^2 by definition is between 0 and 1, where a value of 1 corresponds to a perfect fit.

$$RON/MON_{Predicted} = \beta + \alpha_N \cdot X_N + \alpha_T \cdot X_T + \alpha_E \cdot X_E + \gamma_{NT} \cdot X_N \cdot X_T + \gamma_{NE} \cdot X_N \cdot X_E + \gamma_{TE} \cdot X_T \cdot X_E + \delta_{N^2} \cdot X_N^2 + \delta_{T^2} \cdot X_T^2 + \delta_{E^2} \cdot X_E^2 \quad (7.3)$$

where β is a constant and α, γ and δ are coefficients for linear, interaction, and quadratic terms, respectively, and are generated from the regression model. X_N, X_T, and X_E are fuel concentration in volume fraction for n-heptane, toluene, and ethanol, respectively.

The second step was to validate the accuracy of the regression models, to accomplish this, the RON and MON of 17 fuel blends were predicted and measured according to the EN standard. The validation fuel blends (which are listed in Table 7.2) were selected using both interpolation and extrapolation methods in original the data sets. The original range for toluene and ethanol were 30% and 20% respectively, but the fuel blends in the models were extrapolated up to 38% for both toluene and ethanol. In general the model works remarkable well for both interpolation and extrapolation as can be seen in Figure 7-2 and Table 7-2. However, there is one exception with a significant deviation between predicted and measured MON. This fuel has a large amount of ethanol, 38% while the original model is based on ethanol concentrations up to 20%. Such large extrapolation does apparently limit the accuracy of the MON model, but that the MON model works well except for that one outlier. The predicted MON for all fuels, i.e. blends of ERF, TRF, and TERF showed good agreement with test results, as illustrated in Table 7-2.

Table 7-1 Fuel blends used in regression models to predict RON and MON.

N [v.v%]	T [v.v%]	E [v.v%]	RON measured	MON measured
40	10	5	67.1	63.7
20	10	20	94.7	88.5
20	30	20	97	87.6
40	30	20	80.8	73
30	20	5	79.6	74.5
30	30	12.5	85.3	78.6
40	30	5	71.8	65.8
30	10	12.5	81.6	77.9
20	30	5	90.2	84.1
40	10	20	78.3	74.3
20	10	5	86.1	83.6
40	20	12.5	74.8	68.9
20	20	12.5	92.3	86.4
30	20	20	87.9	81.4
30	20	12.5	83.8	78.2
30	0	0	70.3	70.3
40	0	0	60.6	60.6
30	15	0	74.2	71.9
40	15	0	64.3	62.3
30	0	10	78.7	76.7
40	0	10	69.7	66.8
30	15	10	81.6	77.2
40	15	10	72.2	69
35	7.5	5	71.9	69.4
35	7.5	5	71.9	69.4
35	7.5	5	71.9	69.4
40	7.5	5	66.7	64
30	7.5	5	76.8	74.2
35	15	5	73.5	69.4
35	0	5	70.5	68.7
35	7.5	10	74.9	71.8
35	7.5	0	67.3	66.1

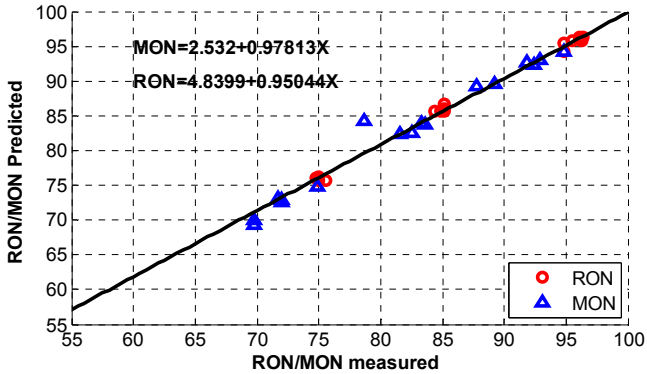

Figure 7-2 The predicted RON and MON from quadratic regression model as a function of measured RON and MON.

Table 7-2 The Predicted RON, MON and S and the tested RON, MON and S used to verify the regression model.

Fuel	N [v %]	T [v %]	E [v %]	I [v %]	RON DoE	RON test	MON DoE	MON test	S DoE	S test
ERF1	10	0	10	80	96,31	96,4	93,09	92,9	3,22	3,5
ERF2	38,5	0	16	45,5	76,17	75	73,19	71,7	2,98	3,3
ERF3	43	0	38	19	85,58	84,4	84,29	78,7	1,29	5,7
TRF1	8,5	22	0	69,5	95,93	96,1	92,75	91,8	3,18	4,3
TRF2	30	20	0	50	75,74	75	72,62	72	3,12	3
TRF3	17,5	12	0	70,5	86,75	85,1	83,98	83,3	2,77	1,8
TRF4	13,5	38	0	48,5	95,48	94,8	89,25	87,8	6,23	7
TRF5	34,5	37	0	28,5	75,64	75,6	69,37	69,8	6,27	5,8
TRF6	20	22	0	58	85,68	85,1	82,43	81,6	3,25	3,5
TERF1	38,5	25	10	26,5	76,1	74,8	70,07	69,8	6,03	5
TERF2	15	21	10	54	95,79	95,5	89,57	89,2	6,22	6,3
TERF3	22,5	7,5	8	62	85,97	85,1	82,65	82,5	3,32	2,6
TERF4	33,5	7,5	8	51	76,11	74,8	72,97	72	3,14	2,8
TERF5	10,5	6	8	75,5	95,78	96,3	92,3	92,4	3,48	3,9
TERF6	19	4	4	73	85,68	84,9	83,84	83,6	1,84	1,3
PRF1	5	0	0	95	94,23	94,8	94,3	94,8	-0,07	0
PRF2	25	0	0	75	75,32	74,8	75,47	74,9	0,2	-0,1

The quadratic regression models were further strengthened and revised by adding the 17 fuel blends presented in Table 7-2 to the previous matrices presented in Table 7-1. This decreased the error using the extrapolation method as illustrated in Figure 7-3. These new models have been verified to other fuel blends found in the literatures and the result showed good agreement. The accuracy of the regression

models were ±0.6. The new regression coefficients for RON and MON are presented in Table 7-3. The coefficient's values are not rounded because they will affect the final results.

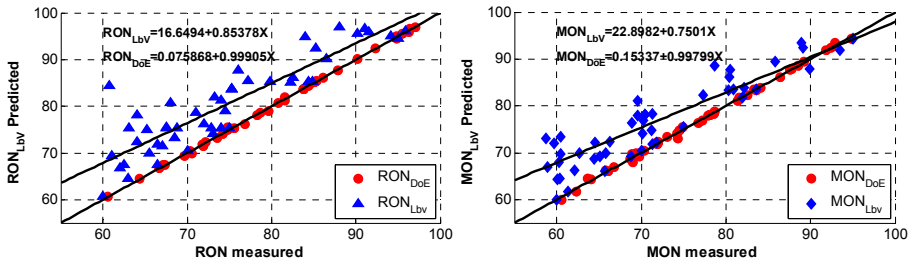

Figure 7-3 The predicted RON and MON from quadratic regression and linear by volume models as a function of measured RON and MON.

Table 7-3 Quadratic regression coefficients for modeling RON and MON.

Regression Coefficients	RON DoE	MON DoE
β	9.93022154471042 E02	9.86850560235952 E02
α_N	-9.4594723945044 E-01	-8.64864845159362E-01
α_T	2.06222143583251E-01	2.00072691374061E-02
α_E	6.86989203401194E-01	3.05420013275534E-01
γ_{NT}	1.13896609766388E-03	2.59735154733907E-03
γ_{NE}	6.48104716520684E-03	1.10360124285118E-02
γ_{TE}	-6.16465224755151E-03	-4.67070201387479E-03
δ_N^2	-5.25603364090350E-04	-2.54416497232109E-03
δ_T^2	9.28989700907245E-05	-4.80768630133682E-04
δ_E^2	-6.90416392044605E-03	-5.21969269652110E-03

Chapter 8

Concluding remarks

This section summarizes the main observations included in the thesis.

The studies in this thesis were performed to improve the understanding of engine performance and emissions in Partially Premixed Combustion. The main focus was on fuel effects but other engine parameters were also systematically studied and modelled to get a more complete picture.

PPC requires a certain level of premixing before ignition which means that the ignition delay can neither be too short nor too long. If the ignition delay is too short the combustion process will be similar to traditional diesel combustion and if it is too long it will be similar to HCCI combustion. The ignition delay is also important for the emission formation within PPC. For example, a longer ignition delay results in a longer mixing-period and greater premixed fraction and thus potentially a reduction of hot, fuel-rich zones associated with high formation rate of soot. Well-defined gasoline fuels, MK1 and oxygenated surrogate fuel blends were tested at similar operating conditions to bring out the most important features of fuel impact on ID. As expected; all studies showed a clear relation between ignition delay and RON where a higher RON gave a longer ID. More interestingly, it was revealed that similar RON resulted in similar ID despite variations in fuel composition. The later was proved to be valid both ways, meaning if fuel blends have similar ID during the same conditions they are likely to have similar RONs as well. This was confirmed by developing a quadratic regression model for ID which was established in Paper III and tested in Paper V. Furthermore, instead of increasing RON the ID can also be extended by a reduction in inlet O_2 concentration. However, it was shown that RON has a larger range for controlling ID since the O_2 level is limited to ambient conditions upwards and an insufficient O_2 concentration may result in incomplete combustion and misfire. An interaction effect between inlet O_2 and RON that was found showed that the impact of RON on ID is stronger at lower O_2 levels.

When the load range for PPC was investigated a relation between load, ignition delay, and RON was found. The ignition delay was shorter at higher loads for all

fuels. This means a fuel having a suitable ignition delay at low load will not be ideal at high loads due to insufficient ignition delay. A typical fuel with such characteristics is diesel fuel. In contrast, gasoline-like fuels will be more suitable at high load. A possible solution is to have a fuel with ignition delay between 6 to 8 degrees at low loads without EGR. Such a fuel facilitates low load operation with a high fraction of premixed combustion. As the load increases the inlet O_2 concentration is reduced in order to maintain a long ID and large premixed fraction. The interaction between RON and O_2 can also be used to decrease the engine out emissions. By reducing inlet O_2 concentration and fine tune the fraction of premixed combustion with RON the emissions of soot and NO_x may be reduced. This is since reduced inlet O_2 concentration will decrease the combustion temperature due to larger heat capacity of the fuel-gas-mixture at any given equivalence ratio. In such an attempt it is important to use sufficient EGR cooling not to increase the global in-cylinder temperature.

A linear correlation between ignition delay and fraction of LTR was observed. The increase of low temperature reactions with increasing ignition delay is a consequence of slowed down initial chemical reactions. The effect of fuel composition on LTR fraction was further investigated in order to understand its behaviour. Therefore a comparison was made between PPC and HCCI combustion. The trends of LTR fraction in HCCI combustion mainly depends on the chemical fuel properties since most of the evaporation and mixing are finished prior to IVC for port injected HCCI. The lack of similarities between LTR trends in PPC and HCCI combustion indicates that the processes behind LTR are more complex in PPC than in HCCI. It is not certain that a fuel with more pronounced chemical prerequisites for LTR will produce more LTR in PPC. The strong relation between LTR and ID indicate that the ignition quality is central for the fraction of LTR in PPC.

The main issue of pollutants in PPC are emissions of HC and CO due to introducing cooled EGR into the cylinder. It was showed that RON has a significant impact on HC and an even more pronounced impact on CO. If the RON value was increased, the HC and CO emissions were increased. In order to understand fuel composition effects on emissions the RON and ignition delay effects were decoupled, by keeping them fixed for a group of fuel blends. The results showed that the main contribution to emissions of HC, NO_x and smoke was the aromatic content in fuel blends. It was concluded that a fuel blend with a RON value between 65 and 75 and with lower aromatic concentration was the most suitable candidate for PPC.

Quadratic regression models were used to map RON and MON for oxygenated surrogate gasoline fuels. The models were validated against 17 fuel blends that first were predicted using the regression models and then measured. In general the

model works remarkably well for both interpolation and extrapolation. These models were further strengthened and revised by adding the 17 fuel blends to the previous matrices. This reduced the error using the extrapolation method. These new models have been verified to other fuel blends found in the literature and the results showed good agreement.

By using the quadratic regression models for predicting ignition delay and RON, it is possible to design a specific fuel with the specifications mentioned previously to meet both emissions legislations and reducing fuel consumption.

Chapter 9

References

[1] C. Lyle Cummins, Jr., “Internal Fire”, Third Revised Edition, Carnot Press, Wilsonville, Oregon, 2000.

[2] European Commission, Climate Action 2012 (August-October 2012), web site www.ec.europa.eu. Projections: Greenhouse Gas from Road Transport.

[3] K. Owen, T, Coley, “Automotive Fuels Reference Book”, second edition, Society of Automotive Engineers, Inc. United State of America 1995.

[4] J.B. Heywood,”Internal Combustion Engine Fundamentals”, International edition, McGraw-Hill, New York, 1988

[5] Bosch, “Automotive Handbook”, sixth edition, published by Robert Bosch, GmbH 2004

[6] Akihama, K., Takatori, Y., Inagaki, K., Sasaki, S. et al., "Mechanism of the Smokeless Rich Diesel Combustion by Reducing Temperature," SAE Technical Paper 2001-01-0655, 2001, doi:10.4271/2001-01-0655.

[7] Onishi, S., Jo, S., Shoda, K., Jo, P. et al., "Active Thermo-Atmosphere Combustion (ATAC) - A New Combustion Process for Internal Combustion Engines," SAE Technical Paper 790501, 1979, doi:10.4271/790501.

[8] Christensen, M., Hultqvist, A., and Johansson, B., "Demonstrating the Multi Fuel Capability of a Homogeneous Charge Compression Ignition Engine with Variable Compression Ratio," SAE Technical Paper 1999-01-3679, 1999, doi:10.4271/1999-01-3679.

[9] Xing-Cai Lü, Wei Chen, Zhen Huang, A fundamental study on the control of the HCCI combustion and emissions by fuel design concept combined with controllable EGR. Part 1. The basic characteristics of HCCI combustion, Fuel, Volume 84, Issue 9, June 2005, Pages 1074-1083, ISSN 0016-2361, http://dx.doi.org/10.1016/j.fuel.2004.12.014.

[10] Takahashi, Y., Suyama, K., Iijima, A., Yoshida, K. et al., "A Study of HCCI Combustion Using Spectroscopic Measurements and Chemical Kinetic Simulations: Effects of Fuel Composition, Engine Speed and Cylinder Pressure on Low-temperature Oxidation Reactions and Autoignition," SAE Int. J. Engines5(1):25-33, 2012, doi:10.4271/2011-32-0524.

[11] Sjöberg, M. and Dec, J., "Influence of Fuel Autoignition Reactivity on the High-Load Limits of HCCI Engines," SAE Int. J. Engines 1(1):39-58, 2009, doi:10.4271/2008-01-0054.

[12] Johansson, T., Johansson, B., Tunestål, P., and Aulin, H., "The Effect of Intake Temperature in a Turbocharged Multi Cylinder Engine operating in HCCI mode," SAE Int. J. Engines 2(2):452-466, 2010, doi:10.4271/2009-24-0060.

[13] Aoyama, T., Hattori, Y., Mizuta, J., and Sato, Y., "An Experimental Study on Premixed-Charge Compression Ignition Gasoline Engine," SAE Technical Paper 960081, 1996, doi:10.4271/960081.

[14] Kitano, K., Nishiumi, R., Tsukasaki, Y., Tanaka, T. et al., "Effects of Fuel Properties on Premixed Charge Compression Ignition Combustion in a Direct Injection Diesel Engine," SAE Technical Paper 2003-01-1815, 2003, doi:10.4271/2003-01-1815.

[15] Splitter, D., Reitz, R., and Hanson, R., "High Efficiency, Low Emissions RCCI Combustion by Use of a Fuel Additive," SAE Int. J. Fuels Lubr. 3(2):742-756, 2010, doi:10.4271/2010-01-2167.

[16] Hanson, R., Kokjohn, S., Splitter, D., and Reitz, R., "Fuel Effects on Reactivity Controlled Compression Ignition (RCCI) Combustion at Low Load," SAE Int. J. Engines 4(1):394-411, 2011, doi:10.4271/2011-01-0361.

[17] Noehre, C., Andersson, M., Johansson, B., and Hultqvist, A., "Characterization of Partially Premixed Combustion," SAE Technical Paper 2006-01-3412, 2006, doi:10.4271/2006-01-3412.

[18] Kimura, S., Aoki, O., Ogawa, H., Muranaka, S. et al., "New Combustion Concept for Ultra-Clean and High-Efficiency Small DI Diesel Engines," SAE Technical Paper 1999-01-3681, 1999, doi:10.4271/1999-01-3681.

[19] Kimura, S., Aoki, O., Kitahara, Y., and Aiyoshizawa, E., "Ultra-Clean Combustion Technology Combining a Low-Temperature and Premixed Combustion Concept for Meeting Future Emission Standards," SAE Technical Paper 2001-01-0200, 2001, doi:10.4271/2001-01-0200.

[20] Kimura, S., Ogawa, H., Matsui, Y., Enomoto, Y., "An expermintal analysis of low-temperature and premixed combustion for simultaneous in direct injection diesel engines," International Journal of Engine Research, August 1, 2002 vol 3 no.4 249-259, doi:10.1243/14680870276223032.

[21] Hiromichi Yanagihara, Yasuo Sato, Jun'ichi Mizuta, A study of DI diesel combustion under uniform higher-dispersed mixture formation, JSAE Review, Volume 18, Issue 4, October 1997, Pages 361-367, ISSN 0389-4304, http://dx.doi.org/10.1016/S0389-4304(97)00031-3.

[22] Hildingsson, L., Persson, H., Johansson, B., Collin, R. et al., "Optical Diagnostics of HCCI and UNIBUS Using 2-D PLIF of OH and Formaldehyde," SAE Technical Paper 2005-01-0175, 2005, doi:10.4271/2005-01-0175.

[23] Lewander, M., Ekholm, K., Johansson, B., Tunestål, P. et al., "Investigation of the Combustion Characteristics with Focus on Partially Premixed Combustion in a Heavy Duty Engine," SAE Int. J. Fuels Lubr. 1(1):1063-1074, 2009, doi:10.4271/2008-01-1658.

[24] Musculus, M., Lachaux, T., Pickett, L., and Idicheria, C., "End-of-Injection Over-Mixing and Unburned Hydrocarbon Emissions in Low-Temperature-Combustion Diesel Engines," SAE Technical Paper 2007-01-0907, 2007, doi:10.4271/2007-01-0907.

[25] Alriksson, M. and Denbratt, I., "Low Temperature Combustion in a Heavy Duty Diesel Engine Using High Levels of EGR," SAE Technical Paper 2006-01-0075, 2006, doi:10.4271/2006-01-0075.

[26] Kim, D., Ekoto, I., Colban, W., and Miles, P., "In-cylinder CO and UHC Imaging in a Light-Duty Diesel Engine during PPCI Low-Temperature Combustion," SAE Int. J. Fuels Lubr. 1(1):933-956, 2009, doi:10.4271/2008-01-1602.

[27] Guibet, J.C.,"Fuel and Engines-Technology , energy, enviroment", Editions Techinp, Paris, 1999

[28] The international Organization for Standardization, "Petroleum products-Determination of knock characteristics of motor and aviation fuels- motor method". Available at: www.iso.org /29-05-2014.

[29] Kalghatgi, G.,"Fuel/Engine Interactions", Published by SAE International with a Product Code of R-409, ISBN of 978-0-7680-6458-2, and 272 pages in a hardbound binding, 2013.

[30] Guilherme B. Machado, José E.M. Barros, Sérgio L. Braga, Carlos Valois M. Braga, Edimilson J. de Oliveira, Antonio H.M. da F.T. da Silva, Leonardo de O. Carvalho, Investigations on surrogate fuels for high-octane oxygenated gasolines, Fuel, Volume 90, Issue 2, February 2011, Pages 640-646, ISSN 0016-2361, http://dx.doi.org/10.1016/j.fuel.2010.10.024.

[31] Kalghatgi, G., "Fuel Anti-Knock Quality - Part I. Engine Studies," SAE Technical Paper 2001-01-3584, 2001, doi:10.4271/2001-01-3584.

[32] Risberg, P., Kalghatgi, G., and Ångstrom, H., "Auto-ignition Quality of Gasoline-Like Fuels in HCCI Engines," SAE Technical Paper 2003-01-3215, 2003, doi:10.4271/2003-01-3215.

[33] Kalghatgi, G. and Head, R., "The Available and Required Autoignition Quality of Gasoline - Like Fuels in HCCI Engines at High Temperatures," SAE Technical Paper 2004-01-1969, 2004, doi:10.4271/2004-01-1969.

[34] Shibata, G. and Urushihara, T., "Auto-Ignition Characteristics of Hydrocarbons and Development of HCCI Fuel Index," SAE Technical Paper 2007-01-0220, 2007, doi:10.4271/2007-01-0220.

[35] Shibata, G., Oyama, K., Urushihara, T., and Nakano, T., "The Effect of Fuel Properties on Low and High Temperature Heat Release and Resulting Performance of an HCCI Engine," SAE Technical Paper 2004-01-0553, 2004, doi:10.4271/2004-01-0553.

[36] Truedsson, I.," The HCCI Fuel Number Measuring and Describing Auto-ignition for HCCI Combustion Engines", ISBN 978-91-7473-949-7, Lund University 2014.

[37] Shibata, G., Oyama, K., Urushihara, T., and Nakano, T., "Correlation of Low Temperature Heat Release With Fuel Composition and HCCI Engine Combustion," SAE Technical Paper 2005-01-0138, 2005, doi:10.4271/2005-01-0138.

[38] Truedsson, I., Tuner, M., Johansson, B., and Cannella, W., "Pressure Sensitivity of HCCI Auto-Ignition Temperature for Primary Reference Fuels," SAE Int. J. Engines 5(3):1089-1108, 2012, doi:10.4271/2012-01-1128.

[39] Shigeyuki Tanaka, Ferran Ayala, James C. Keck, John B. Heywood, Two-stage ignition in HCCI combustion and HCCI control by fuels and additives, Combustion and Flame, Volume 132, Issues 1–2, January 2003, Pages 219-239, ISSN 0010-2180, http://dx.doi.org/10.1016/S0010-2180(02)00457-1.

[40] Tsujimura, T., Pitz, W., Yang, Y., and Dec, J., "Detailed Kinetic Modeling of HCCI Combustion with Isopentanol," *SAE Int. J. Fuels Lubr.* 4(2):257-270, 2011, doi:10.4271/2011-24-0023.

[41] Christensen, M., Hultqvist, A., and Johansson, B., "Demonstrating the Multi Fuel Capability of a Homogeneous Charge Compression Ignition Engine with Variable Compression Ratio," SAE Technical Paper 1999-01-3679, 1999, doi:10.4271/1999-01-3679.

[42] Bunting, B. G., Wildman, C. B., Szybist, J. P., Lewis, S., & Storey, J. (2007 February)Fuel chemistry and cetane effects on diesel homogeneous charge compression ignition performance, combustion, and emissions. *8 (1)*, 15-27. doi:10.1243/14680874JER01306.

[43] Truedsson, I., Tuner, M., Johansson, B., and Cannella, W., "Pressure Sensitivity of HCCI Auto-Ignition Temperature for Gasoline Surrogate Fuels," SAE Technical Paper 2013-01-1669, 2013, doi:10.4271/2013-01-1669.

[44] Neely, G., Sasaki, S., and Leet, J., "Experimental Investigation of PCCI-DI Combustion on Emissions in a Light-Duty Diesel Engine," SAE Technical Paper 2004-01-0121, 2004, doi:10.4271/2004-01-0121.

[45] Okude, K., Mori, K., Shiino, S., and Moriya, T., "Premixed Compression Ignition (PCI) Combustion for Simultaneous Reduction of NOx and Soot in Diesel Engine," SAE Technical Paper 2004-01-1907, 2004, doi:10.4271/2004-01-1907.

[46] Lechner, G., Jacobs, T., Chryssakis, C., Assanis, D. et al., "Evaluation of a Narrow Spray Cone Angle, Advanced Injection Timing Strategy to Achieve Partially Premixed Compression Ignition Combustion in a Diesel Engine," SAE Technical Paper 2005-01-0167, 2005, doi:10.4271/2005-01-0167.

[47] Idicheria, C. and Pickett, L., "Soot Formation in Diesel Combustion under High-EGR Conditions," SAE Technical Paper 2005-01-3834, 2005, doi: 10.4271/2005-01-3834.

[48] Ickes, A., Assanis, D., and Bohac, S., "Load Limits with Fuel Effects of a Premixed Diesel Combustion Mode," SAE Technical Paper 2009-01-1972, 2009, doi:10.4271/2009-01-1972.

[49] Kalghatgi, G., Risberg, P., and Ångström, H., "Advantages of Fuels with High Resistance to Auto-ignition in Late-injection, Low-temperature, Compression Ignition Combustion," SAE Technical Paper 2006-01-3385, 2006, doi: 10.4271/2006-01-3385.

[50] Kalghatgi, G., Hildingsson, L., Harrison, A. J., Johansson, B., "Surrogate fuels for premixed combustion in compression ignition engines," Int. J. of Engine Research, doi:10.1177/1468087411409307, October 2011, vol. 12 no. 5 452-465.

[51] Kitano, K., Nishiumi, R., Tsukasaki, Y., Tanaka, T. et al., "Effects of Fuel Properties on Premixed Charge Compression Ignition Combustion in a Direct Injection Diesel Engine," SAE Technical Paper 2003-01-1815, 2003, doi: 10.4271/2003-01-1815.

[52] Kidoguchi, Y., Yang, C., and Miwa, K., "Effects of Fuel Properties on Combustion and Emission Characteristics of a Direct-Injection Diesel Engine," SAE Technical Paper 2000-01-1851, 2000, doi: 10.4271/2000-01-1851.

[53] Jain, A., Babu, V., Saxena, M., Aigal, A. et al., "Effect of Gasoline Composition (Olefins, Aromatics and Benzene) on Automotive Exhaust Emissions - A Literature Review," SAE Technical Paper 2004-28-0081, 2004, doi:10.4271/2004-28-0081.

[54] Lee, R., Pedley, J., and Hobbs, C., "Fuel Quality Impact on Heavy Duty Diesel Emissions:- A Literature Review," SAE Technical Paper 982649, 1998, doi:10.4271/982649.

[55] Warey, A., Hardy, J., Hennequin, M., Tatur, M. et al., "Fuel Effects on Low Temperature Combustion in a Light-Duty Diesel Engine," SAE Technical Paper 2010-01-1122, 2010, doi: 10.4271/2010-01-1122.

[56] Manente, V., Johansson, B., and Tunestal, P., "Partially Premixed Combustion at High Load using Gasoline and Ethanol, a Comparison with Diesel," SAE Technical Paper 2009-01-0944, 2009, doi: 10.4271/2009-01-0944.

[57] Manente, V., Zander, C., Johansson, B., Tunestal, P. et al., "An Advanced Internal Combustion Engine Concept for Low Emissions and High Efficiency from Idle to Max Load Using Gasoline Partially Premixed Combustion," SAE Technical Paper 2010-01-2198, 2010, doi:10.4271/2010-01-2198.

[58] Borgqvist, P., Andersson, Ö., Tunestål P., Johansson, B.," The Low Load Limit of Gasoline Partially Premixed Cobmustion Using Negative Valve Overlap", the ASME 2012 Internal Combustion Engine Division Fall Technical Conference, ICEF2012-92069.

[59] Kaiadi, M., Johansson, B., Lundgren, M., and Gaynor, J., "Sensitivity Analysis Study on Ethanol Partially Premixed Combustion," SAE Int. J. Engines 6(1):120-131, 2013, doi:10.4271/2013-01-0269.

[60] Shen, M., Tuner, M., and Johansson, B., "Close to Stoichiometric Partially Premixed Combustion -The Benefit of Ethanol in Comparison to Conventional Fuels," SAE Technical Paper 2013-01-0277, 2013, doi:10.4271/2013-01-0277.

[61] B. Johansson, "Förbränningsmotorer" Lund Institute of Technology, Lund University 2006.

[62] Egnell, R., "On Zero-dimensional Modelling of Combustion and NOx Formation in Diesel Engines", Lund University, 2001.

[63] Aronsson, U., Chartier, C., Andersson, Ö., Johansson, B. et al., "Analysis of EGR Effects on the Soot Distribution in a Heavy Duty Diesel Engine using Time-Resolved Laser Induced Incandescence," SAE Int. J. Engines3(2):137-155, 2010, doi:10.4271/2010-01-2104.

[64] Andersson, Ö., "Experiment: Planning, Implementing and Interpreting", First edition, John Wiley & Sons, Ltd, 2012.

[65] Farrell, J. and Bunting, B., "Fuel Composition Effects at Constant RON and MON in an HCCI Engine Operated with Negative Valve Overlap," SAE Technical Paper 2006-01-3275, 2006, doi:10.4271/2006-01-3275.

[66] Ekoto, I., Colban, W., Miles, P., Park, S. et al., "UHC and CO Emissions Sources from a Light-Duty Diesel Engine Undergoing Dilution-Controlled Low-Temperature Combustion," SAE Int. J. Engines 2(2):411-430, 2010, doi:10.4271/2009-24-0043.

[67] Aronsson, U., Andersson, Ö., Egnell, R., Miles, P. et al., "Influence of Spray-Target and Squish Height on Sources of CO and UHC in a HSDI Diesel Engine During PPCI Low-Temperature Combustion," SAE Technical Paper 2009-01-2810, 2009, doi:10.4271/2009-01-2810.

[68] Kee, S., Mohammadi, A., Kidoguchi, Y., and Miwa, K., "Effects of Aromatic Hydrocarbons on Fuel Decomposition and Oxidation Processes in Diesel Combustion," SAE Technical Paper 2005-01-2086, 2005, doi:10.4271/2005-01-2086.

[69] Xioa, Z., Ladommatos, N., Zhao, H., "The Effect of Aromatic Hydrocarbons and Oxygenates on Diesel Engine Emissions", Journal of Automobile Engineering March 1, 2000 vol.214 no.3 307-332, doi: 10.1243/0954407001527448.

[70] Svensson, K., Richards, M., Mackrory, A., and Tree, D., "Fuel Composition and Molecular Structure Effects on Soot Formation in Direct-Injection Flames Under Diesel Engine Conditions," SAE Technical Paper 2005-01-0381, 2005, doi:10.4271/2005-01-0381.

[71] Plee, S. and Ahmad, T., "Relative Roles of Premixed and Diffusion Burning in Diesel Combustion," SAE Technical Paper 831733, 1983, doi:10.4271/831733.

[72] Idicheria, C. and Pickett, L., "Soot Formation in Diesel Combustion under High-EGR Conditions," SAE Technical Paper 2005-01-3834, 2005, doi:10.4271/2005-01-3834.

[73] Aronsson, U., Chartier, C., Andersson, Ö., Egnell, R. et al., "Analysis of the Correlation Between Engine-Out Particulates and Local Φ in the Lift-Off Region of a Heavy Duty Diesel Engine Using Raman Spectroscopy," SAE Int. J. Fuels Lubr. 2(1):645-660, 2009, doi:10.4271/2009-01-1357.

[74] Miles, P. C., et al. "Rate-limiting processes in late-injection, low-temperature diesel combustion regimes." Proc. THIESEL 2004 Conference. 2004.

[75] Koci, C., Ra, Y., Krieger, R., Andrie, M. et al., "Detailed Unburned Hydrocarbon Investigations in a Highly-Dilute Diesel Low Temperature Combustion Regime," SAE Int. J. Engines 2(1):858-879, 2009, doi:10.4271/2009-01-0928.

[76] He, B., Wang, J., Yan, X., Tian, X. et al., "Study on Combustion and Emission Characteristics of Diesel Engines Using Ethanol Blended Diesel Fuels," SAE Technical Paper 2003-01-0762, 2003, doi:10.4271/2003-01-0762.

[77] Neal Morgan, Andrew Smallbone, Amit Bhave, Markus Kraft, Roger Cracknell, Gautam Kalghatgi, Mapping surrogate gasoline compositions into RON/MON space, Combustion and Flame, Volume 157, Issue 6, June 2010, Pages 1122-1131, ISSN 0010-2180, http://dx.doi.org/10.1016/j.combustflame.2010.02.003.

[78] Anderson, J., Leone, T., Shelby, M., Wallington, T. et al., "Octane Numbers of Ethanol-Gasoline Blends: Measurements and Novel Estimation Method from Molar Composition," SAE Technical Paper 2012-01-1274, 2012, doi:10.4271/2012-01-1274.

Chapter 10

Summary of papers

10.1 Paper I

Investigation of Partially Premixed Combustion characteristics in Low Load Range with Regards to Fuel Octane Number in a Light-Duty Diesel Engine

Hadeel Solaka, Ulf Aronsson, Martin Tunér, Bengt Johansson

SAE Technical Paper 2012-01-0684

The objective of this study was to investigate the stable load region as function of RON for PPC. The investigation also focused on classifying the combustion events into four phases: ignition delay, low temperature reactions, premixed combustion and late mixing controlled combustion. The stable load range for PPC at a given EGR rate and air-fuel ratio depended on interactions between ignition delay and RON values. The low load limit was higher at higher octane numbers.

Experiment and post-processing of data were performed by the author. The paper was written by the author in close cooperation with Ulf Aronsson, Bengt Johansson and Martin Tunér.

10.2 Paper II

Investigation on the Impact of Fuel Properties on Partially Premixed Combustion Characteristics in a Light Duty Diesel Engine

Hadeel Solaka, Martin Tunér, Bengt Johansson

ASME Technical Paper ICES2012-81184

This study focused on effects of fuel properties and combustion phasing on combustion events and emissions for PPC. High RON fuels had a small operable combustion phasing region. Engine-out emissions of NO_x and smoke were reduced but HC and CO emissions were increased with increased RON.

Experiment and post-processing of data were performed by the author. The paper was written by the author in cooperation with Bengt Johansson and Martin Tunér.

10.3 Paper III

Analysis of Surrogate Fuels Effect on Ignition delay and Low Temperature Reaction during Partially Premixed Combustion

Hadeel Solaka, Martin Tunér, Bengt Johansson

SAE Technical Paper 2013-01-0903

The focus of this study was on understanding the influence of surrogate fuel mixtures on ignition delay and low temperature reactions. A model predicting the ignition delay and low temperature reaction in context to surrogate fuel mixtures were derived with help of Design of Experiment. Another focus of this work was to study the effect of engine inlet parameters on both ignition delay and low temperature reactions.

Experiment and post-processing of data were performed by the author. The paper was written by the author in cooperation with Bengt Johansson and Martin Tunér.

10.4 Paper IV

Gasoline Surrogate Fuels for Partially Premixed Combustion, of Toluene Ethanol Reference Fuels

Hadeel Solaka, Martin Tunér, Bengt Johansson, William Cannella

SAE Technical Paper 2013-01-2540

The aim of this study was to investigate the influence of surrogate fuel properties such as RON and fuel composition on combustion duration and emissions. NO_x, smoke were increased by increasing toluene content in the blend, while HC and CO were more related to the RON value. Also the effects of inlet O_2 concentration and injection pressure were studied. NO_x emission was reduced by reducing the inlet O_2 while HC and CO increased. The smoke level was reduced with increased injection pressure.

Experiment and post-processing of data were performed by the author. The paper was written by the author in cooperation with Bengt Johansson, Martin Tunér and William Cannella.

10.5 Paper V

Using Oxygenated Gasoline Surrogate Composition to Map RON and MON

Hadeel Solaka Aronsson, Martin Tunér, Bengt Johansson

SAE Technical Paper 2014-01-1303

Quadratic regression models were used to map RON and MON for oxygenated surrogate fuels. Another regression model was used to find three fuel blends with different fuel composition but similar ignition delay. This separates the fuel composition effect from ignition quality effects on combustion and emissions. The models worked remarkably well for predicting RON, MON and ID.

Experiment and post-processing of data were performed by the author. The paper was written by the author in cooperation with Bengt Johansson and Martin Tunér.

10.6 Paper VI

Manuscript submitted to SAE 2014 International Powertrain, Fuels and Lubricant meeting

Comparison of Fuel Effects on Low Temperature Reactions in PPC and HCCI Combustion

Hadeel Solaka Aronsson, Ida Truedsson, Martin Tunér, Bengt Johansson, William Cannella

This work compared fuel effects on the fraction of low temperature reactions (LTR) in PPC and HCCI to sort out the importance of the chemical and physical properties. Ethanol, toluene and isooctane quenched the LTR fraction in HCCI, while they stimulated the LTR fraction in PPC. This is because the fraction of LTR in PPC was more influenced by the ignition quality than the fuel composition.

Experiment and post-processing of data were performed by the author. Experiment data for HCCI was performed by Ida Truedsson. The paper was written by the author in close cooperation with Bengt Johansson and Martin Tunér, Ida Truedsson and William Cannella.

Paper I

Gratis copy for Hadeel Solaka
Copyright 2012 SAE International
E-mailing, copying and internet posting are prohibited
Downloaded Wednesday, March 21, 2012 05:11:13 AM

SAE International®

Investigation of Partially Premixed Combustion Characteristics in Low Load Range with Regards to Fuel Octane Number in a Light-Duty Diesel Engine

2012-01-0684
Published
04/16/2012

Hadeel Solaka
Lund University

Ulf Aronsson
Volvo Group Trucks Technology

Martin Tuner and Bengt Johansson
Lund University

Copyright © 2012 SAE International
doi:10.4271/2012-01-0684

ABSTRACT

The impact of ignition quality and chemical properties on engine performance and emissions during low load partially premixed combustion (PPC) in a light-duty diesel engine were investigated. Four fuels in the gasoline boiling range, together with Swedish diesel (MK1), were operated at loads between 2 and 8 bar $IMEP_g$ at 1500 rpm, with 50% heat released located at 6 crank angle degrees (CAD) after top dead center (TDC). A single injection strategy was used, wherein the start of injection (SOI) and the injection duration were adjusted to achieve desired loads with maintained CA50, as the injection pressure was kept constant at 1000 bar. The objective of this work was to examine the low-load limit for PPC at approximately 50% EGR and λ=1.5, since these levels had been suggested as optimal in earlier studies. The low-load limits with stable combustion were between 5 and 7 bar gross IMEP for the gasoline fuels, higher limit for higher RON values. MK1 had the lowest low-load limit, 3 bar gross IMEP. By increasing λ with the kept EGR ratio, with extended boosting, all the fuels could be operated down to 2 bar $IMEP_g$. The main difference in engine-out emissions between the fuels was the filtered smoke number (FSN), as the gasoline fuels produced much lower smoke than MK1. Higher RON value gave higher levels of carbon monoxide (CO) and unburned hydrocarbon (HC) for the gasoline fuels, while MK1 had the lowest levels of these emissions.

INTRODUCTION

Direct injection compression ignition (DICI) diesel engines for passenger cars have higher efficiency than spark ignition (SI) engines. However, stringent emission legislation demands continued reduction in engine-out emissions especially for particulate matter (PM) and nitrogen oxide (NO_X), but the limits for HC and CO are also demanding. Hence, the challenge is to reduce PM and NO_X without increased levels of CO and HC with new combustion strategies. Many studies in recent years have tried to achieve reduction in emissions by introducing and re-examining different combustion concepts.

Two important pollutants from diesel engines are NO_X and PM. Soot forms at temperatures between 1600 and 2400 K and at an equivalence ratio (Φ) larger than two, while soot oxidization is most pronounced at low equivalence ratios and high temperatures. The level of engine-out soot corresponds to the net difference between formation and oxidation. NO_X is formed either from atmospheric nitrogen or nitrogen from the fuel but with a different mechanism. The major part of NO_X formation during diesel combustion is formed by the thermal mechanism. Its principle reactions have been explained by Zeldovich and Lavoie. NO_X forms above 2000 K at an equivalence ratio lower than two. By introducing large amounts of cooled exhaust gas recirculation (EGR) the combustion temperature can be reduced below the threshold

Gratis copy for Hadeel Solaka
Copyright 2012 SAE International
E-mailing, copying and internet posting are prohibited
Downloaded Wednesday, March 21, 2012 05:11:13 AM

for soot and NO_x formation. The EGR works as a heat absorbing bulk gas, thereby slowing down the kinetic reactions [1,2,3].

Over the last few decades, many concepts have been introduced in order to reduce pollutants from CI engines. One such concept is Homogenous Charge Compression Ignition (HCCI), which was introduced by Onishi [4] in 1979. In HCCI, the fuel and air are fully premixed as in a spark ignition (SI) engine but utilizes compression ignition. HCCI has low NO_x and Soot emissions compared to traditional diesel combustion [5]. However, controlling HCCI combustion is very difficult since auto-ignition chemistry, which determines HCCI combustion timing, depends on pressure, temperature, and on other factors such as fuel chemistry, O_2 concentration [6,7,8,9]. High loads are especially challenging due to high maximum pressure-rise rates, which cause material stress and produce high acoustic noise [10].

Another suggested combustion concept is called Nissan Modulated Kinetics (MK) [11, 12]. This concept proposes late injection, high swirl and high amount of cooled EGR to reduce NO_x and soot.

To overcome the limitation with HCCI and MK combustion concepts, a new concept called Partially Premixed Combustion (PPC) has been introduced [13]. PPC or premixed compression ignition (PCI), imply that an engine operates between fully homogeneous and diffusion control combustion [14] but with a small difference: PPC uses more EGR than PCI, around 50% compared to 30% [15]. In PPC it is desirable to separate the end of injection from the start of combustion [14]. The authors in [11,13,14,15,16,17] described how the separation between end of injection and start of combustion can be achieved, which is to use a large amount of exhaust gas recirculation (EGR), early start of injection, low compression ratio, and fuel with a high octane number (ON).

In 2006, it was demonstrated that using gasoline fuel in a compression ignition engines has potential to produce low levels of engine-out emissions [18,19]. Since gasoline has a higher resistance to auto-ignition compared to diesel fuel, it gives more time for mixing, thus producing a higher fraction of premixed combustion. However, one of the problems of pre-mixed combustion is the high rate of heat release. This leads to higher pressure rise rate and noise, especially if the premixed combustion occurs before top dead center. To overcome this problem a large amount of EGR is used to avoid reaction during the compression stroke and slow down chemistry reaction. This also reduces the combustion temperature and formation of NO_x and soot.

The authors in [17] suggested that the optimum EGR ratio and $\lambda = \frac{A/F}{A/F_s}$ for PPC are about 50% and 1.5 respectively. These settings were shown to give low emissions of soot and NO_x, together with high fuel efficiency. However, it was not possible to achieve stable combustion at low loads for high RON fuels during these conditions, as the experiments were performed in a heavy-duty diesel engine. Thus, the question remains: how does the operating range change when the same conditions are used in a light-duty engine. The aim of this work is to examine the low-load limit for PPC at the suggested settings in [17], approximately 50% EGR and λ=1.5, for four fuels in the gasoline boiling range together with MK1 in a light duty diesel engine.

EXPERIMENTS

ENGINE SETUP

Experiments were performed using an in-line 5-cylinder diesel engine (Volvo D5) operated on one cylinder. Details of the engine are given in Table 1.

Table 1. Engine properties.

Compression ratio, r_c [-]	16.5
Displacement volume [cm^2/cylinder]	480
Bore [mm]	81
Stroke [mm]	93.2
IVC [CAD BTDC]	174
Injection nozzle hole	7
& diameter [mm]	0.14
Included angle [degrees]	140
Injector type	Solenoid
Swirl number [-]	2.2

The engine test rig was equipped with an adjustable exhaust gas recirculation system and adjustable heating of the inlet temperature (see Figure 1).

Gratis copy for Hadeel Solaka
Copyright 2012 SAE International
E-mailing, copying and internet posting are prohibited
Downloaded Wednesday, March 21, 2012 05:11:13 AM

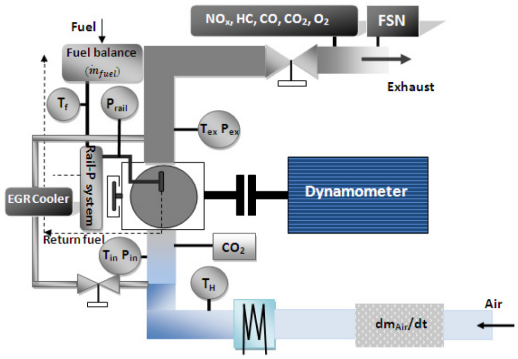

Figure 1. Experimental set-up.

EGR_{RATIO}

The EGR_{ratio} is defined as a ratio between CO_2 concentration in the inlet air to the engine to the CO_2 concentration in the exhaust gases from the engine.

$$EGR_{ratio} = \frac{CO_{2\,Inlet}}{CO_{2\,Exhaust}} \qquad (1)$$

The exhaust gases were cooled in a heat exchanger, using the engine's coolant water as a heat absorber, before it was mixed with the inlet air. The mixture temperature was controlled by heating the fresh charge before it was blended with the EGR, and the temperature target was set to 335 K (see Figure1).

INJECTION SYSTEM

The injection system consisted of common rail, high-pressure pipe, high- and low-pressure pumps and piezo injector. However, during initial experiments it was discovered that the piezo injector had low reliability when operated on gasoline. Running with the piezo injector the combustion died after 15 minutes using gasoline fuels, this could be related to the viscosity difference between gasoline and diesel fuel. To overcome this obstacle, the injection system was modified from piezo to solenoid injector (see Table 1 for injector specifications).

INTAKE AIR and FUEL MASS-FLOW

The intake air mass flow was measured by a thermal mass flow meter (Bronckhorst INFLOW). It was situated approximately 3 m upstream from the intake manifold in order to prevent pressure oscillations to propagate from the engine, or EGR system, into the flow meter. Fuel mass flow was measured by a fuel balance (Sartorius CPA 62025) over a time span of 120 seconds per measurement point.

EMISSIONS

Smoke emissions were measured with the AVL415S smoke meter, while NO_x, HC, exhaust CO_2, CO and intake CO_2 emissions were measured with a Horiba measurement system (MEXA9200DF). NO_x emissions were measured with a chemiluminescence analyzer whereas HC was measured with a hydrogen flame ionization detector (FID) and the piping to the analyzer was heated to approximately 191°C to avoid condensation of unburned fuel components. Oxygen (O_2) was measured by a magneto-pneumatic condenser microphone method (MPA), whereas CO, intake CO_2 and exhaust CO_2 were measured with an infrared analyzer.

FUELS

Five fuels were included in the experiments: four fuels in the gasoline boiling range, and as reference Swedish environmental Class 1 diesel fuel (MK1) (see Table 2). In order to ensure that no damage was caused to the injection system, 500 ppm lubricity additive Infineum R655 was added to each gasoline fuel. The impact, on combustion phasing and emission formation, of the additive is expected to be neglectable at such small fraction.

Table 2. Fuel properties and specifications.

Fuel	RON	MON	CN	C	H/C	O/C	LHV [MJ/kg]	A/F_s
A	69.4	66.1	-	7.11	1.98	0	43.80	14.68
B	78.2	73.4	-	7.16	1.97	0	43.70	14.65
C	87.1	80.5	-	7.20	1.92	0	43.50	14.60
D	88.6	79.5	-	7.21	1.88	0	43.50	14.53
MK1	n.a	-	54	7.2	1.83	0	43.15	14.49

METHODS and DEFINITIONS

The rate of heat release was calculated using the in-cylinder pressure trace from 300 cycles. The method for the rate of heat release calculation,

$$\frac{\partial Q}{\partial \theta} = \frac{\gamma}{\gamma - 1} p \frac{\partial V}{\partial \theta} + \frac{1}{\gamma - 1} V \frac{\partial p}{\partial \theta} + \frac{\delta Q_{losses}}{\delta \theta} \qquad (2)$$

followed the description in Heywood [1]. The convective heat transfer was estimated according to Woschni, and mass losses or blow-by was accounted for assuming choked flow over the piston ring gap [1]. To estimate γ a model described by Egnell was used [20].

From the calculated rate of heat release, information about the combustion events can be extracted. In the analysis, the

Gratis copy for Hadeel Solaka
Copyright 2012 SAE International
E-mailing, copying and internet posting are prohibited
Downloaded Wednesday, March 21, 2012 05:11:13 AM

combustion is divided into four phases: the ignition delay, the low temperature reaction (LTR), the premixed combustion, and the late mixing controlled combustion phase.

The ignition delay is identified by the *endotherm* phase due to fuel heating and evaporation between start of injection (SOI), and start of combustion. The *start of injection* is estimated from the injector current signal. The *start of combustion* (SOC) is defined as the point where the rate of heat release turns positive after SOI, that is 0% heat release completion (CA0) (see Figure 2).

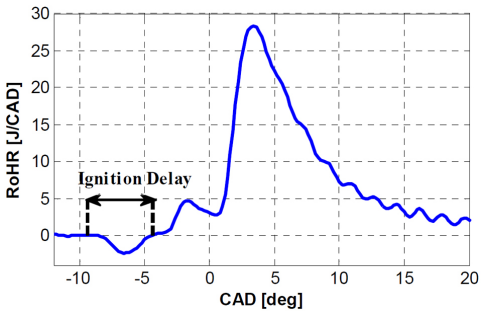

Figure 2. Rate of heat release as a function of crank angle degree at 2 bar gross IMEP. Figure shows ignition delay period.

Low temperature reaction (LTR) is characterized by a small peak before the main premixed heat release. The reason for the lower rate of heat release between those peaks is that the speed of the low temperature reactions decreases with increasing temperature (see Figures 3).

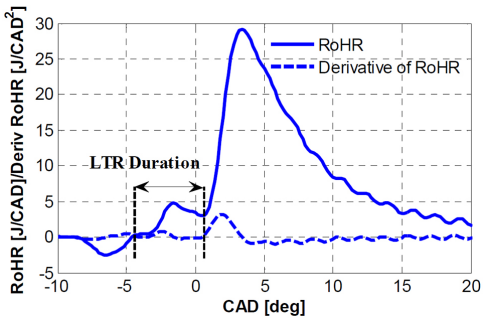

Figure 3. Rate of heat release and gradient of rate of heat release as a function of crank angle degree at 2 bar gross IMEP. Figure shows the low temperature reaction phase.

The *low temperature reaction duration* is defined as the part between SOC and the end of LTR (see Figure 3). The end of LTR is defined as the point where the gradient of rate of heat release reaches 0.05 J/CAD^2. This threshold was selected as the lowest value that gave a robust definition.

The *fraction of low temperature reaction* is the ratio between the accumulated heat release from the LTR and the total heat release.

In the *premixed combustion phase*, the combustible fuel and air mixture burns rapidly [1]. This phase is controlled by chemical kinetics, and reaction speed depends mainly on temperature. In the current study, the premixed- and late- heat release rate are not distinctly separated. This is because parts of the premixed combustion phase are limited by mixing, and parts of the late combustion phase depends on slow reactions rather than mixing. In order to separate the phases in a well defined manner, a Gaussian

$$G(x) = h \cdot e^{-\left(\frac{x-x_0}{2\alpha^2}\right)^2} \qquad (3)$$

profile is fitted to the rising flank of the premixed peak, between the end of LTR and the actual peak, and the integrated area of the profile is used as a measure of the premixed reactions. In Eq. 3 x_0 is the central position of the peak, h and α representing the height and width of the Gaussian profile. Figure 4 shows the rate of heat release as a function of crank angle together with the Gaussian profile. As is evident, the fit follows the premixed heat release closely. The Gaussian profile is a mathematical rather than a physical representation of the premixed reaction phase. However, it provides as a robust measure of the premixed reactions for all the operated cases.

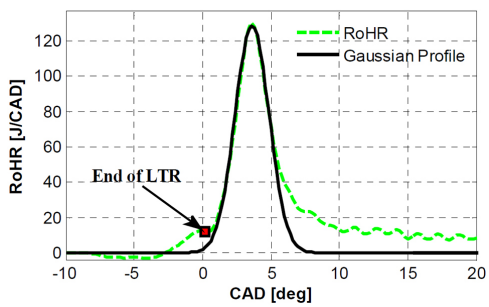

Figure 4. Rate of heat release and Gaussian profile as a function of crank angle degree. Gaussian profile is a fit for the premixed combustion fraction of heat release rate.

Gratis copy for Hadeel Solaka
Copyright 2012 SAE International
E-mailing, copying and internet posting are prohibited
Downloaded Wednesday, March 21, 2012 05:11:13 AM

EXPERIMENTS AND INLET CONDITIONS

The obtainable load region for stable PPC was examined for four fuels in the gasoline boiling range together with MK1 as a reference fuel. The fuels were tested at loads between 2 and 8 bar $IMEP_g$ at 1500 rpm with 50% heat release completion (CA50) at 6 crank angle degree after top dead center (ATDC). A single injection strategy was used, wherein the start of injection (SOI) and the injection duration were adjusted to achieve desired loads with maintained CA50, as the injection pressure was kept constant at 1000 bar. During the experiments the desired λ value was 1.5 at an EGR ratio of approximately 50%. Due to the characteristics of the EGR valve, the target level was set to 53 ±1%. The inlet mixture temperature was kept at 335 K.

As expected higher RON fuels had a higher low-load limit since a high RON value is the same as high resistance to auto-ignition. The low-load limit for higher RON fuels was 7 bar, for low RON fuels it was 5 bar, and for MK1 it was 3 bar $IMEP_g$. With both EGR ratio and λ constant, the inlet pressure was a function of load, meaning that for a certain load the boost level was given. However, in order to maintain a stable combustion below the low-load limits, an extended boosting, with a corresponding increase in λ, was used (see Figures 5 and 6). Figure 5 shows the applied extended boosting at lower loads. This strategy also gives information about the relevance of the target λ =1.5, since different fuels have different low-load limit the emission performance can be compared between both the fuels and in relation to λ. During the experiment the EGR ratio was kept constant at 53%, hence the air-fuel ratio was increased below the low-load limit due to instable combustion or misfire. As RON increased, a greater λ (adjusted with increasing boost) was required to operate stable. Results are shown across a load range, such that as load increased λ converged to 1.5 for all fuels above low-load limits (see Figures 5 and 6).

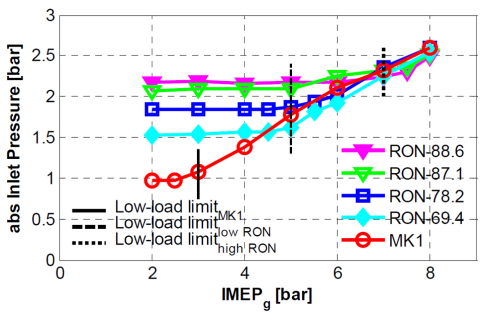

Figure 5. Absolute inlet pressure as a function of load for different fuel.

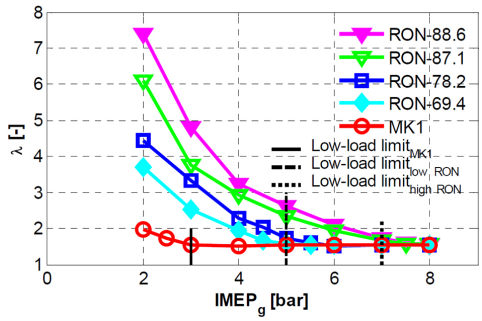

Figure 6. Lambda as a function of load for different fuel.

Figures 7 and 8 show the rate of heat release, in-cylinder pressure, and command signal to the fuel injector as a function of crank angle degree (CAD). In Figure 7, at 2 bar $IMEP_g$ a large variation in the in-cylinder pressure traces were evident due to the variation in the absolute inlet pressure, as λ adjusted to gain stability. However, the rate of heat release traces and the SOI signals were nearly identical for all fuels. At 2 bar $IMEP_g$ the physical properties as lambda adjusted, such as variation in O_2 and CO_2 concentrations, had more effects on the rate of heat release than fuel compositions. At 7 bar $IMEP_g$, shown in Figure 8, the in-cylinder pressure traces were nearly identical for all the fuels with same λ, however the rate of heat release traces and SOI signals were significantly different due to fuel chemistry.

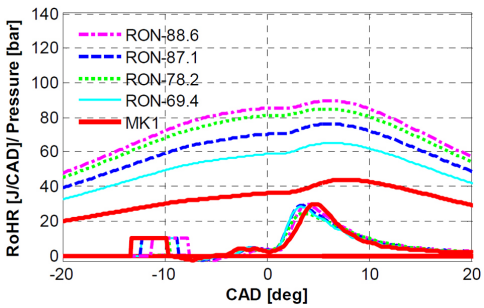

Figure 7. Rate of heat release traces, cylinder pressure traces and injection signals as a function of crank angle degree at 2 bar $IMEP_g$. Operating conditions are injection pressure 1000 bar, and CA50 at 6 CAD ATDC at 1500 rpm.

Gratis copy for Hadeel Solaka
Copyright 2012 SAE International
E-mailing, copying and internet posting are prohibited
Downloaded Wednesday, March 21, 2012 05:11:13 AM

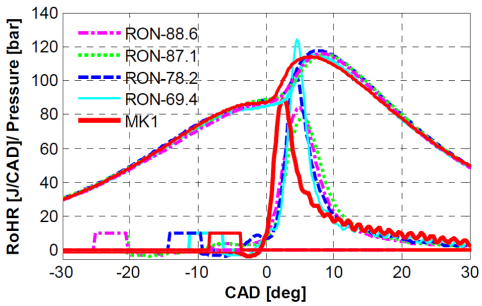

Figure 8. Rate of heat release traces, cylinder pressure traces and injection signals as a function of crank angle degree at 7 bar IMEP$_g$. Operating conditions are injection pressure 1000 bar, and CA50 at 6 CAD ATDC at 1500 rpm.

Figures 9 and 10 are zoomed in version of Figures 7 and 8, which show the LTR phase at 2 and 7 bar IMEP$_g$ respectively. For 2 bar load (Figure 9), the low temperature reaction phase is apparent for all fuels due to low combustion temperature and long ignition delay. At 2 bar IMEP$_g$ as lambda adjusted to gain stability, the variation in oxygen and CO_2 concentrations had a major effects on LTR phase than fuel compositions. For 7 bar load with same lambda (Figure 10), the low temperature reaction region depended largely on the fuel composition. The LTR for diesel fuel was not evident due to short ignition delay and high combustion temperature at higher loads.

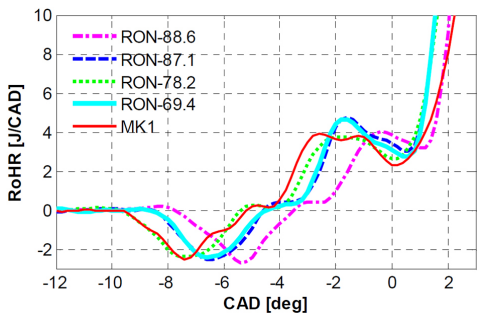

Figure 9. The low temperature reaction phase. LTR is the heat release following the endotherm caused by fuel evaporation at 2 bar IMEP$_g$. Operating conditions are injection pressure 1000 bar, and CA50 at 6 CAD ATDC at 1500 rpm.

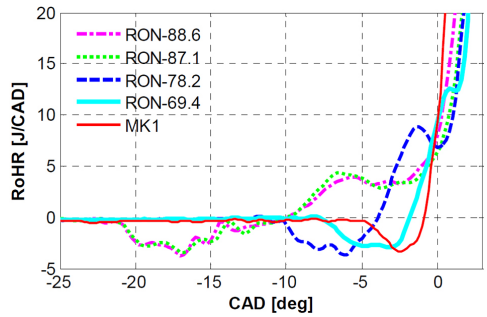

Figure 10. The low temperature reaction phase. LTR is the heat release following the endotherm caused by fuel evaporation at 7 bar IMEP$_g$. Operating conditions are injection pressure 1000 bar, and CA50 at 6 CAD ATDC at 1500 rpm.

RESULTS AND DISCUSSION

Combustion Duration

Figure 11 shows the combustion duration as a function of load. Combustion duration is defined as the time between 10-90% heat release completion, that is CA90-CA10. Diesel fuel had longer combustion duration than the gasoline fuels. The combustion duration increased with increased load for MK1 and for low RON fuels, while it was independent of load for high RON fuels. This was due to premixed combustion, as rapid premixed combustion gives shorter combustion duration while slower diffusion controlled combustion gives longer combustion duration. At loads above 5 bar IMEP$_g$, combustion duration correlates fairly well with RON, with high RON fuels giving shorter combustion duration. At low load no such relation was obvious.

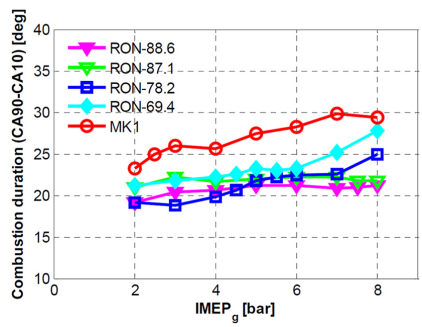

Figure 11. Combustion duration as a function of load for different fuels.

Gratis copy for Hadeel Solaka
Copyright 2012 SAE International
E-mailing, copying and internet posting are prohibited
Downloaded Wednesday, March 21, 2012 05:11:13 AM

Ignition Delay

Figure 12 shows the ignition delay (CAO-SOI) as a function of load for different fuels. Above the low-load limits the ignition delay prolonged with decreased load for all fuels, this was due to the low temperature at SOI (see Figure 13). In this interval, MK1 had the shortest ignition delay, while the gasoline fuels showed increased ignition delay with increased RON. Below the low-load limits, when λ increased the ignition delay decreased again. Apparently, the increased oxygen fraction had a stronger impact on the ignition than the decrease in temperature. All fuels had their actual peak in ignition delay at the identified low-load limit due to low temperature at SOI (see Figure 12 and 13).

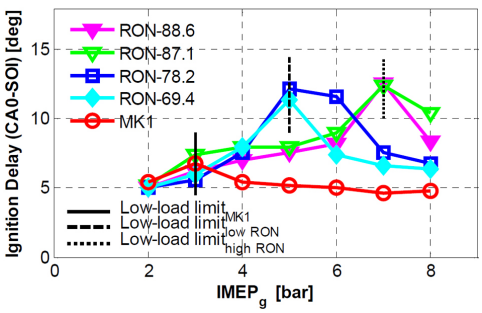

Figure 12. Ignition delay, from the start of combustion to the start of injection, as a function of load.

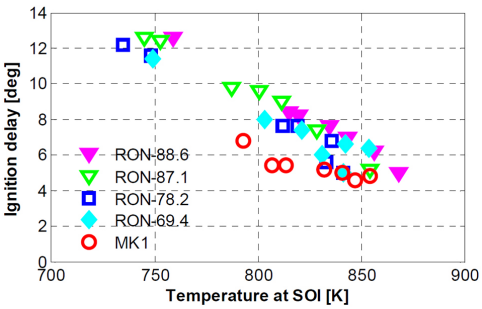

Figure 13. Ignition delay, from the start of combustion to the start of injection, as a function of in cylinder bulk gas temperature at SOI.

Figure 14 shows the start of injection as a function of load. The increment in the ignition delay with earlier or later injection timing occurs because the air temperature and the pressure change significantly close to the top dead center. If the start of injection occurs earlier, the initial pressure and temperature are lower, which leads to lengthening ignition delay [1] (see Figures 12 and 14). The ignition delay was prolonged with advancing the start of injection for gasoline fuels. Above the low-load limits the start of injection was advanced with decreased load, while below the low-load limits the SOI was retarded with decreased load for gasoline fuels to maintain CA50 at 6 CAD after TDC. The start of injection was constant for MK1 between 6 and 8 bar IMEP$_g$.

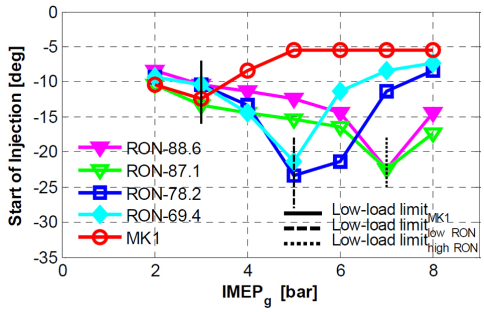

Figure 14. Start of injection as a function of load.

Duration of Low Temperature Reaction

Low temperature reaction phase, which is characterized by a small peak, is usually seen before the main heat release peak. LTR is exothermic, releasing the energy in the apparent heat release trace (see Figures 9 and 10). Low temperature reaction rate of heat release depends both on fuel composition and gas temperature in the cylinder. Fuel chemical composition: containing significant amount of n-paraffin, such as n-heptane, mostly contribute towards a large LTR heating value [21,22]. Tanaka described in [23] the oxidation mechanism of hydrocarbon, where reactions are initiated by abstraction of H from a fuel molecule by O_2 to form alkyl and HO_2. High exothermic reaction occurs at low temperature where alkyl radical reacts with oxygen to generate H_2O and alkyl-peroxide. The high temperature reaction starts to produce H_2O_2 and olefins. This stage occurs between low temperature heat release and high temperature heat release. The temperature gradually increases until H_2O_2 decomposes leading to a branched thermal explosion. For example, if the temperature in the cylinder is very high at start of injection, the early combustion takes place at a high temperature (and there is no possibility of low temperature reaction to occur). Figure 15 shows duration of low temperature reaction as a function of load for different fuels. Since the high temperature reaction started earlier at higher loads, LTR duration decreased by increasing load for MK1. This is because the start of injection was retarded close to the top dead center and thus higher temperature. The duration of LTR increased with decreased load above the low-load limits for gasoline fuels (see Figure 15). However, the LTR duration decreased with decreased load below the low-load limits for all fuels. A correlation between LTR fraction and

Gratis copy for Hadeel Solaka
Copyright 2012 SAE International
E-mailing, copying and internet posting are prohibited
Downloaded Wednesday, March 21, 2012 05:11:13 AM

the RON was evident at constant λ 1.5 above the low-load limits.

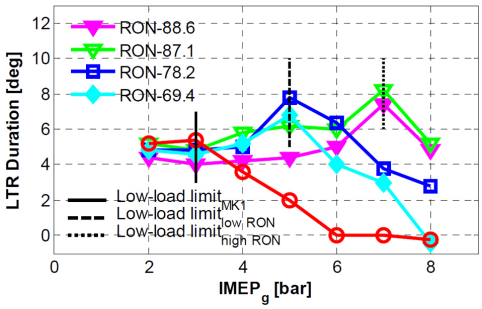

Figure 15. The duration of low temperature reaction as a function of load.

Fraction of Low Temperature Reaction Rate of Heat Release

Figure 16 shows the fraction of LTR as a function of load. The LTR fraction increased with decreased load due to temperature reduction. The LTR fraction for MK1 depends largely on the load compared to the gasoline fuels. At low loads MK1 has the highest fraction due to low temperature, while at high loads the fraction of LTR for MK1 disappeared due to high temperature. The fraction of LTR for MK1 drops from 6-0% due to temperature increment. For the gasoline fuels the fraction of LTR increased by decreasing the load due to temperature reduction. Above the low-load limits, the gasoline fuels showed higher fraction of LTR than MK1 was likely due to fuel chemical properties.

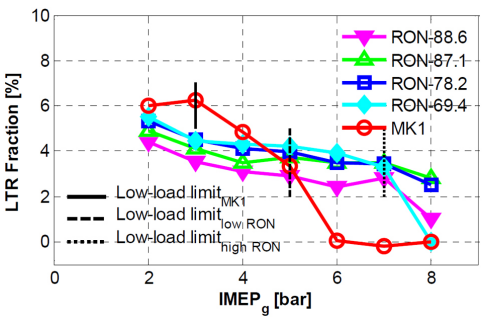

Figure 16. Fraction of low temperature reaction as a function of load.

Premixed Combustion Fraction

Figure 17 shows the calculated premixed combustion using Gaussian profile fit (shown in Figure 3 and described with Equation 4). The increment in premixed fraction for MK1 with decreased load was due to a prolonged ignition delay. At low load below 4 bar $IMEP_g$, MK1 had a higher portion of the premixed combustion than the gasoline fuels, which was due to prolonged ignition delay and fuel compositions. For the gasoline fuels the fraction of premixed combustion increased from 8 bar $IMEP_g$ to the low-load limit at constant lambda 1.5 due to prolonged ignition delay. The fraction of premixed combustion decreased with decreased load below the low-load limit for gasoline fuels, this was due to a shortened ignition delay (see Figure 18), a high boosting level (high lambda values) and a high temperature.

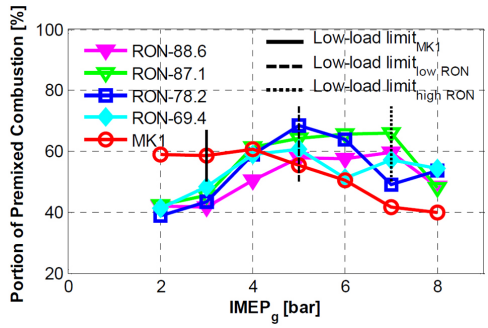

Figure 17. The fraction of the premixed combustion as a function of load.

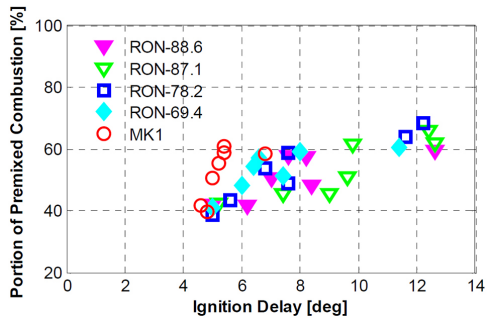

Figure 18. The fraction of the premixed combustion as a function of ignition delay.

EMISSIONS

Smoke

The smoke emissions as a function of the load are shown in Figure 19. Between 2 and 4 bar $IMEP_g$, all fuels had smoke levels below the detection limit 0.01 FSN. The 69.4 RON gasoline fuel had detectable smoke at 8 bar $IMEP_g$, while MK1 produced significant smoke levels between 5 and 8 bar

Gratis copy for Hadeel Solaka
Copyright 2012 SAE International
E-mailing, copying and internet posting are prohibited
Downloaded Wednesday, March 21, 2012 05:11:13 AM

$IMEP_g$. The rate of soot oxidation depends mostly on turbulence, temperature and available oxygen. Above the low-load limits, all fuels operated at the same oxygen fraction and since the ambient density temperature and injection pressure are similar; the conditions for soot oxidation are likely the same for all fuels. The difference in smoke is thereby likely to be connected to the soot formation. Apparently the gasoline fuels had a weak tendency for soot formation than diesel. The soot formation is mainly affected of the fuel characteristics, the mixing between fuel and air, and the combustion temperature. Since similar combustion phasing, boosting and inlet temperature are used at the highest load for all fuels, the soot formation can be expected to depend on fuel characteristics and mixture formation. The difference in ignition delay is, however, small between the low RON fuels and MK1 at the highest loads. It is thereby indicated that the fuel composition had a far stronger influence on the smoke level than any characteristics of the combustion process. [3,8,16,24,25,26]

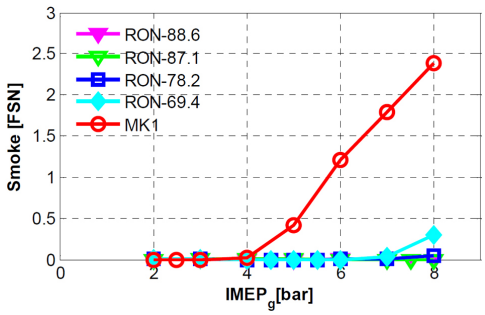

Figure 19. Smoke as a function of load.

NO_x

Figure 20 shows the emission index of NO_x, gram NO_x per kilogram fuel as a function of load. The NO_x formation is strongest at high combustion temperatures and at high oxygen fractions. Also for a given diesel engine, there are three major factors that influence NO_x formation including air-fuel ratio, EGR and combustion phasing. During the experiment both EGR and combustion phasing kept constant at 53% and CA50 at 6 degrees ATDC respectively. Also the NO_x level depended both on fuel properties and λ. For the gasoline fuels, the NO_x level was close to 0.2 g/kg fuel down to the low-load limits. At lower loads, below the low-load limit, the NO_x level increased rapidly as the load decreased mostly due to increased λ (high O_2 fraction) and thus higher local temperature. At the lowest load the level was between 1.2 and 2 g/kg fuel. A correlation between the RON (and also λ) and the NO_x emission index can be seen except for the fuel with the RON 78, since the RON 78 had the shortest combustion duration at low load between 2 to 5 bar $IMEP_g$. The combustion temperature increases with shorter combustion duration, which thereby also affects the NO_x formation. For MK1 the NO_x level was less dependent on the load and varied between 0.2 and 0.5 g/kg fuel.

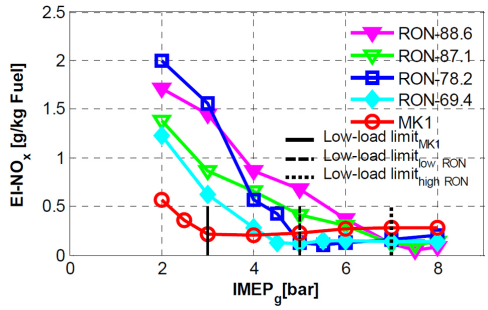

Figure 20. Emission index NO_x as a function of load.

HC and CO

The emission index and PPM level for unburned hydrocarbon (HC) as a function of load are shown in Figures 21 and 22 respectively. HC increased with decreased load due to low temperature during the expansion at low loads. At lean mixtures most of HC is oxidized or converted to CO above 1200 K [27]. The HC level was highest for the high RON fuels and lowest for diesel. This is likely to be connected either to the advanced injection timing for the high RON fuel (an earlier SOI places more fuel in the squish volume) which is less likely to be fully oxidized, or due to longer ignition delay which creates more over-lean (fuel-air) mixture and thus more incomplete combustion. A correlation between the RON and the HC emission index was apparent (see Figure 21). HC emission index could not be measured at low load for all the fuels due to measurement saturation at 1400 ppm (see Figure 22). The high RON fuels saturated faster than the low RON fuels and MK1 probably due to low temperature combustion and incomplete combustion.

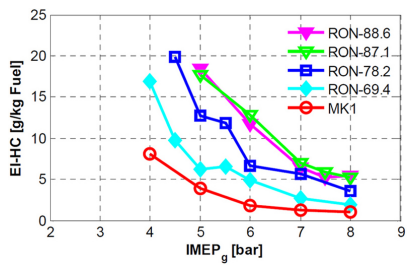

Figure 21. The HC emission index as a function of load.

Gratis copy for Hadeel Solaka
Copyright 2012 SAE International
E-mailing, copying and internet posting are prohibited
Downloaded Wednesday, March 21, 2012 05:11:13 AM

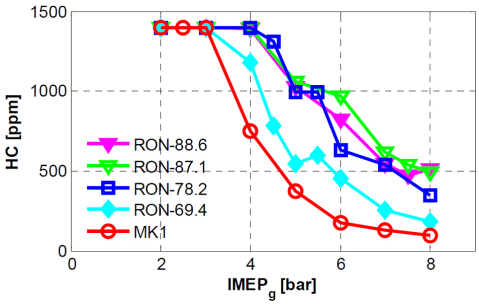

Figure 22. HC emission in ppm as a function of load.

The carbon monoxide (CO) emission index as a function of load is shown in Figure 23. The CO increased with decreased load due to the low temperature during the expansion at low loads. At lean mixtures and combustion temperature between 800 K and 1400 K, a high fraction of CO can be expected. The CO was lower for MK1 than the gasoline fuels due to more complete oxidation. A correlation between the RON and the CO emission index was evident (see Figure 23).

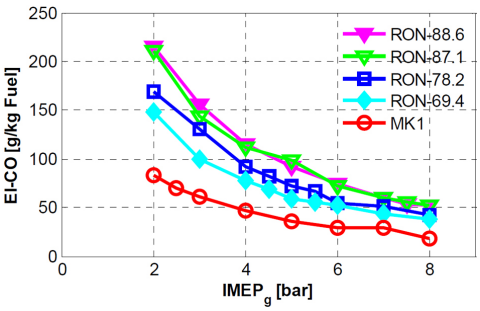

Figure 23. Emission index CO as a function of load.

Indicated Efficiency

Figure 24 shows the gross indicated efficiency as a function of load for different fuels. The gross indicated efficiency ($\eta_{Indicated}$) is calculated from the fuel energy in the cylinder and IMEP gross. The gross indicated efficiencies decreased with decreased load for all fuels. MK1 showed slightly higher efficiency than gasoline fuels; however the efficiencies at the highest load were about 46-49%. Above 5 bar IMEP$_g$, MK1 had higher gross indicated efficiency comparing to gasoline fuels due to more complete combustion (high combustion efficiency).

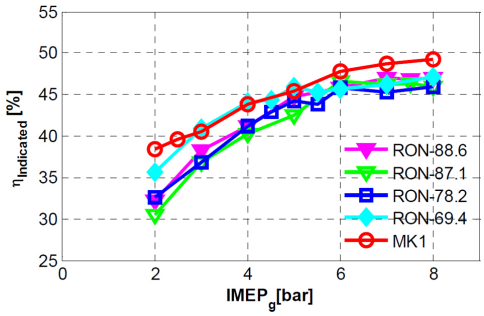

Figure 24. Indicated efficiency as a function of load.

SUMMARY/CONCLUSIONS

The low-load limit for stable PPC operation using ≈50% EGR at λ=1.5 was determined for four gasoline fuels and Swedish diesel fuel (MK1) in a HSDI diesel engine. The engine was operated at loads between 2 and 8 bar IMEP$_g$ at 1500 rpm with 50% heat release completion (CA50) at 6 CAD after the top dead center. A single injection strategy was used, wherein the start of injection (SOI) and the injection duration was adjusted to achieve the desired loads with the maintained combustion phasing, as the injection pressure was kept constant at 1000 bar. The inlet was fed with an exhaust gas recirculation (EGR) ratio of 53 ±1%, and the inlet mixture temperature was kept at 335 K.

• The low-load limit with the stable combustion at λ=1.5 was between 5 and 7 bar IMEP$_g$ for the gasoline fuels, and a higher limit for the higher RON values. MK1 had the lowest low-load limit at 3 bar IMEP$_g$.

• By increasing λ with kept EGR ratio, with extended boosting, all fuels could be operated down to 2 bar IMEP$_g$. The higher oxygen fraction in combination with the higher pressure at the top dead center favored the combustion stability.

• The portion of premixed combustion was not distinctly different between the MK1 and the gasoline fuels, however MK1 showed the longest combustion duration independently on load. This was an indication of a slower reaction rate during the premixed combustion for MK1.

• The duration of the low temperature reaction depended on the ignition delay, where a prolonged ignition delay gave an increased duration of LTR.

• The portion of the low temperature reaction decreased with increased load from about 5% at 2 bar IMEP$_g$ to about 3% at 8 bar IMEP$_g$. MK1 had a similar fraction as the gasoline fuels at low loads, but above 5 bar IMEP$_g$ the LTR was not apparent.

Gratis copy for Hadeel Solaka
Copyright 2012 SAE International
E-mailing, copying and internet posting are prohibited
Downloaded Wednesday, March 21, 2012 05:11:13 AM

• Smoke was higher for the MK1 than for the gasoline fuels. The engine out smoke is the net result of formation and oxidation. The rate of soot oxidation depends mostly on turbulence, temperature and available oxygen. Above the low-load limits all fuels were operated at the same oxygen fraction and since the ambient density temperature and injection pressure are similar; the conditions for soot oxidation are likely the same for all fuels. The difference in smoke is thereby likely to be connected to the soot formation. The soot formation is mainly affected of the fuel characteristics, the mixing between fuel and oxygen, and the combustion temperature. At the highest loads similar combustion phasing, and TDC conditions are used for all fuels. The ignition delay was also similar for MK1 and the low RON fuels. The soot formation can thereby be expected to depend mostly on fuel characteristics.

• CO and HC decreased with increased load for all fuels due to increased temperature during the expansion, which favors a sufficient late oxidation. The levels of HC and CO were lower for the MK1 compared to the gasoline fuels. HC and CO were correlated to RON.

• Some conclusions can be drawn when comparing the different fuels potential to produce clean PPC. Above the low-load limits the gasoline fuels had better emission performance than MK1 even if the level of HC and CO was slightly higher. Below the low-load limit the emission performance was significantly worse for the gasoline fuels and MK1 had the lowest emission levels. This verifies that the target level of λ=1.5 is relevant.

REFERENCES

1. Heywood, J.B., 1988, *"Internal Combustion Engine Fundamentals"*, McGraw Hill Book Co.

2. Warnatz, J., Maas, U., DiBble, R.W., 2006, *"Combustion Physical and Chemical Fundamentals, Modeling and Simulation, Experiments, Pollutant Formation"* 4th edition, Springer Berlin Heidelberg New York.

3. Aronsson, U., Chartier, C., Andersson, Ö., Johansson, B. et al., "Analysis of EGR Effects on the Soot Distribution in a Heavy Duty Diesel Engine using Time-Resolved Laser Induced Incandescence," *SAE Int. J. Engines* 3(2):137-155, 2010, doi:10.4271/2010-01-2104.

4. Onishi, S., Jo, S., Shoda, K., Jo, P. et al., "Active Thermo-Atmosphere Combustion (ATAC) - A New Combustion Process for Internal Combustion Engines," SAE Technical Paper 790501, 1979, doi: 10.4271/790501.

5. Christensen, M., Hultqvist, A., and Johansson, B., "Demonstrating the Multi Fuel Capability of a Homogeneous Charge Compression Ignition Engine with Variable Compression Ratio," SAE Technical Paper 1999-01-3679, 1999, doi:10.4271/1999-01-3679.

6. Lu, X.C., Chen, W., Huang, Z., 2005, *"A Fundamental Study on the Control of the HCCI Combustion and Emissions by Fuel Design Concept Combined with Controllable EGR. Part 1. The Basic Characteristics of HCCI Combustion"*, Fuel 84 (2005) 1074-1083

7. Takahashi, Y., Suyama, K., Iijima, A., Yoshida, K. et al., "A Study of HCCI Combustion Using Spectroscopic Measurements and Chemical Kinetic Simulations: Effects of Fuel Composition, Engine Speed and Cylinder Pressure on Low-temperature Oxidation Reactions and Autoignition," SAE Technical Paper 2011-32-0524, 2011, doi: 10.4271/2011-32-0524.

8. Sjöberg, M. and Dec, J., "Influence of Fuel Autoignition Reactivity on the High-Load Limits of HCCI Engines," SAE Int. J. Engines 1(1):39-58, 2009, doi:10.4271/2008-01-0054.

9. Johansson, T., Johansson, B., Tunestål, P., and Aulin, H., "The Effect of Intake Temperature in a Turbocharged Multi Cylinder Engine operating in HCCI mode," SAE Int. J. Engines 2(2):452-466, 2010, doi:10.4271/2009-24-0060.

10. Kitano, K., Nishiumi, R., Tsukasaki, Y., Tanaka, T. et al., "Effects of Fuel Properties on Premixed Charge Compression Ignition Combustion in a Direct Injection Diesel Engine," SAE Technical Paper 2003-01-1815, 2003, doi:10.4271/2003-01-1815.

11. Kimura, S., Aoki, O., Ogawa, H., Muranaka, S. et al., "New Combustion Concept for Ultra-Clean and High-Efficiency Small DI Diesel Engines," SAE Technical Paper 1999-01-3681, 1999, doi:10.4271/1999-01-3681.

12. Kimura, S., Aoki, O., Kitahara, Y., and Aiyoshizawa, E., "Ultra-Clean Combustion Technology Combining a Low-Temperature and Premixed Combustion Concept for Meeting Future Emission Standards," SAE Technical Paper 2001-01-0200, 2001, doi:10.4271/2001-01-0200.

13. Noehre, C., Andersson, M., Johansson, B., and Hultqvist, A., "Characterization of Partially Premixed Combustion," SAE Technical Paper 2006-01-3412, 2006, doi: 10.4271/2006-01-3412.

14. Suzuki, H., Koike, N., and Odaka, M., "Combustion Control Method of Homogeneous Charge Diesel Engines," SAE Technical Paper 980509, 1998, doi: 10.4271/980509.

15. Okude, K., Mori, K., Shiino, S., and Moriya, T., "Premixed Compression Ignition (PCI) Combustion for Simultaneous Reduction of NOx and Soot in Diesel Engine," SAE Technical Paper 2004-01-1907, 2004, doi: 10.4271/2004-01-1907.

16. Musculus, M., "Multiple Simultaneous Optical Diagnostic Imaging of Early-Injection Low-Temperature Combustion in a Heavy-Duty Diesel Engine," SAE Technical Paper 2006-01-0079, 2006, doi:10.4271/2006-01-0079.

17. Manente, V., Zander, C., Johansson, B., Tunestal, P. et al., "An Advanced Internal Combustion Engine Concept for Low Emissions and High Efficiency from Idle to Max Load Using Gasoline Partially Premixed Combustion," SAE

Gratis copy for Hadeel Solaka
Copyright 2012 SAE International
E-mailing, copying and internet posting are prohibited
Downloaded Wednesday, March 21, 2012 05:11:13 AM

Technical Paper 2010-01-2198, 2010, doi: 10.4271/2010-01-2198.

18. Kalghatgi, G., Risberg, P., and Ångström, H., "Advantages of Fuels with High Resistance to Auto-ignition in Late-injection, Low-temperature, Compression Ignition Combustion," SAE Technical Paper 2006-01-3385, 2006, doi:10.4271/2006-01-3385.

19. Kalghatgi, G., Risberg, P., and Ångström, H., "Partially Pre-Mixed Auto-Ignition of Gasoline to Attain Low Smoke and Low NOx at High Load in a Compression Ignition Engine and Comparison with a Diesel Fuel," SAE Technical Paper 2007-01-0006, 2007, doi:10.4271/2007-01-0006.

20. Egnell, R., "Combustion Diagnostics by Means of Multizone Heat Release Analysis and NO Calculation," SAE Technical Paper 981424, 1998, doi: 10.4271/981424.

21. Shibata, G., Oyama, K., Urushihara, T., and Nakano, T., "Correlation of Low Temperature Heat Release With Fuel Composition and HCCI Engine Combustion," SAE Technical Paper 2005-01-0138, 2005, doi:10.4271/2005-01-0138.

22. Truedsson, I., Tuner, M., Johansson, B., and Cannella, W., "Pressure Sensitivity of HCCI Auto-Ignition Temperature for Primary Reference Fuels," SAE Technical Paper 2012-01-1128, 2012.

23. Tanaka, S., Ayala, F., Keck, J.C., Heywood, J.B., 2002 *"Two-Stage Ignition in HCCI Combustion and HCCI Control by Fuels and Additives"*, Combustion and Flame 132 (2003) 219-239

24. Dec, J., "A Conceptual Model of DI Diesel Combustion Based on Laser-Sheet Imaging*," SAE Technical Paper 970873, 1997, doi: 10.4271/970873.

25. Andersson, Ö., *"Diesel Combustion, in Handbook on Combustion"*, vol. 3, Ed. Winter, F., Wiley-VHC books, Weinheim, 2010

26. Aronsson, U., Chartier, C., Andersson, Ö., Egnell, R. et al., "Analysis of the Correlation Between Engine-Out Particulates and Local Φ in the Lift-Off Region of a Heavy Duty Diesel Engine Using Raman Spectroscopy," *SAE Int. J. Fuels Lubr.* 2(1):645-660, 2009, doi:10.4271/2009-01-1357.

27. Kim, D., Ekoto, I., Colban, W., and Miles, P., "In-cylinder CO and UHC Imaging in a Light-Duty Diesel Engine during PPCI Low-Temperature Combustion," *SAE Int. J. Fuels Lubr.* 1(1):933-956, 2009, doi: 10.4271/2008-01-1602.

CONTACT INFORMATION

hadeel.solaka@energy.lth.se

ACKNOWLEDGMENTS

The author would like to acknowledge the Competence Center Combustion Processes, KCFP, and the Swedish Energy Agency for the financial support, Bill Cannella from Chevron for supplying fuels and Patrick Borgqvist for implementing the control system.

DEFINITIONS/ABBREVIATIONS

ATDC
After top dead center

CAD
Crank angle degree

CA50
Crank angle at 50% completion of heat release

CN
Cetane number

CO
Carbon monoxide

CO_2
Carbon dioxide

EGR
Exhaust gas recirculation

$IMEP_g$
Indicated mean effective pressure gross

LTR
Low temperature reaction

MON
Motor octane number

NO_x
Nitrogen oxides e.i. NO, NO_2

ON
Octane number

PM
Particulate matter

RON
Research octane number

Gratis copy for Hadeel Solaka
Copyright 2012 SAE International
E-mailing, copying and internet posting are prohibited
Downloaded Wednesday, March 21, 2012 05:11:13 AM

SOC
Start of combustion

SOI
Start of injection

TDC
Top dead center

UHC
Unburned hydrocarbons

The Engineering Meetings Board has approved this paper for publication. It has successfully completed SAE's peer review process under the supervision of the session organizer. This process requires a minimum of three (3) reviews by industry experts.

All rights reserved. No part of this publication may be reproduced, stored in a retrieval system, or transmitted, in any form or by any means, electronic, mechanical, photocopying, recording, or otherwise, without the prior written permission of SAE.

ISSN 0148-7191

Positions and opinions advanced in this paper are those of the author(s) and not necessarily those of SAE. The author is solely responsible for the content of the paper.

SAE Customer Service:
Tel: 877-606-7323 (inside USA and Canada)
Tel: 724-776-4970 (outside USA)
Fax: 724-776-0790
Email: CustomerService@sae.org
SAE Web Address: http://www.sae.org
Printed in USA

Paper II

Internal Combustion Engine Division Spring Technical Conference

ICES2012

May 6-9, 2012, Torino, Italy

ICES2012-81184

Investigation on the Impact of Fuel Properties on Partially Premixed Combustion Characteristics in a Light Duty Diesel Engine

Hadeel Solaka
Author
Lund, Sweden

Martin Tunér
Co-Author
Lund, Sweden

Bengt Johansson
Co-Author
Lund, Sweden

ABSTRACT

The impact of fuel composition on the emission performance and combustion characteristics for partially premixed combustion (PPC) were examined for four fuels in the gasoline boiling range together with Swedish diesel MK1. Experiments were carried out at 8 bar $IMEP_g$ and 1500 rpm with 53±1% EGR and $\lambda = 1.5$. This relation gave inlet mole fractions of approximately 5% CO_2 and 13% O_2. The combustion phasing was adjusted by means of start of injection (SOI), for all fuels, over the range with stable combustion and acceptable pressure rise rate combined with maintained λ, EGR ratio, inlet pressure, and load. The operating range was limited by combustion instability for the high RON fuels, while MK1 and the low RON fuels could be operated over the whole MBT plateau. The largest difference in engine-out emissions between the fuels was the filtered smoke number (FSN), as the gasoline fuels produced a much lower FSN value than MK1. Higher RON value gave higher levels of carbon monoxide (CO) and unburned hydrocarbon (HC) for the gasoline fuels, while MK1 had the lowest levels of these emissions.

INTRODUCTION

Direct injection compression ignition (DICI) diesel engines for passenger cars have higher efficiency than spark ignition engines (SI). However, stringent emission legislation demands continued reduction in engine-out emissions especially for particulate matter (PM) and nitrogen oxide (NO_x), but the limits for HC and CO are also demanding. Hence, the challenge is to reduce PM and NO_x without increased levels of CO and HC with new combustion strategies. Many studies in recent years have tried to achieve reduction in emissions by introducing and re-examining different combustion concepts.

Two important pollutants from diesel engines are NO_x and PM. To a significant degree, PM consists of combustion generated soot. Soot forms at temperatures between 1600 and 2400 K and at an equivalence ratio (Φ) larger than two, while soot oxidization is most pronounced at low equivalence ratios and high temperatures. The level of engine-out soot corresponds to the net difference between formation and oxidization. NO_x is formed either from atmospheric nitrogen or nitrogen from the fuel but with a different mechanism. The major part of NO_x formation during diesel combustion is formed by the thermal mechanism. Its principle reactions have been explained by Zeldovich and Lavoie. NO_x forms above 2000 K at an equivalence ratio lower than two. By introducing large amounts of cooled exhaust gas recirculation (EGR) the combustion temperature can be reduced below the threshold for soot and NO_x formation. The EGR works as a heat absorbing bulk gas, thereby slowing down the kinetic reactions [1,2,3].

Over the last few decades, many concepts have been introduced in order to reduce pollutants from CI engines. One such concept is Homogenous Charge Compression Ignition (HCCI), which was introduced by Onishi [4] in 1979. In HCCI, the fuel and air are fully premixed as in a spark ignition (SI) engine but utilizes compression ignition. HCCI has low NO_x and soot emissions compared to traditional diesel combustion [5]. However, controlling HCCI combustion is very difficult since auto-ignition chemistry, which determines HCCI combustion timing, depends on pressure, temperature, and on other factors such as fuel chemistry and O_2 concentration [6-9]. High loads are especially challenging due to high maximum pressure-rise rates, which cause material stress and produce high acoustic noise [10].

Another suggested combustion concept is called Nissan Modulated Kinetics (MK) [7,8]. This concept proposed late injection, high swirl, and high amount of cooled EGR to reduce NO_x and Soot.

To overcome the limitation with HCCI and MK combustion concepts, a new concept called Partially Premixed

Copyright © 2012 by ASME

Combustion (PPC) has been introduced [13]. PPC or premixed compression ignition (PCI), imply that an engine operates between fully homogeneous and diffusion control combustion [14] but with a small difference: PPC uses more EGR than PCI, around 50% compared to 30% [15]. In PPC it is desirable to separate the end of injection from the start of combustion [14]. The authors in [11,13-17] described how the separation between end of injection and start of combustion can be achieved, which is to use a large amount of exhaust gas recirculation (EGR), early start of injection, low compression ratio, and fuel with a high octane number.

In 2006, it was demonstrated that using gasoline fuel in a compression ignition engines has potential to produce low levels of engine-out emissions [18,19]. Since gasoline has a higher resistance to auto-ignition compared to diesel fuel, it gives more time for mixing, thus producing a higher fraction of premixed combustion. However, one of the problems of pre-mixed combustion is the high rate of heat release. This leads to a higher pressure rise rate and noise, especially if the premixed combustion occurs before top dead center (TDC). To overcome this problem a large amount of EGR is used to avoid reaction during the compression stroke and to slow down chemical reactions. This also reduces the combustion temperature and formation of NO_x and soot.

The authors in [17] suggested that the optimum EGR ratio and $\lambda = {}^{A}/_{A_{F_S}}$ for PPC are about 50% and 1.5 respectively. These settings were shown to give low emissions of soot and NO_x, together with high fuel efficiency. However, it was not possible to achieve stable combustion at low loads for high RON fuels during these conditions, as the experiments were performed in a heavy-duty diesel engine. In [20] the low load limits for four fuels in the gasoline boiling range together with MK1 with the settings suggested in [17] were investigated in a light duty diesel engine, by the authors of this paper. It was concluded that the low-load limit with the stable combustion at λ=1.5 and 50% EGR was between 5 and 7 bar $IMEP_g$ for the gasoline fuels, higher limit for the higher RON values. Diesel had the lowest low-load limit, 3 bar $IMEP_g$. In this investigation the heat release and emission performance using the same fuels are investigated just above the highest low-load limit, at 8 bar $IMEP_g$ with respect to combustion phasing.

EXPERIMENTS

ENGINE SETUP—Experiments were performed using an in-line 5-cylinder diesel engine (Volvo D5) operated on one cylinder. Details of the engine are given in Table 1.

Table 1. ***Engine properties***.

Compression ratio, r_c [-]	16.5
Displacement volume [cm^2/cylinder]	480
Bore [mm]	81
Stroke [mm]	93.2
IVC [CAD BTDC]	174
Injection nozzle holes	7
Injection holes diameter [mm]	0.14
Included angle [degrees]	140
Injector type	Solenoid
Swirl number [-]	2.2

The engine test rig was equipped with an adjustable exhaust gas recirculation system and adjustable heating of the inlet air temperature (see Figure 1).

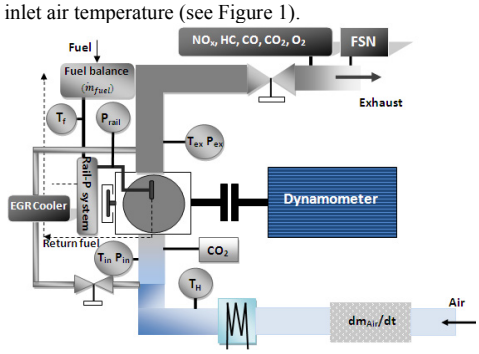

Figure 1. Experimental setup.

EGR_{ratio}—The EGR_{ratio} is defined as a ratio between the concentration of CO_2 in the inlet air to the engine to the concentration of CO_2 in the exhaust gases from the engine.

$$EGR_{ratio} = \frac{CO_{2_{Inlet}}}{CO_{2_{Exhaust}}} \qquad (1)$$

The exhaust gases were cooled in a heat exchanger, using the engine's coolant water as a heat absorber, before it was mixed with the inlet air. The mixture temperature was controlled by heating the fresh charge before it was blended with the EGR, and the temperature target was set to 335 K (see Figure 1).

INJECTION SYSTEM—The injection system consisted of a common rail, a high-pressure pipe, high- and low-pressure pumps and piezo injector. However, during the initial experiments it was discovered that the piezo injector had low

Copyright © 2012 by ASME

Table 2. Fuel properties and specifications.

Fuel	RON	MON	CN	C	H/C	O/C	LHV[MJ/kg]	A/F_s	N-paraffin	Iso-paraffin	Olefins
A	69.4	66.1	-	7.11	1.98	0	43.80	14.7	6.89x	1.08y	2.94z
B	78.2	73.4	-	7.16	1.97	0	43.70	14.7	5.71x	1.13y	z
C	87.1	80.5	-	7.20	1.92	0	43.50	14.6	2.77x	1.46y	4z
D	88.6	79.5	-	7.21	1.88	0	43.50	14.5	x	y	16.4z
MK1	n.a	-	54	16	1.87	0	43.15	14.4	38.2%	-	1%

reliability when operated on gasoline. Running with the piezo injector the combustion died after 15 minutes using gasoline fuels, this could be related to the viscosity difference between the gasoline and diesel fuel. To overcome this obstacle, the injection system was modified from piezo to solenoid injector (see Table 1 for injector specifications).

INTAKE AIR and FUEL MASS-FLOW—The intake air mass flow was measured by a thermal mass flow meter (Bronckhorst IN-FLOW). It was situated approximately 3 m upstream from the intake manifold in order to prevent pressure oscillations to propagate from the engine, or EGR system, into the flow meter. Fuel mass flow was measured by a fuel balance (Sartorius cp8201) over a time span of 120 seconds per measurement point.

EMISSIONS—Smoke were measured with the AVL415S smoke meter, while NO_x, HC, CO, intake CO_2 and exhaust CO_2 emissions were measured with a Horiba measurement system (MEXA9200DF). NO_x emissions were measured with a chemiluminescence analyzer whereas HC was measured with a hydrogen flame ionization detector (FID) and the piping to the analyzer was heated to approximately 191°C to avoid condensation of unburned fuel components. Oxygen (O_2) was measured by a magneto-pneumatic condenser microphone method (MPA), whereas CO, intake CO_2 and exhaust CO_2 were measured with an infrared analyzer.

FUELS—Five fuels were included in the experiments: four fuels in the gasoline boiling range, and as a reference Swedish environmental Class 1 diesel fuel (MK1) (see Table 2). In Table 2 the x, y and z are normalized value of the fuel components. In order to ensure that no damage was caused to the injection system, 500 ppm lubricity additive *Infineum R655* was added to each gasoline fuel. The impact of the additive on combustion phasing and emission formation is expected to be neglectable at such small fraction.

The variations in n-paraffin, iso-paraffin and olefin content on emissions performance were investigated in this study. Olefins are also known as alkenes, which are unsaturated hydrocarbons and have influence on anti-knock but as well on emission performance. They serve as a component into blend in fuel to increase the octane number (ON). Earlier investigations have shown that olefins may decrease the combustion duration and thereby increase the combustion temperature [21].

Paraffins are also known as alkanes, which are saturated hydrocarbons. N-paraffins are a proper component to blend in fuel to decrease the octane number. N-paraffin has a straight chain, while iso-paraffin has a shorter branched chain.

METHODS and DEFINITIONS—The rate of heat release was calculated using the in-cylinder pressure trace from 300 cycles. The method for the rate of heat release calculation,

$$\frac{\partial Q}{\partial \theta} = \frac{\gamma}{\gamma - 1} p \frac{\partial V}{\partial \theta} + \frac{1}{\gamma - 1} V \frac{\partial p}{\partial \theta} + \frac{\delta Q_{losses}}{\delta \theta} \qquad (2)$$

followed the description in Heywood [1]. The convective heat transfer was estimated according to Woschni, and mass losses or blow-by was accounted by assuming choked flow over the piston ring gap [1]. To estimate γ a model described by Egnell was used [22].

From the calculated rate of heat release, information about the combustion events can be extracted. In the analysis, the combustion is divided into four phases: the ignition delay, the low temperature reactions (LTR), the premixed combustion, and the late mixing controlled combustion phase (see Figure 2).

Copyright © 2012 by ASME

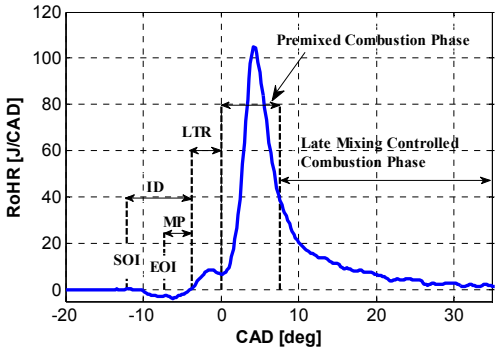

Figure 2. The rate of heat release as a function of crank angle degree. Figure shows combustion phases.

The *ignition delay* (ID) is identified by the *endotherm* phase due to fuel heating and vaporization between start of injection (SOI) and start of combustion (SOC) (see Figure 2).

The *start of injection* (SOI) is determined from the gradient of the injection pressure. The SOI is the point where the gradient reaches the maximum value before its minimum value due to needle lift (see Figure 3). The *start of combustion* (SOC) is defined as the point where the rate of heat release turns positive after (SOI), that is 0% heat release completion (CA0) (see Figure 2).

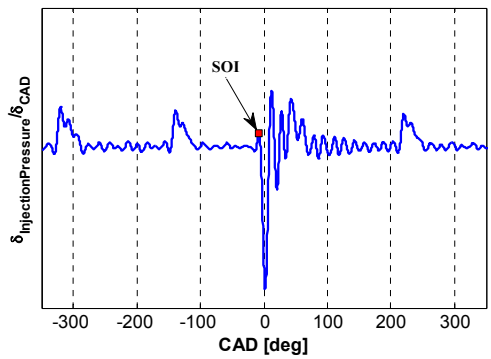

Figure 3. The gradient of injection pressure as a function of crank angle degree. Figure shows SOI.

The *Mixing Period* (MP) is identified as the period between end of injection and start of combustion (see Figure 2). The MP can be used to determine the fuel air mixing prior combustion. A positive mixing period gives a strong indication that the combustion event will be highly premixed.

Low temperature reaction (LTR) is characterized by a small peak before the main premixed heat release (see Figure 2). The reason for the lower rate of heat release between those peaks is that the speed of the low temperature reactions decreases with increasing temperature

The *low temperature reaction duration* is defined as the part between SOC and the end of LTR (see Figure 2). The end of LTR is defined as the point where the gradient of rate of heat release reaches 0.05 J/CAD^2. This threshold was selected as the lowest value that gave a robust definition.

The *fraction of low temperature reaction* is the ratio between the accumulated heat release from the LTR and the total heat release.

In the *premixed combustion phase*, the combustible fuel and air mixture burns rapidly [1]. This phase is controlled by chemical kinetics, and reaction speed depends mainly on temperature. In the current study, the premixed- and late heat release rate are not distinctly separated. This is because parts of the premixed combustion phase are limited by mixing, and parts of the late combustion phase depends on slow reactions rather than mixing. In order to separate the phases in a well defined manner, a Gaussian

$$G(x) = h \cdot e^{-\left(\frac{x-x_0}{2\alpha^2}\right)^2} \qquad (3)$$

profile is fitted to the rising flank of the premixed peak, between end of low temperature reactions and the actual peak, and the integrated area of the profile is used as a measure of the premixed reactions. In Eq. 3 x_0 is the central position of the peak, h and α representing the height and width of the Gaussian profile. Figure 4 shows the rate of heat release as a function of crank angle together with the Gaussian profile.

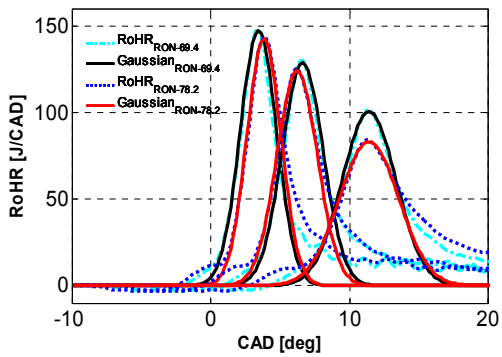

Figure 4. The rates of heat release and Gaussian profiles as a function of crank angle degree. The Gaussian profile is a fit for the premixed combustion portion of the heat release rate.

As is evident, the fit follows the premixed heat release closely. The Gaussian profile is a mathematical rather than a

Copyright © 2012 by ASME

physical representation of the premixed reaction phase. However, it is provided as a robust measure of the premixed reactions for all the operated cases.

EXPERIMENTS AND INLET CONDITIONS

Fuel aspect on PPC was examined for four fuels in the gasoline boiling range together with Swedish MK1 as a reference fuel. The experiments were performed at 8 bar $IMEP_g$ and 1500 rpm. A single injection strategy was used where the start of injection (SOI) and the injection duration were adjusted to achieve the desired load and CA50. The injection pressure was kept constant at 1000 bar. During the experiments the desired λ value was 1.5 at an EGR ratio of 53±1%. This relation gave an inlet mole fraction of approximately 5% CO_2 and 13% O_2. The inlet mixture temperature and pressure were kept at 335 K and 2.5 bar respectively. The exhaust pressure was controlled with a back-pressure valve to maintain 0.2 bar above the inlet air pressure, that is 2.7 bar.

The combustion phasing was adjusted by means of start of injection (SOI), for all fuels, over the range with stable combustion and acceptable pressure rise rate combined with maintained λ, EGR ratio, inlet pressure, and load (see Figure 5). For MK1 and the low RON fuels the range was limited by a decrease in λ due to an increased fueling when the phasing was outside the maximum brake torque (MBT) plateau. For the high RON fuels the range was limited by combustion instability: a too early injection timing places more fuel in the squish volume which has less chance to burn, while too late injection does not give enough time for a sufficient mixing before the temperature drop during the expansion. As expected higher RON fuels had a more advanced SOI since a high RON value is the same as high resistance to auto-ignition. MK1 showed the largest span in achievable combustion phasing range. The high RON fuels CA50 are insensitive to injection timing because with an early injection the fuel and air become over-mixed and essentially homogeneous.

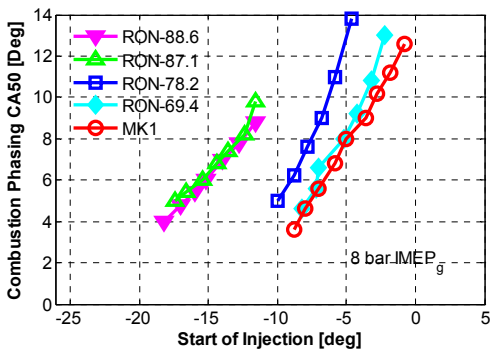

Figure 5. Combustion phasing as a function of start of injection.

During the experiment the maximum accepted pressure rise rate was 14 bar/CAD and maximum accepted coefficient of variance (COV) of $IMEP_g$ was 2%. Generally MK1 had a much lower pressure rise rate and a lower COV of $IMEP_g$. Figure 6 shows that MK1 has a different rate of heat release compared to the gasoline fuels.

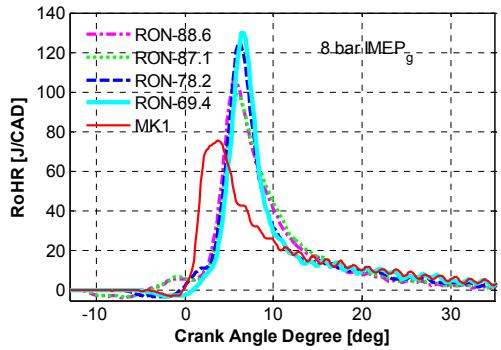

Figure 6. Rate of heat release as a function of crank angle degree CA50 maintained at 8 CAD after TDC.

RESULTS AND DISCUSSION

Ignition Delay

Figure 7 shows the ignition delay (CA0-SOI) as a function of combustion phasing. MK1 had the shortest ignition delay while the gasoline fuels showed an increased ignition delay with increasing RON. The ignition delay was independent of combustion phasing for MK1 and low RON fuels, while it decreased for cases with late CA50 for high RON fuels. The ignition delay seems to be related to the n-paraffin concentration (see Table 2). A high concentration of n-paraffin for MK1 gives a shorter ignition delay and low concentration for high RON fuels gives a prolonged ignition delay.

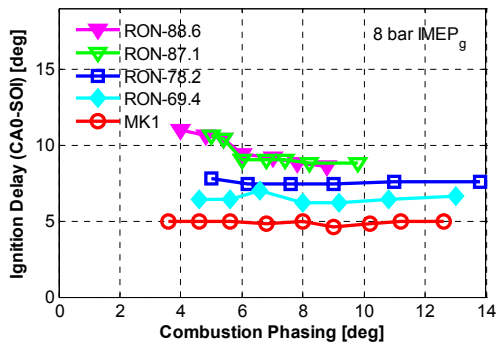

Figure 7. Ignition delay as a function of combustion phasing.

Copyright © 2012 by ASME

Figure 8 shows the average in-cylinder temperature at SOI as a function of start of injection. The increment in the ignition delay with earlier injection timing for the high RON fuels (see Figure 7) occurs because the air temperature and pressure change significantly close to the top dead center. If the start of injection occurs earlier, the initial pressure and temperature are lower which gives a longer ignition delay [1]. The temperatures at start of injection for MK1 and low RON fuels do not change much with the injection timing since these fuels are injected close to TDC, where there is small change in in-cylinder volume. However, for the high RON fuels the temperature at SOI was 40 K higher for the latest injection timing compared to the earliest. This explains the observed trend in Figure 8 with shorter ignition delay for later injection timing for the high RON fuels.

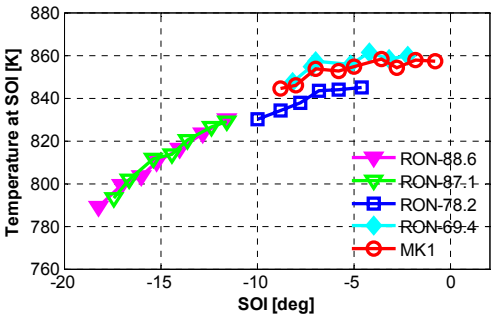

Figure 8. Temperature at SOI as a function of the crank angle of SOI.

Duration and fraction of low temperature reaction

The low temperature reaction phase is characterized by a small peak before the main heat release peak. The auto-ignition of hydrocarbon-air mixtures has been investigated experimentally and theoretically.

These investigations show that heavy hydrocarbons ignite in a two-stage process involving a low temperature phase followed by a high temperature phase. This continues until the temperature rises to a level where olefins and HO_2 are generated, which is important to terminate the first-stage of the combustion. At this point, the second-stage begins and the rate of temperature rise drops rapidly. Tanaka described in [23] the oxidation mechanism of hydrocarbons, where the reaction started with the abstraction of H from a fuel molecule by O_2 to form an alkyl and HO_2. The highly exothermic reaction occurs at low temperatures producing H_2O and alkyl-peroxide. Later, the temperature continues to rise slowly until the reaction produces OH radicals, which is important to terminate the second-stage and start a branched thermal explosion.

The LTR- and high temperature reaction (HTR) rate of heat release depend both on fuel composition, fuel structure and gas temperature in the cylinder. A significant fraction of n-paraffins, such as n-heptane, mostly contribute towards high fraction of LTR [24,25]. For example, if the in-cylinder temperature is very high at start of injection, the main combustion takes place at a high temperature (and there is no possibility of low temperature reaction to occur). Figure 9 shows duration of LTR as a function of combustion phasing. The duration of the LTR phase is insensitive to combustion phasing for all fuels. However, LTR phase for MK1 and the lowest RON fuel was not present due to high temperature at CA0. This is because the high temperature reactions started earlier with late injection timing. The high RON fuels showed to have the longest duration of LTR due to low temperature and pressure at CA0 (see Figure 9). It seems that n-paraffin concentration has an effect on the duration of the LTR phase. High concentration gives late injection timing and therefore a higher temperature. This is the reason why the LTR phase was not present for MK1 and the lowest RON fuel.

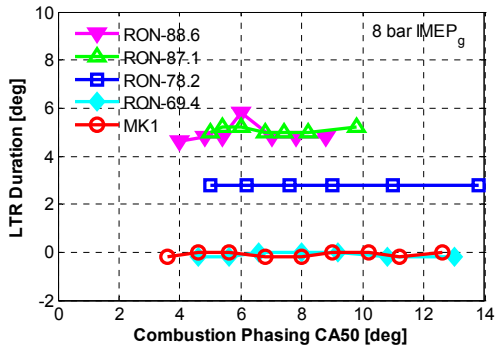

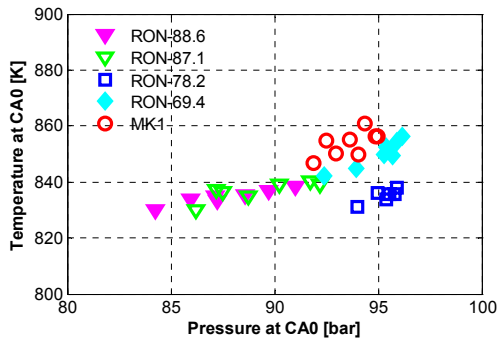

Figure 9. The duration of low temperature reaction as a function of combustion phasing (left) and average in-cylinder temperature at CA0 as a function of in-cylinder pressure at CA0 (right).

Copyright © 2012 by ASME

Figure 10 shows the fraction of LTR as a function of combustion phasing. As mentioned before, MK1 and the lowest RON fuel do not have a LTR phase. The fractions of LTR phase for the other gasoline fuels are between 2 and 3.5%. The 78.2 RON fuel had a high fraction of LTR phase due to the low temperature at CA0 (see Figure 10). However, RON 78.2 had a shorter duration compared to high RON fuels due to the high in-cylinder pressure at CA0 (see Figure 9 right). The 78.2 RON fuel is more sensitive to in-cylinder temperature and pressure than the other tested gasoline fuels.

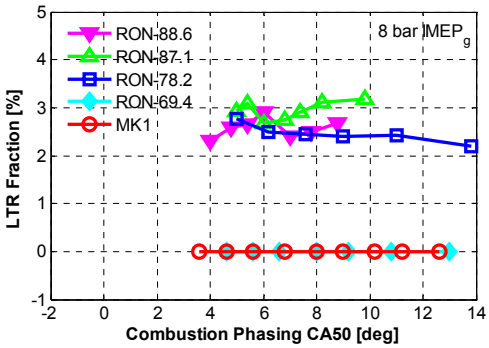

Figure 10. Fraction of low temperature reaction as a function of combustion phasing.

Premixed combustion fraction

Figure 11 shows the calculated premixed combustion using Gaussian profile fit (shown in Figure 4 and described with Equation 3). The premixed fractions for gasoline fuels are insensitive to CA50, while it increases for MK1 with late combustion phasing. The fraction of premixed combustion phase is connected to the n-paraffin concentration for gasoline fuels (see Table 2). High concentration of n-paraffin gives a high fraction of premixed combustion; however this was not the case for MK1 due to fuel chemistry and high temperature.

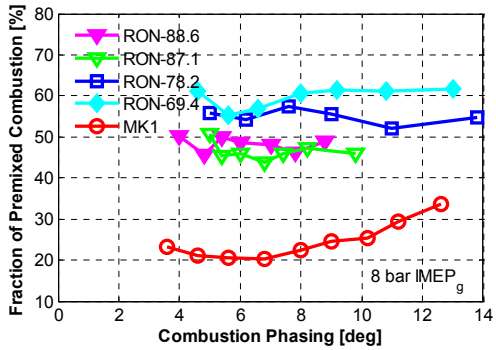

Figure 11. The fraction of the premixed combustion as a function of combustion phasing.

Combustion duration

Figure 12 shows the combustion duration as a function of combustion phasing. Combustion duration is defined as the length of the crank angle interval between 10% and 90% accumulated heat release, that is CA90-CA10. Diesel fuel had longer combustion duration than the gasoline fuels. The combustion duration for MK1 and for the lowest RON fuel was insensitive to combustion phasing, while it increased for the other gasoline fuels with retarding combustion phasing. This was due to premixed combustion, as a rapid premixed combustion gives shorter combustion duration, while slower diffusion controlled combustion gives longer combustion duration. The combustion duration was longest for MK1 and shortest for the high RON fuels.

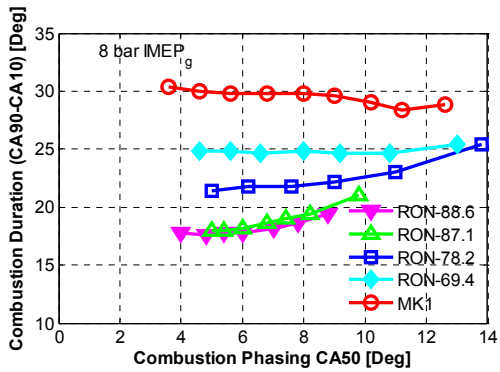

Figure 12. Combustion duration as a function of combustion phasing CA50.

Figure 13 shows that the maximum RoHR decreases with retarding combustion phasing for all fuels. However, the maximum RoHR for MK1 was quite insensitive to CA50. This is connected to the trend in premixed heat release fraction. The

Copyright © 2012 by ASME

increased premixed fraction at a later combustion phasing prevents the maximum rate to decrease for MK1.

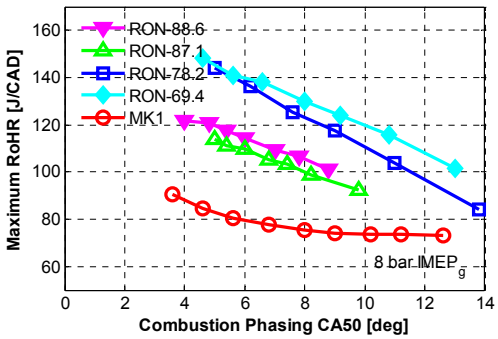

Figure 13. Maximum rate of heat release as a function of combustion phasing CA50.

Emissions

Smoke

The smoke emissions as a function of combustion phasing are shown in Figure 14. The smoke level for MK1 was largely influenced of the combustion phasing and peaked at 2.8 for CA50=10. The lowest RON fuel had a smoke level around 0.3 FSN, while other gasoline fuels had smoke levels below the detection limit 0.01 FSN. The rate of soot oxidation depends mostly on turbulence, temperature and available oxygen. All fuels operated at the same oxygen fraction and since the ambient density temperature and injection pressure are similar; the conditions for soot oxidation are likely the same for all fuels. The difference in smoke is thereby likely to be connected to the soot formation.

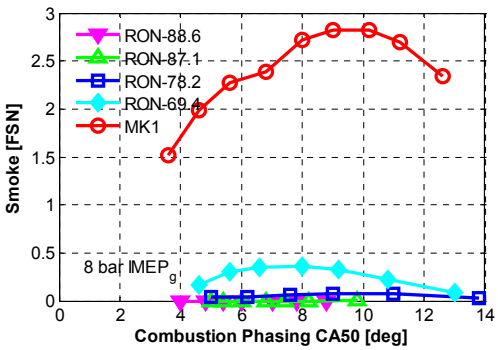

Figure 14. Smoke as a function of combustion phasing.

The soot formation is mainly affected by the fuel characteristics, the mixing between fuel and air, and the combustion temperature. Since boosting and inlet temperature are comparable for all fuels the soot formation can be expected to depend on fuel characteristics and mixture formation. The difference in ignition delay is, however, small between the low RON fuels and MK1. It is thereby indicated that the fuel composition had a far stronger influence on the smoke level than any characteristics of the combustion process. [3,8,16,26,27,28]

NO_x

Figure 15 shows the emission index of NO_x, g/kg-fuel, as a function of combustion phasing. The NO_x formation is strongest at high combustion temperatures and high oxygen fractions. There are three major factors that influence NO_x formation for a given diesel engine; air-fuel ratio, EGR ratio, and combustion phasing. For the gasoline fuels the NO_x level was close to 0.2 g /kg fuel. NO_x decreased with retarding combustion phasing due to low combustion temperature. MK1 had significantly higher NO_x level than gasoline fuels due to inhomogeneous combustion and thus higher in combustion temperature. A correlation between olefin concentration and NO_x was evident, high concentration of olefin resulted in low NO_x level (see Figure 15 and table 2).

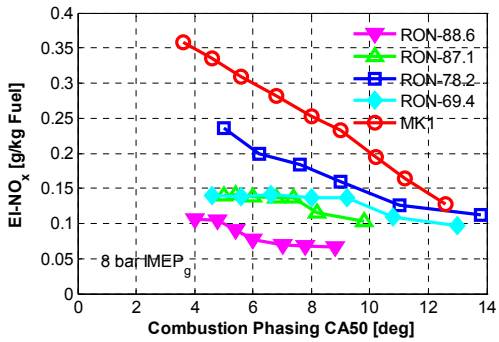

Figure 15. The emission index NO_x as a function of combustion phasing.

HC, CO and Combustion Efficiency

The emission indices for unburned hydrocarbon (HC) and carbon monoxide (CO) as a function of combustion efficiency are shown in Figure 16. HC increased with decreased combustion efficiency due to low combustion temperature during the expansion. At lean mixtures and above 1200 K most of HC is oxidized or converted to CO [29]. The HC level was highest for the high RON fuels and lowest for MK1. This is likely to be connected either to the advanced injection timing for the high RON fuel (an earlier SOI places more fuel in the squish volume, which is less likely to be fully oxidized), or due to longer ignition delay which creates more over-lean (fuel-air) mixture and thus more incomplete combustion. The HC level increased with retarding combustion phasing due to

Copyright © 2012 by ASME

low combustion temperature and it was lowest for MK1 due to efficient combustion.

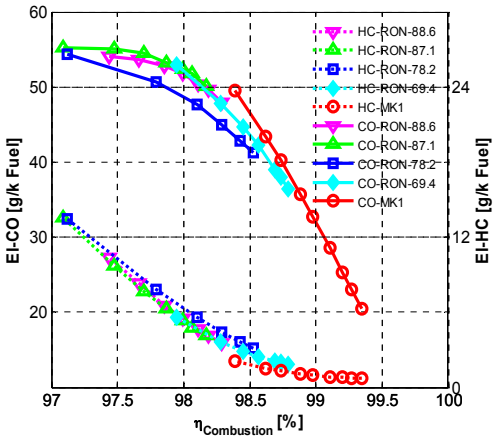

Figure 16. The emission index CO and HC as a function of combustion efficiency.

The reduction in CO with increased combustion efficiency is due to a high combustion temperature during the expansion. At lean mixtures and a combustion temperature between 800 K and 1400 K, a high fraction of CO can be expected. The CO was lower for MK1 than the gasoline fuels due to a more complete oxidation. The CO level increased with late combustion phasing and this was due to the low combustion temperature. A correlation between the RON and the CO emission index was evident, see Figure 16. The reason that high HC and CO was observed for the high RON fuels is because with such early injection timing the fuel and air become over-mixed.

Combustion efficiency ($\eta_{Combustion}$) increased with advanced combustion phasing due to high combustion temperature. Combustion efficiency was highest for MK1 and lowest for the low RON fuels. The inlet conditions are considered to be similar between the fuels, the difference thereby is likely due to the temperature rise because of in-homogeneity in the combustion for MK1.

SUMMARY AND CONCLUSIONS

Fuel aspects on PPC were examined for four fuels in the gasoline boiling range together with MK1 as a reference fuel. The experiments were performed at 8 bar $IMEP_g$ and 1500 rpm. During the experiments the desired λ value was 1.5 at an EGR ratio of 53±1%. This relation gave approximate inlet mole fraction of 5% CO_2 and 13% O_2. SOI where adjusted to detect the range in CA50 with stable combustion and acceptable pressure rise rate combined with maintained λ, EGR ratio, inlet pressure, and load.

- The combustion phasing range for MK1 and low RON fuels was limited by decrease in λ, while for high RON fuels the combustion phasing range was limited by combustion instability.
- MK1 showed the largest span in achievable CA50 range, approximately 10 CAD while the high RON fuel only had a range of 6 CAD.
- The ignition delay was related to n-paraffin concentration in the fuel. A high concentration of n-paraffin gave a short ignition delay, while low concentration gave a prolonged ignition delay.
- The duration and fraction of LTR depended on the ignition delay, where a prolonged ignition delay gave an increased duration.
- Smoke was higher for MK1 than the gasoline fuels. Considering the similar conditions for soot oxidation this was concluded to be related to the soot formation characteristics.
- MK1 showed a low concentration of HC and CO emissions compared to the gasoline fuels. The high RON fuels had the highest concentration of HC and CO plausible due to over-mixing.

REFERENCES

1. Heywood, J.B., 1988, "*Internal Combustion Engine Fundamentals*", McGraw Hill Book Co.
2. Warnatz, J., Maas, U., Dibble, R.W., 2006, "*Combustion Physical and Chemical Fundamentals, Modeling and Simulation, Experiments, Pollutant Formation*" 4th edition, Springer Berlin Heidelberg New York.
3. Aronsson, U., Chartier, C., Andersson, Ö., Johansson, B. et al., 2010 , "*Analysis of EGR Effects on the Soot Distribution in a Heavy Duty Diesel Engine Using Time-Resolved Laser Induced Incandescence*", SAE 2010-01-2104
4. Onishi, S., Hong Jo, S., Shado, K., Do Jo, P., Kato, S., "*Active Thermo-Atmosphere Combustion (ATAC) - A NEW Combustion Process for Internal Combustion Engine*", SAE 790501
5. Christiansen, M., Hultqvist, A., Johansson, B., 1999, "*Demonstrating the Multi Fuel Capability of a Homogenous Charge Compression Ignition Engine with Variable Compression Ratio*", SAE 1999-01-3679
6. Lu, X.C., Chen, W., Huang, Z., 2005, "*A Fundamental Study on the Control of the HCCI Combustion and Emissions by Fuel Design Concept Combined with Controllable EGR. Part 1. The Basic Characteristics of HCCI Combustion*", Fuel 84 (2005) 1074-1083
7. Takahashi, Y., Suyama, K., Lijima, A., Yoshida, K., Shoji, H., 2011, "*A Study of HCCI Combustion Using Spectroscopic Measurements and Chemical Kinetic Simulations: Effects of Fuel Composition, Engine Speed and Cylinder Pressure on Low-temperature Oxidation Reactions and Autoignition*", SAE Technical Papers 2011-32-0524

Copyright © 2012 by ASME

8. Sjöberg, M., Dec, J.E., 2008, "*Influence of Fuel Autoignition Reactivity on the High-Load Limits of HCCI Engines*", SAE Technical Paper 2008-01-0054
9. Johansson, T., Johansson, B., Tunestål, P., Aulin, H., 2009, "*The Effect of Intake Temperature in a Turbocharged Multi Cylinder Engine Operating in HCCI Mode*", SAE Technical Paper 2009-24-0060
10. Kitano, K., Nishiumi, R., Tsukasaki, Y., Tanaka, T. and Morinaga, M., 2003 , "*Effects of Fuel Properties on Pre-Mixed Charge Compression Ignition Combustion in a Direct Injection Diesel Engine*", JSAE 20030117 and SAE 2003-01-1815, 2003
11. Kimura, S., Aoki, O., Ogawa, H., Muranaka, S., Enomoto, Y., 1999, "*New Combustion Concept for Ultra-Clean and High-Efficiency Small DI Diesel Engines*", SAE 1999-01-3681
12. Kimura, S., Aoki, O., Kitahara, Y., Aiyoshizawa, E., 2002, "*Ultra-Clean Combustion Technology Combining a Low-Temperature and Premixed Combustion Concept for Meeting Future Emission Standards*", SAE 2002-01-0200
13. Andersson, M., et al., 2006, "*Characterization of Partially Premixed Combustion*", SAE 2006-01-3412
14. Suzuki, H., et al., 1998, "*Combustion Control Method of Homogeneous Charge Diesel Engine*", SAE 980509
15. Okude, K., Moir, K., Shiino, S., Moriyama, T., 2004, "*Premixed Compression Ignition (PCI) combustion for Simultaneous Reduction of NOx and Soot in Diesel Engine*", SAE 2004-01-1907
16. Musculus, Mark P. B., 2006, "*Multiple Simultaneous Optical Diagnostic Imaging of Early-Injection Low-Temperature Combustion in Heavy-Duty Diesel Engine*", SAE 2006-01-0079
17. Manente, V., Zander, C., Johansson, B., Tunestal, P., et al., 2010, "*An Advanced Internal Combustion Engine Concept for Low Emissions and High Efficiency from Idle to Max Load Using Gasoline Partially Premixed Combustion*", SAE 2010-01-2198.
18. Kalghatgi, G T., Risberg, P., Ångström, H., 2006, "*Advantages of Fuels with High Resistance to Auto-Ignition in Late-Injection, Low-temperature, Compression Ignition Combustion*", SAE 2006-04-3385
19. Kalghatgi, G., Risberg, P., Ångström, H., 2007, "*Partially Pre-mixed Auto-Ignition of Gasoline to Attain Low Smoke and Low NOx at High Load in a Comparison with a Diesel Fuel*", SAE 2007-01-0006
20. Solaka, H., Tuner, M., Johansson, B., "*Investigation of Partially Premixed Combustion Characteristics in Low Load Range with Regards to Fuel Octane Number in a Light Duty Diesel Engine*", SAE Technical Paper 2012-01-0684.
21. Yitao, S., Shijin, S., Jianxin, W., Jianhua, X., "*Optimization of Gasoline Hydrocarbon Compositions for Reducing Exhaust Emissions*", Jornal of Environmental Sciences, ISSN 1001-0742
22. Egnell., R, "*Combustion Diagnostics by means of Multizone Heat Release Analysis an NO Calculation*", SAE paper no. 891424 (1988)
23. Tanaka, S., Ayala, F., Keck, J.C., Heywood, J.B., 2002 "*Two-Stage Ignition in HCCI Combustion and HCCI Control by Fuels and Additives"*, Combustion and Flame 132 (2003) 219-239
24. Shibata, G., OYama, K., et al., 2005,"*Correlation of Low Temperature Heat Release with Fuel Composition and HCCI Engine Combustion*", SAE Technical Paper 2005-01-0138.
25. Truedsson, I., Tuner, M., Johansson, B., Cannella, W., "*Pressure Sensitivity of HCCI Auto-Ignition Temperature for Primary Reference Fuels*", SAE Techincal Paper 2012-01-1128
26. Dec, J.E., *"A Conceptual Model of DI Diesel Combustion Based on Laser-Sheet Imaging",* SAE Technical Paper 970873, 1997
27. Andersson, Ö., "*Diesel Combustion, in Handbook on Combustion",* vol. 3, Ed. Winter F., Wiley-VHC books, Weinheim, 2010
28. Aronsson, U., Chartier, C., Andersson, Ö., Egnell, R., Sjöholm, J., Richter, M., and Aldén, M., *"Analysis of the Correlation Between Engine-Out Particulates and Local Φ in the Lift-Off Region of a Heavy Duty Diesel Engine Using Raman Spectroscopy*", SAE Technical Paper 2009-01-1357, 2009
29. Kim, D., Ekoto, I., Colban, W.F., and Miles, P.C., 2008 "*In-Cylinder CO and UHC Imaging in a Light-Duty Diesel Engine During PPCI Low-Temperature Combustion*", SAE Technical Paper 2008-01-1602.

CONTACT INFORMATION

Hadeel.Solaka@energy.lth.se

ACKNOWLEDGMENTS

The author would like to acknowledge the Competence Center Combustion Processes, KCFP, and the Swedish Energy Agency for the financial support, Bill Cannella from Chevron for supplying fuels and Patrick Borgqvist for implementing control system.

NOMENCLATURE

ATDC	After top dead center
CAD	Crank angle degree
CA50	Crank angle at 50% completion of heat release
CA0	Crank angle at 0% completion of heat release
CN	Cetane number
CO	Carbon monoxide
CO_2	Carbon dioxide
COV	Coefficient of variance
EGR	Exhaust gas recirculation
EOI	End of injection

Copyright © 2012 by ASME

HC	Unburned hydrocarbon
$IMEP_g$	Indicated mean effective pressure gross
LTR	Low temperature reactions
MON	Motored octane number
MP	Mixing period
NO_x	Nitrogen oxides e.i. NO, NO_2
PM	Particulate Matter
RoHR	Rate of heat release
RON	Research octane number
SOC	Start of combustion
SOI	Start of injection
TDC	Top dead center
UHC	Unburned hydrocarbons

Copyright © 2012 by ASME

Paper III

13PFL-0914

Analysis of Surrogate Fuels Effect on Ignition delay and Low Temperature Reaction during Partially Premixed Combustion

Hadeel Solaka, Martin Tunér and Bengt Johansson
Lund University

Copyright © 2013 SAE International

ABSTRACT

Fuel effects on ignition delay and low temperature reactions (LTR) during partially premixed combustion (PPC) were analyzed using Design of Experiments (DoE). The test matrix included seventeen mixtures of n-heptane, isooctane, toluene and ethanol covering a broad range of ignition quality and fuel chemistry. Experiments were performed on a light duty diesel engine at 8 bar IMEPg, 1500 rpm with a variation in combustion phasing, inlet oxygen concentration and injection pressure. A single injection strategy was used and the start of injection and injection duration were adjusted to achieve the desired load and combustion phasing. The experimental data show that fuels with higher RON values generally produced longer ignition delays. In addition, the alcohol content had significantly stronger effect on ignition delay than the aromatic. Fuels with more ethanol gave longer ignition delays and a combination of high level of ethanol and toluene produced the longest ignition delay. An increased inlet oxygen concentration shortened the ignition delay. Surprisingly and in contradiction to what has been reported for HCCI combustion, ethanol amplified the LTR phase, while n-heptane suppressed it. Finally, the LTR phase was proportional to ignition delay. Longer ignition delay resulted in higher fraction of LTR.

INTRODUCTION

Compression ignited (CI) engines generally have higher efficiency than spark ignited (SI) engines. However the most common combustion concept in CI engines, conventional diesel combustion, struggles with high levels of particulate matter (PM) and NO_x emissions. A significant portion of the PM consists of combustion generated soot. The soot and NO_x emissions can be individually suppressed but generally there is a tradeoff, methods that reduce NO_x emissions lead to increased soot emissions and vice-versa. One reason for this is that conditions leading to a sufficient soot oxidation also lead to high NO_x formation. However, by introducing large amount of cooled exhaust gas recirculation (EGR) the combustion temperature can be suppressed which leads to lower formation of both soot and NO_x [1-3]. This is utilized in partially premixed combustion (PPC). In PPC it is desirable to have separation between the end of injection and the start of combustion [4,5]. This can be achieved using large amount of exhaust gas recirculation (EGR), early start of injection, and fuel with high octane number (ON) [6-9].

In 2006 it was demonstrated that using gasoline fuel in compression ignition engines may reduce the levels of engine-out emissions [10-15]. Since gasoline has a higher resistance to auto-ignition compared to the diesel fuel, it gives more time for mixing, and thus producing a higher fraction of premixed combustion. Using both EGR and gasoline fuels with high octane number further extends the time for pre-mixing. The fuel effects on the combustion process is dependent of the course of events on the early stages, i.e. mixing period, ignition delay and low temperature reaction phase (LTR). Therefore, understanding the fuel effect of these properties is critical to understand fuel effects on PPC.

Fuel effects on ignition delay have been studied previously for diesel, Homogenous Charge Compression Ignition (HCCI) and PPC combustion. The ignition delay plays an important role in partially premixed combustion. Achieving the desired premixed combustion requires increasing the mixing of the fuel and air prior to ignition. The ignition delay depends on two factors; physical and chemical processes. The physical delay is when the fuel is injected, droplet evaporates, mixes with air and heats up to the auto ignition temperature [16], while the chemical delay takes place after the contact has been made between fuel and oxygen. This engages kinetics of chemical reactions which form free radicals and other intermediates that are necessary for ignition [16,17]. It is known that the two-stage, low temperature reactions (LTR), occurs in HCCI operations for fuels with a cetane number higher than 34. The amount of low temperature reactions heat release in each case increases with decreasing octane number and increasing cetane number, respectively. It is known that LTR phase increases with high concentration of n-heptane in the fuel during HCCI combustion. In [18-20], it was realized that the aromatics, some of the naphthenes, olefins and ethanol have a mechanism that reduces the LTR phase in HCCI combustion. In [20], Shibata mentioned that inlet oxygen concentration have a mechanism that affect the LTR phase, decreasing the inlet oxygen decreases the LTR. The LTR phase is mostly depends on the chemical reactions and the structure of the fuel composition. However, very few

researchers have studied the effect on fuel properties on LTR phase in partially premixed combustion.

The authors have studied fuel effects on PPC previously [21,22]. It was observed that higher octane number fuels have longer ignition delay, as expected. Higher n-paraffin content resulted in shorter ignition delay and smaller LTR phase. Previously by the author also was observed that there was a relationship between ignition delay and LTR, longer ignition delay resulted in higher LTR. Therefore, this research study seeks to understand the connection between fuel properties (in particular alcohol, aromatic and alkane) and combustion events. There are three main goals of the research study: **Firstly** to understand which chemical and physical properties that affect ignition delay. Ignition delay is an important factor in partially premixed combustion, increasing the ignition delay allows for improved fuel-air mixing and thus resulting in a more substantial premixed burn. **Secondly** to investigate the chemical and physical parameters influence on the LTR phase. The LTR is an indication of low temperature combustion. Previous study by Shibata [20] showed that ethanol and high level of exhaust gas recirculation suppress LTR while n-heptane amplifies LTR in HCCI combustion. Hence, the focus of this study tries to capture the same trend but in PPC instead of HCCI operating conditions. **Thirdly** investigate if there is a correlation between ignition delay and LTR and if this correlation is influenced by ethanol or inlet oxygen concentration. Therefore in this study, four surrogate fuels, n-heptane, isooctane, toluene and ethanol, were analyzed using design of experiment. The test matrix included seventeen mixtures of n-heptane, isooctane, toluene and ethanol covering a broad range of ignition quality and fuel chemistry. The model is used to map the n-heptane, toluene and ethanol influence on ignition delay and LTR-phase. Fuel effects were quantified across a range of inlet oxygen concentration, combustion phasing and injection pressure to identify secondary parameter interactions.

EXPERIMENTAL SETUP AND DIAGNOSTICS

Engine setup

The presented investigations were performed in a Volvo D5 five cylinder passenger car diesel engine. The engine operated on only one cylinder while the other four were motored. The cylinder head and injection system with the following specifications are shown in Table 1. The engine test rig was equipped with an adjustable exhaust gas recirculation system and adjustable heating of the inlet temperature.

Table 1. Engine Specifications

Engine specifications	
Engine type	Volvo D5
Number of cylinders	1
Bore [mm]	81
Stroke [mm]	93.2
Displacement Volume [cm^2/cylinder]	480
IVC [CAD BTDC]	174
Compression ratio	16.5
Swirl ratio	2.2
Number of intake valves	2
Number of exhaust valves	2
Injector	
Type	Solenoid
Injection nozzle holes	7
Injection nozzle diameter [mm]	0.14
Included angle [degrees]	140

Fuels

Fuels used in this study are a mixture of n-heptane, isooctane, toluene and ethanol in different volume fractions. In order to ensure that no damage was caused to the injection system, 100 ppm lubricity additive *Infineum R655* was added to each fuel mixture. The impact, on combustion phasing and emission formation, of the additive is expected to be neglectable at such small fraction. Fuel specifications are shown in Table 2. Isooctane and n-heptane mixtures are called primary reference fuels (PRF), and these fuels define the RON and MON scales with 100 and 0 respectively. Toluene and ethanol are octane enhancers. However, there is no direct link between fuel mixture (compositions of PRF and toluene or PRF and ethanol or altogether) and octane number. In Table 2 the RON value increases for a fuel mixture that consists of toluene or ethanol or both, this RON called "Blending RON". Toluene blending RON is a nonlinear relation. However, its RON value increases from 120 to 126* if the fuel mixture consists of 15% [23]. Ethanol RON value increases from 107 to 140** if the fuel mixture consists of 10% [24].

Measurement instrument

Data acquisition

Cylinder pressure is measured with Kistler 6056 to monitor cylinder pressure for heat release calculations. This sampled with the resolution of 0.2 crank angle degrees (CAD). The crank shaft position was determined by an encoder which provided five pulses per crank angle degree providing a resolution of 0.2 CAD. There are many parameters that measured from the engine such as the inlet and exhaust pressure which are measured with a pressure sensor of type Keller. The inlet air, inlet mixture and exhaust temperature are measured by Pentronic type K thermocouples.

Table 2. Fuel Specifications

Fuels Properties	n-Heptane	Toluene	Ethanol	Isooctane
RON	0	120	107	100
MON	0	109	89	100
Blending RON	0	126*	140**	100
Auto-Ignition temperature [°C]	203.85	529	425	411
Molecular formula	C_7H_{16}	C_7H_8	C_2H_6O	C_8H_{18}
Molar mass [g/mol]	100.23	92.15	46.07	114.26
Density [kg/m^3]	679.5	866.9	789	688
Boiling point [°C]	98	110.6	78.5	99

Fuel and air mass flows

The intake air mass flow is measured by a thermal mass flow meter (Bronckhorst IN-FLOW). It is situated approximately 3 m upstream from the intake manifold in order to prevent pressure oscillations to propagate from the engine, or EGR system, into the flow meter. Fuel mass flow is measured as the mean value of the mass gradient by a fuel balance (Sartorius CPA 62025).

Emission measurement

Smoke emissions were measured with the AVL415S smoke meter, while NO_x, HC, exhaust CO_2, CO and intake CO_2 emissions were measured with a Horiba measurement system (MEXA9200DF). NO_x emissions were measured with a chemiluminescence analyzer whereas HC was measured with a hydrogen flame ionization detector (FID) and the piping to the analyzer was heated to approximately 191°C to avoid condensation of unburned fuel components. Inlet and exhaust oxygen (O_2) was measured by a magneto-pneumatic condenser microphone method (MPA), whereas CO, intake CO_2 and exhaust CO_2 were measured with infrared analyzes.

Inlet oxygen concentration

The intake oxygen concentration is measured with a Horiba measurement system. The oxygen concentration in the intake manifold was controlled by a valve that provides the amount of EGR into the intake system. The EGR was drawn off the main exhaust pipe through EGR cooler to decrease the EGR temperature. Typical EGR coolers, including the cooler used on the production 5-cylinder version of this engine, cool the EGR by circulating engine coolant through a heat exchanger which uses the engine cooling loop. Later the EGR and the heated air in the inlet system are mixed to a temperature of 345 K before the intake air mixture goes into the cylinder as shown in Figure 1.

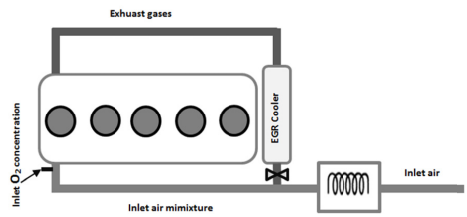

Figure 1. EGR and oxygen measurement in the inlet system.

METHODS AND DEFINITIONS

Design of experiments

Seventeen blends of isooctane, n-heptane, and toluene and ethanol mixture are created according to experimental design of mixture. A central composite design of two-level full factorial where axes are drawn through the center of the cube and the axial points are located at the face of the cube [25], as shown in Figure 2, are used in this study. The experiment used n-heptane, toluene and ethanol in a center composite two-level, three factor, full factorial design. A fourth factor, isooctane was added to allow calculation of a four factor. The approach was used as it was believed that there could be meaningful interactions among the first three factors that could be calculated with center composite full factorial design.

Table 4. Surrogate fuel matrix.

Fuels	n-heptane [vol %]	Toluene [vol %]	Ethanol [vol %]	Isooctane [vol %]	RON	MON
1	30	0	0	70	70.3	70.4
2	40	0	0	60	60.6	60.8
3	30	15	0	55	74.2	71.9
4	40	15	0	45	64.3	62.3
5	30	0	10	60	78.7	76.7
6	40	0	10	50	69.7	66.8
7	30	15	10	45	81.6	77.2
8	40	15	10	35	72.2	69.0
9_{cp}	35	7.5	5	52.5	71.9	69.4
10_{cp}	35	7.5	5	52.5	71.9	69.4
11_{cp}	35	7.5	5	52.5	71.9	69.4
12	40	7.5	5	47.5	66.6	64.0
13	30	7.5	5	57.5	76.8	74.2
14	35	15	5	45	73.5	69.4
15	35	0	5	60	70.5	68.7
16	35	7.5	10	47.5	74.9	71.8
17	35	7.5	0	57.5	67.3	66.1

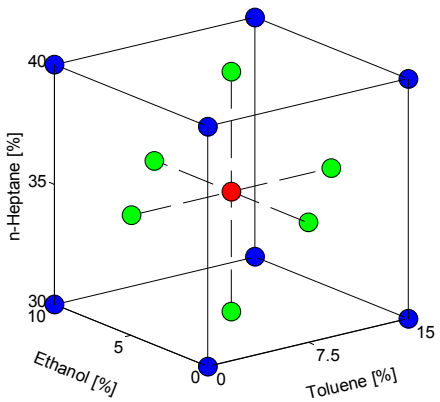

Figure 2. A central composite of two-level full factorial design.

The settings for the three factors are given in Table 3 and graphically in Figure 2. However, the isooctane content in the mixtures was calculated according to Eq. 1. The levels were chosen to model gasoline fuel in a wide range of ignition quality.

Table 3. Surrogate fuel compositions.

Fuel	High [%]	Average [%]	Low [%]
n-Heptane	40	35	30
Toluene	15	7.5	0
Ethanol	10	5	0

$$Isooctane_{C_I} = 100 - \left(nheptane_{C_N} + toluene_{C_T} + ethanol_{C_E}\right) \quad (1)$$

Where C_I is the isooctane composition in the mixture, C_N, C_T, and C_E are n-heptane, toluene and ethanol compositions respectively in the mixture. In order to include isooctane in the test matrix, it was decided that the sum of n-heptane, toluene and ethanol mixture concentration should be less than 100 and the rest represented by isooctane as shown in Table 4.

The test matrix consisted of 15 fuel mixtures as shown in Table 4. The number of experiments can be described as $2^{k-p}+2k+cp$, where k is the number of studied variables, p is the fractionalization element (p=0, full design) and *cp* is the number of the central points. The center point was replicated three times thus meaning that test matrix consisted of 17 ($2^3+2x3+3$) set point combinations in total as seen in Table 4. The research octane number (RON) and the motor octane number (MON) were determined by ASTM D2699 and D2700 respectively in CFR engine.

Heat release characteristic

From the calculated rate of heat release information about the combustion events can be extracted. The combustion events are divided into four phases; ignition delay (ID), low temperature reactions (LTR), premixed combustion phase and late mixing controlled combustion phase as seen in Figure 3. In this study, two phases were studied; ignition delay and low temperature reaction phase.

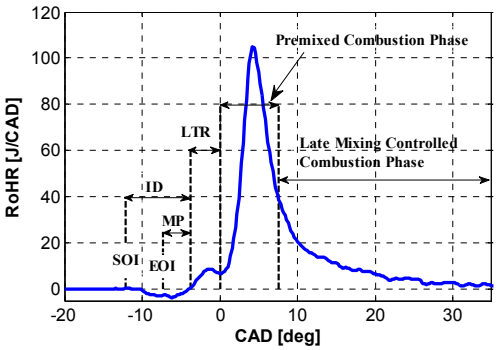

Figure 3. Typical PPC heat release diagram identifying different PPC phases.

Ignition delay phase

The ignition delay is the period between the start of injection (SOI) and the start of combustion (SOC) as shown in Figure 3. The start of injection was determined from the gradient of injection pressure where the gradient reached its maximum value due to needle lift as shown in Figure 4. The start of combustion is defined as the location where rate of heat release returns to zero after the negative period. When the fuel is injected the cylinder gas temperature decreases due to fuel evaporation, showing the negative rate of heat release. At the point where the rate of heat release return to zero established the start of combustion and, or the start of low temperature reactions.

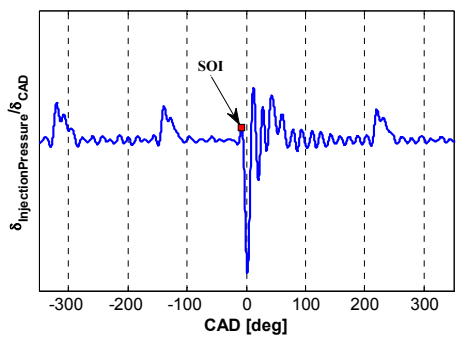

Figure 4. Gradient of injection pressure as a function of crank angle degree. Start of injection in red square.

Low temperature reaction phase

The Low temperature reactions are the first heat release with very low reaction temperature, where several reactions occur simultaneously and lead to real combustion. The LTR phase is characterized by a small peak before the main premixed rate of heat release. LTR fraction is used in this study and it was compared for different surrogate fuels. There are two methods used by the author to define the LTR phase. In the current study a method established and used to define the end of LTR phase in a good and robust way because at times the end of LTR is indistinct from the main rate of heat release. In order to separate the phases (LTR phase and premixed combustion phase) in a well-defined manner, a Gaussian profile is fitted to the raising flank of the premixed peak, between 15 J/CAD and the actual peak. The rate of heat release is then subtracted from the Gaussian profile, and the integrated area between the start of combustion and the threshold point is used as a measure of the LTR fraction as shown in Figure 5.

$$G(x) = h \cdot e^{-\left(\frac{x-x_0}{2\alpha^2}\right)^2} \qquad (2)$$

In Equation (2) x_0 is the central position of the peak, h and α representing the height and width of the Gaussian profile.

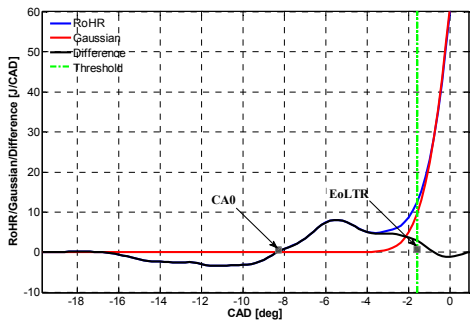

Figure 5. Gaussian profile (red), RoHR (blue), and difference (black) as a function of CAD. Figure shows the LTR phase.

OPERATING CONDITIONS

The testing condition used for this part of work center around the base conditions: 1500 rpm with a 8 bar $IMEP_g$ as in previous studies by the author [21,22]. A single injection strategy was used where the start of injection and the injection duration were adjusted to achieve the desired load and combustion phasing (CA50) as shown in Table 5. Combustion phasing is defined as the crank angle degree where 50% of the total heat is released (CA50). The inlet mixture temperature and pressure were kept constant at 345 K and 2.8±0.2 bar respectively. At this condition, several parameters were varied to examine surrogate fuel effect and engine behavior during PPC. These parameters included inlet oxygen concentration, combustion phasing and injection pressure. The inlet oxygen concentration was set to three different volume fractions: 11, 13 and 15%. At each oxygen concentration level, the combustion phasing and injection pressure were varied. The combustion phasing was set to 3, 6, 8 and 10 degrees after top dead center, while injection pressure was set to, at each

oxygen concentration and combustion phasing 800, 1000 and 1200 bar as shown in Table 6.

Table 5. Constant inlet conditions.

Engine speed [rpm]	1500
Inlet temperature mixture [K]	345
Loads $IMEP_g$ [bar]	8
Absolut inlet pressure [bar]	2.8±0.2

Table 6. Operating conditions.

Inlet oxygen concentration [%]	11 (Low)	13 (Base)	14 (High)
CA50 [ATDC deg]	3, 6, 8 &10	3, 6, 8 &10	3, 6, 8 &10
Injection Pressure [bar]	800 (Low)	1000 (Base)	1200 (High)

RESULTS AND ANALYSIS

Ignition Delay

The time difference between the start of injection (SOI) and the start of combustion (SOC) is called ignition delay. There are two factors that affect the ignition delay; physical and chemical factors. The physical factors that affect the fuel spray characteristics and the cylinder chamber conditions (such as temperature, velocity and pressure) will influence the ignition delay. On the other hand, the chemical properties of the fuels are much more important.

One of the physical factors is the injection system variables. These variables are injection quantity (duration), injection timing, and injection pressure. Other physical factors are air charge conditions, load, engine speed, combustion chamber geometry, and swirl rate. In this study, the engine speed, air charge temperature and pressure, combustion chamber geometry, swirl ratio and load were constant. The injection timing and injection duration were adjusted to obtain the desire load at 8 bar $IMEP_g$ and combustion phasing at 3, 6, 8 and 10 crank angle degree after top dead center (ATDC) for all operating conditions. The injection pressure and inlet oxygen concentration were varied as shown Table 6.

The ignition quality for three PRF fuels (PRF60, PRF70 and PRF80) were analyzed and compared to TRF (a mixture of toluene and PRF) and ERF (a mixture of ethanol and PRF). This analysis will help to understand n-heptane, effect on ignition delay in the surrogate fuel matrix. Figure 6 shows the ignition delay for the three PRF fuels at different oxygen concentrations. The effect of RON value on the ignition delay is clear, with distinct difference between each fuel of different RON value. The increases in ignition delay as RON value was increased. This is expected, since a high RON value is the same as high resistance to auto-ignition. In order to achieve the same CA50 for all PRF fuels, the SOI was adjusted. Hence, PRF80 was injected earlier due to its high RON value. The prolonged ignition delay with earlier or later injection timing occurs because the air temperature and the pressure change significantly close to the top dead center. If the start of injection occurs earlier, the initial pressure and temperature are lower which results in longer ignition delay [16]. For example: having CA50 at 3 degrees after top dead center (earliest SOI), the ignition delay increases with increasing PRF by almost one degree for the case with the lowest inlet oxygen concentration and similar trend is captured with other inlet oxygen concentrations. However, the inlet oxygen concentration has more influence on ignition delay than fuel compositions for PRF fuels as shown in Figure 6. The ignition delay decreases with increasing oxygen concentration in the inlet air charge. Ignition delay is prolonged for PRF80 (black square marker) by decreasing oxygen concentration. In order to achieve the same CA50 at 3 CAD ATDC for different oxygen concentration the injection timing is adjusted. Due to insufficient oxygen and longer mixing time the injection timing is advanced for the lowest oxygen concentration. The same trend is captured for the other fuels at different inlet oxygen concentrations. The equivalent ignition delay for different PRF is maintained by varying the inlet oxygen concentration. PRF80 with 15% O_2 (black square and dotted line), PRF70 with 13% O_2 (red circle and dashed line) and PRF60 with 11% O_2 (blue triangle and solid line) have similar ignition delay as shown in Figure 6.

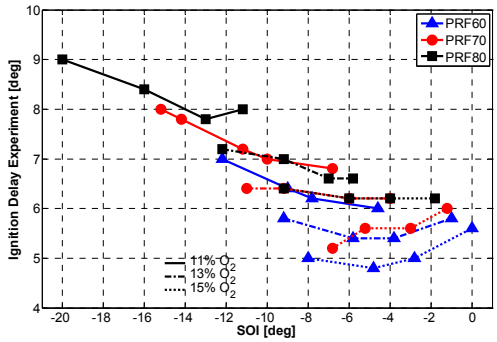

Figure 6. Ignition delay as a function of start of injection. PRF60 (blue triangle), PRF70 (red circle), PRF80 (black square) with different inlet oxygen concentrations; 11% O_2 solid lines, 13% O_2 dashed lines and 15% O_2 dotted lines with CA50 at 3 degrees ATDC and 1000 bar injection pressure.

The ignition delay as a function of the start of injection for PRF, TRF and ERF are shown in Figure 7. To understand the influence of fuel compositions on ignition delay, base fuel PRF70 (30% n-heptane and 70% isooctane) was compared to two different fuel compositions TRF and ERF. In this case, n-heptane concentration was kept constant at 30% volume fraction whereas isooctane concentration was replaced by toluene for TRF fuel and by ethanol for ERF fuel. The ignition delay was prolonged by replacing 15% of isooctane in PRF70 with toluene (blue square dashed line). Whereas replacing 10% of isooctane in PRF70 with ethanol (black triangle dotted line), the ignition delay was boosted by 1.5 degree at CA50 3 CAD ATDC (earliest injection) as shown in Figure 7. As it

was mentioned previously, the injection timing was advanced for higher RON fuel to achieve the same CA50 due to high auto-ignition resistance.

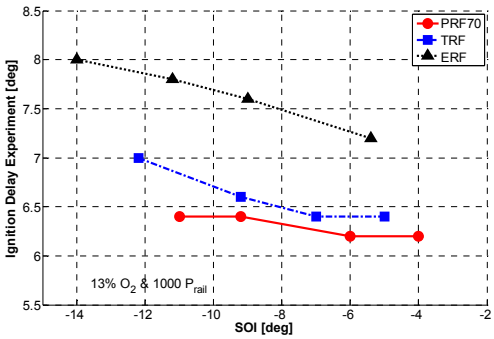

Figure 7. Ignition delay as a function of start of injection. Figure shows PRF70 (red circle solid line), TRF (blue square dashed line) and ERF (black triangle dotted line) at constant oxygen concentration 13% and 1000 bar injection pressure.

The general trends from the DoE analysis of the measurements are shown in Figure 8 to Figure 11 and Figure 14 to Figure 17. The levels on the abscissa of these figures refer to the values given in Table 4 and Table 6. The markers represent the experimental data and the curves represent the DoE regression model fit. As seen in the following figures the curves from the DoE regression model do not match the experimental data exactly. However, the regression model for a response is based on the whole data set (17 data points) as shown in Table 4, but few of the surrogate fuel mixtures are plotted in the following figures. These surrogate mixtures are: ***PRF***, ***TRF*** (which consist of 15% toluene and PRF), ***ERF*** (which consists of 10% ethanol and PRF), ***$TERF_{critical}$*** (critical point which consists of 15% toluene, 10% ethanol and PRF) and ***$TERF_{cp}$*** (center point which consists of 7.5% toluene, 5% ethanol and PRF). The rest of the surrogate mixtures captured the same trends.

Figure 8 shows the ignition delay trends and fuel compositions. Ignition delay depends on chemical reaction that occurs inside the combustion chamber. These chemical reactions depend on fuel composition and conditions in the combustion chamber. In this study the inlet operating conditions were kept constant at all points as shown in Table 5. Figure 8 shows the base case where the engine control parameters are at 13% O_2, 1000 bar injection pressure and with CA50 at 3 CAD ATDC. This helps to investigate and grasp the effect of surrogate fuels on ignition delay. As expected, ignition delay decreases with increasing n-heptane concentration in the mixtures. The ignition quality of a fuel is defined by its cetane number (CN), N-heptane has high cetane number, and fuels with high cetane number will generally have a shorter ignition delay. For PRF fuel (black solid line), increasing isooctane content in the fuel did not have much influence on ignition delay. Then the rest of the fuels are compared with PRF as the base fuel at the lowest n-heptane concentration. For TRF (green dash-dot line) ignition delay is higher by a. For $TERF_{cp}$ (red dashed line) ignition delay is higher by one and half degree. For ERF (black dotted line) ignition delay is higher by two degrees. For $TERF_{critical}$ (red dotted line) ignition delay is higher by four degrees. Fuel slope varies from a horizontal line to a sharp slope depending on fuel RON value. Hence, the difference in ignition delay and its slope between fuels is relatively proportional to their separation in RON value. R^2 for each model are given in the figures. By definition R^2 range is between 0 and 1, where a value of 1 corresponds to a perfect fit. The same trend was captured at different CA50 with variation of inlet oxygen concentration and injection pressure for all surrogate mixtures.

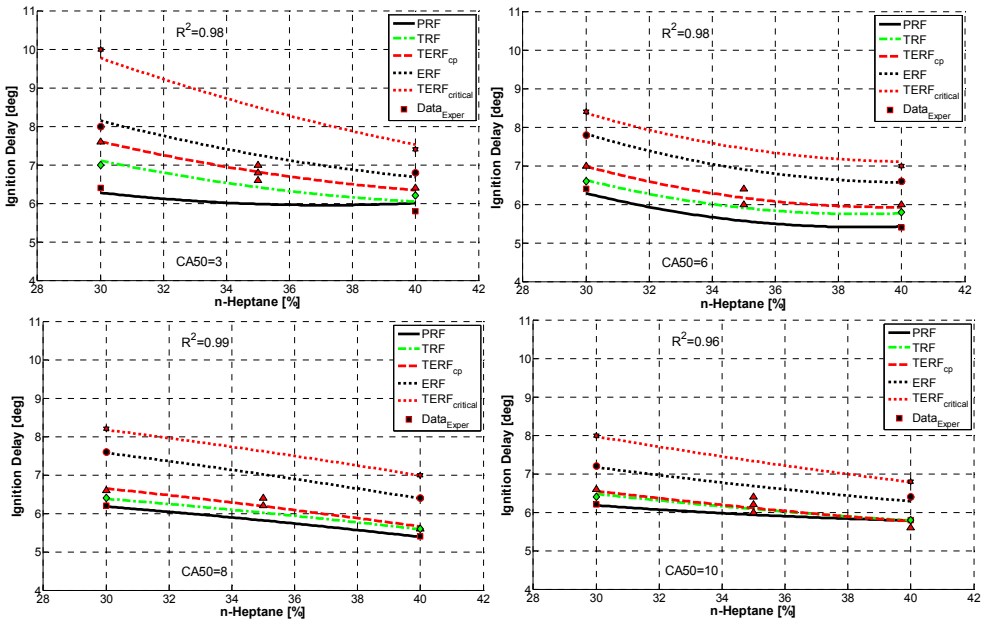

Figure 8. Ignition delay as a function of n-heptane. Figure shows PRF (black solid line and squares), TRF (green dash-dot line and diamonds), ERF (black dotted line and circles), $TERF_{cp}$ (red dashed line and triangles) and $TERF_{critical}$ (red dotted line and hexagrams) at constant oxygen concentration 13%, 1000 injection pressure and CA50 at 3, 6, 8 and 10 CAD ATDC.

As expected, ignition delay increased with increasing RON value for different cases of SOC as shown in Figure 9. The chemical characteristics of the fuel are very important. The dependence of RON value on fuel molecular structure is as follows: straight-chain paraffinic compounds (n-heptane) have the highest ignition quality comparing to the branched-chain (isooctane), which means the auto-ignition resistance is higher for isooctane. Aromatic and alcohol have poor ignition quality which means the auto-ignition resistance is very high. The results shown in Figure 9 are under the same operating condition as in Table 5 at 13% inlet oxygen concentration and 1000 bar injection pressure with variation of combustion phasing. Keeping the CA50 constant at 3, 6, 8 and 10 CAD ATDC resulted in a wide range of SOC for different fuel combinations. The ignition delay decreases with retarding SOC until it reaches its minimum around SOC 0 CAD ATDC, then it increases again. The increase in ignition delay with earlier SOC (at -6 and -3 degree) is because the air temperature and pressure are lower. However, the decrease in ignition delay with later SOC (at 0 degree) is because the air temperature and pressure are slightly higher close to top dead center (TDC). After TDC the air temperature and pressure are slightly lower therefore the increase in ignition delays at SOC (3 and 6 degree).

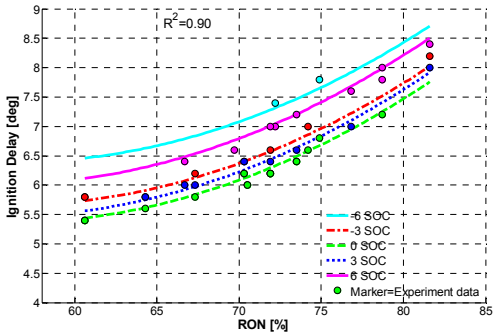

Figure 9. Ignition delay as a function of RON for different cases of SOC. Figure shows SOC -6 (cyan solid line), SOC -3 (blue dotted line and), SOC 0 (green dashed line), SOC 3 (red dash-dot line) and SOC 6 (red solid line) at 1000 bar injection pressure, 13% inlet oxygen concentration and CA50 at 3, 6, 8 and 10 CAD ATDC.

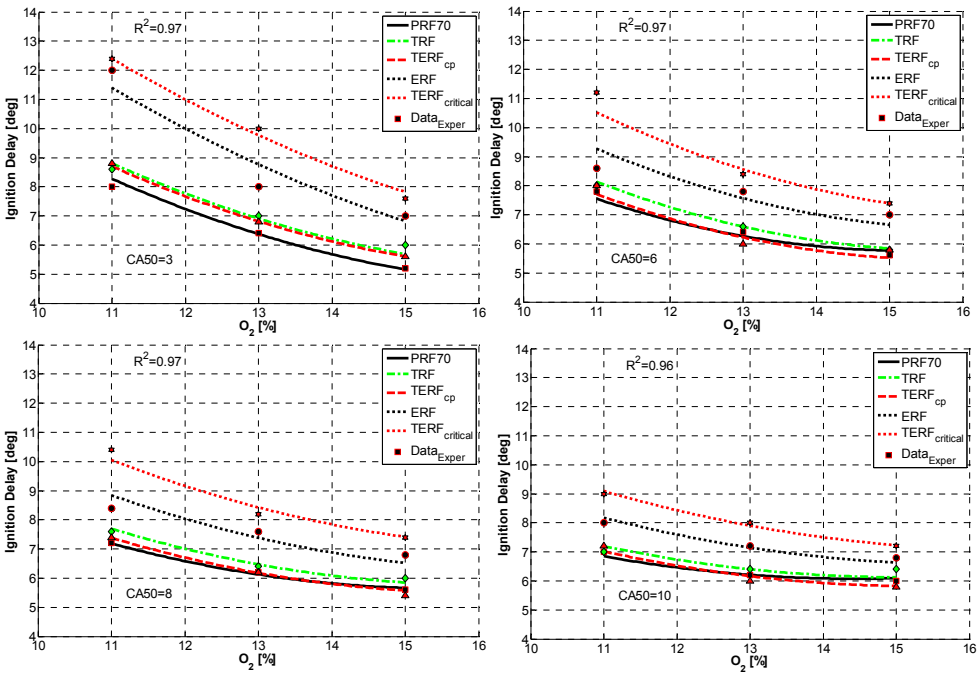

Figure 10. Ignition delay as a function of inlet oxygen concentration. Figure shows PRF (black solid line and squares), TRF (green dash-dot line and diamonds), ERF (black dotted line and circles), $TERF_{cp}$ (red dashed line and triangles) and $TERF_{critical}$ (red dotted line and hexagrams) at 1000 bar injection pressure and CA50 at 3, 6, 8 and 10 CAD ATDC.

As seen in Figure 10 ignition delay increased with decreasing inlet oxygen concentration. For $TERF_{critical}$ and ERF, ignition delay was increased by four degrees moving from the highest inlet oxygen concentration to the lowest. While for PRF, $TERF_{cp}$ and TRF, ignition delay was increased by three degrees moving from the highest to the lowest inlet oxygen concentration. The total amount of air charge entering the cylinder was the same but the volume fraction of oxygen was lower. Therefore, the increase in ignition delay was due to insufficient oxygen in the inlet air charge, thus allows more time for the injected fuel to react with the available oxygen. The inlet oxygen concentration had stronger influence on ignition delay. These trends did not change with variation in injection pressure or combustion phasing was used. However, the ignition delay levels decreased by approximately three degrees by retarding the combustion phasing.

Generally, increasing injection pressure advances the combustion phasing due to improved spray breakup and shorter physical mixing time, yielding a shorter ignition delay [26]. However, in this study ignition delay is insensitive to injection pressure, as shown in Figure 11, at constant operating condition as shown in Table 5, and at 13% O_2 with CA50 at 3 degree ATDC. Results obtained at other inlet oxygen concentrations and combustion phases are similar. This is due to similarity in SOI at different injection pressure for the same fuel.

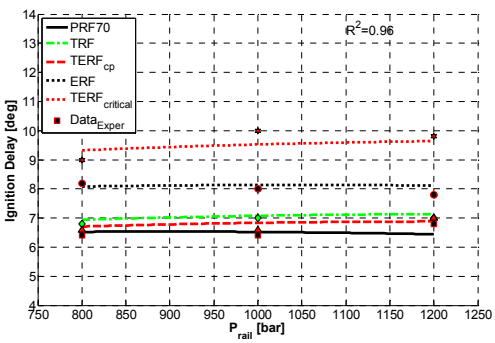

Figure 11. Ignition delay as a function of injection pressure. Figure shows PRF (black solid line and squares), TRF (green dash-dot line and diamonds), ERF (black dotted line and circles), $TERF_{cp}$ (red dashed line and triangles) and $TERF_{critical}$ (red dotted line and hexagrams) at 1000 injection pressure and CA50 at 3 CAD ATDC.

Low Temperature Reactions Phase

The low temperature reaction phase is defined from the start of combustion to the end of LTR. The end of LTR is defined as the minimum value between the main peak of heat release rate and the second peak of LTR, as shown in Figure 5. Low temperature reactions phase depends mainly on chemical process (such as fuel composition and fuel structure) and physical (such as in-cylinder temperature and pressure and the conditions for the inlet air charge as well). Earlier studies showed that LTR increases with n-heptane while it decreases with isooctane in HCCI combustion [18,19]. Shibata in [20] mentioned that ethanol and high EGR rate suppress LTR in HCCI combustion. Therefore this work tries to capture the same trend but in PPC type of combustion. Three different PRF fuels are studied to clarify the effect of n-heptane on LTR. These three fuels, as mentioned in previous section, are; PRF60 (blue triangle markers), PRF70 (red circle markers) and PRF80 (black square markers). The most striking feature observed in Figure 12 is the increase in the LTR as n-heptane decreased and EGR rate increased. To achieve the same CA50, SOI was advanced for high RON fuels. Advancing the SOI generally tends to increase LTR phase because the in-cylinder temperature and pressure are lower. The inlet oxygen concentration had stronger impact on low temperature reaction than fuel composition for PRF fuel.

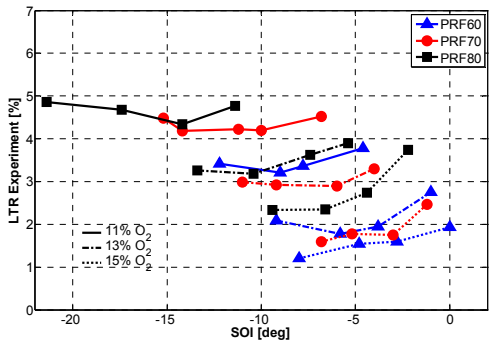

Figure 12. LTR fraction as a function of start of injection. PRF60 (blue triangle), PRF70 (red circle), PRF80 (black square) with different inlet oxygen concentrations; 11% O_2 solid lines, 13% O_2 dashed lines and 15% O_2 dotted lines.

LTR fraction as a function of start of injection for PRF, TRF and ERF are shown in Figure 13 (left). To understand the influence of fuel composition especially aromatic and alcohol on LTR phase, a base fuel PRF70 (red solid line) was compared to TRF (blue dash-dot line) and ERF (black dotted line). The n-heptane concentration was kept constant for all fuels at 30% volume fraction, whereas isooctane in PRF70 was replaced by 15% toluene for TRF fuel and by 10% for ERF fuel. The SOI was advanced for TRF by one degree to maintain same CA50 at 3 CAD ATDC (earliest SOI). Accordingly the increase in LTR fraction for TRF was achieved. The LTR fraction increased for ERF by half percent at same CA50 in comparison to PRF. Advancing the SOI tends to decrease cylinder temperatures and pressures. However, the LTR fraction for all fuels increased by retarding the SOI. This is because the SOC occurs after TDC and thus cylinder temperatures are lower as shown in Figure 13 (right).

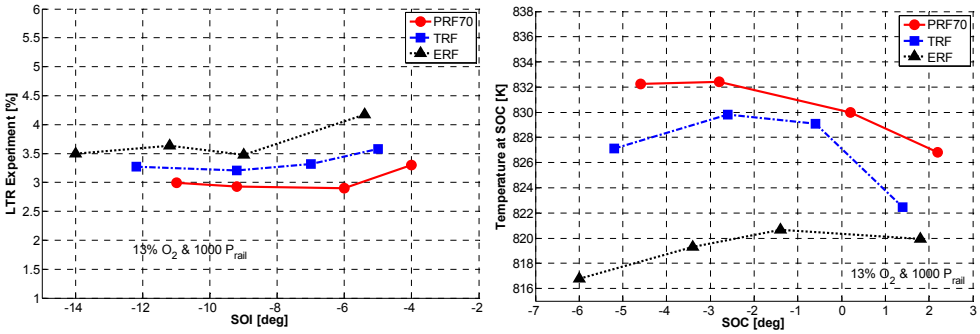

Figure 13. LTR fraction as a function of start of injection (left) and in-cylinder temperature at SOC as a function of SOC (right). Figure shows PRF70 (red circle solid line), TRF (blue square dashed line) and ERF (black triangle dotted line) at constant oxygen concentration 13% and 1000 bar injection pressure.

Figure 14 shows LTR trends and fuel compositions. The most remarkable characteristic observed here is the increase in LTR as n-heptane content increased for all surrogate fuel combinations. The operating conditions that are used for this analysis are shown in Table 5 with base case (13% O_2 and 1000 bar injection pressure) at CA50 3 degrees ATDC. In order to better understand the influence of surrogate components on LTR, analyses were done at constant operating conditions. The results are contradictory to what was expected, for PRF (black solid line) the LTR reaction decreases as n-heptane increased. Thus, the start of injection retarded as the octane number was decreased to achieve the same CA50. However, the in-cylinder temperature and pressure are slightly higher as the SOI is retarded near the top dead center. For TRF fuel (green dash-dot line) the LTR is slightly higher than PRF. The increase in LTR, in this case, is due to increase in octane number because toluene has higher octane number than isooctane. Thus, the in-cylinder temperature and pressure are lower with advanced SOI. For ERF (black dotted line) and $TERF_{cp}$ (red dashed line) fuels, the LTR are slightly different from each other and TRF. Generally, the similarities in LTR for these fuels are due to similarities in the cylinder temperature. For $TERF_{critical}$ (red dotted line), LTR is higher than the rest of the fuels due to high octane number at 30% n-heptane. As mentioned previously, the SOI is advanced for fuels with higher RON and thus the in-cylinder temperature and pressure are lower. Also, it can be noted that the slopes of LTR, predicted from the regression model, are different for each fuel due to fuel composition. Results obtained at other combustion phasing and injection pressure show similar trends.

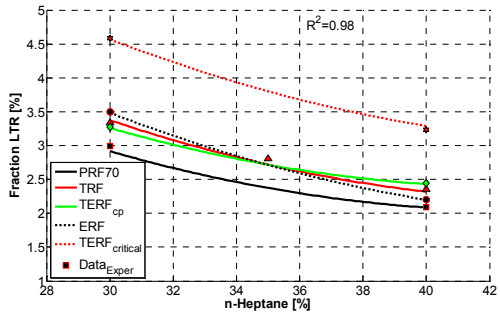

Figure 14. LTR as a function of n-heptane. Figure shows PRF (black solid line and squares), TRF (green dash-dot line and diamonds), ERF (black dotted line and circles), $TERF_{cp}$ (red dashed line and triangles) and $TERF_{critical}$ (red dotted line and hexagrams) at constant oxygen concentration 13%, 1000 injection pressure and CA50 at 3 CAD ATDC.

Figure 15 (left) illustrates the LTR trends and fuel compositions as a function of SOC. As expected the LTR increases with early SOC due to low cylinder temperature and pressure. The reason that TERFcritical (red dashed line) has advanced SOC is due to its higher RON value. Accordingly, matching combustion phasing between fuels requires different injection timings for different octane number fuels, with higher RON fuels needing earlier injection timings and thus results in an earlier SOC as shown in Figure 15. However, it was observed that LTR have their minimum values because in-cylinder temperature and pressure are slightly higher near top dead center. Figure 15 (right) shows temperature at SOC (TaSOC) which is calculated from in-cylinder pressure trace and has a significant influence on LTR. The effect of RON value on in-cylinder temperature is clear, with distinct difference between each fuel of different RON value. The difference in TaSOC between fuels is fairly proportional to

their separation in RON value. In Figure 15 (right) it was observed that even for the same SOI for different fuels, marked in the rectangular area, the TaSOC increases as RON value decreased. To summaries this, in order to achieve the same CA50 different SOI was required for different RON fuels which resulted in different SOC. The increase in LTR as the RON value increased was due to decreased in TaSOC.

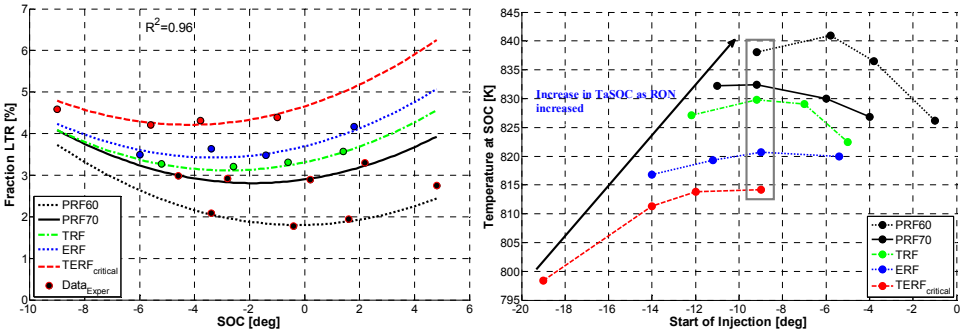

Figure 15. LTR as a function of SOC (left) and Temperature at SOC as a function of SOI (right). Figure shows PRF60 (black dotted line), PRF70 (black solid line), TRF (green dash-dot line), ERF (blue dotted line), and $TERF_{critical}$ (red dashed line) with base case (oxygen concentration 13%, 1000 injection pressure) with variation of CA50 at 3, 6, 8 and 10 CAD ATDC.

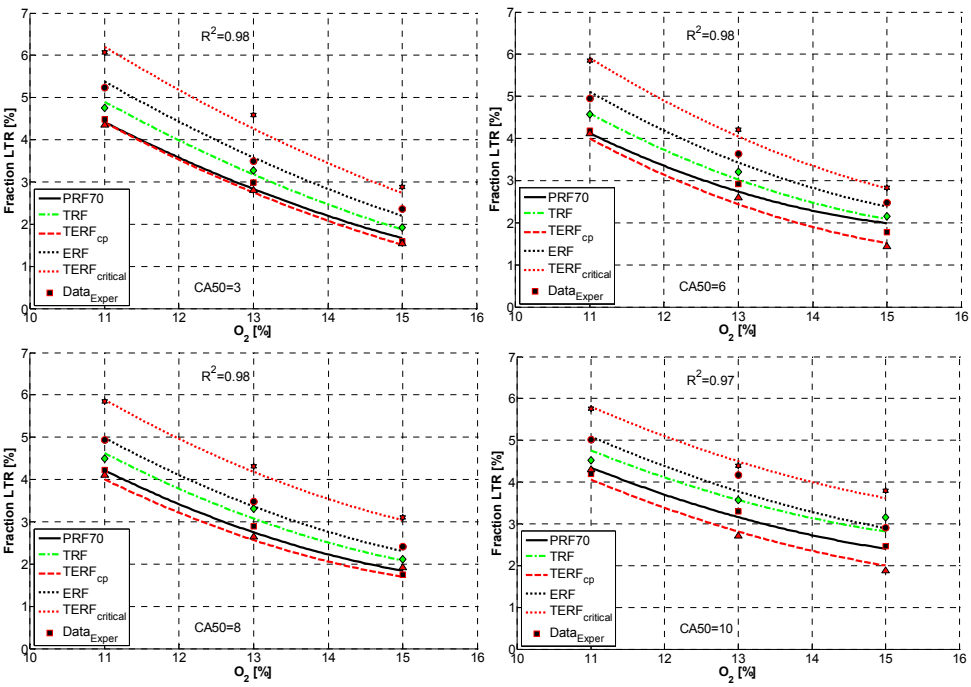

Figure 16. LTR as a function of inlet oxygen concentrations. Figure shows PRF70 (black solid line), TRF (green dash-dot line), ERF (black dotted line), $TERF_{cp}$ (red dashed line), and $TERF_{critical}$ (red dotted line) with variation of CA50 at 3, 6, 8 and 10 CAD ATDC.

Figure 16 presents the LTR trends and fuel compositions as the inlet oxygen concentration was varied from 11% to 15%. In obtaining these data, the operating conditions were fixed as shown in Table 5, while the injection pressure kept constant at 1000 bar and the CA50 at 3 degrees ATDC. Two factors contribute to the effect on LTR: the chemical factors and the physical factors. Previously, it was mentioned that one of the aims of this study is to understand the influence of inlet oxygen concentration (O_2) on LTR phase and if O_2 has the much more influence on LTR than fuel compositions. Shibata states in [20] that LTR decreases as EGR rates increases in a HCCI engine. However, in this study it was found that the LTR increased as the inlet oxygen concentration decreases. Therefore, the increase in LTR is due to slow chemical reaction rates. This is an expected consequence of longer mixing times when temperatures are dropping rapidly. Decreasing the inlet oxygen concentration from 15 to 11% the LTR increased by 3% for the fuels presented in figure 16. A similar trend was captured independently of CA50 for all fuels used in the experiments. However, moving from PRF70 to $TERF_{critical}$ at 11% O_2 the LTR increased by 1.5%. To conclude, the inlet oxygen volume fraction had much more influence on the LTR than the fuel compositions.

The slight increases in fractions of LTR as the injection pressure increases as shown in Figure 17 is due to very small different in cylinder temperatures. Nevertheless, these tests were carried out at constant operating conditions as shown in Table 5 and at 13% O_2, which produced similar SOI for same fuel at different injection pressures.

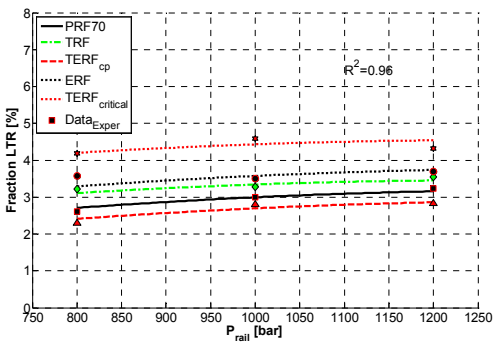

Figure 17. LTR as a function of injection pressure. Figure shows PRF70 (black solid line), TRF (green dash-dot line), ERF (black dotted line), $TERF_{cp}$ (red dashed line), and $TERF_{critical}$ (red dotted line) at 13% O_2 CA50 at 3 CAD ATDC.

Low Temperature Reaction Phase versus Ignition Delay

In Previous sections was found that both ignition delay and LTR phase had similar features with fuel compositions, inlet oxygen concentrations and injection pressure. Thus, a correlation is found between the LTR and ignition delay as shown in Figure 18 at different oxygen concentrations. It is in interest to know if this is influenced by inlet oxygen concentration or alcohol concentration. At 15% O_2, moving from PRF60 to ERF (replacing 10% of isooctane in PRF with ethanol) the LTR increased as ignition delay was increased by 1% per 2 degrees respectively. The increase in LTR and ignition delay is because the increase in RON value tends to advance SOI. Advancing the SOI tends to lower the in-cylinder temperatures. There is additional time available for fuel-air premixing at advanced injection timing due to prolonged ignition delay. Therefore, the chemical reactions occur slowly and as a result the LTR increases. However, reducing the O_2 from 15% to 11% for PRF60 the LTR increased as the ignition delay was increased by 2% per 2 degrees respectively. The increases in LTR as ignition delay increase is due to insufficient oxygen concentration in the inlet air charge, thus allows more time for the injected fuel to react with the available oxygen. Figure 18 shows that the slopes between fuels are different. At 15% O_2, the slope between PRF60 and PRF70 is sharp, meaning the LTR increases more than ignition delay. The slopes between PRF70-TRF and TRF- ERF are weak, meaning the ignition delay is longer than LTR. However, the slope between ERF and TERF is steepest, meaning LTR increases more than ignition delay.

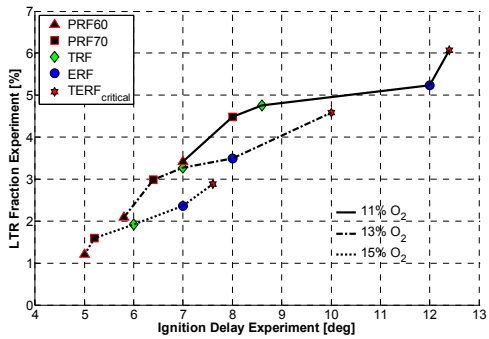

Figure 18. LTR as a function of ignition delay. Figure shows PRF60 (black triangle markers), PRF70 (black square markers), TRF (green diamond markers), ERF (blue circle markers), and $TERF_{critical}$ (red hexagrams) at 11% O_2 (black solid line), 13% O_2 (black dash-dot line) and 15% O_2 (black dashed line) with CA50 at 3 CAD ATDC.

The relations between LTR and ignition delay at different inlet oxygen concentration and with different CA50 are shown in Figure 19 at constant injection pressure 1000 bar. At 11% O_2, the LTR-ID slope is insensitive to ignition delay at the earliest and latest CA50 (3 and 10 degrees ATDC) due to lower cylinder temperature and pressure. Thus, the chemical reactions occur slower. However, the LTR-ID slope is more

sensitive as the inlet oxygen increases. This is due to sufficient oxygen in the inlet air charge, thus the injected fuel is mixed faster with the available air and ignition occur faster. Therefore the in-cylinder temperatures are higher and the chemical reactions occur rapidly. This trend is well captured with 15% O_2 (green solid line) in comparison with the other cases as shown in Figure 19 and Table 7.

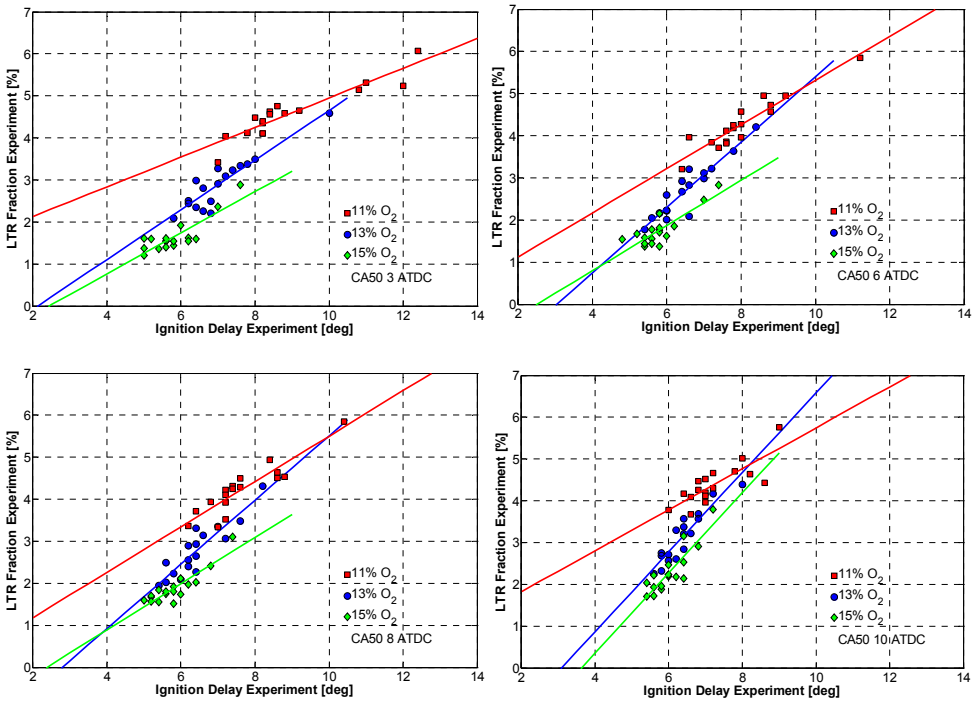

Figure 19. LTR as a function of ignition delay. Figure shows 11% O_2 (red solid line with squares) 13% O_2 (blue solid line with circles) and 15% O_2 (green solid line with diamonds) for all seventeen fuels at different CA50 and 1000 bar injection pressure.

Table 7. The LTR-ID slope Equations

11% O_2	
CA50 [deg ATDC]	**Slope Eq.**
3	y =1.423+0.353x
6	y= 0.0789+0.523x
8	y = 0.0984+0.541x
10	y =0.8455+0.49x
13% O_2	
CA50 [deg ATDC]	**Slope Eq.**
3	y =-1.263+0.592x
6	y= -2.343+0.775x
8	y =-2.141+0.765x
10	y =-2.943+0.953x
15% O_2	
CA50 [deg ATDC]	**Slope Eq.**
3	y =-1.198+0.4899x
6	y =-1.347+0.536x
8	y =-1.313+0.551x
10	y =-3.475+0.959x

SUMMARY AND CONCLUSIONS

In this study seventeen fuel mixtures designed with DoE were tested in a light duty diesel engine at 8 bar $IMEP_g$ and 1500 rpm with an absolute inlet pressure of 2.28±0.2 bar. A single injection strategy was used where the start of injection and the injection duration were adjusted to achieve the desired load and combustion phasing. The inlet oxygen concentration, combustion phasing, and injection pressure were all varied during the experiments at constant inlet mixture temperature of 345 K.

1. The ignition delay was more influenced by alcohol than aromatic due to increases in RON value and thus better mixing due to advance the SOI.
2. The increase in ignition delay as RON value increased was due to advanced SOI. The difference in ignition delay between fuels was relatively proportional to their separation in RON value. This was expected, since a high RON value is the same as high resistance to auto-ignition.
3. At lower inlet oxygen concentration, more ambient fluid must be mixed with the fuel to release the same amount of heat. Thus, additional time is expected in order to mix the same amount of O_2 with unburned fuel which tends to increase the ignition delay.
4. In contradiction to what has been reported for HCCI combustion, ethanol and toluene amplified the LTR phase, while n-heptane suppressed it in PPC type of combustion. However, ethanol had stronger influence on LTR than toluene.
5. Running the test as constant operating conditions and having similar SOI for same fuel at different injection pressure, the LTR and ignition delay were insensitive to injection pressure.
6. Reducing O_2 from 15% to 11% increased LTR as much as increasing ethanol concentration from 0% to 10%.
7. A proportional correlation between LTR and ignition delay was found. This slope was more influenced by inlet oxygen concentration than alcohol content in the fuel. However, the LTR-ID slope was sensitive at different combustion phases and especially for the case with the highest inlet oxygen concentration.

REFERENCES

1. Ladommatos, N., Abdelhalim, S., Zhao, H., "*The Effects of Exhaust Gas Recirculation on Diesel Combustion and Emissions*", International Journal of Engine Research, vol. 1, no. 1, pp. 107-126, 2000.
2. Idicheria, C., A., Pickett, L., M., "*Soot Formation in Diesel Combustion under High-EGR Conditions*", SAE Technical Paper Series, 2005-01-3834.
3. Aronsson, U., Chartier, C., Andersson, Ö., Johansson, B. et al., 2010 , "*Analysis of EGR Effects on the Soot Distribution in a Heavy Duty Diesel Engine Using Time-Resolved Laser Induced Incandescence*", SAE 2010-01-2104.
4. Manente, V., "*Gasoline Partially Premixed Combustion: An Advanced Internal Combustion Engine Concept Aimed to High Efficiency, Low Emission and Low Acoustic Noise in the Whole load Range"*, Media-Tryck, Lund, Sweden, 2010.
5. Lewander M., "Characterization and Control of Multi-Cylinder Partially Premixed Combustion", Media-Tryck, Lund, Sweden, 2011.
6. Andersson, M., et al., "*Characterization of Partially Premixed Combustion*", SAE 2006-01-3412.
7. Kitano, K., et al., "*Effects of Fuel Properties on Premixed Charge Compression Ignition Combustion in a Direct Injection Diesel Engine*", JSAE 20030117, SAE 2003-01-1815.
8. Kimura, S., Aoki, O., Ogawa, H., Muranaka, S., Enomoto, Y.,"*New Combustion Concept for Ultra-Clean and High-Efficiency Small DI Diesel Engines*", SAE 1999-01-3681.
9. Kimura, S., Aoki, O., Kitahara, Y., Aiyoshizawa, E.,"*Ultra-Clean Combustion Technology Combining a Low-Temperature and Premixed Combustion Concept for Meeting Future Emission Standards*", SAE 2002-01-0200.
10. Johansson, B., "*High-load Partially Premixed Combustion in a Heavy-Duty Diesel engine*", Diesel Engine Emissions Reduction (DEER) Conference Presentation and Posters
11. Okude, K., Moir, K., Shiino, S., Moriyama, T.,"*Premixed Compression Ignition (PCI) combustion for Simultaneous Reduction of NOx and Soot in Diesel Engine*", SAE 2004-01-1907.
12. Musculus, Mark P. B.,"*Multiple Simultaneous Optical Diagnostic Imaging of Early-Injection Low-Temperature Combustion in Heavy-Duty Diesel Engine*", SAE 2006-01-0079.
13. Manente, V., Zander, C., Johansson, B., Tunestal, P., et al.,"*An Advanced Internal Combustion Engine Concept for Low Emissions and High Efficiency from Idle to Max Load Using Gasoline Partially Premixed Combustion*", SAE 2010-01-2198.
14. Kalghatgi, G T., Risberg, P., Ångström, H.,"*Advantages of Fuels with High Resistance to Auto-Ignition in Late-Injection, Low-temperature,*

Compression Ignition Combustion", SAE 2006-04-3385.
15. Kalghatgi, G., Risberg, P., Ångström, H.,"*Partially Pre-mixed Auto-Ignition of Gasoline to Attain Low Smoke and Low NOx at High Load in a Comparison with a Diesel Fuel*", SAE 2007-01-0006.
16. Heywood, J.B., "*Internal Combustion Engine Fundamentals*", McGraw Hill Book Co, 1988.
17. Warnatz, J., Maas, U., DiBble, R.W., "*Combustion Physical and Chemical Fundamentals, Modeling and Simulation, Experiments, Pollutant Formation*" 4th edition, Springer Berlin Heidelberg New York, 2006.
18. Shibata, G., OYama, K., et al,"*Correlation of Low Temperature Heat Release with Fuel Composition and HCCI Engine Combustion*", SAE Technical Paper 2005-01-0138.
19. Tanaka, S., Ayala, F., Keck, J.C., Heywood, J.B.,"*Two-Stage Ignition in HCCI Combustion and HCCI Control by Fuels and Additives"*, Combustion and Flame 132 (2003) 219-239.
20. Shibata, G., Ogawa, H., "*HCCI Combustion Control by DME-Ethanol Binary Fuel and EGR*", SAE Technical Paper 2012-01-1577.
21. Solaka, H., Aronsson, U., Tuner, M., and Johansson, B., "*Investigation of Partially Premixed Combustion Characteristics in Low Load Range with Regards to Fuel Octane Number in a Light-Duty Diesel Engine*," SAE Technical Paper 2012-01-0684, 2012, doi:10.4271/2012-01-0684.
22. Solaka, H., Tuner, M., and Johansson, B., "*Investigation on impact of fuel properties on partially premixed combustion characteristics in a light duty diesel engine*," ASME Technical Paper 2012-0-81184, 2012.
23. Morgan, N., Smallbone, A., et al., "*Mapping surrogate gasoline compositions into RON/MON space*", Journal of combustion and flame.
24. Wyman, C., E., "*Ethanol from lignocellulosic biomass: Technology, economics, and opportunities*", Journal of Bioresource Technology, Volume 50, Issue 1, 1994, Pages 3-15, ISSN 0960-8524, 10.1016/0960-8524(94) 90214-3.
25. Andersson, Ö., "*Experiment: Planning, Implementing and Interpreting*", First edition, John Wiley & Sons, Ltd, 2012.
26. Plee, S. and Ahmad, T., "*Relative Roles of Premixed and Diffusion Burning in Diesel Combustion*," SAE Technical Paper 831733, 1983, doi:10.4271/831733.

CONTACT INFORMATION

hadeel.solaka@energy.lth.se

ACKNOWLEDGMENTS

The author would like to acknowledge the Competence Center Combustion Processes, KCFP, and the Swedish Energy Agency for the financial support, William Cannella from Chevron for supplying fuels.

DEFINITIONS/ABBREVIATIONS

ATDC	After top dead center
CAD	Crank angle degree
CA0	Crank angle at 0% completion of heat release
CA50	Crank angle at 50% completion of heat release
CN	Cetane number
DoE	Design of experiment
EGR	Exhaust gas recirculation
ERF	Primary reference fuel with ethanol
ID	Ignition delay
$IMEP_g$	Indicated mean effective pressure gross
LTR	Low temperature reaction
MON	Motor octane number
NO_x	Nitrogen oxides e.i. NO, NO_2
ON	Octane number
PM	Particulate matter
PRF	Primary reference fuel
RON	Research octane number
SOC	Start of combustion
SOI	Start of injection
TaSOC	Temperature at start of combustion
TDC	Top dead center
$TERF_{cp}$	Primary reference fuel with toluene and ethanol, center point
$TERF_{critical}$	Primary reference fuel with toluene and ethanol, critical point
TRF	Primary reference fuel with toluene

Paper IV

Downloaded from SAE International by Hadeel Solaka Aronsson, Monday, May 12, 2014 05:12:40 AM

SAE INTERNATIONAL™

Gasoline Surrogate Fuels for Partially Premixed Combustion, of Toluene Ethanol Reference Fuels

2013-01-2540
Published
10/14/2013

Hadeel Solaka, Martin Tuner, and Bengt Johansson
Lund University

William Cannella
Chevron USA Inc.

Copyright © 2013 SAE International and Copyright © 2013 KSAE

doi:10.4271/2013-01-2540

ABSTRACT

Partially premixed combustion (PPC) is intended to improve fuel efficiency and minimize the engine-out emissions. PPC is known to have the potential to reduce emissions of nitrogen oxides (NO_x) and soot, but often at the expense of increased emissions of unburned hydrocarbons (HC) and carbon monoxide (CO). PPC has demonstrated remarkable fuel flexibility and can be operated with a large variety of liquid fuels, ranging from low-octane, high-cetane diesel fuels to high-octane gasolines and alcohols. Several research groups have demonstrated that naphtha fuels provide a beneficial compromise between functional load range and low emissions. To increase the understanding of the influence of individual fuel components typically found in commercial fuels, such as alkenes, aromatics and alcohols, a systematic experimental study of 15 surrogate fuel mixtures of n-heptane, isooctane, toluene and ethanol was performed in a light-duty PPC engine using a design of experiment methodology. The impacts of oxygen concentration, injection pressure, combustion phasing and premixed fraction were investigated for all fuel blends. The investigation also produced data for future kinetics modeling that can expand the understanding of fuel effects on PPC.

The experiments were performed at 8 bar $IMEP_g$ and at an engine speed of 1500 rpm using a single injection strategy.

HC and CO emissions increased greatly with increasing ethanol and decreased greatly with increasing n-heptane concentration. NO_x emissions increased with an increasing oxygen fraction and decreased with increasing ethanol concentration. Although soot levels were near zero in many of the experiments, we observed that high levels of n-heptane increased soot, while high ethanol reduced it. The premixed fraction was impossible to predict due to data variation. No correlation was found between the premixed fraction and soot levels.

INTRODUCTION

Manufacturing diesel engines to meet future emissions standards requires significant development of the combustion system. Several new strategies for diesel combustion have been proposed, such as premixed charge compression ignition (PCCI) [1], premixed compression ignition (PCI) [2], partially premixed compression ignition (PPCI) [3], and Nissan LTC's modulated kinetics (MK) [4,5]. These concepts all share general features and similar objectives.

The main advantage of these combustion strategies is low levels of engine-out soot and NO_x. The common method for achieving this is to use a high level of cooled exhaust gas recirculation (EGR); this increases the heat capacity, reducing the combustion temperature and avoiding zones with high production of soot and NO_x. EGR also slows the kinetic reactions, resulting in more fuel and air being premixed before ignition. However, there are significant drawbacks, as high EGR rates elevate CO and HC emissions [6]. In addition, high EGR rates can affect soot oxidation late in the cycle [7]. At low loads, high EGR rates are avoided due to incomplete combustion. To achieve long ignition delay and a sufficient time for fuel and air to mix before ignition without using high EGR rates, different fuel properties can be used.

Downloaded from SAE International by Hadeel Solaka Aronsson, Monday, May 12, 2014 05:12:40 AM

Compression-ignited (CI) engines generally have higher efficiency than do spark-ignition engines. However, the most common combustion concept in CI engines, conventional diesel combustion, struggles with high particulate matter (PM) and NO_x emissions. Therefore, new combustion strategies are used in CI engines to reduce engine-out PM and NO_x emissions. One such promising strategy, partially premixed combustion (PPC), is analyzed here. Independently of its properties, if a combustion concept is to be put into production in the near future, it must use the fuels available on the market. It is important to understand how PPC responds to fuel properties, especially research octane number (RON) and ignition quality.

It has been demonstrated that using gasoline fuel in compression ignition engines may reduce the levels of engine-out emissions [8, 9, 10, 11, 12, 13]. Since gasoline has a higher resistance to auto-ignition than does diesel fuel, it allows more mixing time, producing a higher fraction of premixed combustion. Using both EGR and high-octane gasoline fuels further extends the premixing time. However, a drawback of using gasoline fuels is that their high RONs are limiting at lower loads. The fuel effects on the combustion process depend on the course of events in the early stages of combustion, i.e., the ignition delay (ID), mixing period (MP), and premixed fraction phase (PF), as shown in Figure 1. Therefore, understanding fuel effects on these properties is critical in understanding fuel effects on PPC.

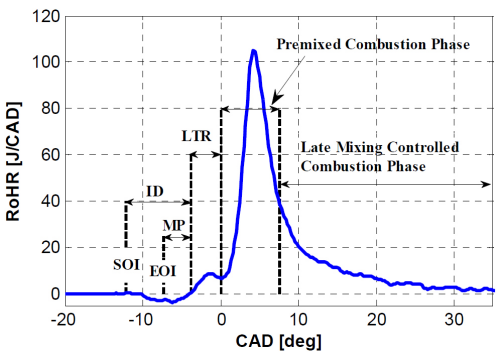

Figure 1. Typical PPC heat release diagram identifying different PPC phases.

Fuel effects on emissions such as HC and CO have previously been studied in diesel combustion. However, few studies of the effect of fuel composition on partially premixed combustion have been performed. These studies were performed in PPC using gasoline fuels, but it was difficult to analyze fuel composition effects on combustion events and emissions due to the great variation in the concentrations of fuel components. Beside the effects of fuel composition on engine-out emissions, combustion chamber geometry and operating conditions are also a source of engine-out emissions, especially of HC and CO. The sources of engine-out HC emissions in conventional diesel combustion also apply in PPC: trapped fuel in the crevice volume, significant variation in local fuel equivalence ratio, bulk quenching of oxidation reactions due to low combustion temperature, and spray impingement causing liquid film in the squish volume and on the combustion chamber wall resulting in incomplete fuel evaporation and oxidation [14]. Previous studies have investigated the sources of HC and CO under low-temperature combustion conditions. The major contributors to bulk-gas HC and CO late in the cycle are nozzle dribble and ejected fuel droplets [15]. Other studies demonstrate that the spray target and squish height affect HC and CO emissions [16].

The authors have previously studied fuel effects on engine-out emissions and combustion characteristics for commercial fuels such as diesel and various types of gasoline [17, 18]. It was observed that gasoline fuels had a higher premixed fraction than did diesel. However, the relationship between premixed fraction and fuel composition among the gasoline fuels was not fully understood. The wide range of fuel compositions inhibited the possibility of isolating the impacts of the paraffin, olefin, and aromatic contents. Therefore, this study focuses on understanding the influence of individual fuel components, such as alkanes, aromatics, and alcohols, typically found in commercial fuels. For example: the most common aromatics in gasoline is toluene and recently ethanol has been added in gasoline up to 10% with the aim to reduce CO_2 emissions. Machado et al. [19] concluded that mixtures of n-heptane, isooctane, ethanol and toluene could be used as surrogate fuels for oxygenated gasoline. To this end, a systematic study of 15 surrogate fuel mixtures of n-heptane, isooctane, toluene, and ethanol was performed in a light-duty PPC engine using a design of experiment (DoE) methodology. Similar fuel has been run in HCCI combustion [20]. Moreover, we also studied varying operating conditions, such as injection pressure, combustion phasing, and inlet oxygen concentration, resulting in 612 operating points. These data are used to strengthen the quadratic regression models of the premixed fraction and emissions. In addition, the data will be used in future kinetics modeling to increase the understanding of fuel effects on PPC.

Objective

The main objective of this study is to predict the premixed combustion fraction for different fuel compositions and operating conditions. The premixed combustion fraction is a key parameter in PPC since it affects both engine-out emissions and fuel consumption. A second objective is to understand the impact of fuel composition on engine-out emissions in PPC.

EXPERIMENTAL SETUP AND DIAGNOSTICS

Engine Setup

The presented investigations were performed in a Volvo D5 five-cylinder passenger car diesel engine. The engine

Downloaded from SAE International by Hadeel Solaka Aronsson, Monday, May 12, 2014 05:12:40 AM

operated on only one cylinder while the other four were motored. The specifications of the cylinder head and injection system are shown in Table 1. The engine test rig was equipped with an adjustable exhaust gas recirculation system and adjustable heating of the inlet charge temperature.

Table 1. Engine specifications

Engine specifications	
Engine type	Volvo D5
Number of cylinders	1
Bore [mm]	81
Stroke [mm]	93.2
Displacement Volume [cm^2/cylinder]	480
IVC [CAD BTDC]	174
Compression ratio	16.5
Swirl ratio	2.2
Number of intake valves	2
Number of exhaust valves	2
Injector	
Type	Solenoid
Injection nozzle holes	7
Injection nozzle diameter [mm]	0.14
Included angle [degrees]	140

Fuels

The fuels used here were mixtures of n-heptane, isooctane, toluene, and ethanol in different volume fractions. To prevent damage to the injection system, 100 ppm of the lubricity additive Infineum R655 was added to each fuel mixture. The impact of such a small amount of additive on combustion phasing and emission formation is expected to be negligible. Fuel specifications are shown in Table 2. Isooctane and n-heptane mixtures are called primary reference fuels (PRF), and these fuels define the RON and motor octane number (MON) scales, which each extend from 100 to 0. Toluene and ethanol are octane enhancers. However, there is no direct link between fuel mixture (compositions of PRF and toluene, PRF and ethanol, or all four) and octane number. Toluene and ethanol increase RON when added to primary reference fuels, but this increase is not linearly related to the volume percent added; this can be seen from the results presented in Table 4.

Table 2. Fuel specifications

Fuels properties	n-Heptane	Toluene	Ethanol	Isooctane
RON	0	120	107	100
MON	0	109	89	100
Auto-ignition temperature [°C]	203.85	529	425	411
Molecular formula	C_7H_{16}	C_7H_8	C_2H_6O	C_8H_{18}
Molar mass [g/mol]	100.23	92.15	46.07	114.26
Density [kg/m^3]	679.5	866.9	789	688
Boiling point [°C]	98	110.6	78.5	99

Measurement Equipment

Data Acquisition

Cylinder pressure was measured using a Kistler 6056 piezoelectric pressure sensor for heat release calculations. It was sampled at a resolution of 0.2 crank angle degrees (CAD). The inlet and exhaust pressures were measured using a Keller pressure sensor. The inlet air, inlet mixture, and exhaust temperature were measured using Pentronic type-K thermocouples.

Fuel and Air Mass Flows

The intake air mass flow was measured using a Bronckhorst IN-FLOW thermal mass flow meter. It was situated approximately 3 m upstream from the intake manifold to prevent pressure oscillations propagating from the engine, or EGR system, into the flow meter. The fuel mass flow was measured as the mean value of the mass gradient using a Sartorius CPA 62025 fuel balance.

Emission Measurement

Smoke emissions were measured using an AVL415S smoke meter, while NO_x, HC, exhaust CO_2, CO, and intake CO_2 emissions were measured using a Horiba MEXA9200DF measurement system. NO_x emissions were measured using a chemiluminescence analyzer, whereas HC was measured using a flame ionization detector (FID); the piping to the FID analyzer was heated to approximately 191°C to prevent condensation of unburned fuel components. Inlet and exhaust oxygen (O_2) were measured using a magneto-pneumatic condenser microphone method (MPA), whereas CO, intake CO_2, and exhaust CO_2 were measured using infrared analyzers.

Inlet Oxygen Concentration

The inlet oxygen concentration was measured using a Horiba measurement system. The oxygen concentration in the intake manifold was controlled by a valve that regulates the amount of EGR entering the intake system. The EGR was drawn off the main exhaust pipe through the EGR cooler to reduce the EGR temperature. Typical EGR coolers, including the cooler used on the production five-cylinder version of this engine, cool the EGR by circulating engine coolant water through a heat exchanger. Later, the EGR and the heated air in the inlet system are mixed and heated to a temperature of 345 K before the intake air mixture enters the cylinder, as shown in Figure 2.

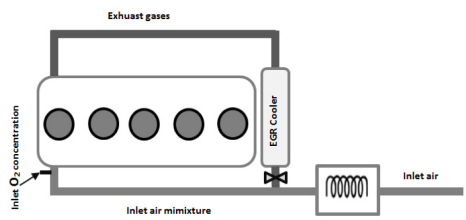

Figure 2. EGR and oxygen measurement in the inlet system.

Downloaded from SAE International by Hadeel Solaka Aronsson, Monday, May 12, 2014 05:12:40 AM

Table 3. Surrogate fuel compositions.

Fuel	High [%]	Average [%]	Low [%]
n-Heptane	40	35	30
Toluene	15	7.5	0
Ethanol	10	5	0

Table 4. Surrogate fuel matrix.

Fuels	n-heptane [vol %]	Toluene [vol %]	Ethanol [vol %]	Isooctane [vol %]	RON	MON
2	40	0	0	60	60.6	60.8
4	40	15	0	45	64.3	62.3
17	35	7.5	0	57.5	67.3	66.1
12	40	7.5	5	47.5	66.6	64.0
1	30	0	0	70	70.3	70.4
8	40	15	10	35	72.2	69.0
15	35	0	5	60	70.5	68.7
3	30	15	0	55	74.2	71.9
6	40	0	10	50	69.7	66.8
14	35	15	5	45	73.5	69.4
9_{cp}	35	7.5	5	52.5	71.9	69.4
10_{cp}	35	7.5	5	52.5	71.9	69.4
11_{cp}	35	7.5	5	52.5	71.9	69.4
16	35	7.5	10	47.5	74.9	71.8
13	30	7.5	5	57.5	76.8	74.2
5	30	0	10	60	78.7	76.7
7	30	15	10	45	81.6	77.2

METHODS AND DEFINITIONS

Design of Experiments

Fifteen blends of isooctane, n-heptane, toluene, and ethanol were created according to the experimental design. A central composite two-level full-factorial design in which axes are drawn through the center of the cube and the axial points are located on the face of the cube [21], as shown in Figure 3, is used in this study.

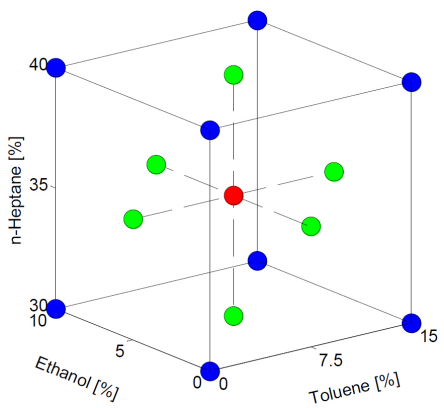

Figure 3. A central composite two-level full factorial design.

The settings for the three factors are given in Table 3 and shown graphically in Figure 3.

Isooctane levels were chosen to model gasoline fuel over a wide ignition-quality range. The isooctane contents of the mixtures were calculated according to Eq. 1,

$$\text{Isooctane}_{C_I} = 100 - \left(\text{nheptane}_{C_N} + \text{toluene}_{C_T} + \text{ethanol}_{C_E}\right) \quad (1)$$

where C_I is the isooctane percentage in the mixture and C_N, C_T, and C_E are the n-heptane, toluene, and ethanol percentages in the mixture, respectively.

The test matrix consisted of 15 fuel mixtures as shown in Table 4. The number of experiments can be described as $2^{k-p} + 2k + cp$, where k is the number of studied variables, p is the fractionalization element ($p = 0$, full design), and cp is the number of center points. The center point was replicated three times, meaning that test matrix consisted of 17, i.e., $2^3 + (2 \times 3) + 3$, set point combinations as seen in Table 4. The RON and the MON were determined using the ASTM D2699 and D2700 standard methods, respectively, in a CFR engine.

Heat Release Characteristics

Information about the combustion event can be extracted from the calculated rate of heat release. The heat losses are included in the rate of heat release calculation using the Woschni model. The combustion event is divided into four phases, i.e., ignition delay (ID), LTR, premixed combustion phase, and late mixing controlled combustion, as seen in Figure 1.

Downloaded from SAE International by Hadeel Solaka Aronsson, Monday, May 12, 2014 05:12:40 AM

Premixed Combustion Phase

In the *premixed combustion phase*, the combustible fuel and air mixture burns rapidly. This phase is controlled by chemical kinetics and the reaction speed depends mainly on temperature.

In the present study, the premixed and late heat release rates are not separated. This is because parts of the premixed combustion phase are limited by mixing, and parts of the late combustion phase depend on slow reactions rather than mixing. To separate the phases in a well-defined manner, a Gaussian profile is fitted to the rising flank of the premixed peak, between the end of low-temperature reactions and the actual peak, and the integrated area of the profile is used as a measure of the premixed reactions. In Eq. 2,

$$G(x) = h \cdot e^{-\left(\frac{x-x_0}{2\alpha^2}\right)^2} \quad (2)$$

x_0 is the central position of the peak, and h and α represent the height and width of the Gaussian profile, respectively. Figure 4 shows the rate of heat release as a function of crank angle together with the Gaussian profile. As is evident, the fit closely follows the premixed heat release. The Gaussian profile is a mathematical rather than a physical representation of the premixed reaction phase. However, it provides as a robust measure of the premixed reactions under all operating conditions.

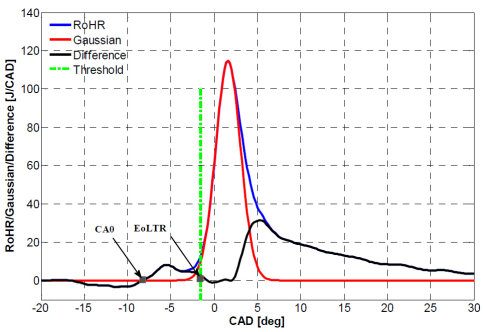

Figure 4. Gaussian profile as a fit for the premixed combustion proportion of heat release rate.

OPERATING CONDITIONS

The test conditions used here centered on the base conditions, i.e., 1500 rpm at 8 bar $IMEP_g$, used in previous studies by the author [17,18,22]. A single-injection strategy was used in which the start of injection and duration were adjusted to achieve the desired load and combustion phasing, as shown in Table 5. Combustion phasing is defined as 50% heat release completion (CA50). The inlet mixture temperature and pressure were kept constant at 345 K and 2.28 ± 0.02 bar, respectively. Under these conditions, several parameters were varied to examine surrogate fuel effect and engine behavior during PPC. These parameters included inlet oxygen concentration, combustion phasing, and injection pressure. The inlet oxygen concentration was set to three different volume fractions: 11, 13, and 15%. At each oxygen concentration, the combustion phasing and injection pressure were varied. The combustion phasing was set to 3, 6, 8, and 10 degrees after top dead center. Three different injection pressures, i.e., 800, 1000, and 1200 bar, were applied for each combination of oxygen concentration and combustion phasing, as shown in Table 6.

Table 5. Constant inlet conditions.

Engine speed [rpm]	1500
Inlet temperature mixture [K]	345
Load $IMEP_g$ [bar]	8
Absolute inlet pressure [bar]	2.28±0.02

Table 6. Parameter variations

Inlet O_2 concentration [%]	11 (low)	13 (base)	15 (high)
CA50 [ATDC deg]	Early, mid, late	Early, mid, late	Early, mid, late
Injection pressure [bar]	800 (low)	1000 (base)	1200 (high)

RESULTS AND ANALYSIS

Premixed Fraction

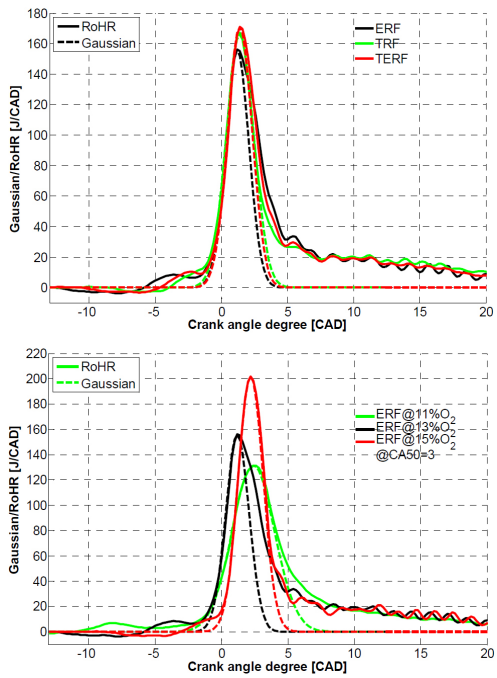

Figure 5. Rate of heat release (RoHR) and Gaussian profile for different fuels at baseline (CA50 at 3 CAD, 13% O_2, and 1000 bar injection pressure) and for ERF at different inlet O_2 concentrations.

Downloaded from SAE International by Hadeel Solaka Aronsson, Monday, May 12, 2014 05:12:40 AM

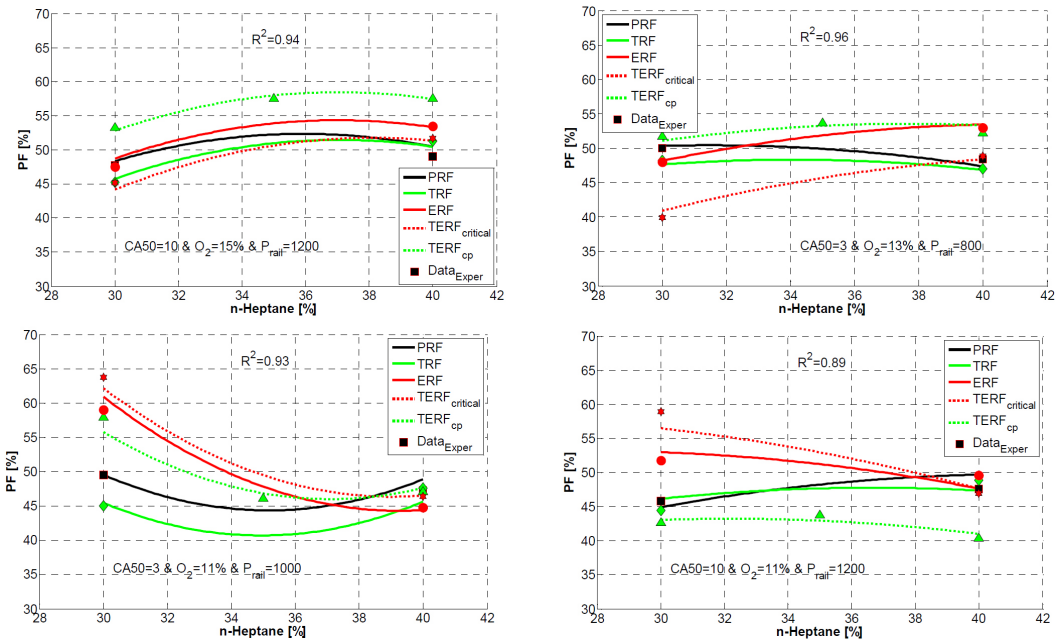

Figure 6. Premixed fraction as a function of n-heptane for different surrogate mixtures under different operation conditions.

The premixed fraction (PF), a central concept in PPC, is known to influence both thermodynamic efficiency and engine-out emissions. For example, a correlation between PF and engine-out emissions, especially soot, is shown in [23]. The present work examined the effect of fuel composition and operating conditions on PF.

According to Figure 5, the Gaussian profile follows the premixed combustion well independently of fuel composition and operating conditions.

Regression models are used to study fuel effects on PF at different oxygen concentrations, CA50s, and injection pressures. The R^2 values for the models are shown in Appendix Tables 1, 2, 3. A model with $R^2 = 1$ explains all variation in the data while a model with $R^2 = 0$ explains none of the variation in the data. Generally, the R^2 values here are quite low, indicating that the observations from the models might be uncertain. However, some exceptions with higher R^2 values are shown in Figure 6, where PF is plotted as a function of the n-heptane fraction. The trends in PF depend on the operating conditions for all fuels, but some fuels display equal trends under given operating conditions. TRF and PRF have the same trend and slope in PF, while ERF, $TERF_{critical}$, and $TERF_{cp}$ have similar trends and slopes. The different trends in PF under different operating conditions indicate that there are interaction effects between fuel composition and operating conditions. This also means that it is difficult to draw general conclusions about fuel effects on PF. For example, it can be concluded that a changed n-heptane fraction will have a similar impact on PF for ERF and $TERF_{critical}$, but that the impact will differ under different operating conditions.

Peak Rate of Heat Release (PRoHR)

An important parameter during combustion is the peak rate of heat release (PRoHR). The fuel composition and derived parameter influence have been studied here. The predicted PRoHR is calculated according to Eq. 3. The data matrix together with the regression coefficients give the predicted parameter. β_0 is a constant term while β_{CA50}, β_{O2}, β_{Prail}, β_N, β_T, and β_E (shown in red) are linear terms for CA50, inlet O_2 concentration, injection pressure, n-heptane, toluene, and ethanol, respectively. The interaction coefficients (shown in black) include β_{NT} (interaction between n-heptane and toluene), β_{NE} (interaction between n-heptane and ethanol), and β_{TE} (interaction between toluene and ethanol). The quadratic coefficients (shown in green) include β_{NN} (n-heptane quadratic), β_{TT} (toluene quadratic), and β_{EE} (ethanol quadratic). N, T, and E are the volume fractions [%] of n-heptane, toluene, and ethanol, respectively, while CA50, inlet oxygen concentration, and injection pressure are presented in degrees ATDC, volume fraction [%], and bar, respectively.

Downloaded from SAE International by Hadeel Solaka Aronsson, Monday, May 12, 2014 05:12:40 AM

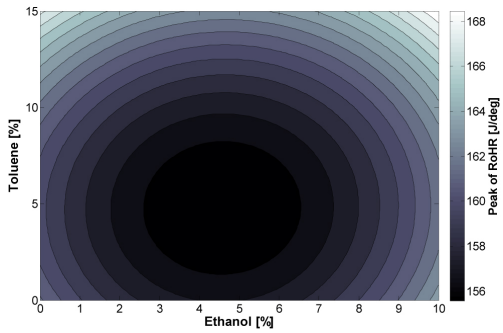

Figure 7. Peak rate of heat release as a function of fuel composition (toluene, ethanol, and PRF) at baseline (with CA50 at 3 CAD ATDC, 13% O2, and injection pressure at 1000 bar).

$$PRoHR_{Predicted} = \beta_0 + \beta_{CA50} \cdot CA50 + \beta_{O_2} \cdot O_2 + \beta_{P_{rail}} \cdot P_{rail} + \beta_N \cdot N + \beta_T \cdot T + \beta_E \cdot E + \beta_{CA50 \cdot O_2} \cdot CA50 \cdot O_2 + \beta_{CA50 \cdot P_{rail}} \cdot CA50 \cdot P_{rail} + \beta_{CA50 \cdot N} \cdot CA50 \cdot N + + \beta_{CA50 \cdot T} \cdot CA50 \cdot T + + \beta_{CA50 \cdot E} \cdot CA50 \cdot E + \beta_{O_2 \cdot P_{rail}} \cdot O_2 \cdot P_{rail} + \beta_{O_2 \cdot N} \cdot O_2 \cdot N + \beta_{O_2 \cdot T} \cdot O_2 \cdot T + \beta_{O_2 \cdot E} \cdot O_2 \cdot E + \beta_{P_{rail} \cdot N} \cdot P_{rail} \cdot N + \beta_{P_{rail} \cdot T} \cdot P_{rail} \cdot T + \beta_{P_{rail} \cdot E} \cdot P_{rail} \cdot E + \beta_{N \cdot T} \cdot N \cdot T + \beta_{N \cdot E} \cdot N \cdot E + \beta_{T \cdot E} \cdot T \cdot E + \beta_{CA50 \cdot CA50} \cdot CA50^2 + \beta_{O_2 \cdot O_2} \cdot {O_2}^2 + \beta_{P_{rail} \cdot P_{rail}} \cdot {P_{rail}}^2 + \beta_{N \cdot N} \cdot {P_N}^2 + \beta_{T \cdot T} \cdot {P_T}^2 + \beta_{E \cdot E} \cdot {P_E}^2$$

Equation 3

Figures 7 and 8 show the predicted PRoHR, where the R^2 is 0.95 for the entire dataset. The PRoHR has its minimum circle zone at 5% ethanol and toluene, as shown in Figure 7. A similar trend was observed under different operating conditions, but the minimum zone shifts depending on inlet oxygen concentration and CA50. Reducing inlet O_2 concentration shifts the zone to the left, and at late CA50s the zone is shifted upwards. This behavior is expected because the chemical reactions occur slowly for a longer period at late CA50s. The minimum occurs around 5% ethanol and toluene due to a shorter mixing period and thus a smaller proportion of premixed combustion.

Furthermore, the PRoHR is sensitive to inlet oxygen concentration and injection pressure, as shown in Figure 8. However, the PRoHR was less sensitive to the injection pressure at the lowest inlet oxygen concentration. This is because lack of oxygen gives more time for air and fuel to mix, resulting in a longer ignition delay. On the other hand, the injection pressure significantly influences PRoHR at the highest inlet oxygen concentration. This is because the spray momentum at high injection pressure creates more turbulence and thus better mixing between air and fuel. Therefore, the lowest PRoHR is achieved at the lowest level of inlet O_2 concentration and injection pressure, while the highest peak is achieved at the highest level of inlet O_2 concentration and injection pressure.

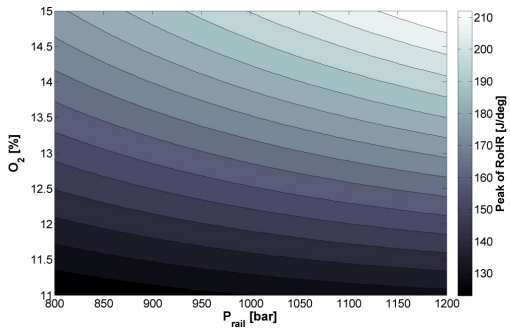

Figure 8. Peak rate of heat release as a function of inlet oxygen concentration and injection pressure for TERF (15% toluene, 10% ethanol, and 40% n-heptane) with CA50 at 3 CAD ATDC.

Combustion Duration

The combustion duration (CD), defined as CA90-CA10, is plotted as a function of PRoHR for a sweep in CA50 at three oxygen concentrations in Figure 9. At all oxygen concentrations, retarded combustion gave a lower peak rate of heat release, indicating that the reaction rate during the most rapid part of the premixed combustion was decaying. The trend in CD, however, was not consistent for the different oxygen concentrations. Retarded combustion phasing gave an increased CD at the lowest oxygen fraction, while the CD was stable at the medium oxygen concentration and decreased at the high oxygen concentration. This observation can be explained by differences between early and late combustion. From Figure 10 it is evident that combustion starts later when CA50 is retarded at all oxygen concentrations, which also means that CA10 is retarded. At the lowest oxygen concentration, late combustion is slower, leading to a larger retardation in CA90 than in CA10 as well as increased CD. At a higher oxygen concentration, the reaction rate is higher and CA90 is more stable than CA10, while at the medium oxygen concentration, the retardation in CA10 and CA90 is about the same.

Downloaded from SAE International by Hadeel Solaka Aronsson, Monday, May 12, 2014 05:12:40 AM

The fuel effect on CD was studied using a DoE. The predicted CD was calculated using Eq. 3 and R^2 = 0.93. The results indicate that the maximum CD was found with a 5% ethanol concentration and toluene concentration as shown in Figure 11. The CD shortened as ethanol and toluene concentrations were increased. However, increasing the nheptane concentration increases the radius of the maximum zone, which still displays a similar trend. Likewise, the CD as a function of toluene and ethanol concentrations displayed similar trends under different operating conditions. The shorter CD as toluene and ethanol concentrations increased was due to advanced SOI and thus resulted in a larger proportion of premixed combustion.

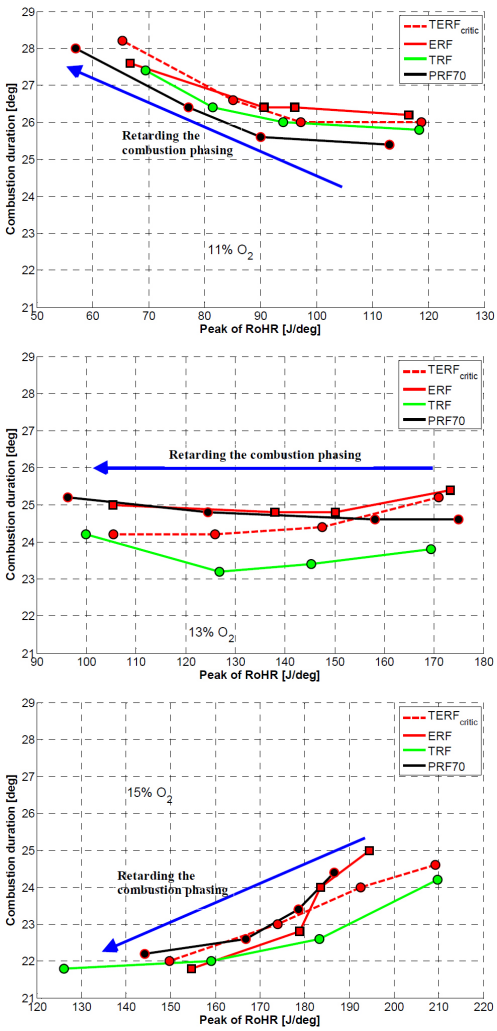

Figure 9. Combustion duration as a function of PRoHR for different fuels at different inlet O_2 concentrations.

Furthermore, the CD shortened as the inlet oxygen concentration and injection pressure increased, as shown in Figure 12. Higher oxygen concentration increases the reaction rate, leading to shorter CDs. Higher injection pressures give faster fuel and air mixing leading to a larger proportion of combustible mixture.

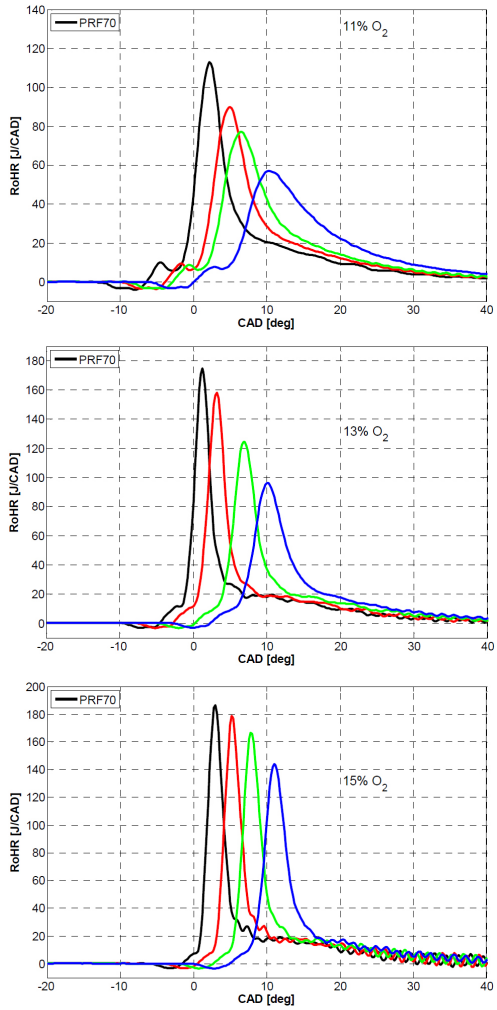

Figure 10. Rate of heat release as a function of crank angle degree for PRF70 at different inlet O_2 concentrations for different CA50.

Downloaded from SAE International by Hadeel Solaka Aronsson, Monday, May 12, 2014 05:12:40 AM

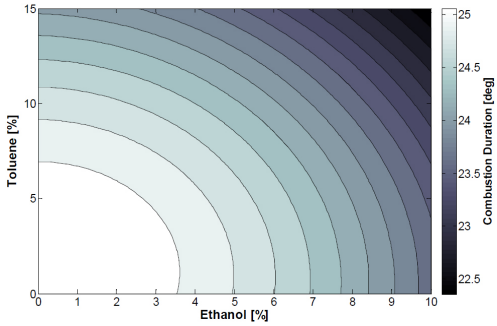

Figure 11. Combustion duration as a function of fuel composition at baseline (with CA50 at 3 CAD, 13% O_2, and injection pressure at 1000 bar).

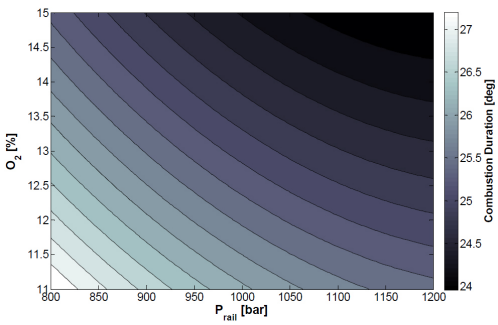

Figure 12. Combustion duration as a function of inlet oxygen concentration and injection pressure with TERF (15% toluene, 10% ethanol, and 40% n-heptane).

Emissions

Fuel Effects on Emissions

A higher PRoHR and more advanced CA50 resulted in higher NO_x and lower HC and CO emissions due to a higher combustion temperature (not shown); similar trends have previously been observed [15, 16, 24]. The effects of fuel composition on NO_x, CO, and HC emissions are presented in Figure 13. Increasing the ethanol concentration gave lower NO_x and higher HC and CO emissions. The effect is equally strong independently of toluene concentration for HC and CO but weaker at low toluene concentration for NO_x.

Increasing the toluene concentration gave more emissions of NO_x, HC, and CO. At a low ethanol concentration, the effect is stronger for NO_x, weaker for HC, and almost nonexistent for CO. Similar trend was observed at other cases.

It has previously been reported that fuels with aromatics extend the duration of NO_x formation due to local high-temperature regions with combustion of decomposed hydrocarbons [25]. HC and CO increased with increasing ethanol and toluene concentrations, since SOI had to be advanced to maintain CA50. An earlier SOI places more fuel in the squish volume, which has less chance to be fully oxidized because it might be trapped in overly lean zones, rich zones, or liquid fuel film. Aronsson *et al.* observed that during PCCI combustion in an optical engine the squish volume was a significant source of HC emissions and a dominant source of CO emissions [16].

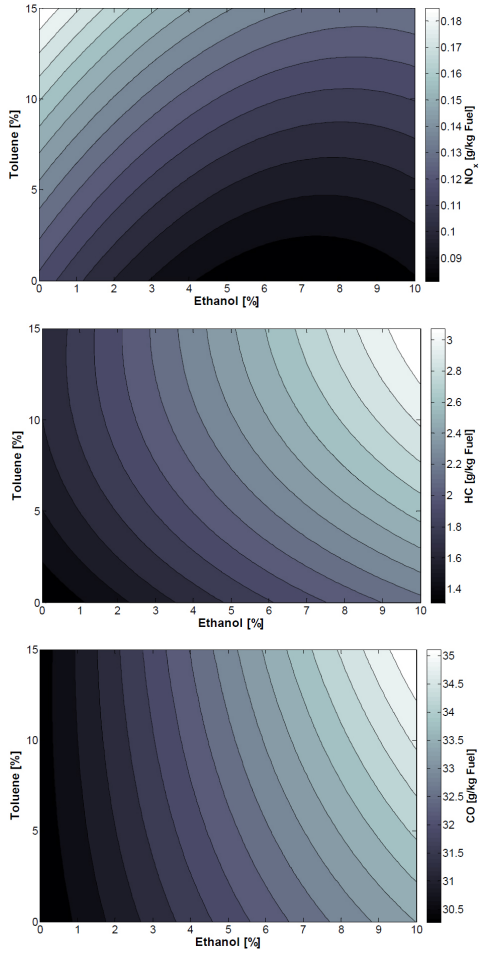

Figure 13. Emission index NO_x, HC, and CO as a function of fuel composition at baseline (with CA50 at 6 CAD, 13% O_2, and injection pressure at 1000 bar).

The spray target is lowered as the SOI is retarded. Lowering the spray target will help inject the fuel into the bowl. However, fuels with higher RONs need to be injected earlier to achieve the same CA50. It is known that toluene and ethanol are octane enhancers. As a result, the HC and CO emissions are higher for a fuel mixture that consists of toluene, ethanol, or both, see Figure 1 in Appendix. The spray

Downloaded from SAE International by Hadeel Solaka Aronsson, Monday, May 12, 2014 05:12:40 AM

divides into two parts if it hits the edge of the squish volume, one part entering the bowl and the second part ending up in the squish volume as a liquid film. The amount of the second part of the spray determines the level of HC and CO emissions.

Inlet Parameter Effects on Emissions

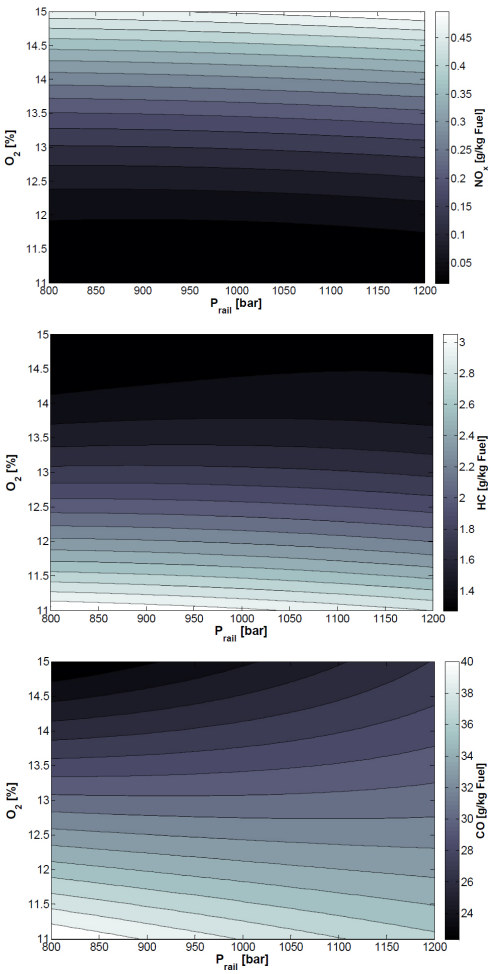

Figure 14. Emission index NO_X as a function of inlet oxygen concentration, combustion phasing, and injection pressure with TERF (15% toluene, 10% ethanol, and 40% n-heptane).

The inlet oxygen concentration significantly influences emissions, as shown in Figure 14. As the inlet oxygen concentration is deceased the local combustion temperatures are lower, leading to substantial increases in HC and CO emissions. CO and HC emissions are typically higher for PPC than conventional diesel combustion. The increased HC and CO emissions in PPC with reduced inlet oxygen concentrations are believed to be caused by a combination of a general decay in oxidation rate and an advance SOI which place a large amount of fuel in the squish volume.

At a lower inlet oxygen concentration, the light components of the fuel evaporate easily due to longer ID and LTR. However, heavier components will remain on the combustion chamber walls. These heavier components evaporate during the expansion stroke but, due to a shortage of oxygen, their oxidation reactions suffer [26].

As well as the inlet oxygen concentration, the effect of injection pressure on emissions was also examined, revealing that injection pressure did not greatly influence NO_X, HC, or CO emissions.

Smoke Emissions

The smoke emissions were very low, so it was difficult to create a model using the data obtained from the measurement experiment. However, smoke values above the threshold for the AVL415S smoke meter (≥0.01 FSN) were analyzed, yielding results for 188 of 612 measurement points under different operating conditions. Ethanol produced very low levels of smoke, as seen in Figure 15, followed by TRF and PRF with early combustion phasing. Hence, when retarding the combustion phasing above 6 CAD ATDC, the smoke number for TRF increased but still displayed a trend similar to that of PRF. However the heat release rate for PRF and TRF are similar with different combustion phasings, as seen in Figure 16. The increasing smoke number for the TRF mixture with retarded combustion phasing is perhaps due to fuel composition. Toluene has double bonding between its carbon atoms, which requires high energy and higher temperature to break. One of Azetsu *et al.*'s [27] findings was that the flame temperature increases with fuel aromatic content. The higher flame temperature of the test fuel containing aromatics is attributed to the higher H/C ratio of the molecular structure. Increasing the flame temperature, especially at the upstream location where the fuel concentration is much higher, increases the local soot concentration since the soot oxidation rate is hindered by the insufficient oxygen [28]. At the latest combustion phasing, the smoke number decreased; as this is due to incomplete combustion, soot will not form.

In addition, the injection pressure strongly affected the smoke levels. As the injection pressure increased from 800 to 1200 bar, the smoke levels declined by approximately 0.4 FSN for TRF fuel. This is because the soot residence time, which is characterized by the duration between the start of soot inception and the start of soot oxidation, declines as the injection pressure increases. The ERF fuel had lower levels of smoke due to soot oxidation, since this mixture contains sufficient oxygen.

Downloaded from SAE International by Hadeel Solaka Aronsson, Monday, May 12, 2014 05:12:40 AM

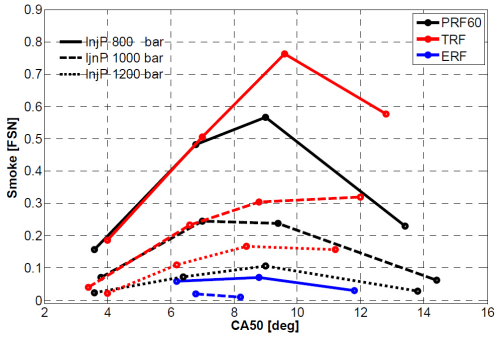

Figure 15. Smoke as a function of combustion phasing for different injection pressures at 13% inlet oxygen concentration (n-heptane concentration was kept constant at 40%; toluene 15% and ethanol 10%).

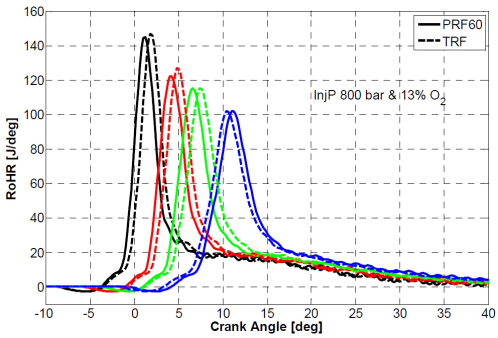

Figure 16. Rate of heat release as a function of crank angle degree with different combustion phasings, 800 bar injection, pressure, and 13% inlet oxygen concentration (n-heptane concentration was kept constant at 40%; toluene 15%).

Efficiencies

Combustion Efficiency

The effects of fuel composition on combustion efficiency were examined under constant operating conditions. The highest combustion efficiency was achieved by increasing the n-heptane concentration in the mixture and the lowest combustion efficiency was found with the highest concentrations of ethanol and toluene.

In contrast, combustion phasing and inlet oxygen concentration strongly affected combustion efficiency. Figure 17 shows combustion efficiency as a function of CA50 and inlet O_2 concentration for different surrogate mixtures. Generally, high combustion efficiency is achieved at early CA50s and at high inlet oxygen concentrations. At lower inlet O_2 concentrations, the combustion efficiency is affected more by changing CA50 than at higher inlet O_2 concentrations. This is because at higher inlet O_2 concentrations there is more oxygen, which helps oxidize the HC and CO and achieve complete combustion. On the other hand, at lower O_2 concentrations, the combustion efficiency is sensitive to changes in CA50 due to a lack of oxygen, so the combustion temperature will significantly influence the combustion efficiency. However, with increasing RON, the combustion efficiency is more sensitive to CA50 than to inlet oxygen concentration. This is because high-RON fuels advance the SOI, placing more fuel in the squish volume.

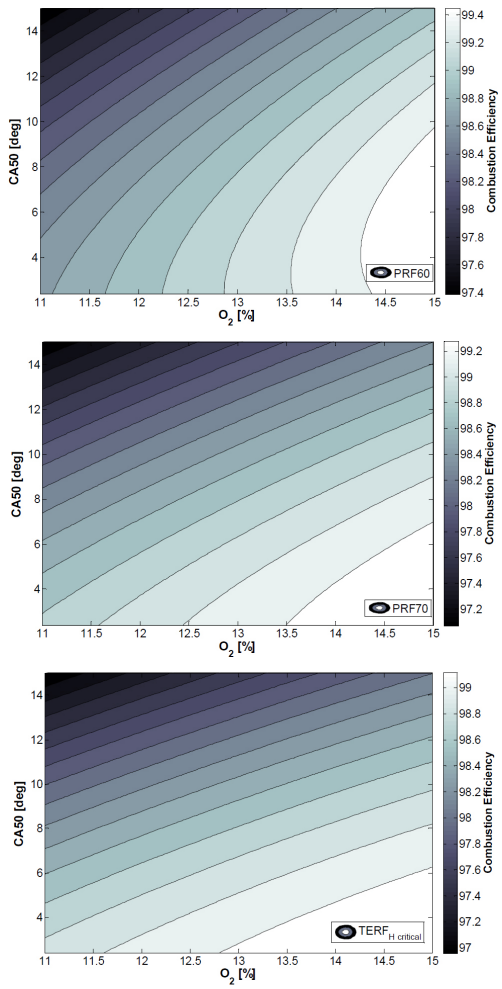

Figure 17. Combustion efficiency as a function of combustion phasing and inlet O_2 concentration for different fuels.

Downloaded from SAE International by Hadeel Solaka Aronsson, Monday, May 12, 2014 05:12:40 AM

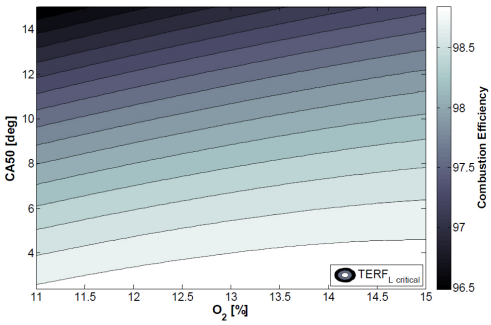

Figure 17. (cont.) Combustion efficiency as a function of combustion phasing and inlet O_2 concentration for different fuels.

Gross Indicated Efficiency

Besides the combustion efficiency, indicated efficiency was examined. Unfortunately, it was difficult to predict the indicated efficiency using DoE. The fuel effect on gross indicated efficiency was very small. From the measured data (612 points), it was possible to find fuels and derive parameter coefficient effects on $\eta_{Undicated}$, as shown in Table 7. The gross indicated efficiency increased with increasing n-heptane concentration in the mixture, but decreased with increasing ethanol concentration. This is due to higher combustion temperature with increasing n-heptane concentration because of its high ignition quality. Injection pressure had no effect on the indicated efficiency; on the other hand, combustion phasing significantly influenced $\eta_{Undicated}$. As expected, retarding the CA50 reduced the $\eta_{Undicated}$ due to less expansion work. However, increasing the inlet oxygen concentration increased the indicated efficiency by making enough oxygen available, resulting in complete combustion. In addition, $\gamma = \frac{c_p}{c_v}$ is higher for air than EGR, which results in higher thermal efficiency.

Table 7. Fuel composition and derived parameter coefficient effects on gross indicated efficiency.

Parameters	Effect on $\eta_{Undicated}$	Coefficient
Retarding CA50	↓	0.27
Increasing inlet O_2 concentration	↑	0.22
Injection pressure	-	0.0003
Increasing N	↑	0.04
Increasing T	-	0.003
Increasing E	↓	0.028

CONCLUSIONS

Effects on heat release and engine-out emissions were investigated in a light-duty diesel engine undergoing partially premixed combustion. A DoE matrix containing 15 fuel blends was experimentally evaluated with variation in CA50, injection pressure, and inlet oxygen concentration.

1. Despite good agreement between a Gaussian profile and the premixed combustion phase, it was difficult to obtain an accurate regression model of the proportion of premixed combustion.

2. The relationship between PRoHR and combustion duration depended on the inlet O_2 concentration. At the lowest inlet O_2 concentration, the CD decreased as PRoHR increased, while at a medium O_2 concentration, the CD was insensitive to PRoHR and at highest O_2 concentration the CD increased as the PRoHR increased.

3. The minimum PRoHR and the maximum CD coincided at 5% toluene and 5% ethanol contents.

4. As PRoHR increased, HC and CO emissions decreased while NO_x emissions increased due to a higher combustion temperature.

5. High-RON fuels produced high HC and CO emissions, since an early SOI was needed to maintain CA50, placing more fuel in the squish volume. Fuel placed in the squish volume has less chance to be fully oxidized, since it can be trapped in overly lean zones, rich zones, or as fuel film on the piston top or cylinder head.

6. Lower inlet O_2 concentrations gave more HC and CO emissions for the same reason as above in combination with a general decay in oxidation rate.

7. The smoke levels were near zero in much of the experiment, leading to a poor general regression model. However, some observations of the smoke level were still made. High levels of n-heptane increased the smoke level while ethanol decreased it. Smoke was lowest at the highest O_2 levels, which were connected to stronger soot oxidation. The smoke level decreased with increasing injection pressure.

FUTURE WORK

A dataset consisting of 612 PPC engine experiments using different mixtures of n-heptane, isooctane, toluene and ethanol has been produced for future kinetics modeling.

REFERENCES

1. Neely, G., Sasaki, S., and Leet, J., "Experimental Investigation of PCCI-DI Combustion on Emissions in a Light-Duty Diesel Engine," SAE Technical Paper 2004-01-0121, 2004, doi:10.4271/2004-01-0121.

2. Okude, K., Mori, K., Shiino, S., and Moriya, T., "Premixed Compression Ignition (PCI) Combustion for Simultaneous Reduction of NOx and Soot in Diesel Engine," SAE Technical Paper 2004-01-1907, 2004, doi: 10.4271/2004-01-1907.

3. Lechner, G., Jacobs, T., Chryssakis, C., Assanis, D. et al., "Evaluation of a Narrow Spray Cone Angle, Advanced Injection Timing Strategy to Achieve Partially Premixed

Downloaded from SAE International by Hadeel Solaka Aronsson, Monday, May 12, 2014 05:12:40 AM

Compression Ignition Combustion in a Diesel Engine," SAE Technical Paper 2005-01-0167, 2005, doi: 10.4271/2005-01-0167.

4. Kimura, S., Aoki, O., Ogawa, H., Muranaka, S. et al., "New Combustion Concept for Ultra-Clean and High-Efficiency Small DI Diesel Engines," SAE Technical Paper 1999-01-3681, 1999, doi:10.4271/1999-01-3681.

5. Kimura, S., Aoki, O., Kitahara, Y., and Aiyoshizawa, E., "Ultra-Clean Combustion Technology Combining a Low-Temperature and Premixed Combustion Concept for Meeting Future Emission Standards," SAE Technical Paper 2001-01-0200, 2001, doi:10.4271/2001-01-0200.

6. Colban, W., Miles, P., and Oh, S., "Effect of Intake Pressure on Performance and Emissions in an Automotive Diesel Engine Operating in Low Temperature Combustion Regimes," SAE Technical Paper 2007-01-4063, 2007, doi: 10.4271/2007-01-4063.

7. Idicheria, C. and Pickett, L., "Soot Formation in Diesel Combustion under High-EGR Conditions," SAE Technical Paper 2005-01-3834, 2005, doi:10.4271/2005-01-3834.

8. Noehre, C., Andersson, M., Johansson, B., and Hultqvist, A., "Characterization of Partially Premixed Combustion," SAE Technical Paper 2006-01-3412, 2006, doi: 10.4271/2006-01-3412.

9. Okude, K., Mori, K., Shiino, S., and Moriya, T., "Premixed Compression Ignition (PCI) Combustion for Simultaneous Reduction of NOx and Soot in Diesel Engine," SAE Technical Paper 2004-01-1907, 2004, doi: 10.4271/2004-01-1907.

10. Musculus, M., "Multiple Simultaneous Optical Diagnostic Imaging of Early-Injection Low-Temperature Combustion in a Heavy-Duty Diesel Engine," SAE Technical Paper 2006-01-0079, 2006, doi:10.4271/2006-01-0079.

11. Manente, V., Zander, C., Johansson, B., Tunestal, P. et al., "An Advanced Internal Combustion Engine Concept for Low Emissions and High Efficiency from Idle to Max Load Using Gasoline Partially Premixed Combustion," SAE Technical Paper 2010-01-2198, 2010, doi: 10.4271/2010-01-2198.

12. Kalghatgi, G., Risberg, P., and Ångström, H., "Advantages of Fuels with High Resistance to Auto-ignition in Late-injection, Low-temperature, Compression Ignition Combustion," SAE Technical Paper 2006-01-3385, 2006, doi:10.4271/2006-01-3385.

13. Kalghatgi, G., Risberg, P., and Ångström, H., "Partially Pre-Mixed Auto-Ignition of Gasoline to Attain Low Smoke and Low NOx at High Load in a Compression Ignition Engine and Comparison with a Diesel Fuel," SAE Technical Paper 2007-01-0006, 2007, doi:10.4271/2007-01-0006.

14. Heywood, J.B., "*Internal Combustion Engine Fundamentals*", McGraw Hill Book Co, 1988

15. Ekoto, I., Colban, W., Miles, P., Park, S. et al., "UHC and CO Emissions Sources from a Light-Duty Diesel Engine Undergoing Dilution-Controlled Low-Temperature Combustion," *SAE Int. J. Engines* 2(2):411-430, 2009, doi: 10.4271/2009-24-0043.

16. Aronsson, U., Andersson, Ö., Egnell, R., Miles, P. et al., "Influence of Spray-Target and Squish Height on Sources of CO and UHC in a HSDI Diesel Engine During PPCI Low-Temperature Combustion," SAE Technical Paper 2009-01-2810, 2009, doi:10.4271/2009-01-2810.

17. Solaka, H., Aronsson, U., Tuner, M., and Johansson, B., "Investigation of Partially Premixed Combustion Characteristics in Low Load Range with Regards to Fuel Octane Number in a Light-Duty Diesel Engine," SAE Technical Paper 2012-01-0684, 2012, doi: 10.4271/2012-01-0684.

18. Solaka, H., Tuner, M., and Johansson, B., "*Investigation on impact of fuel properties on partially premixed combustion characteristics in a light duty diesel engine*," ASME Technical Paper 2012-0-81184, 2012.

19. Machado, G.B., Barros, J.E.M., Braga, S.L., Braga, C.V.M., Oliviera, E.J., Silva, A.H.M..F.T, Carvalho, L.O., 2011, "Investigation on surrogate fuels for high-octane oxygenated gasolines", Fuel, 90, pp.640-646.

20. Truedsson, I., Tuner, M., Johansson, B., and Cannella, W., "Emission Formation Study of HCCI Combustion with Gasoline Surrogate Fuels," SAE Technical Paper 2013-01-2626, 2013, doi:10.4271/2013-01-2626.

21. Andersson, Ö., "*Experiment: Planning, Implementing and Interpreting*", First edition, John Wiley & Sons, Ltd, 2012.

22. Solaka, H., Tuner, M., and Johansson, B., "Analysis of Surrogate Fuels Effect on Ignition Delay and Low Temperature Reaction during Partially Premixed Combustion," SAE Technical Paper 2013-01-0903, 2013, doi:10.4271/2013-01-0903.

23. Leermakers, C., Bakker, P., Somers, L., de Goey, L. et al., "Commercial Naphtha Blends for Partially Premixed Combustion," *SAE Int. J. Fuels Lubr.* 6(1):199-216, 2013, doi:10.4271/2013-01-1681.

24. Opat, R., Ra, Y., Gonzalez D., M., Krieger, R. et al., "Investigation of Mixing and Temperature Effects on HC/CO Emissions for Highly Dilute Low Temperature Combustion in a Light Duty Diesel Engine," SAE Technical Paper 2007-01-0193, 2007, doi:10.4271/2007-01-0193.

25. Kee, S., Mohammadi, A., Kidoguchi, Y., and Miwa, K., "Effects of Aromatic Hydrocarbons on Fuel Decomposition and Oxidation Processes in Diesel Combustion," SAE Technical Paper 2005-01-2086, 2005, doi: 10.4271/2005-01-2086.

26. Koci, C., Ra, Y., Krieger, R., Andrie, M. et al., "Detailed Unburned Hydrocarbon Investigations in a Highly-Dilute Diesel Low Temperature Combustion Regime," *SAE Int. J. Engines* 2(1):858-879, 2009, doi:10.4271/2009-01-0928.

27. Azetsu, A., Sato, Y., and Wakisaka, Y., "Effects of Aromatic Components in Fuel on Flame Temperature and Soot Formation in Intermittent Spray Combustion," SAE

Downloaded from SAE International by Hadeel Solaka Aronsson, Monday, May 12, 2014 05:12:40 AM

Technical Paper 2003-01-1913, 2003, doi: 10.4271/2003-01-1913.

28. Kuti, O., Zhang, W., Nishida, K., Wang, X. et al., "Effect of Injection Pressure on Ignition, Flame Development and Soot Formation Processes of Biodiesel Fuel Spray," *SAE Int. J. Fuels Lubr.* 3(2):1057-1070, 2010, doi: 10.4271/2010-32-0053.

CONTACT INFORMATION

hadeel.solaka@energy.lth.se

ACKNOWLEDGMENTS

The authors would like to acknowledge the Competence Center Combustion Processes, KCFP, and the Swedish Energy Agency for the financial support, William Cannella from Chevron for supplying fuels.

DEFINITIONS/ABBREVIATIONS

ATDC - After top dead center

CAD - Crank angle degree

CA50 - Crank angle at 50% completion of heat release

CD - Combustion duration

CN - Cetane number

DoE - Design of experiment

EGR - Exhaust gas recirculation

ERF - Primary reference fuel with ethanol

ID - Ignition delay

$IMEP_g$ - Indicated mean effective pressure, gross

LTR - Low temperature reaction

MON - Motor octane number

NO_x - Nitrogen oxides, i.e., NO and NO_2

ON - Octane number

PF - Premixed fraction

PM - Particulate matter

PRoHR - Peak rate of heat release

PRF - Primary reference fuel

RON - Research octane number

SOC - Start of combustion

SOI - Start of injection

TDC - Top dead center

$TERF_{cp}$ - Primary reference fuel with toluene and ethanol, center point

$TERF_{critical}$ - Primary reference fuel with toluene and ethanol, critical point

TRF - Primary reference fuel with toluene

Downloaded from SAE International by Hadeel Solaka Aronsson, Monday, May 12, 2014 05:12:40 AM

APPENDIX

Table 1. R^2 for premixed fraction at 11% O2 at different CA50s and injection pressures.

R^2	O_2 [%]	Inj pressure [bar]	CA50 [deg]
0.77	11	1200	3
0.74	-	-	6
0.69	-	-	8
0.89	-	-	10
0.93	-	1000	3
0.36	-	-	6
0.65	-	-	8
0.39	-	-	10
0.70	-	800	3
0.35	-	-	6
0.30	-	-	8
0.43	-	-	10

Table 2. R^2 for premixed fraction at 13% O_2 at different CA50s and injection pressures.

R^2	O_2 [%]	Inj pressure [bar]	CA50 [deg]
0.85	13	1200	3
0.88	-	-	6
0.83	-	-	8
0.77	-	-	10
0.85	-	1000	3
0.85	-	-	6
0.94	-	-	8
0.68	-	-	10
0.96	-	800	3
0.75	-	-	6
0.86	-	-	8
0.89	-	-	10

Table 3. R^2 for premixed fraction at 15% O_2 at different CA50s and injection pressures.

R^2	O_2 [%]	Inj Pressure [bar]	CA50 [deg]
0.84	15	1200	3
0.90	-	-	6
0.88	-	-	8
0.94	-	-	10
0.85	-	1000	3
0.70	-	-	6
0.47	-	-	8
0.65	-	-	10
0.76	-	800	3
0.87	-	-	6
0.72	-	-	8
0.58	-	-	10

Downloaded from SAE International by Hadeel Solaka Aronsson, Monday, May 12, 2014 05:12:40 AM

The predicted PoRoHR, CD, NOx, HC, CO and Combustion efficiency is calculated according to Equation 3 and Table 4 in Appendix. The data matrix (dataset) together with the regression coefficients give the predicted parameter. β_0 is a constant term while β_{CA50}, β_{O2}, β_{Prail}, β_N, β_T, and β_E (shown in red) are linear terms for CA50, inlet O_2 concentration, injection pressure, n-heptane, toluene, and ethanol, respectively. The interaction coefficients (shown in black) include β_{NT} (interaction between n-heptane and toluene), β_{NE} (interaction between n-heptane and ethanol), and β_{TE} (interaction between toluene and ethanol). The quadratic coefficients (shown in green) include β_{NN} (n-heptane quadratic), β_{TT} (toluene quadratic), and β_{EE} (ethanol quadratic). N, T, and E are the volume fractions [%] of n-heptane, toluene, and ethanol, respectively, while CA50, inlet oxygen concentration, and injection pressure are presented in degrees ATDC, volume fraction [%], and bar, respectively.

$$Parameter_{Predicted} = \beta_0 + \beta_{CA50} \cdot CA50 + \beta_{O_2} \cdot O_2 + \beta_{P_{rail}} \cdot P_{rail} + \beta_N \cdot N + \beta_T \cdot T + \beta_E \cdot E + \beta_{CA50 \cdot O_2} \cdot CA50 \cdot O_2 + \beta_{CA50 \cdot P_{rail}} \cdot CA50 \cdot P_{rail} + \beta_{CA50 \cdot N} \cdot CA50 \cdot N + + \beta_{CA50 \cdot T} \cdot CA50 \cdot T + + \beta_{CA50 \cdot E} \cdot CA50 \cdot E + \beta_{O_2 \cdot P_{rail}} \cdot O_2 \cdot P_{rail} + \beta_{O_2 \cdot N} \cdot O_2 \cdot N + \beta_{O_2 \cdot T} \cdot O_2 \cdot T + \beta_{O_2 \cdot E} \cdot O_2 \cdot E + \beta_{P_{rail} \cdot N} \cdot P_{rail} \cdot N + \beta_{P_{rail} \cdot T} \cdot P_{rail} \cdot T + \beta_{P_{rail} \cdot E} \cdot P_{rail} \cdot E + \beta_{N \cdot T} \cdot N \cdot T + \beta_{N \cdot E} \cdot N \cdot E + \beta_{T \cdot E} \cdot T \cdot E + \beta_{CA50 \cdot CA50} \cdot CA50^2 + \beta_{O_2 \cdot O_2} \cdot {O_2}^2 + \beta_{P_{rail} \cdot P_{rail}} \cdot {P_{rail}}^2 + \beta_{N \cdot N} \cdot {P_N}^2 + \beta_{T \cdot T} \cdot {P_T}^2 + \beta_{E \cdot E} \cdot {P_E}^2$$

Table 4. Regression coefficients.

Regression model coefficient	PoRoHR	CD	NOx	HC	CO	$\eta_{combustion}$
β_0	36.78169	36.34	3.108	27.306	147.6675	93.05046
β_{CA50}	-6.32553	1.22	0.131	2.0057	2.405021	-0.26822
β_{O_2}	12.99155	0.27	-0.601	-3.037	-8.20477	0.527386
$\beta_{P_{rail}}$	-0.16695	-0.02	-0.0004	-0.002	-0.08866	0.002809
β_N	0.294777	0.035	-0.002	-0.509	0.937745	0.026936
β_T	0.158755	-0.18	-0.005	0.089	-1.57403	0.037172
β_E	-2.16633	-0.69	0.013	0.302	-3.12393	0.04904
β_{CA50O_2}	-0.14792	-0.092	-0.013	-0.143	-0.04378	0.01552
$\beta_{CA50P_{rail}}$	-0.00382	-8.67E-06	-3.906E-6	0.0003	0.000537	-4.61E-05
β_{CA50N}	0.149433	-0.014	-0.0005	-0.035	-0.00635	0.003668
β_{CA50T}	-0.03099	-0.0004	-0.0003	0.012	-0.00567	-0.00099
β_{CA50E}	-0.08487	0.006	0.0004	0.033	-0.01242	-0.00319
$\beta_{O_2P_{rail}}$	0.017325	0.0003	0.00003	0.0002	0.005846	-0.00019
β_{O_2N}	0.10209	-0.041	0.0008	0.014	-0.27088	0.006598
β_{O_2T}	0.022999	0.002	0.0011	-0.004	0.11175	-0.00283
β_{O_2E}	-0.03678	0.028	-0.0022	-0.013	0.293596	-0.00675
$\beta_{P_{rail}N}$	0.00223	-0.0001	-3.77E-06	-0.0001	-8.42E-05	9.13E-06
$\beta_{P_{rail}T}$	-0.0005	0.00005	1.49E-06	0.00002	6.85E-05	-3.93E-06
$\beta_{P_{rail}E}$	-0.00161	0.0001	4.2E-06	0.00009	4.24E-05	-1.11E-05
β_{NT}	-0.0188	0.004	-0.0002	-0.002	0.003797	8.12E-05
β_{NE}	0.081953	0.007	-0.00007	-0.011	-0.00937	0.001469
β_{TE}	-0.00439	-0.001	-0.00016	0.004	0.012246	-0.00075
β_{CA50}^2	0.093745	0.026	0.0022	0.067	-0.01165	-0.00635
$\beta_{O_2}^2$	-0.6105	0.024	0.029	0.111	0.200829	-0.01659
$\beta_{P_{rail}}^2$	-2.68E-05	8.00E-06	1.26E-7	-6.525E-7	5.85E-06	-1.07E-07
β_{NN}^2	-0.0729	0.011	0.00003	0.009	0.032724	-0.00189
β_{TT}^2	0.073399	-0.006	0.00006	-0.002	-0.00128	0.000301
β_{EE}^2	0.224161	-0.018	0.0008	-0.002	-0.00538	0.000165
R^2	0.95	0.93	0.91	0.93	0.97	0.97

Downloaded from SAE International by Hadeel Solaka Aronsson, Monday, May 12, 2014 05:12:40 AM

High-RON fuels produced high HC and CO emissions, since an early SOI was needed to maintain CA50, placing more fuel in the squish volume, see Figure 1. Fuel placed in the squish volume has less chance to be fully oxidized, since it can be trapped in overly lean zones, rich zones, or as fuel film on the piston top or cylinder head.

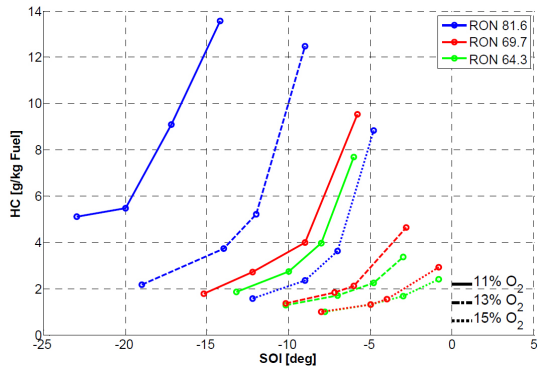

Figure 1. HC emission as a function of start of injection for three different RON values at different inlet oxygen concentrations.

The Engineering Meetings Board has approved this paper for publication. It has successfully completed SAE's peer review process under the supervision of the session organizer. This process requires a minimum of three (3) reviews by industry experts.

All rights reserved. No part of this publication may be reproduced, stored in a retrieval system, or transmitted, in any form or by any means, electronic, mechanical, photocopying, recording, or otherwise, without the prior written permission of SAE.

ISSN 0148-7191

Positions and opinions advanced in this paper are those of the author(s) and not necessarily those of SAE. The author is solely responsible for the content of the paper.

SAE Customer Service:
Tel: 877-606-7323 (inside USA and Canada)
Tel: 724-776-4970 (outside USA)
Fax: 724-776-0790
Email: CustomerService@sae.org
SAE Web Address: http://www.sae.org
Printed in USA

Paper V

Downloaded from SAE International by Hadeel Solaka Aronsson, Monday, May 12, 2014 05:14:35 AM

SAE INTERNATIONAL

Using Oxygenated Gasoline Surrogate Compositions to Map RON and MON

2014-01-1303
Published 04/01/2014

Hadeel Solaka Aronsson, Martin Tuner, and Bengt Johansson
Lund Univ.

CITATION: Solaka Aronsson, H., Tuner, M., and Johansson, B., "Using Oxygenated Gasoline Surrogate Compositions to Map RON and MON," SAE Technical Paper 2014-01-1303, 2014, doi:10.4271/2014-01-1303.

Copyright © 2014 SAE International

Abstract

Gasoline fuels are complex mixtures which consist of more than 200 different hydrocarbon species. In order to decrease the chemical and physical complexity, oxygenated surrogate components were used to enhance the fundamental understanding of partially premixed combustion (PPC). The ignition quality of a fuel is measured by octane number. There are two methods to measure the octane number: research octane number (RON) and motor octane number (MON). In this paper, RON and MON were measured for a matrix of n-heptane, isooctane, toluene, and ethanol (TERF) blends spanning a wide range of octane number between 60.6 and 97. First, regression models were created to derive RON and MON for TERF blends. The models were validated using the standard octane test for 17 TERF blends. Second, three different TERF blends with an ignition delay (ID) of 8 degrees for a specific operating condition were determined using a regression model. This was done to examine the model accuracy for ID and study fuel composition effect on combustion events and emissions.

The results showed a good agreement between predicted and tested RON and MON with an accuracy of ±0.6. The model also had high accuracy during extrapolation for some fuel blends. For toluene and reference fuel blend (TRF) the model was more accurate for MON than for RON, while the situation was the opposite for ethanol and reference fuel blend (ERF) i.e. the model worked better for RON than for MON during extrapolation. The ignition delay was similar for all three TERF blends despite the differences in their composition. However, high concentration of toluene resulted in higher levels of HC, NO_x, and smoke emissions.

Introduction

Automotive gasoline contains about 200 different hydrocarbons compounds. The concentrations of the compounds vary significantly depending on the source of crude oil, refinery process, and product specifications. Generally, hydrocarbon distribution consists of alkanes, alkenes, isoalkanes, cycloalkanes, cycloalkenes, and aromatics. Gasoline can vary widely in composition: even those with the same octane number may be quite different, not only in the physical properties, but also in the molecular structure of the components [1].

Performance and quality of an automotive gasoline is determined by its resistance to knock. The antiknock quality of the fuel limits the power and economy for SI-engine using that fuel. The higher the antiknock quality of the fuel is the more the power and efficiency of the engine. Therefore, the performance of the gasoline fuel is measured by the octane number. Octane numbers are obtained by two methods: those obtained by the first method are called research octane numbers (RON) (ASTM D-2699 and ASTM D-2722). Those obtained by second method called motor octane number (MON) (ASTM D-2700 and ASTM D-2723). Gasoline octane numbers are not blends linearly thus are measured because their blending behavior is dependent on the other components that are present in the blend. Therefore it is difficult to predict the octane quality of a gasoline. Generally, engines in vehicles differ broadly in the way they respond to octane parameters and the level of octane quality they require. There are even large variations between different cars of the same model. This means that in order to define the octane requirement of a fuel with good accuracy, it is necessary to test at least a dozen of examples [2]. Manufacturing gasoline with different octane qualities are costly and time consuming. Therefore many researchers have developed surrogate fuels to represent gasoline combustion behavior in chemical kinetic simulation, optical studies, and CFD [3, 4, 5].

The simplest surrogate fuels for gasoline consist of single components. For example: isooctane is often used to represent gasoline, especially in optical studies, CFD, and chemical kinetic simulations [6, 7] because of its high octane number, and compared to gasoline, relatively simple fuel chemistry. On

Downloaded from SAE International by Hadeel Solaka Aronsson, Monday, May 12, 2014 05:14:35 AM

the other hand, n-heptane is often used to represent diesel fuel due to its low octane number (high cetane number). Normally, blends of iso-octane and n-heptane, which are primary reference fuels (PRF), are used to represent gasoline fuel with different octane numbers [8]. Researchers have presented studies about surrogate fuels that describe possible components and classifying their importance [4]. These studies suggested three necessary components for gasoline surrogates: n-heptane, isooctane and toluene. Toluene is typically the most representative of the aromatic compound in gasoline. Recently ethanol is considered to be used in surrogate fuels due to recent increase in the use of ethanol in USA and Europe. The reason to introduce toluene and ethanol to PRF fuel as surrogate is that the sensitivity of any PRF fuel, unlike commercial gasoline, is zero. The sensitivity of a fuel is obtained as

$$Senstivity\ (S) = RON - MON \tag{1}$$

Generally, the linear by volume (*LbV*) method is used to calculate RON and MON for any PRF fuel. This is a sum of the contribution of the two components weighted by their volume fractions, the equation can be written as

$$RON = \propto_N \cdot x_N + \propto_I \cdot x_I \tag{2}$$

Where $\propto_N$ and $\propto_I$ are the coefficients for n-heptane (*N*) and isooctane (*I*) and are equal to 0 and 100. Where x_N and x_I are the volume fractions of n-heptane and isooctane respectively.

There is a direct link between fuel composition and RON value for *PRF* fuels. However, with blends of n-heptane, isooctane, and toluene (*TRF*), n-heptane, isooctane, and ethanol (*ERF*), and n-heptane, isooctane, ethanol, and toluene (*TERF*), no such link exists. The octane numbers (*ON*) change in a nonlinear correlation by adding ethanol or toluene to any PRF. This makes it impossible to determine and estimate the RON or MON value for *TRF*, *ERF*, and *TERF* blends using the *LbV* method, and it is time consuming and costly to send a fuel to be tested according to ASTM methods. Many researchers and modelers ask the same question; if it is possible to re-create RON and MON for a gasoline fuel using surrogate fuel. In order to mimic a fuel we need a sufficient and accurate method to determine RON and MON.

Primarily this investigation address the problem using a regression model from design of experiment (DoE) to map the n-heptane, toluene, ethanol, and isooctane space with respect to RON and MON. The model will allow estimation of RON and MON for any *TRF*, *ERF*, and *TERF* surrogate and/or determine the required blend for achieving a fuel with a desired RON and MON. This is an efficient method that can be used by other research groups or industry to meet their specific fuel requests. Also it is interesting to remark that RON and MON are two characteristics that nowadays are widely used also for the CI engine community. Secondly, the relation between ignition delay and RON is examined. From previous studies it is known that fuels with the same RON value have similar ignition delays in PPC [9]. The objective is to investigate if fuels with the same ignition delay (with different composition) will have similar RON values. Finally, the possibility to control the combustion events by using fixed ignition delay for different fuels with different compositions is examined.

Surrogate Fuels Selection Methodology

Component and Concentration Selections

The motivation for the selection of the components and concentration for the surrogate fuel is to mimic gasoline fuels. Aromatics are significant component in gasoline fuel and could vary significantly based on the origin. Toluene is the main aromatic component in gasoline. Recently ethanol is blended into most gasoline at a concentration of 10% by volume in United State and at a concentration of 5% in European Union [10]. Isooctane and n-heptane are also important components for controlling the octane rating.

Therefore, for the primary investigation two design of experiment fuel matrices from previous studies [11, 12, 13] are combined. This allows expanding the RON and MON space with different combinations of surrogate fuel compositions.

These studies showed that ethanol octane blending is more sensitive in relations to RON than toluene [11]. Therefore, the selections of fuels for the rest of the investigations are based on the ratio between toluene to ethanol.

Fuel Properties

The fuels used in this investigation are blends of n-heptane, isooctane, toluene, and ethanol. Fuel properties are presented in Table 1. These fuels were blended in volume fraction to create surrogate fuels. The fuels were individually tested according to ASTDM to determine the values of RON and MON. The stoichiometric air/fuel ratio and lower heating value were calculated based on the C:H:O ratio of each blend.

The RON and MON values for first part of the investigation are found in [11, 12, 13]. Fuel properties for the remaining part of the investigation are presented in Table 2.

Table 1. Fuel specifications.

Fuels properties	n-Heptane	Toluene	Ethanol	Isooctane
RON	0	120	107	100
MON	0	109	89	100
Auto-ignition temperature [^{o}C]	203.85	529	425	411
Molecular formula	C7H16	C7H8	C2H6O	C8H18
Molar mass [g/mol]	100.23	92.15	46.07	114.26
Density [kg/m^{3}]	679.5	866.9	789	688
Boiling point [^{o}C]	98	110.6	78.5	99

Table 2 shows fuel properties for the second part of the investigation. *N*, *T*, *E*, and *I* are abbreviations for n-heptane, toluene, ethanol, and isooctane, respectively. These fuels were prepared that the ratios of toluene/ethanol (*T/E*) are: 3, 0.75, and 0. The choice of these ratios is due to: higher sensitivity of ethanol than toluene, their predicated ignition delay were

Downloaded from SAE International by Hadeel Solaka Aronsson, Monday, May 12, 2014 05:14:35 AM

similar at the specific operating conditions (CA50= 3 degree ATDC, P_{rail}= 1000 bar, inlet O_2=13%), and the regression model for ignition delay is reliable during that range.

Table 2. Fuel composition and octane rating.

Fuel T/E	N [v%]	T [v%]	E [v%]	I [v%]	RON DoE	MON DoE
3	31.52	15	5	48.48	77.28	73.6
0.75	35.66	7.5	10	46.84	75.58	73.12
0	34.24	0	10	55.76	75.58	72.15

Fuel Design

Thirty blends of oxygenated surrogate fuels were created according to a design of experiment method. The central composite two-level full-factorial design used, in which axes are drawn through the center of the cube and the axial points are located on the face of the cube [14], is shown in Figure 1.

Isooctane levels were chosen to model gasoline fuel over a wide ignition-quality range. The isooctane contents of the blends were calculated according to Eq. 3,

$$\mathrm{Isooctane}_{C_I} = 100 - \left(\mathrm{nheptane}_{C_N} + \mathrm{toluene}_{C_T} + \mathrm{ethanol}_{C_E}\right) \quad (3)$$

Where C_I is the volume percentage of isooctane in the blend, and C_N, C_T, and C_E are the volume percentages of n-heptane, toluene, and ethanol in the blend, respectively.

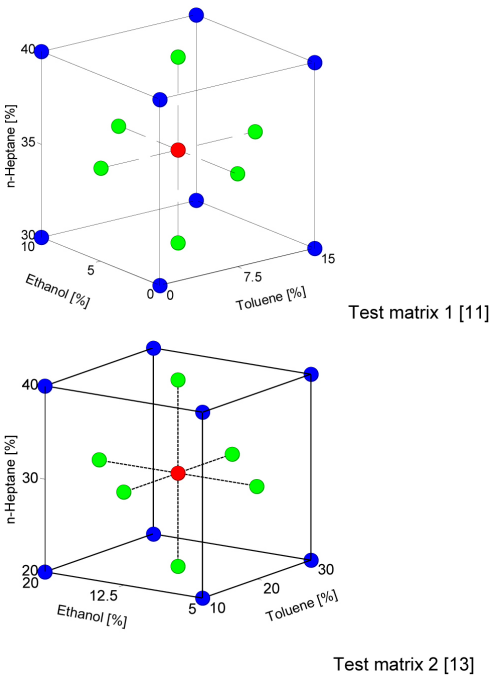

Figure 1. A central composite two-level full factorial design for test matrix 1 and 2.

The two test matrices consisted of 15 fuel blends each. The number of experiments can be described for each cube as $2^{k-p}+2k+cp$, where k is the number of studied variables, p is the fractionalization element (p = 0, full design), and cp is the number of center points. The center point was replicated three times, meaning that test matrix consisted of 17, i.e., $2^3 + (2 \times 3) + 3$, set point combinations as seen in Figure 1.

Experimental

Test Methodology

Fuel blends were prepared by determining the volume fraction for each component required achieving the desired blend at a temperature of 295 K. RON and MON were measured according to ASTM D2699 and D2700 standard methods. The accuracy of RON and MON was about ±0.2. Beside the fuel matrices from authors' research facility [11, 13], another three test matrices were prepared to validate the regression models of RON and MON presented in this work. These test matrices were prepared to design fuels either with same sensitivity but different RONs and/or fuels with same RON but with different sensitivities as seen in Figure 2. This allows studying fuels at broader range and understanding fuel composition concentration effect on RON and MON.

In a previous study by the authors [11] a regression model was used to predict the ignition delay for surrogate fuel blend. In this study, the ignition delay model is validated using three fuels (with different compositions) of an ID of 8 degrees. These fuels were prepared with the ratios of toluene/ethanol to: 3, 0.75, and 0 as seen in Table 2. The choice of these ratios is due to the higher sensitivity of RON for ethanol blends than toluene blends. From a previous study, it is known that similar RON results in similar ignition delay [9]. Therefore in this work, the statement is reversed and the question becomes: Do fuels with similar ignition delay have similar RON? By applying a constant ignition delay the fuel composition effect on combustion event and emissions can be investigated.

Thirty liters of each mixture was prepared for fuel-line cleaning and test execution. The fuels were tested under identical operating conditions as presented in Table 3. To prevent damage to the injection system, 100 ppm of the lubricity additive *Infineum R655* was added to each fuel mixture. The impact of such a small amount of additive on combustion phasing and emission formation is expected to be negligible.

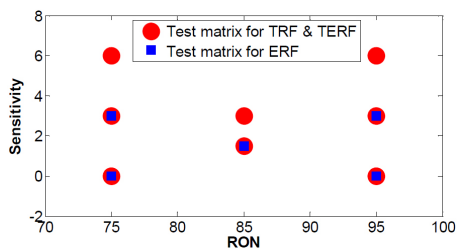

Figure 2. The test matrices for ERF (blue square markers), TRF and TERF mixtures for different RONs and sensitivities.

Downloaded from SAE International by Hadeel Solaka Aronsson, Monday, May 12, 2014 05:14:35 AM

Table 3. Operating conditions.

Engine speed [rpm]	1500
Inlet temperature mixture [K]	345
Load $IMEP_g$ [bar]	8
Absolute inlet pressure [bar]	2.3
Combustion phasing CA50 [deg]	3, 6, 8 &10
Inlet oxygen concentration [%]	13
Injection pressure [bar]	1000
Injection strategy	Single injection

Table 4. Engine specifications.

Engine specifications for one cylinder	
Engine type	Volvo D5
Number of cylinders	1
Bore [mm]	81
Stroke [mm]	93.2
Displacement Volume [cm^2/cylinder]	480
IVC [CAD BTDC]	174
Compression ratio	16.5
Swirl ratio	2.2
Number of intake valves	2
Number of exhaust valves	2
Injector	
Type	Solenoid
Injection nozzle holes	7
Injection nozzle diameter [mm]	0.14
Included angle [degrees]	140

Test Cell

The experimental engine was a five cylinder passenger car diesel engine operated on one cylinder. The engine and injector specifications are shown in Table 4. The engine test rig was equipped with an adjustable EGR system and adjustable heating for varying the inlet air temperature.

Smoke emissions were measured using an AVL415S smoke meter, while NO_x, HC, exhaust CO_2, CO, and intake CO_2 emissions were measured using a Horiba MEXA9200DF measurement system. NO_x emissions were measured using a chemiluminescence analyzer, whereas HC was measured using a flame ionization detector (FID); the piping to the FID analyzer was heated to approximately 191°C to prevent condensation of unburned fuel components. Inlet and exhaust oxygen (O_2) were measured using a magneto-pneumatic condenser microphone method (MPA), whereas CO, intake CO_2, and exhaust CO_2 were measured using infrared analyzers. The inlet oxygen concentration was measured using a Horiba measurement system. The oxygen concentration in the intake manifold was controlled by a valve that regulates the amount of exhaust gas recirculation (EGR) entered the intake system.

Heat Release Characteristics

From the calculated rate of heat release, information about the combustion events can be extracted. The heat losses are included in the rate heat release calculation using the Woschni model. The combustion events are divided into four phases; ignition delay (ID), low temperature reaction (LTR), premixed fraction and late mixing controlled combustion phases as seen in Figure 3.

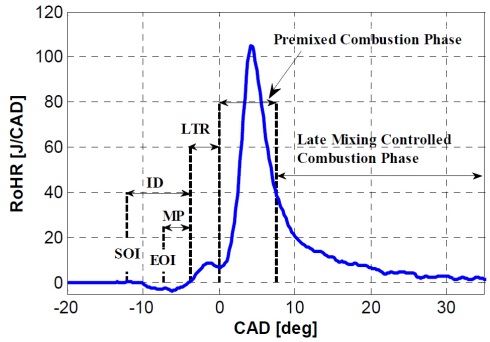

Figure 3. Typical PPC heat release diagram identifying different PPC combustion phases at 8 bar $IMEP_g$.

The ignition delay is the period between the start of injection (SOI) and the start of combustion (SOC) as shown in Figure 3. The start of injection was determined from the first maximum in the evolution of the pressure gradient in the common rail (not shown). The start of combustion is defined as the location where the rate of heat release returns to zero after the negative period. When the fuel is injected into the combustion chamber the gas temperature decreases due to fuel evaporation, showing the negative rate of heat release. The point where the rate of heat release returns to zero establishes the start of combustion and/or the start of low temperature reaction (LTR).

In order to separate the phases (LTR phase and premixed combustion phase) in a well-defined manner, a Gaussian profile is fitted to the rising flank of the premixed peak, between 15 J/CAD and the actual peak. Different values for the threshold have been tested but with very small impact on the LTR phase. The rate of heat release is then subtracted from the Gaussian profile, and the integrated area between the SC and the threshold point is used as a measure of the LTR fraction.

$$G(x) = h \cdot e^{-\left(\frac{x-x_0}{2\propto^2}\right)^2} \quad (4)$$

In Equation (4) x_0 is the central position of the peak, h and $\propto$ representing the height and width of the Gaussian profile, respectively.

Results and Discussion

Fitting Responses

Quadratic regression models were used to map RON and MON for the oxygenated surrogate gasoline fuels. Each regression model was fitted using data (thirty four surrogate fuels) generated previously at the authors' research facility [11, 13]. Later the modeled RON and MON were calculated according to equations 5.

$$RON_{Predicted} = \beta + \alpha_N \cdot X_N + \alpha_T \cdot X_T + \alpha_E \cdot X_E + \gamma_{NT} \cdot X_N \cdot X_T + \gamma_{NE} \cdot X_N \cdot X_E + \gamma_{TE} \cdot X_T \cdot X_E + \delta_{N^2} \cdot X_N^2 + \delta_{T^2} \cdot X_T^2 + \delta_{E^2} \cdot X_E^2 \quad (5)$$

Downloaded from SAE International by Hadeel Solaka Aronsson, Monday, May 12, 2014 05:14:35 AM

where β is a constant and α, γ and δ are coefficients for linear, interaction, and quadratic terms, respectively, and are generated from the regression model. The coefficients for each model are shown in Table B in the Appendix. X_N, X_T, and X_E are fuel concentration in volume fraction for n-heptane, toluene, and ethanol, respectively.

As seen in figure 4 the modeled RON values are presented in solid, dash-dotted, and dotted lines, while the measured RON values are presented as *x*-markers. The different line styles represent the different concentrations of n-heptane. The curves are fitted to the data points where the R^2 for RON is 0.999 and for MON is 0.997. It should be noted that the regression model for a response is based on the whole data set (34 data points) and not only on two or three points as shown in the figures. R^2 values for each model are given in the figures. R^2 by definition is between 0 and 1, where a value of 1 corresponds to a perfect fit.

Figure 4 shows the modeled RON as a function of ethanol and toluene. Measured RON values are shown as a reference. Figure 5 shows the modeled RON and MON versus the measured RON and MON. It can be observed that residuals are normally distributed and equally scattered around the model. The coefficient of determination R^2 is equal to 0.99 for both models, indicating an excellent fit of the data by the model.

However, the simplest mixing model is the *LbV* model. This is simply a sum of the contributions of the four components weighted by their volume fractions, denoted *X*. Equation 2 can be re-written as

$$RON = \theta_N X_N + \theta_T X_T + \theta_E X_E + \theta_I X_I \quad (6)$$

Where the θs represent the coefficients for n-heptane (*N*), toluene (*T*), ethanol (*E*) and isooctane (*I*) and are equal to 0, 120, 107 and 100 respectively. The *LbV* models lack the ability to predict RON for a mixture consisting of all four components due to the non-linear behavior of toluene and ethanol blends. For example; if the X_n is 40%, X_T is 15%, X_E is 10% and X_I is 35%, the predicted RON from *LbV* is 63.7 and from quadratic regression model is 72.26, while the measured RON is 72.2.

The RON slope as a function of ethanol is steeper than toluene as seen in Figure 4. It could be noticed that increasing ethanol or toluene concentration the RON value increases but it is stronger for ethanol. It is worth mentioning that while increasing the ethanol or toluene concentration the isooctane concentration decreases.

Comparing *ERF*, *TRF* and *TERF* at the same n-heptane concentration some statement can be made:

- RON is amplified by TERF rather than ERF alone
- The slope for TERF and ERF are similar and steeper than for TRF.

However, increasing n-heptane concentration decreases RON value for any surrogate mixture.

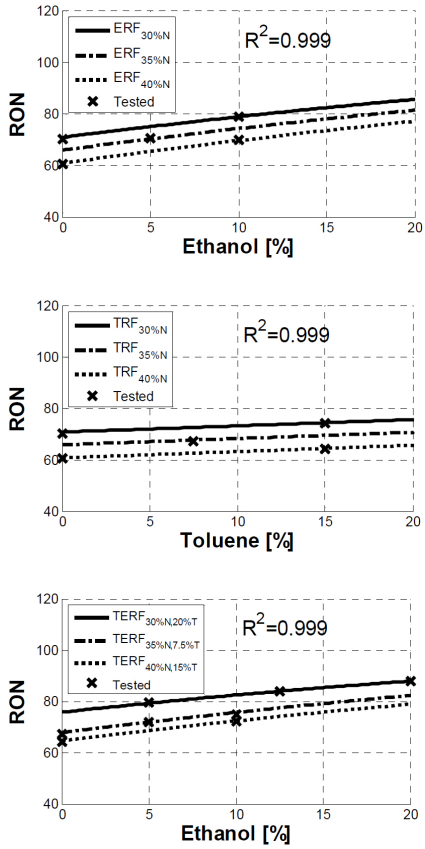

Figure 4. Modeled RON (solid, dash-dots and dotted lines) as a function of ethanol and toluene. Measured RON values are shown as a reference.

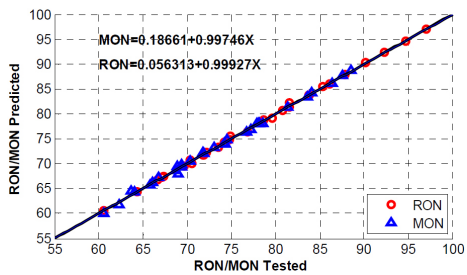

Figure 5. Predicted RON and MON versus tested RON and MON.

Model Validation

The quadratic regression models are used to model the sensitivity and RON values for three test matrices of *ERF*, *TRF*, and *TERF* as shown in Figure 2. In this case, it is possible to choose the composition of a mixture with a

Downloaded from SAE International by Hadeel Solaka Aronsson, Monday, May 12, 2014 05:14:35 AM

specified RON and sensitivity for seventeen fuels. RON and MON for all seventeen fuels were measured as well to validate the accuracy of the model. The fuel composition, RON, and MON modeled and measured for the three test matrices are shown in Table A in the Appendix.

Figure 6 and 7 show the modeled RON from the quadratic regression model and the validated RON for the chosen fuel blends as shown in Figure 2. Figure 5 shows the accuracy of the regression model for the modeled RON as black x-markers and the validated RON (measured) as red o-markers for different surrogate fuels. Extrapolation was used in the regression model to achieve the desired sensitivity for the ERF and TRF mixtures. TRF mixtures have the mildest incline in comparison to TERF and ERF, with the latest having the steepest incline.

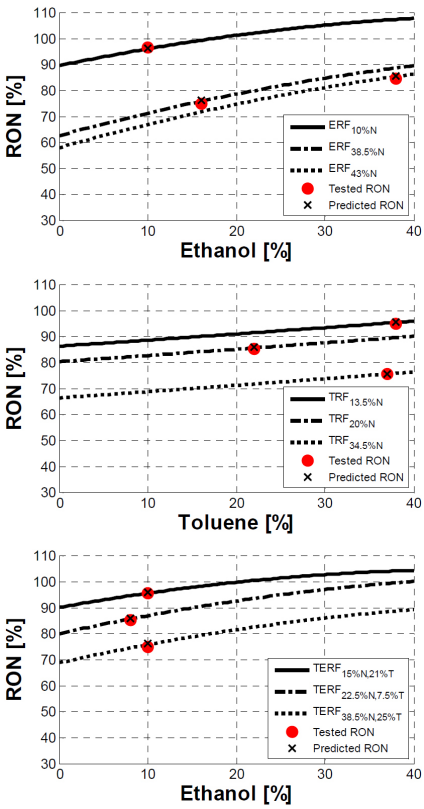

Figure 6. Predicted RON (solid, dash-dots and dotted line), desired predicted RON (x-markers) and tested RON (o-markers) for ERF, TRF and TERF.

In contrary to predicted RON, the predicted MON value for extrapolated sensitivity of ERF mixture did not show a good agreement with the tested MON value. The predicted MON value of 84.3 for the sensitivity of ERF mixture did not show a good agreement with the tested MON value of 78.7 as shown in Figure 6. This is due to using extrapolation outside the DoE limit which is 20% in volume for ethanol and 30% in volume for toluene. On other hand, the predicted MON values for the rest of the ERF, TRF, and TERF showed good agreement with the validated/tested MON. However, in order to strengthen the regression model, the RON and MON of seventeen fuels were added to the models. This decreased the error using the extrapolation method for ERF mixtures to predict MON value. The new regression coefficients for RON and MON are presented in Table B in the Appendix.

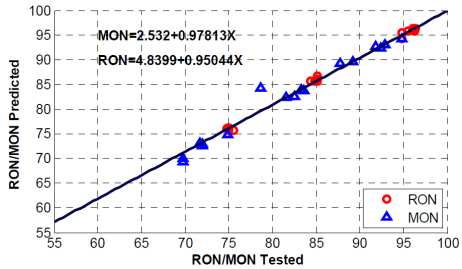

Figure 7. Model validation for predicted RON/MON versus tested RON/MON.

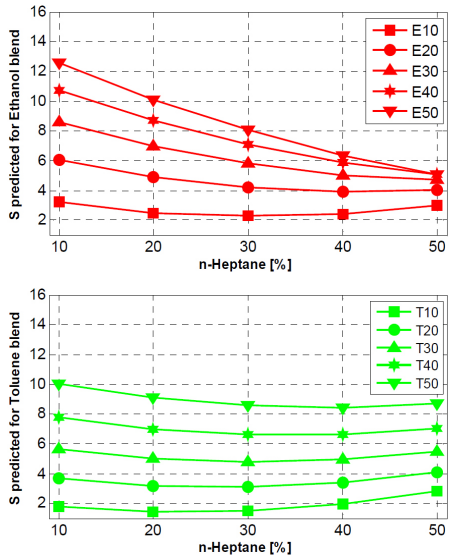

Figure 8. The predicted sensitivity of ethanol and toluene blends as a function of n-heptane.

According to Figure 8, the sensitivity (*S*) effect of ethanol differs from that of toluene, shown as function of n-heptane concentration. The sensitivity of ethanol blends decreases as n-heptane concentration increases and isooctane decreases. By increasing ethanol concentration, the sensitivity of a blend increases. However, looking at E10 (fuel containing 10 vol.% of ethanol), the blend sensitivity decreases as n-heptane increases, until it reaches a minimum value around 30 vol.% of n-heptane and starts to increase again. At low ethanol concentration, the sensitivity of a blend is less sensitive to the change in the n-heptane and isooctane concentrations. As opposite to ethanol, the sensitivities of toluene blends were

Downloaded from SAE International by Hadeel Solaka Aronsson, Monday, May 12, 2014 05:14:35 AM

less sensitive to the change in the n-heptane and isooctane concentrations. Though, at low toluene concentration such as T10 to T30, the sensitivity of the blend is increased as n-heptane concentration is increased and isooctane decreased.

Fuel Composition Effects at Similar ID

The ID was predicted with a length of about 8 degrees using a regression model from previous study by the authors [11]. This was achieved for three surrogate mixtures with T/E ratio of 0, 0.75 and 3 at constant operating conditions. The fuel properties are presented in Table 2. Previous works have shown that similar RON resulted in similar ID [9]. However, in this work the ID was fixed for three surrogate mixture with different composition. This showed that with similar ID similar RON was attained as seen in Table 2. The RON and MON value were predicted using equation 5 with the latest regression coefficients as was explained in previous section, and shown in Table B in the Appendix. With similar ID and RON value it will be easier to see fuel composition effect on combustion events and emissions.

Fuel Composition Effect on Combustion Process

The combustion phasing (CA50) was varied at 3, 6, 8, and 12 degrees for the three surrogate fuels. According to Figure 9, the ignition delays for the three surrogate fuels are similar. This proves that the regression model from previous study is reliable. It can also be concluded that fuel composition with similar RON have negligible influence on ignition delay.

Figure 10 shows the low temperature reaction (LTR) fraction as a function of start of injection (SOI). The LTR fraction is described as the total area between the start of combustion (SOC) and end of LTR to the total accumulative heat release. The LTR fraction is not affected by fuel composition. In previous study by the authors [11] showed that there is a relation between ID and LTR fraction.

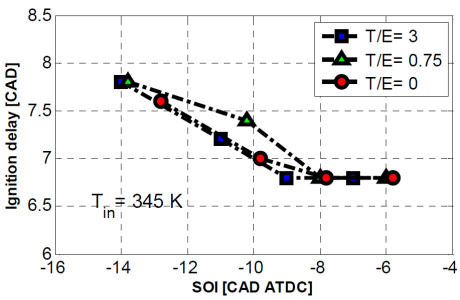

Figure 9. Ignition delay as a function of SOI for the three surrogate mixtures.

The ID and LTR fraction decrease as the SOI is retarded since the in-cylinder temperature is higher closer to top dead center (TDC). The T/E=0.75 at SOI of −10 in Figure 9 and T/E=3 at later SOI in Figure 10 do not follow the trend of the other fuels exactly. This difference comes, partly from the coarse resolution of the pressure trace, 0.2 CAD, which limits the accuracy of SOI, SOC, and end of LTR.

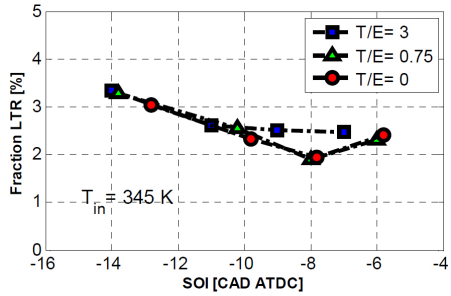

Figure 10. LTR as a function of SOI for the three surrogate mixtures.

Figure 11 shows the combustion duration (CD) as a function of SOI. The CD is the difference between CA90 and CA10. It can be noticed that the fuel composition do not influence the combustion duration. However, the combustion duration for all fuels is insensitive to the retardation in combustion phasing, except at the latest combustion phasing where the combustion duration increases. This increment is due to the slower diffusion controlled combustion and thus prolonged CD.

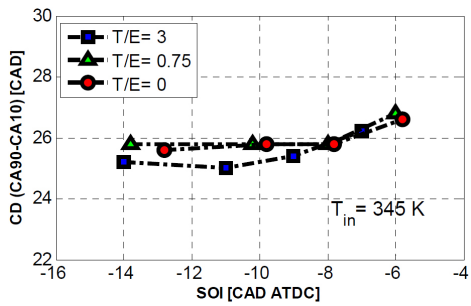

Figure 11. Combustion duration as a function of SOI for the three surrogate mixtures.

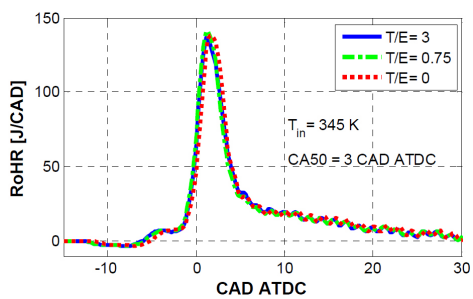

Figure 12. Rate of heat release as a function of crank angle degree for the three surrogate mixtures.

At constant operating conditions, the surrogate fuels have similar heat release rates as shown in Figure 12. Despite the differences between the surrogate fuel compositions, the

Downloaded from SAE International by Hadeel Solaka Aronsson, Monday, May 12, 2014 05:14:35 AM

combustion events are similar for all fuels. This leads us to the conclusion that the fuel composition does not affect the combustion event, if the fuels have similar RON and ID.

Comparing the three surrogate fuels, some statement can be made;

- Fuels with similar ID have similar RON
- The combustion events in PPC are controlled by ID and RON of a fuel rather than the fuel composition.

Fuel Composition Effect on Emissions

Figure 13 shows emissions as function of combustion phasing. The fuel composition has an influence on emissions. With a fixed ID and RON, it is easier to see the fuel composition impact on emissions. Increasing the ratio of toluene to ethanol (T/E), increase the emissions of NO_x, smoke and HC. It has previously been reported that fuels with aromatics extend the duration of NO_x formation due to local high-temperature regions with combustion of decomposed hydrocarbons [15]. Also, it is known that increasing aromatics content in the fuel leads an increased production of soot [16, 17]. However, the smoke levels are in general below the detecting limit of 0.01 FSN of the AVL smoke meter. The smoke values shown in Figure 13 are a mean value of three recording points at each CA50. It is worth mentioning that the NO_x and smoke emissions are below Euro 6 emission levels.

The trend of increasing the ratio of T/E is clear with HC emissions. Increasing the toluene concentration in the blend resulted in an increment in HC emissions [16]. However, CO emissions were not affected by the fuel composition.

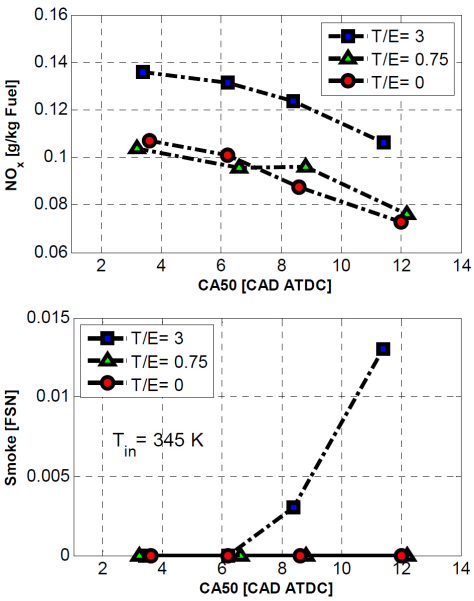

Figure 13.

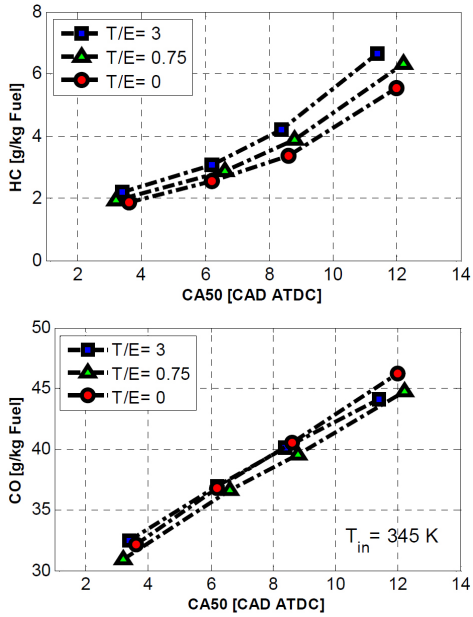

Figure 13. (cont.) Emissions as a function of CA50 for the three surrogate mixtures.

Summary/Conclusions

Quadratic regression models were used to map RON and MON for oxygenated surrogate gasoline fuels. Also, the blends for three different TERFs, all with an ignition delay of 8 degrees for a specific operating condition, were determined using a third quadratic regression model. This was done to separate the fuel composition effects from ignition quality effects on combustion events and emissions.

1. The quadratic regression model was shown to be more accurate than the linear by volume equation for determining RON and MON for oxygenated surrogate fuels.
2. RON was increased by increasing the concentrations of toluene and ethanol, and thus reducing concentration of isooctane.
3. The fuel sensitivity of ethanol blends were affected by the fraction of n-heptane and isooctane. The same was true for the sensitivity of toluene blends, however not to the same extent.
4. It was possible to predict the ignition delay accurately, using the quadratic regression model.
5. Similar ignition delays of fuels, independent of the fuel composition, gave similar RON values.
6. For a similar RON value the fuel composition did not have a significant influence on the combustion process at a constant ID, giving identical RoHR.
7. RON and ID are key factors to control the combustion process in PPC.

Downloaded from SAE International by Hadeel Solaka Aronsson, Monday, May 12, 2014 05:14:35 AM

8. The fuel composition at a constant ID was important for NO_x, smoke, and HC emissions. Higher concentrations of toluene gave higher levels of these emissions.
9. The CO emissions were insensitive to the fuel composition.

References

1. Speight James G., 2008, "Synthetic Fuels Handbook", McGRaw-Hill Companies.
2. Owen, K. and Coley, T., "Automotive Fuels Reference Book," - Second Edition Society of Automotive Engineers, Inc., Warrendale, PA, ISBN 978-1-56091-589-8, 1995.
3. Smallbone, A., Morgan, N., Bhave, A., Kraft, M. et al., "Simulating Combustion of Practical Fuels and Blends for Modern Engine Applications Using Detailed Chemical Kinetics," SAE Technical Paper 2010-01-0572, 2010, doi:10.4271/2010-01-0572.
4. Pitz, W., Cernansky, N., Dryer, F., Egolfopoulos, F. et al., "Development of an Experimental Database and Chemical Kinetic Models for Surrogate Gasoline Fuels," SAE Technical Paper 2007-01-0175, 2007, doi:10.4271/2007-01-0175.
5. Morgan Neal, Smallbone Andrew, Bhave Amit, Kraft Markus, Cracknell Roger, Kalghatgi Gautam, Mapping surrogate gasoline compositions into RON/MON space, Combustion and Flame, Volume 157, Issue 6, June 2010, Pages 1122-1131, ISSN 0010-2180.
6. Mehl Marco, Pitz William J., Westbrook Charles K., Curran Henry J., Kinetic modeling of gasoline surrogate components and mixtures under engine conditions, Proceedings of the Combustion Institute, Volume 33, Issue 1, 2011, Pages 193-200, ISSN 1540-7489, http://dx.doi.org/10.1016/j.proci.2010.05.027.
7. Kosaki, H., Yamashita, A., Adnin bin Hamidi, M., and Tezaki, A., "Chemical Kinetic Mechanism of Compression Ignition Derived from Intermediate Species for PRF and Toluene/n-Heptane Fuel Systems," *SAE Int. J. Fuels Lubr.* 5(1):28-33, 2011, doi:10.4271/2011-01-1784.
8. Koopmans, L., Strömberg, E., and Denbratt, I., "The Influence of PRF and Commercial Fuels with High Octane Number on the Auto-ignition Timing of an Engine Operated in HCCI Combustion Mode with Negative Valve Overlap," SAE Technical Paper 2004-01-1967, 2004, doi:10.4271/2004-01-1967.
9. Solaka, H., Tuner, M., and Johansson, B., "Investigation on impact of fuel properties on partially premixed combustion characteristics in a light duty diesel engine," ASME Technical Paper 2012-0-81184, 2012
10. Stradling, R., Antunez Martel, F-J., et al., "Volatility and vehicle drivability performance of ethanol/gasoline blends: a literature review", 2009, CONCAWE, Brussels, report no. 8/09, ec.europa.eu/energy/renewables/studies
11. Solaka, H., Tuner, M., and Johansson, B., "Analysis of Surrogate Fuels Effect on Ignition Delay and Low Temperature Reaction during Partially Premixed Combustion," SAE Technical Paper 2013-01-0903, 2013, doi:10.4271/2013-01-0903.
12. Solaka, H., Tuner, M., Johansson, B., and Cannella, W., "Gasoline Surrogate Fuels for Partially Premixed Combustion, of Toluene Ethanol Reference Fuels," SAE Technical Paper 2013-01-2540, 2013, doi:10.4271/2013-01-2540.
13. Truedsson, I., Tuner, M., Johansson, B., and Cannella, W., "Pressure Sensitivity of HCCI Auto-Ignition Temperature for Gasoline Surrogate Fuels," SAE Technical Paper 2013-01-1669, 2013, doi:10.4271/2013-01-1669.
14. Andersson, Ö., "Experiment: Planning, Implementing and Interpreting", First edition, John Wiley & Sons, Ltd, 2012.
15. Kee, S., Mohammadi, A., Kidoguchi, Y., and Miwa, K., "Effects of Aromatic Hydrocarbons on Fuel Decomposition and Oxidation Processes in Diesel Combustion," SAE Technical Paper 2005-01-2086, 2005, doi:10.4271/2005-01-2086.
16. Xioa, Z., Ladommatos, N., Zhao, H., "The Effect of Aromatic Hydrocarbons and Oxygenates on Diesel Engine Emissions", Journal of Automobile Engineering March 1, 2000 vol.214 no.3 307-332, doi:10.1243/0954407001527448.
17. Svensson, K., Richards, M., Mackrory, A., and Tree, D., "Fuel Composition and Molecular Structure Effects on Soot Formation in Direct-Injection Flames Under Diesel Engine Conditions," SAE Technical Paper 2005-01-0381, 2005, doi:10.4271/2005-01-0381.

Contact Information

hadeel.solaka@energy.lth.se

Acknowledgments

The authors would like to acknowledge the Competence Center for Combustion Processes, KCFP, and the Swedish Energy Agency for the financial support, and William Cannella from Chevron for supplying fuels.

Definitions/Abbreviations

ATDC - After top dead center

CA50 - Crank angle at 50% completion of heat release

CAD - Crank angle degree

CD - Combustion duration

DoE - Design of experiment

E - Ethanol

E10 - 10 vol.% ethanol concentration

ERF - Ethanol and primary reference fuel

I - Isooctane

ID - Ignition delay

LTR - Low temperature reaction

MON - Motor octane number

N - n-heptane

PPC - Partially premixed combustion

RoHR - Rate of heat release

Downloaded from SAE International by Hadeel Solaka Aronsson, Monday, May 12, 2014 05:14:35 AM

RON - Research octane number

S - Sensitivity of a blend, S=RON-MON

SOC - Start of combustion

SOI - Start of injection

T - Toluene

T10 - 10 vol.% toluene concentration

TERF - Toluene, ethanol and primary reference fuel

TRF - Toluene and primary reference fuel

Downloaded from SAE International by Hadeel Solaka Aronsson, Monday, May 12, 2014 05:14:35 AM

APPENDIX

In Table A, the RON and MON values were predicted using the quadratic regression model (with 34 data points). Later, these blends were sent to testing of their RON and MON, in order to validate the accuracy of the model.

Table A. Predicted RON, MON, and S and tested RON, MON, and S for the seventeen surrogate fuels.

N [v %]	T [v %]	E [v %]	I [v %]	RON DoE	RON test	MON DoE	MON test	S DoE	S test
10	0	10	80	96,31	96,4	93,09	92,9	3,22	3,5
38,5	0	16	45,5	76,17	75	73,19	71,7	2,98	3,3
43	0	38	19	85,58	84,4	84,29	78,7	1,29	5,7
8,5	22	0	69,5	95,93	96,1	92,75	91,8	3,18	4,3
30	20	0	50	75,74	75	72,62	72	3,12	3
17,5	12	0	70,5	86,75	85,1	83,98	83,3	2,77	1,8
13,5	38	0	48,5	95,48	94,8	89,25	87,8	6,23	7
34,5	37	0	28,5	75,64	75,6	69,37	69,8	6,27	5,8
20	22	0	58	85,68	85,1	82,43	81,6	3,25	3,5
38,5	25	10	26,5	76,1	74,8	70,07	69,8	6,03	5
15	21	10	54	95,79	95,5	89,57	89,2	6,22	6,3
22,5	7,5	8	62	85,97	85,1	82,65	82,5	3,32	2,6
33,5	7,5	8	51	76,11	74,8	72,97	72	3,14	2,8
10,5	6	8	75,5	95,78	96,3	92,3	92,4	3,48	3,9
19	4	4	73	85,68	84,9	83,84	83,6	1,84	1,3
5	0	0	95	94,23	94,8	94,3	94,8	-0,07	0
25	0	0	75	75,32	74,8	75,47	74,9	0,2	-0,1

In Table B, the regression coefficients are calculated from 51 fuel blends (the two DoE models and the seventeen validated fuels). With these coefficients the results are more accurate and the model has been validated (RON and MON) for well-known fuel blends.

$$RON_{Predicted} = \beta + \alpha_N \cdot X_N + \alpha_T \cdot X_T + \alpha_E \cdot X_E + \gamma_{NT} \cdot X_N \cdot X_T + \gamma_{NE} \cdot X_N \cdot X_E + \gamma_{TE} \cdot X_T \cdot X_E + \delta_{N^2} \cdot X_N^2 + \delta_{T^2} \cdot X_T^2 + \delta_{E^2} \cdot X_E^2 \quad (5)$$

Where β is a constant coefficient predicted from the regression model. Where α, γ and δ are coefficients for linear, interaction, and quadratic terms, respectively. X_N, X_T, and X_E are fuel concentration in volume fraction for n-heptane, toluene and ethanol, respectively and the remaining is isooctane. For example: if X_N =40 vol.%, X_T =0 vol.%, X_E =10 vol.%, the isooctane will be then 50 vol.% in this blend, and thus the RON and MON are 69.39 and 66.96, respectively.

Table B. Quadratic regression coefficients for modeling RON and MON.

Regression Coefficients	RON DoE	MON DoE
β	99,3022154471042	98,6850560235952
α_N	-0,94594723945044	-0,864864845159362
α_T	0,206222143583251	0,0200072691374061
α_E	0,686989203401194	0,305420013275534
γ_{NT}	0,00113896609766388	0,00259735154733907
γ_{NE}	0,00648104716520684	0,0110360124285118
γ_{TE}	-0,00616465224755151	-0,00467070201387479
δ_N^2	-0,00052560336409035	-0,00254416497232109
δ_T^2	0,000092898700907245	-0,000480768630133682
δ_E^2	-0,00690416392044605	-0,0052196926965211

Downloaded from SAE International by Hadeel Solaka Aronsson, Monday, May 12, 2014 05:14:35 AM

The Engineering Meetings Board has approved this paper for publication. It has successfully completed SAE's peer review process under the supervision of the session organizer. The process requires a minimum of three (3) reviews by industry experts.

All rights reserved. No part of this publication may be reproduced, stored in a retrieval system, or transmitted, in any form or by any means, electronic, mechanical, photocopying, recording, or otherwise, without the prior written permission of SAE International.

Positions and opinions advanced in this paper are those of the author(s) and not necessarily those of SAE International. The author is solely responsible for the content of the paper.

ISSN 0148-7191

http://papers.sae.org/2014-01-1303

Paper VI

Manuscript is submitted to SAE 2014 International Powertrain, Fuels and Lubricants meeting

Comparison of Fuel Effects on Low Temperature Reactions in PPC and HCCI Combustion

Hadeel Solaka Aronsson, Ida Truedsson, Martin Tuner, Bengt Johnsson
Lund University

William Cannella
Chevron

Copyright © 2014 SAE International

Abstract

The current research focus on fuel effects on low temperature reactions (LTR) in Homogeneous Charge Compression Ignition (HCCI) and Partially Premixed Combustion (PPC). LTR result in a first stage of heat release with decreasing reaction rate at increasing temperature. This makes LTR important for the onset of the main combustion. However, auto-ignition is also affected by other parameters and all fuel does not exhibit LTR. Moreover, the LTR does not only depend on fuel type but also on engine conditions. This research aims to understand how fuel composition affects LTR in each type of combustion mode and to determine the relative importance of chemical and physical fuel properties for PPC. For HCCI the chemical properties are expected to dominate over physical properties, since vaporization and mixing are completed far before start of combustion. The HCCI experiments were carried out in a Co-operative Fuel Research (CFR) engine, while the PPC experiments were carried out in a single cylinder high speed direct injected (HSPDI) diesel engine. A Gaussian profile was fitted to the data and used to determine the fraction of LTR for each type of combustion. The fuels used in this study are blends of ethanol, n-heptane, and isooctane (ERF), blends of toluene, n-heptane, and isooctane (TRF), and blends of toluene, ethanol, n-heptane and isooctane (TERF). The fractions of ethanol and toluene were varied at three levels to examine the influence on LTR for both HCCI and PPC. The result showed that increasing ethanol and toluene concentration in the ERF and TERF blends increases the LTR fraction in PPC while they decreased the LTR fraction for HCCI combustion. Ethanol had a stronger impact than toluene. Increasing isooctane and decreasing n-heptane concentration increased the LTR fraction for PPC while it decreased LTR fraction for HCCI. The lack of agreement between fuel effects in PPC and HCCI indicate that the processes behind LTR are more complex in PPC than in HCCI. It is not certain that a fuel with more pronounced chemical prerequisites for LTR will produce more LTR. The strong relation between LTR and ID for PPC indicate that the ignition quality is central for the fraction of LTR in PPC.

Introduction

In response to the strict legislation on engine-out emissions, especially on particulate matter (PM) and nitrogen oxides (NO and NO_2, here combines as NO_x), new strategies for combustion have been developed. Overall, these strategies can be classified into a group called Low Temperature Combustion (LTC). These strategies, such as Homogeneous Charge Compression Ignition (HCCI) [1-3], Premixed Charge Compression Ignition (PCCI) [4], Reactivity Controlled Compression Ignition (RCCI) [5], and Partially Premixed Combustion (PPC) [6-10], are used to reduce NO_x and PM and have historically been very sensitive to fuel chemistry.

The main advantage of these combustion strategies is low levels of engine out soot and NO_x. The common method for some of the strategies is to use high levels of cooled EGR, which increase heat capacity, resulting in a reduced combustion temperature, avoiding zones with high production of soot and NO_x. The EGR also slows down the kinetic reactions which results in a greater amount of fuel and air being premixed before ignition.

One of the challenges of HCCI combustion is control of combustion. The difficulty lies in controlling the auto-ignition phenomena. This is due to variation in temperature and fuel composition. Each fuel component has its specific auto-ignition temperature. Therefore, the combustion with diesel or gasoline fuel, which can contain hundreds to thousands of components, in an HCCI engine is difficult to explain and predict. However, there are some methods to control combustion such as varying the inlet temperature, compression ratio or to use dual fuel in which the two fuels have very different auto-ignition temperatures. Since gasoline has a higher resistance to auto-ignition compared to diesel fuel, it provides more time for mixing, and thus producing a higher fraction of premixed combustion. Using both EGR and gasoline fuels with high octane number further extends the time for pre-mixing. However, there is a drawback of using gasoline fuel: due to the high RON value a limitation at lower loads is present. Fuel effects on the combustion process are dependent of the course

of events in the early stages, i.e. mixing period, ignition delay, and low temperature reaction phase (LTR). Therefore, understanding fuel effects on these properties is critical to understand fuel effects on PPC.

A well-known phenomenon in HCCI combustion are the low temperature reactions (LTR), which is seen by a characteristic initial bump in the rate of heat release. This bump occurs before the main rate of heat release. Low temperature reactions depend both on fuel composition and gas temperature in the cylinder. Tanaka [13] indicates that in HCCI, the oxidation mechanism of hydrocarbons is initiated by abstraction of an H atom from a fuel molecule (RH) by O_2 to form an alkyl radical R• and HO_2•. At low temperatures, the LTR addition of R•+O2 to form RO2• then initiates a highly exothermic cycle that produces H_2O and an alkylperoxide. This continues until the temperature has reached a value where competing reactions starts to produce H_2O_2 and olefins. This intermediate stage occurs between the low temperature heat release and the high temperature heat release, and is referred to as intermediate temperature heat release (ITHR) [14]. The temperature then gradually increases until H_2O_2 decomposes leading to a branched thermal explosion. Fuel containing significant amounts of n-paraffin, such as n-heptane, exhibit a large low temperature reaction fraction [11,12]. LTR is also present in combustion of most diesel fuels. Christensen et al. [15] noted that LTR appears for HCCI type operation with gasoline-like fuels with an octane number lower than 83, while Bunting et al. [16] observed that diesel-like fuels or high cetane number fuels exhibit LTR, but no LTR was detected with a cetane number lower than 34.

In [17], Shibata et al. concluded that the structure of the hydrocarbons is strongly related to the LTR. They mention that aromatics, olefins and some naphthenes have a mechanism that reduces the LTR. In [18] Shibata et al. noted that a small change in chemical composition can change the HCCI combustion characteristics, such as the amount and phasing of LTR. Ethanol and toluene have a quenching effect on LTR and it is strongest for ethanol [19].

Fuel effects on ignition delay have been studied previously for diesel combustion, Homogenous Charge Compression Ignition, and Partially Premixed combustion. The ignition delay plays an important role in partially premixed combustion. Achieving the desired premixed combustion requires increasing the mixing of the fuel and air prior to ignition. The ignition delay depends on both physical and chemical processes. The physical delay is when the fuel is injected, droplet evaporates, mixes with air and are heated up to the auto ignition temperature [20], while the chemical delay takes place after the contact has been made between fuel and oxygen. This engages kinetics of chemical reactions, which form free radicals and other intermediates that are necessary for ignition [20,21].

The authors have studied fuel effects on LTR in PPC previously [22]. It was observed that a higher octane number fuel had a longer ignition delay. Higher n-paraffin content resulted in a shorter ignition delay and a smaller LTR phase. A relationship between ignition delay and LTR was also found, where a longer ignition delay resulted in higher LTR. It was also seen that, for the same ignition delay and RON values, independent of fuel composition, the LTR phase was the same [23].

This research study seeks to understand the connection between fuel property effects on LTR in PPC and HCCI combustion. One part in this is understanding the different effects of ethanol and toluene on LTR phase in both combustion modes.

Surrogate fuels selection methodology

Fuel properties

Fuels used in this investigation are blends of n-heptane, isooctane, toluene, and ethanol. Fuel properties are listed in Table 1. These fuels were blended in volume fraction to create the surrogate fuels. The fuels were individually tested according to DIN EN ISO 5164 standard (RON), and DIN EN ISO 5163 standard (MON) to determine the values of RON and MON, respectively. The stoichiometric air/fuel ratio and lower heating value were calculated based on the C:H:O ratio of each blend.

Table 1. Fuel properties.

Fuels properties	n-Heptane	Toluene	Ethanol	Isooctane
RON	0	120	107	100
MON	0	109	89	100
Auto-ignition temperature [°C]	203.85	529	425	411
Molecular formula	C7H16	C7H8	C2H6O	C8H18
Molar mass [g/mol]	100.23	92.15	46.07	114.26
Density [kg/m^3]	679.5	866.9	789	688
Boiling point [°C]	98	110.6	78.5	99

Component and concentration selections

The components and concentrations for the surrogate fuels were selected for fuels to have gasoline-like properties. Eight fuels from the PPC and HCCI test matrices were chosen to compare the composition effects in both types of combustion. The compositions and octane values of these fuels are found in Tables 2 to 3. Table 2 shows fuel specifications for PPC and HCCI operation, where both n-heptane and toluene concentration were kept constant, while ethanol concentration increased from 0 to 10 vol.% for PPC, and from 5 to 20 vol.% for HCCI. Table 3 shows fuel specifications where n-heptane and ethanol concentration were kept constant, while toluene concentration increased from 0 to 15 vol.% for PPC and from 10 to 30 vol.% for HCCI. In all cases, as the concentration of ethanol or toluene increased, the concentration of isooctane correspondingly decreased. Table 4 shows primary reference fuels (PRF) that are used for both PPC and HCCI combustion.

Table 2. Fuel specifications for PPC and HCCI operation where ethanol concentration increased.

Test matrix	n-hept (vol.%)	Toluene (vol.%)	Ethanol (vol.%)	Iso-oct (vol.%)	RON	MON	S
PPC	35	7.5	0	57.5	67.3	66.1	1.2
PPC	35	7.5	5	52.5	71.9	69.4	2.5
PPC	35	7.5	10	47.5	74.9	71.8	3.1
HCCI	30	20	5	45	79.6	74.5	5.1
HCCI	30	20	12.5	37.5	83.8	78.1	5.7
HCCI	30	20	20	30	87.9	81.4	6.5

Table 3. Fuel specifications for PPC and HCCI operation where toluene concentration increased.

Test matrix	n-hept (vol.%)	Toluene (vol.%)	Ethanol (vol.%)	Iso-oct (vol.%)	RON	MON	S
PPC	35	0	5	60	70.5	68.7	1.8
PPC	35	7.5	5	52.5	71.9	69.4	2.5
PPC	35	15	5	45	73.5	69.4	4.1
HCCI	30	10	12.5	47.5	81.6	77.9	3.7
HCCI	30	20	12.5	37.5	83.8	78.1	5.7
HCCI	30	30	12.5	27.5	85.3	78.6	6.7

Table 4. Fuel specifications for PPC and HCCI operation where isooctane concentration increased.

Test matrix	n-hept (vol.%)	Toluene (vol.%)	Ethanol (vol.%)	Iso-oct (vol.%)	RON	MON	S
PPC/HCCI	40	0	0	60	60	60	0
PPC/HCCI	30	0	0	70	70	70	0
PPC/HCCI	20	0	0	80	80	80	0

Experimental

Test methodology

PPC was examined for 8 fuels that are listed in Tables 2 to 4. Experiments were performed using an in-line 5-cylinder diesel engine (Volvo D5) operated on one cylinder. Details of the engine are given in Table 5. The fuels were tested at 8 bar $IMEP_g$ at 1500 rpm with a 50% heat release completion (CA50) at 3 crank angle degrees after top dead center (ATDC). A single injection strategy was used, wherein the start of injection (SOI) and the injection duration were adjusted to achieve the desired load with a constant, fixed value for CA50, as the injection pressure was kept constant at 800 bar. During the experiments the desired inlet oxygen concentration was 11% and the inlet mixture temperature and pressure were kept at 345 K and 2.3 bar.

The results for HCCI were obtained from experiments performed in a CFR engine, and the engine specifications and further details on the experiments can be found in reference [12]. All fuels were tested with an inlet temperature of 248 K and the combustion phasing with CA50 at 3±1 degrees ATDC was held by adjusting the compression ratio. The engine was run naturally aspirated. For each operating point, fuel amount was adjusted to achieve an equivalence ratio of 0.33. The HCCI experiments were performed at an engine speed of 600 rpm.

Table 5. Engine specifications.

Engine specifications for one cylinder	
Engine type	Volvo D5
Number of cylinders	1
Bore [mm]	81
Stroke [mm]	93.2
Displacement Volume [cm^3/cylinder]	480
IVC [CAD BTDC]	174
Compression ratio	16.5
Swirl ratio	2.2
Number of intake valves	2
Number of exhaust valves	2
Injector	
Type	Solenoid
Injection nozzle holes	7
Injection nozzle diameter [mm]	0.14
Included angle [degrees]	140

Heat release characteristics

From the calculated rate of heat release, information about the combustion event can be extracted. The heat losses are included in the rate of heat release calculation using the Woschni model [20]. For PPC, the combustion events are divided into four phases; ignition delay (ID), low temperature reactions (LTR), premixed fraction and late mixing controlled combustion phases as seen in Figure 1.

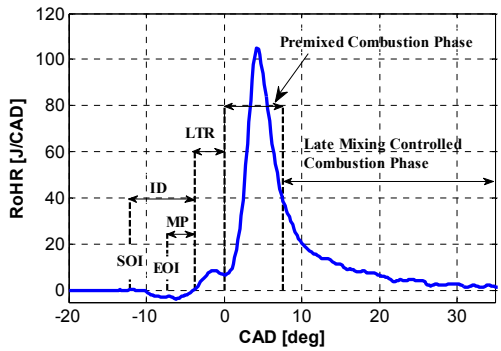

Figure 1. Typical PPC heat release diagram identifying different PPC combustion phases at 8 bar $IMEP_g$.

For PPC, the ignition delay is the period between the start of injection (SOI) and the start of combustion (SOC=CA0) as shown in Figure 1. The start of injection was determined from the first maximum in the evolution of the pressure gradient in the common rail (not shown). The start of combustion is defined as the location where the rate of heat release returns to zero after the negative period. When the fuel is injected into the combustion chamber the gas temperature decreases due to fuel evaporation, showing the negative rate of heat release. The point where the rate of heat release returns to zero establishes the start of combustion and/or the start of low temperature reaction (LTR).

In order to separate the LTR and premixed combustion phases in a well-defined manner, in the PPC heat release curves a Gaussian profile is fitted to the rising flank of the premixed peak, between 15 J/CAD and the actual peak. Different values for the threshold have been tested but with very small impact on the LTR phase. The rate of heat release is then subtracted from the Gaussian profile, and the integrated area between the SOC and the threshold point is used as a measure of the LTR fraction as shown in Figure 2.

$$G(x) = h \cdot e^{-\left(\frac{x-x_0}{2\propto^2}\right)^2} \qquad (4)$$

In Equation (4) x0 is the central position of the peak, h and ∝ representing the height and width of the Gaussian profile, respectively.

For the HCCI heat release curves, a Gaussian profile was fitted to the rising flank of the LTR peak, between the 0.16 J/CAD and the actual peak of LTR. The integrated area is then used as a measure of the LTR fraction for HCCI as shown in Figure 3. The Gaussian profile was fitted to the main heat release rate for PPC case due to inseparable phases of LTR and premixed fraction. In HCCI case there is a distinguish time between the main heat release and the LTR phase. This period between the main heat release and LTR is called Inter mediate heat release.

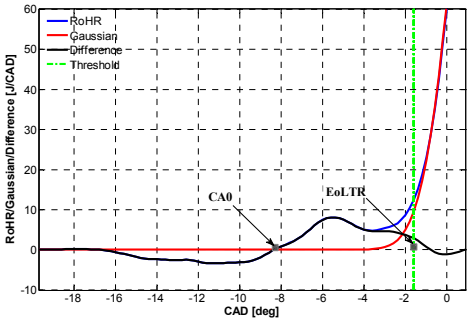

Figure 2. Gaussian profile (red), RoHR (blue), and difference (black) as a function of crank angle degree. Figure shows the LTR phase for PPC.

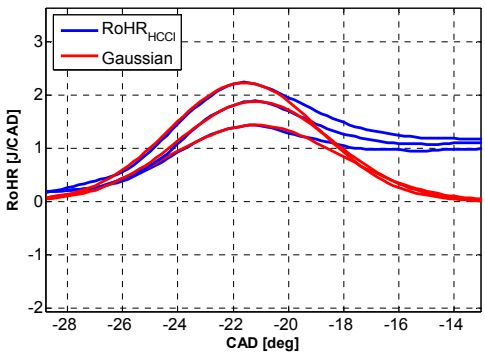

Figure 3. Gaussian profile fit for HCCCI LTR phase (red), and HCCI RoHR (blue) as a function of crank angle degree.

Results and discussion

Effects of ethanol on LTR

Figure 5 shows the LTR fraction as a function of ethanol concentration for the fuels in Table 2. This represents the net effect of replacing some of the isooctane with ethanol (with constant n-heptane and toluene concentrations). For the PPC tests, as ethanol concentration increases from 0 to 10% the LTR fraction increases with a slope of 0.08. However for the HCCI tests, as ethanol concentration increases from 5 to 20% the LTR fraction decreases with a slope of -0.1. The ethanol concentration has a stronger impact on the LTR fraction in HCCI than PPC. Previous work by the authors has shown similar trends in PPC and HCCI combustion [12, 22]. In PPC, the trend was explained by the ignition delay. A high concentration of ethanol resulted in longer ignition delay. The trend in HCCI is due to a change in the compression ratio required to initiate auto-ignition. A higher concentration of ethanol requires a higher compression ratio. The reasons for these trends are discussed below.

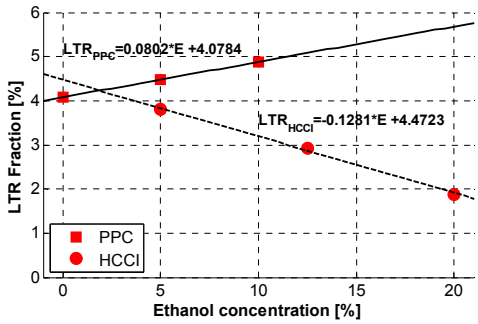

Figure 5. LTR fraction as a function of ethanol concentration.

Figure 6 shows the ignition delay (ID) for PPC and compression ratio (Rc) required for auto-ignition for a constant CA50 in HCCI combustion as a function of the ethanol concentration. The ID increases as ethanol concentration increases due to the advance in the start of injection (SOI) required maintaining the same CA50. Injecting fuel at early SOI the cylinder temperature and pressure are lower, which helps slow the chemical reaction and thus prolongs the time of mixing between fuel and air. It is known that ID is influenced by the chemical and physical properties of a fuel. It is difficult to determine exactly the vaporization time partially because the ignition occurs before vaporization has been completed. It is mentioned in previous paragraph that the increment of LTR is due to a prolonged in ID. The Rc increases as ethanol concentration increases to achieve same CA50 around 3 degrees ATDC. Increasing the Rc result in an increase in cylinder temperature and pressure. A higher cylinder temperature and pressure helps accelerate the main reactions to the point where they are dominant and LTR is minimized. The ethanol concentration has stronger impact on ID rather than Rc by comparing their slopes. The slope for ID is 3 times steeper than for Rc.

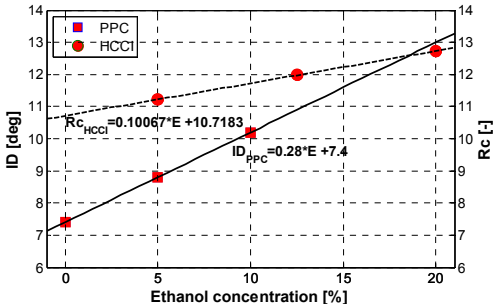

Figure 6 Ignition delay and compression ratio as a function of ethanol concentration in the blend.

According to Figure 7, a linear relation between the LTR fraction and ID, and LTR fraction and Rc are observed. As the ID increased, the LTR fraction increased due to additional time for the low temperature chemical reactions to occur. In contrast, increasing Rc in HCCI had the opposite effect on LTR. This was because the cylinder temperature and pressure were higher, resulting in acceleration of the main reactions and minimization of LTR. The LTR fraction slope is steeper for Rc in HCCI than ID in PPC. The slope is 1.4 times more for HCCI than PPC. In order to see ethanol effect on LTR phase in PPC, the ID effect should be excluded. However, this task is difficult to achieve with the conditions available in this work.

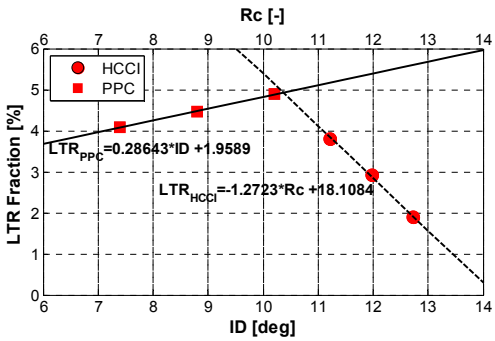

Figure 7 LTR fractions as a function of ignition delay and compression ratio.

It is difficult to explain the LTR fraction trend in PPC due to a complex combustion phenomena happening in the combustion chamber. However, with help of the global cylinder temperature, which is calculated from the pressure trace some observations can be made. The ignition temperature, which is the temperature that is calculated from the cylinder pressure at the start of LTR phase, decreased when increasing the ethanol concentration in the blend for PPC. The trend and the ignition temperature interval were different for HCCI (Figure not shown). It is known that the cylinder temperature influences the LTR phase. As the temperature rises above a threshold level the LTR decreases (the radicals driving the low temperature reaction chain branching are decomposed and high temperature heat release starts to dominate).

The slope for LTR fraction as a function of ethanol can mathematically be calculated using two other slopes as shown in equations 5 and 6.

$$LTR_{\ PPC}\ f(E) = ID\ f(E) \cdot LTR\ f(ID) \qquad (5)$$

$$LTR_{\ HCCI}\ f(E) = Rc\ f(E) \cdot LTR\ f(Rc) \qquad (6)$$

The calculated LTR as a function of ethanol for PCC and HCCI combustion are similar to the slopes presented in Figure 5..

Effects of Toluene on LTR

The net effect of adding toluene, with a corresponding reduction in isooctane at constant n-heptane and ethanol levels, was studied using the fuels in Table 3. The results are shown in Figure 8. In PPC, the LTR fraction first increased as the toluene level increased from 0 to 7.5 vol.% and then levels off. In contrast, the LTR decreased in HCCI combustion as toluene concentration was increased from 10 to 30 vol.%. For both PPC and HCCI, the steepness of the slopes are similar but with different direction. For both combustion modes, toluene concentration had a weaker influence on LTR phase than for ethanol. The LTR fraction was insensitive to the increase in toluene concentration from 7.5 to 15% for PPC case. This is can due to small changes in the injection timing. The small changes in LTR fraction in PPC and HCCI can be explained by ID and Rc respectively.

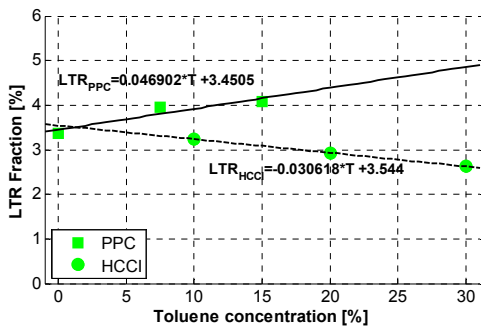

Figure 8. LTR fraction as a function of toluene concentration.

The ID increased as toluene concentration was increased from 0 to 7.5%, while ID was shown to be insensitive to toluene concentration between 7.5 and 15% as seen in Figure 9. This was due to the advance of the SOI at earlier case while keeping a similar SOI at later cases (Figure not shown) to maintain the same CA50. The Rc was increased to keep CA50 constant as toluene concentration increased. Toluene had a stronger impact on Rc than ID. The Rc slope was twice more than the ID slope. As mentioned previously, increasing the Rc resulted in a reduction of the LTR phase. It seemed that if the ID is similar despite the increase in toluene concentration, the LTR fraction is also similar for PPC. Similar IDs are due to similar SOI and thus similar mixing time for the fuel and air.

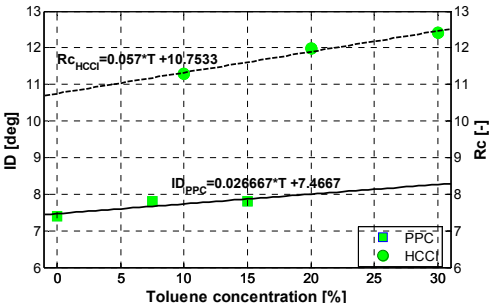

Figure 9. Ignition delay and compression ratio as a function of toluene concentration.

The relation between LTR and ID for PPC, and LTR and Rc for HCCI, is shown in Figure 10. The LTR slope dependence on ID is steeper than for Rc, this may partially be due to similar value of ID. The ID influence on the LTR slope is stronger for toluene than ethanol in the PPC case. The Rc impact on LTR slope is stronger for ethanol than toluene in HCCI case.

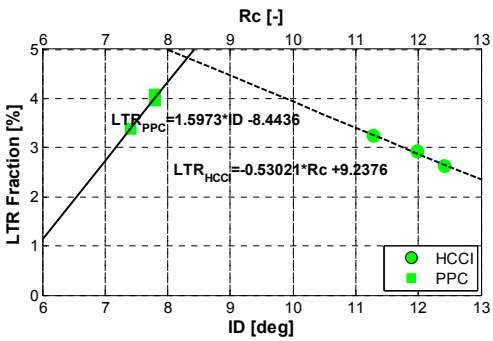

Figure 10. LTR fraction as a function of ignition delay and compression ratio.

Mathematically the slope for LTR fraction as function of toluene can be calculated from Figures 9 and 10 for both PPC and HCCI using equation 7 and 8.

$$LTR_{PPC}\, f(T) = ID\, f(T) \cdot LTR\, f(ID) \quad (7)$$

$$LTR_{HCCI}\, f(T) = Rc\, f(T) \cdot LTR\, f(Rc) \quad (8)$$

The calculated slopes for LTR fraction is similar to the slopes presented in Figure 8. It is possible to calculate the LTR fraction as a function of toluene for PPC and HCCI by using two functions as presented in equation 7 and 8.

Effects of Isooctane on LTR

LTR fraction increased when the isooctane concentration was increased in the blend for PPC, while it decreased for HCCI as shown in Figure 11. The LTR fractions for PRF60 and PRF70 were higher for HCCI than for PPC, however for PRF80 the LTR fraction was higher for PPC. The slope for PPC is about 6 times steeper than for HCCI. This behavior was explained by a prolonged ID in PPC, which allows sufficient time for fuel and air to mix. This helped slow the chemical reaction and thus the LTR increased. The decrease in LTR for HCCI was explained by the change in Rc. By increasing isooctane concentration, required Rc increased.

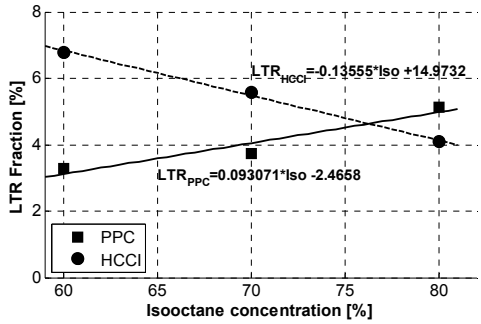

Figure 11 LTR fractions as a function of isooctane concentrations.

The ID and Rc increased when increasing the isooctane concentration as shown in Figure 12. The increase in ID as isooctane concentration was increased was due to the advance of the SOI to maintain a similar CA50. Injecting fuel earlier the cylinder temperature and pressure are lower and thus the reactions occur slowly. The Rc increases as increasing isooctane to achieve similar CA50, however, increasing the Rc the cylinder temperature and pressure are higher and thus the reactions occur rapidly. The slope for ID is steeper than for Rc as a function of isooctane.

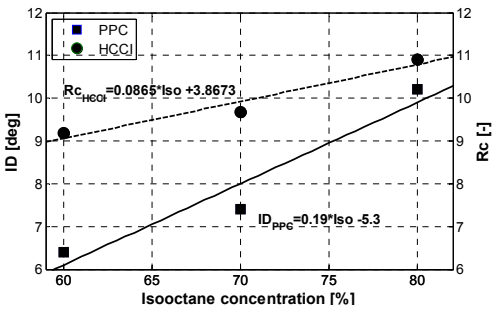

Figure 12 Ignition delay and compression ratio as a function of isooctane concentrations.

As expected, the LTR fraction decreased when increasing the Rc, while it increased when prolonging the ID as seen in Figure 13. This was mainly due to the cylinder temperature and pressure variation caused by changing the Rc and SOI. However, the LTR fraction slope is steeper for Rc than for ID and thus more sensitive to the change in Rc than SOI.

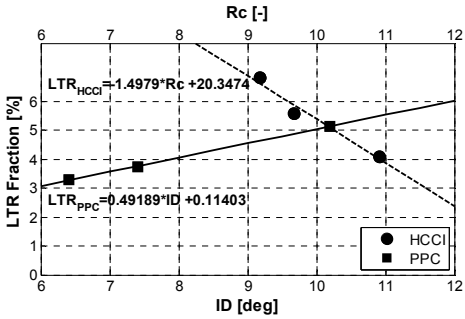

Figure 13 LTR fractions as a function of ignition delay and compression ratio.

The slope for LTR fraction as function of isooctane can be calculated mathematically from Figures 12 and 13.

$$LTR_{PPC}\, f(Iso) = ID\, f(Iso) \cdot LTR\, f(ID) \qquad (9)$$

$$LTR_{HCCI}\, f(Iso) = Rc\, f(Iso) \cdot LTR\, f(Rc) \qquad (10)$$

The calculating slope is similar to the slope shown in Figure 11 for LTR fraction. This means that the LTR as function of isooctane can be described as two other functions as seen in equation 9 for PPC and equation 10 for HCCI.

Factors that affect the ID and LTR fraction can be divided into two groups: the chemical and the physical properties. The ID increased when increasing ethanol, toluene, and isooctane concentrations in the blend. This was due to increase of the RON value of the blend. Previously the authors showed that by increasing the ethanol concentration, the RON value increased in a nonlinear process. It was also shown that ethanol had the strongest effect on RON values, compared to toluene and isooctane. RON is a measure of fuel auto-ignition quality, by doing knock measurements. A higher RON means a higher resistance to auto-ignition. The ID was prolonged when the RON was increased due to the advance of SOI to maintain a constant CA50. The ID was highest for ethanol and lowest for toluene, as RON increased, as seen in Figure 14. Beside the fuel effect on ignition delay, the physical effects from for example SOI plays a major role in prolonging the ID. Advancing the SOI decreases the cylinder temperature and pressure, which give the chemical reactions more time to occur.

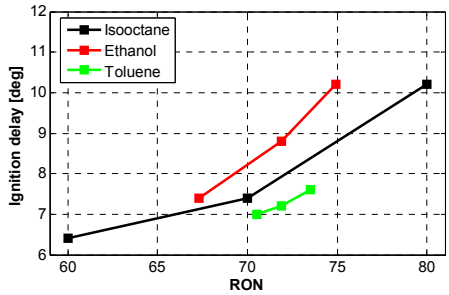

Figure 14 Ignition delays as a function of RON.

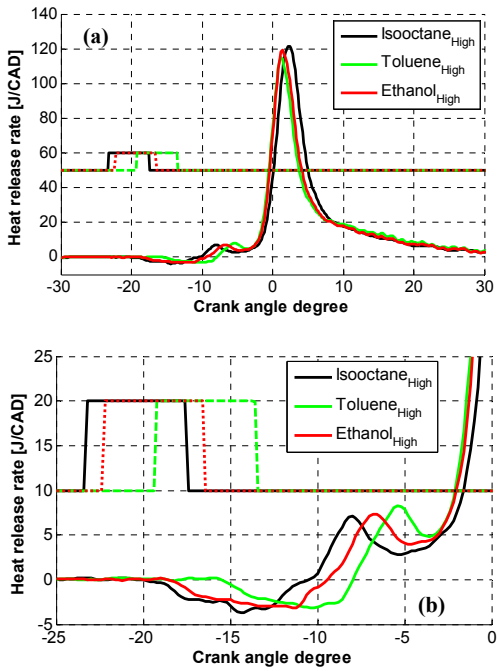

Figure 15 (a) Heat release rate as a function of crank angle degree for the highest concentrations of isooctane, toluene and ethanol at CA50 3 degrees ATDC. Figure (b) is a zoomed version of (a) showing heat of vaporization, LTR phase.

The heat release rates showing the low temperature reactions and the endothermic phases are presented in Figure 15 for the highest concentration of isooctane, toluene, and ethanol at CA50 3 degrees ATDC. Despite the similarity in CA50, both the fuel vaporization period and LTR phase are different as seen in Figure 15 b. The differences in vaporization period are partially due to the change in SOI and partially to the different fuel composition. As seen, the SOI is earlier for isooctane with RON 80 and the latest is for toluene with RON 73. As

mentioned in previous sections, an early SOI will result in lower cylinder temperature and pressure and thus giving more time for mixing. The amount of energy for heat of vaporization (the negative dip in heat of release) from isooctane and ethanol are the same at the highest concentration (figure not shown). Isooctane is injected earlier, when cylinder temperature and pressures are lower, which help to prolong the vaporization period. However for the ethanol blend, the SOI is later than for isooctane, and thus the cylinder temperature is higher, which will shorten the vaporization time. For the toluene blend the vaporization period is even shorter due to late injection timing and thus higher cylinder temperature.

Conclusions

This work compares fuel effects on the low temperature reaction (LTR) fraction in PPC and HCCI combustion to sort out the limiting factors for fraction of LTR in PPC. Experiments were carried out in a single cylinder light-duty diesel engine for PPC and in a CFR engine for HCCI. The combustion phasing, CA50, was kept close to 3 degrees ATDC by adjusting the start of injection (SOI) for PPC and the compression ratio for HCCI. Fuel blends were divided into three groups to test the effect of ethanol, toluene, and isooctane in each combustion mode. The isooctane concentration was used to balance the variation of ethanol and toluene in the first and second group while n-heptane was used to balance the variation in isooctane concentration in the third group. The following observations were made:

1. As ethanol or toluene concentration increases, the LTR fraction increases for PPC while it decreases for HCCI.
2. Ethanol had a stronger impact on LTR fraction than toluene.
3. Increasing isooctane and decreasing n-heptane concentration increased the LTR fraction for PPC while it decreased for HCCI.
4. A prolonged ignition delay gave a higher fraction of LTR for PPC. As when the SOI has to be advanced at higher RON values.

In summary, the observed fuel effect on LTR in PPC was reversed compared to HCCI. Chemical fuel effects will dominate over physical effects for port injected HCCI since the fuel can be expected to be vaporized and fairly well mixed when the inlet valve close. The lack of agreement between fuel effects in PPC and HCCI indicate that:

1. The processes behind LTR are more complex in PPC than in HCCI. It is not certain that a fuel with more pronounced chemical prerequisites for LTR will produce more LTR.
2. The strong relation between LTR and ID for PPC indicate that the ignition quality is central for the fraction of LTR in PPC.

Future work

Comparing fuels with similar RON value but with different fuel composition to examine fuel composition effect on combustion process in both PPC and HCCI combustion. Having fuel with similar RON values could result in similar ignition delay for PPC and using the same compression ratio in HCCI.

References

1. Onishi, S., Hong Jo, S., Shado, K., Do Jo, P., Kato, S., “Active Thermo-Atmosphere Combustion (ATAC) - A NEW Combustion Process for Internal Combustion Engine”, SAE 790501
2. Christiansen, M., Hultqvist, A., Johansson, B., 1999, “Demonstrating the Multi Fuel Capability of a Homogenous Charge Compression Ignition Engine with Variable Compression Ratio”, SAE 1999-01-3679
3. Johansson, T., Johansson, B., Tunestål, P., Aulin, H., 2009, ”The Effect of Intake Temperature in a Turbocharged Multi Cylinder Engine Operating in HCCI Mode”, SAE Technical Paper 2009-24-0060
4. Lee, S. and Reitz, R., "Spray Targeting to Minimize Soot and CO Formation in Premixed Charge Compression Ignition (PCCI) Combustion with a HSDI Diesel Engine," SAE Technical Paper 2006-01-0918, 2006, doi:10.4271/2006-01-0918.
5. Splitter, D., Hanson, R., Kokjohn, S., and Reitz, R., "Reactivity Controlled Compression Ignition (RCCI) Heavy-Duty Engine Operation at Mid-and High-Loads with Conventional and Alternative Fuels," SAE Technical Paper 2011-01-0363, 2011, doi:10.4271/2011-01-0363.
6. Manente, V., Johansson, B., and Tunestal, P., "Partially Premixed Combustion at High Load using Gasoline and Ethanol, a Comparison with Diesel," SAE Technical Paper 2009-01-0944, 2009, doi:10.4271/2009-01-0944
7. Borgqvist, P., Tunestal, P., and Johansson, B., "Gasoline Partially Premixed Combustion in a Light Duty Engine at Low Load and Idle Operating Conditions," SAE Technical Paper 2012-01-0687, 2012, doi:10.4271/2012-01-0687.
8. Kaiadi, M., Johansson, B., Lundgren, M., and Gaynor, J., "Sensitivity Analysis Study on Ethanol Partially Premixed Combustion," SAE Int. J. Engines 6(1):120-131, 2013, doi:10.4271/2013-01-0269.
9. Shen, M., Tuner, M., Johansson, B., and Cannella, W., "Effects of EGR and Intake Pressure on PPC of Conventional Diesel, Gasoline and Ethanol in a Heavy Duty Diesel Engine," SAE Technical Paper 2013-01-2702, 2013, doi:10.4271/2013-01-2702.
10. Solaka, H., Aronsson, U., Tuner, M., and Johansson, B., "Investigation of Partially Premixed Combustion Characteristics in Low Load Range with Regards to Fuel Octane Number in a Light-Duty Diesel Engine," SAE Technical Paper 2012-01-0684, 2012, doi:10.4271/2012-01-0684.
11. Shibata, G., OYama, K., et al., 2005,”Correlation of Low Temperature Heat Release with Fuel Composition and HCCI Engine Combustion”, SAE Technical Paper 2005-01-0138.
12. Truedsson, I., Tuner, M., Johansson, B., and Cannella, W., "Pressure Sensitivity of HCCI Auto-Ignition Temperature for Primary Reference Fuels," SAE Int. J. Engines 5(3):1089-1108, 2012, doi:10.4271/2012-01-1128.
13. Tanaka, S., Ayala, F., Keck, J.C., Heywood, J.B., 2002 “Two-Stage Ignition in HCCI Combustion and HCCI Control by Fuels and Additives”, Combustion and Flame 132 (2003) 219-239.

14. Tsujimura, T., Pitz, W., Yang, Y., and Dec, J., "Detailed Kinetic Modeling of HCCI Combustion with Isopentanol," SAE Int. J. Fuels Lubr. 4(2):257-270, 2011, doi:10.4271/2011-24-0023.
15. Christensen, M., Hultqvist, A., and Johansson, B., "Demonstrating the Multi Fuel Capability of a Homogeneous Charge Compression Ignition Engine with Variable Compression Ratio," SAE Technical Paper 1999-01-3679, 1999, doi:10.4271/1999-01-3679.
16. Bunting, B. G., Wildman, C. B., Szybist, J. P., Lewis, S., & Storey, J. (2007 February) Fuel chemistry and cetane effects on diesel homogeneous charge compression ignition performance, combustion, and emissions. 8 (1), 15-27. doi:10.1243/14680874JER01306
17. Shibata, G., Oyama, K., Urushihara, T., and Nakano, T., "Correlation of Low Temperature Heat Release With Fuel Composition and HCCI Engine Combustion," SAE Technical Paper 2005-01-0138, 2005, doi:10.4271/2005-01-0138.
18. Shibata, G., Oyama, K., Urushihara, T., and Nakano, T., "The Effect of Fuel Properties on Low and High Temperature Heat Release and Resulting Performance of an HCCI Engine," SAE Technical Paper 2004-01-0553, 2004, doi:10.4271/2004-01-0553.
19. Truedsson, I., Tuner, M., Johansson, B., and Cannella, W., "Pressure Sensitivity of HCCI Auto-Ignition Temperature for Gasoline Surrogate Fuels," SAE Technical Paper 2013-01-1669, 2013, doi:10.4271/2013-01-1669.
20. Heywood, J.B., "Internal Combustion Engine Fundamentals", McGraw Hill Book Co, 1988.
21. Warnatz, J., Maas, U., DiBble, R.W., "Combustion Physical and Chemical Fundamentals, Modeling and Simulation, Experiments, Pollutant Formation" 4th edition, Springer Berlin Heidelberg New York, 2006.
22. Solaka, H., Tuner, M., and Johansson, B., "Analysis of Surrogate Fuels Effect on Ignition Delay and Low Temperature Reaction during Partially Premixed Combustion," SAE Technical Paper 2013-01-0903, 2013, doi:10.4271/2013-01-0903.
23. Solaka Aronsson, H., Tuner, M., and Johansson, B., "Using Oxygenated Gasoline Surrogate Compositions to Map RON and MON," SAE Technical Paper 2014-01-1303, 2014.

Contact Information

hadeel.solaka@energy.lth.se

Acknowledgments

The authors would like to acknowledge the Competence Center for Combustion Processes, KCFP, and the Swedish Energy Agency for the financial support, and William Cannella from Chevron for supplying fuels.

Definitions/Abbreviations

ATDC	After top dead center
CA50	Crank angle at 50% completion of heat release
CAD	Crank angle degree
DoE	Design of experiment
E	Ethanol
E10	10 vol.% ethanol concentration
ERF	Ethanol and primary reference fuel
I	Isooctane
ID	Ignition delay
IT	Ignition temperature
LTR	Low temperature reaction
MON	Motor octane number
N	n-heptane
PPC	Partially premixed combustion
Rc	Compression ratio
RoHR	Rate of heat release
RON	Research octane number
S	Sensitivity of a blend, S=RON-MON
SOC	Start of combustion
SOI	Start of injection
T	Toluene
T10	10 vol.% toluene concentration
TERF	Toluene, ethanol and primary reference fuel
TRF	Toluene and primary reference fuel